Miniaturization of Process Analytical Technology: from Concept to Reality

Neves Sao Pedro, M.

DOI
10.4233/uuid:ec3f81c3-1bb4-4724-9f97-fff46e3c1c66

Publication date
2023

Document Version
Final published version

Citation (APA)
Neves Sao Pedro, M. (2023). *Miniaturization of Process Analytical Technology: from Concept to Reality*. [Dissertation (TU Delft), Delft University of Technology]. https://doi.org/10.4233/uuid:ec3f81c3-1bb4-4724-9f97-fff46e3c1c66

Miniaturization of Process Analytical Technology

From Concept to Reality

Mariana Neves São Pedro

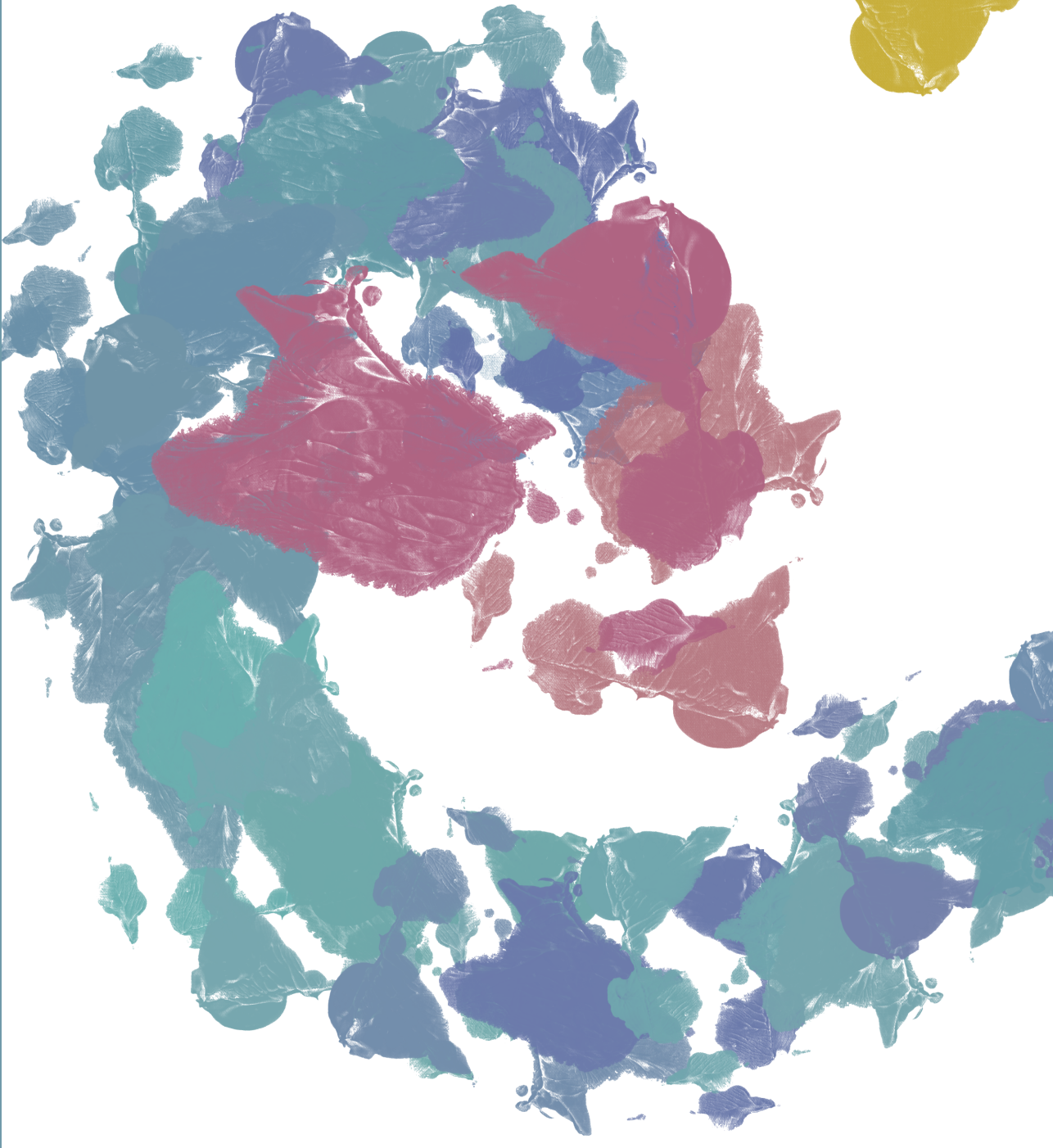

Miniaturization of Process Analytical Technology

From Concept to Reality

MINIATURIZATION OF PROCESS ANALYTICAL TECHNOLOGY

FROM CONCEPT TO REALITY

Dissertation

for the purpose of obtaining the degree of doctor
at Delft University of Technology,
by the authority of the Rector Magnificus, prof. dr. ir. T.H.J.J. van der Hagen,
chair of the Board of Doctorates
to be defended publicly on
Friday 27th October 2023 at 10:00 o'clock

by

Mariana NEVES SÃO PEDRO

Master of Science in Biotechnology,
Instituto Superior Técnico, Portugal,

born in Lisbon, Portugal

This dissertation has been approved by the promotors.

Composition of the doctoral committee:

Rector Magnificus	chairperson
Prof. dr. ir. M. Ottens	Delft University of Technology, promotor
Prof. dr. ing. M.H.M. Eppink	Wageningen University / Byondis, promotor

Independent members:

Prof. dr. M.R. Aires-Barros	Instituto Superior Técnico
Prof. dr. J.J. Hubbuch	Karlsruhe Institute of Technology
Prof. dr. ir. L.A.M. van der Wielen	Delft University of Technology
Prof. dr. F. Hollmann	Delft University of Technology
dr. M. Pabst	Delft University of Technology

This work falls into the European Union's Horizon 2020 research and innovation programme under the Marie Skłodowska-Curie grant agreement No 812909 CODOBIO, within the Marie Skłodowska-Curie European Training Networks framework.

Printed by Proefschriftspecialist

Cover illustration and design: David Calderón Franco

ISBN: 978-94-6384-473-4

An electronic version of this dissertation is available at http://repository.tudelft.nl/

Contents

Summary

Continuous biomanufacturing is considered the future phase for the optimization of production processes in the biopharmaceutical industry. Productivity, product quality and consistency are greatly improved while production costs and environmental footprint are drastically reduced. The manufacturing of monoclonal antibodies (mAbs), an important biopharmaceutical in the treatment of cancers, autoimmune disorders, and, more recently, COVID-19, is eligible for this continuous processing due to patent expiration and the subsequent need to lower manufacturing costs. An extensive state-of-art into continuous biomanufacturing, resulting from data collected from academia and industry participants in a conference workshop, is presented in **Chapter 2**. The major gaps in high-throughput process development, with the main needs and possible solutions to achieve end-to-end continuous biomanufacturing, are comprehensively discussed.

An important conclusion was that, for a continuous process implementation, real-time information on each unit operation must be obtained in an adequate timeframe which allows process monitoring and control. Process analytical technologies (PAT) are thus essential by allowing real-time analysis of the raw materials or the in-process critical quality attributes (CQAs). With the information collected from the manufacturing process, minor adjustments in the operation conditions can be executed, ensuring that the process remains in the proper specifications. However, for downstream processing, PAT tools have been mostly unexplored.

A major CQA during mAb production is protein aggregation, which, when present in the biopharmaceutical's final formulation, might lead to an adverse immune response. To create the necessary PAT tool for aggregate detection, the measurement must be immediate, being available in a time range of a few seconds to minutes. Miniaturized sensors, placed after each unit operation, are a potential solution to speed up the analytical measurement. Short reaction times and small sample size (in the µL or nL-scale) are just two of the major benefits of working in a microfluidic environment. Thus, creating a miniaturized analytical technique significantly decreases the measurement time to potentially only a few seconds. Several analytical methods which provide an aggregate measurement (Dynamic Light Scattering and Raman spectroscopy as examples) were extensively evaluated for the possibility of being miniaturized in **Chapter 3**.

Fluorescent dyes (FDs), when in the presence of mAb aggregates, strongly enhance their fluorescence when compared to in the presence of the monomer form. Thus, FDs were chosen to develop a real-time miniaturized PAT tool for aggregate detection. An

immediate and straightforward result in possible size differences of mAb species is achieved. To mix a FD with the mAb sample to be analysed, a microfluidic mixing channel was first designed. Due to the presence of laminar flow, the mixing in the microfluidic scale is an inherently slow process. To enhance the mixing efficiency, passive mixing methods, where the structure or configuration of the microfluidic channel is altered, were used. In **Chapter 4**, a screening into possible geometries was performed, employing computational fluid dynamic (CFD) modelling. A zigzag microchannel, with a total of 30 mixing units with a 45^0 angle each, showed the highest mixing efficiency, higher than 90%, validated with colour dyes, and later with a fluorescent-tagged mAb molecule.

Nevertheless, the ability of the proposed micromixer to actually detect aggregates still needed to be assessed. In **Chapter 5**, the developed PAT tool was validated by resorting to an UV detector, using mAb samples with diverse levels of aggregation and four independent and well-established FDs. The required concentration of FDs to produce a measurable signal was initially assessed resorting to a liquid handling system, the Tecan. Additionally, several known induction factors were used to produce mAb samples with different levels of aggregation, such as temperature or low pH. The micromixer was able to detect aggregation across all the induced aggregation samples by a rise of the UV signal, whereas, for the mAb purified sample with 0% of high molecular weight species, no measurable increase was observed.

Lastly, the developed micromixer was implemented in a chromatographic system, an ÄKTA™ unit. The validation was firstly performed in a simple anion exchange chromatographic operation for aggregate removal, followed by a final validation in an integrated continuous downstream process. A viral inactivation and two chromatographic polishing steps were reproduced, where a pool sample after each unit operation was directly sent to the microfluidic sensor for analysis, described in detail in **Chapter 6**. A real-time measurement for protein aggregation was then achieved, in just below 10 minutes.

The work here developed shows that the miniaturization of an analytical technique is a good solution to expedite the measurement and create the needed PAT tool for aggregation detection. Furthermore, the micromixer requires no extra equipment to perform the analytical measurement next to an UV monitor, using relatively affordable fabrication materials, which makes the implementation of this PAT tool in an industrial setting achievable.

Samenvatting

Continue procesvoering wordt gezien als de volgende fase in de optimalisatie van productieprocessen in de biofarmaceutische industrie. Productiviteit, productkwaliteit en productconsistentie worden aanzienlijk verbeterd, terwijl productiekosten en milieu-impact drastisch worden verminderd. Monoklonale antilichamen (mAbs) zijn belangrijke biofarmaceutisch producten voor de behandeling van kanker, auto-immuunziekten en, meer recentelijk COVID-19. De productie van deze mAbs is geschikt voor continue procesvoering omdat patenten binnenkort verlopen en daardoor de productiekosten ook verlaagd dienen te worden. Een uitgebreid overzicht van de huidige toegepaste technieken in continue bioproductie wordt gegeven in **Hoofdstuk 2**. Dit overzicht is gebaseerd op gegevens verzameld tijdens een conferentie workshop met zowel academische als industriële deelnemers. De belangrijkste tekortkomingen van *high-throughput process development* (HTPD: combinatie van snel experimenteel testen en het ontwikkelen van een productieproces) en benodigdheden in de ontwikkeling met mogelijke oplossingen om continue bioproductie te bereiken worden uitvoerig besproken.

Een belangrijke conclusie met betrekking tot de implementatie van een continu proces is dat er real-time informatie over elke processtap moet worden verkregen binnen een bepaalde tijd om procesmonitoring en -controle mogelijk te maken. *Process Analytical Technology* (PAT) is essentieel omdat dit real-time analyse van de grondstoffen en de "kritieke kwaliteitskenmerken" tijdens het proces mogelijk maakt. Met de op deze manier verzamelde informatie uit het productieproces kunnen kleine aanpassingen in de operationele omstandigheden worden uitgevoerd, zodat het proces binnen de juiste specificaties blijft. Echter, op dit moment zijn PAT-tools nog niet uitgebreid onderzocht voor toepassing in het zuiveringsproces (downstream processing) van bio-producten.

Eiwitaggregatie is een belangrijk zogenaamd "kritieke kwaliteitskenmerk" tijdens de productie van mAbs, dat kan leiden tot een ongewenste immuunrespons als dat aanwezig is in de uiteindelijke formulering van het biofarmaceutische product. Om een PAT-tool voor aggregatiedetectie te creëren, zou de meting enkele seconden tot minuten moeten duren. Een mogelijke oplossing zou zijn om geminiaturiseerde sensoren na elke processtap te plaatsen om zo de analytische meting te versnellen. Korte reactietijden en kleine monsters (in de µL- of nL-schaal) zijn slechts twee van de belangrijkste voordelen van microfluidics. Dus het creëren van een

geminiaturiseerde analytische techniek kan de meettijd aanzienlijk verminderen tot mogelijk slechts enkele seconden. Verschillende analytische methoden voor een aggregaatmeting (zoals Dynamic Light Scattering en Raman spectroscopie) worden uitgebreid besproken en beoordeeld op hun miniaturisatie potentieel in **Hoofdstuk 3**.

Fluorescerende kleurstoffen (FD's) versterken fluorescentie van mAb-aggregaten in vergelijking met het mAb monomeer. Daarom zijn FD's gekozen om een real-time geminiaturiseerde PAT-tool voor aggregaatdetectie te ontwikkelen. Hiermee kunnen verschillen in grootte tussen mAbs onmiddellijk en eenvoudig worden gedetecteerd. Om een FD te mengen met het te analyseren mAb-monster, wordt eerst een microfluïdische mengkanaal ontworpen. Vanwege de aanwezigheid van laminaire stroming is menging op microfluïdisch niveau een inherent langzaam proces. Om de efficiëntie van mengen te verbeteren, worden passieve mengmethoden gebruikt waarbij de structuur of configuratie van het microfluïdische kanaal wordt gewijzigd. In **Hoofdstuk 4** wordt een screening uitgevoerd naar mogelijke geometrieën van het microfluidische kanaal met behulp van computationele vloeistofdynamica (CFD)-modellering. Een zigzag-microkanaal, met in totaal 30 mengeenheden met elk een hoek van 45^0 toont de hoogste mengefficiëntie (hoger dan 90%) en is gevalideerd met kleurstoffen en later met een fluorescent-gemarkeerd mAb-molecuul.

Desalniettemin dient het vermogen van de voorgestelde micromixer om aggregaten daadwerkelijk te detecteren nog worden beoordeeld. In **Hoofdstuk 5** wordt de ontwikkelde PAT-tool gevalideerd met behulp van een UV-detector, door mAb-monsters met verschillende aggregatieniveaus en vier onafhankelijke en bekende FD's te analyseren. De vereiste concentratie van FD's om een meetbaar signaal te produceren wordt in eerste instantie beoordeeld met behulp van een *liquid handling system* (LHS), de Tecan. Bovendien worden verschillende bekende inductiefactoren gebruikt om mAb-monsters met verschillende niveaus van aggregatie te produceren, zoals temperatuur of een lage pH. De micromixer blijkt in staat om aggregatie te detecteren bij alle geïnduceerde aggregatiemonsters door een toename van het UV-signaal te meten, terwijl bij het gezuiverde mAb-monster met 0% van de hoogmoleculaire soorten geen meetbare toename wordt waargenomen.

Ten slotte wordt de ontwikkelde micromixer geïmplementeerd in een chromatografisch zuiveringssysteem, een ÄKTA™. De validatie wordt eerst uitgevoerd in een eenvoudige anionenwisseling chromatografisch proces om aggregaten te verwijderen. Daarna wordt de uiteindelijke validatie in een geïntegreerd continu

downstream-proces uitgevoerd. Een virale inactivatie en twee chromatografische polijst stappen worden gereproduceerd, waarbij een monster na elke processtap direct naar de microfluïdische sensor wordt gestuurd om te analyseren, zoals in detail beschreven in **Hoofdstuk 6**. Een bijna real-time meting voor eiwitaggregatie wordt vervolgens bereikt in iets minder dan 10 minuten.

Het ontwikkelde werk toont aan dat de miniaturisatie van een analytische techniek een goede oplossing is om metingen te versnellen en daarmee de benodigde PAT-tool voor aggregatiedetectie te vervaardigen. Bovendien vereist de micromixer geen extra apparatuur om de analytische meting uit te voeren naast een UV-monitor. Tezamen met het gebruik van relatief goedkope fabricagematerialen maakt dit de implementatie van deze PAT-tool in een industriële omgeving uiteindelijk haalbaar.

Chapter 1

Introduction

2.1. Background and Aim

Monoclonal antibodies (mAbs) are highly specific molecules which can recognize and eliminate pathogenic and disease antigens, being used in the treatment of several diseases such as cancers [1], autoimmune disorders [2] and, more recently, COVID-19 [3]. Some examples of mAbs which are found in the marked are described in **Table 1.1**, focusing on its commercial name and target disease. The global mAb market was valued at around 185 billion dollars in 2021 and is forecasted to reach 380 billion dollars by 2024 [4].

***Table 1.1** – Examples of mAbs in clinical use, with its commercial name and its disease target. Based on Grilo* et al. *[5].*

mAb	Commercial Name	Disease target
Dupilumab	DUPIXENT	Atopic dermatitis
Trastuzumab	HERCEPTIN	Breast cancer, gastric or gastroesophageal junction adenocarcinoma
Infliximab	REMICADE	Crohn's disease, ulcerative colitis, rheumatoid arthritis, psoriatic arthritis, plaque psoriasis
Rituximab	RITUXAN	Non-Hodgkin's lymphoma, chronic lymphocytic leukemia
Basiliximab	SIMULECT	Prevent transplanted kidney rejection

Their basic structure (Figure 1.1), in a Y-shape, is composed of two heavy and two light chains. At each tip of the Y lies the fragment antigen-binding (Fab) portion of the antibody which is responsible for recognition of a specific antigen. The fragment crystallisable (Fc) region located at the base of the Y structure mediates interactions between the antibody and the immune system [1].

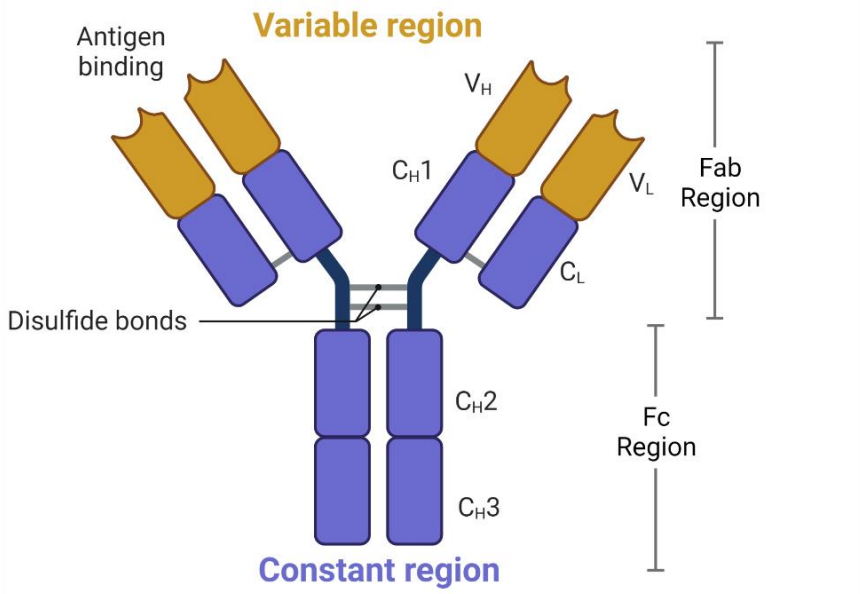

Figure 1.1 – Basic structure of a monoclonal antibody molecule.

To achieve an effective treatment, mAbs are required at high doses, being administrated in a chronic regime. Their production obliges extremely high levels of purity, at the highest yield, and with minimum costs associated to loss of product. Therefore, biopharmaceutical industry is making efforts to create more effective and productive manufacturing processes. Additionally, the rise of biosimilars, due to the expiration of mAb patents held by the biopharmaceutical companies, has led to the need of reducing manufacturing costs [2]. Continuous biomanufacturing has been recognized as the next step for further optimization of production processes, in particular, for the manufacturing of biopharmaceuticals [3]. An improvement in productivity, product quality and consistency can be achieved while drastically reducing production costs, facility and environmental footprint [4, 5].

A continuous process is composed of integrated (physically connected) continuous unit operations with zero or minimal hold volumes, where a continuous unit operation is capable of processing a continuous flow input as long as the operation runs [1, 2]. For the production of mAbs, it was demonstrated that an integrated

continuous biomanufacturing platform (Figure 1.2) allowed a 55% reduction of costs when compared to the conventional batch processing [6].

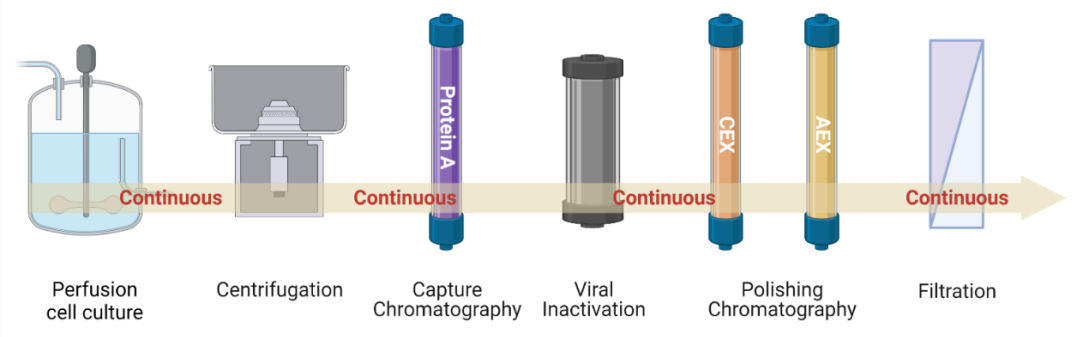

Figure 1.2 – Representation of a fully end-to-end integrated continuous process for the biomanufacturing of the biopharmaceutical mAb. Firstly, to produce the mAb, a perfusion cell culture is performed, followed by an initial clarification to remove the cells. After, a capture step, Protein A chromatography, is executed, tailed by a viral inactivation step and two polishing steps: cation (CEX) and anion exchange (AEX) chromatography. Finally, before sending the biopharmaceutical to the final formulation step, ultrafiltration/diafiltration is performed to concentrate the product. Based on Konstantinov et al. [6].

However, to implement an end-to-end continuous process, adequate real-time information for each unit operation has to be available in a time-frame necessary to facilitate control [6]. Therefore, the development and implementation of process analytical technologies (PAT) which can gather this information is crucial. PAT has been defined as "a system for designing, analysing, and controlling manufacturing through timely measurements (i.e., during processing) of critical quality and performance attributes of raw and in-process materials and processes, with the goal of ensuring final product quality" [10]. The goal is to establish and develop processes that consistently guarantee a defined level of quality in the final product. This can be achieved by real-time monitoring raw materials or in-process product attributes to control the process, the critical quality attributes (CQAs) [11, 12]. Accompanying the PAT approach, the biopharmaceutical industry also adopted the Quality by Design (QbD) framework. QbD was defined as "a systematic approach to development that begins with predefined objectives and emphasizes product and process understanding and process control, based on sound science and quality risk management" [13]. Hence, QbD is helped by the implementation of PAT by enhancing process comprehension and ensuring a consistent product quality.

PAT needs to be integrated with control strategies to ensure that the continuous process remains within the defined specifications. For example, when impurities arise within the manufacturing process, adjustments in operating conditions based on the

information collected can be performed [14]. While continuous processes stand to benefit greatly from PAT implementation, these tools have been largely unexplored [12]. For the upstream part, this was already achieved in the bioreactor operation, as demonstrated by the existing commercial perfusion processes. Classical sensors were incorporated which can provide information on process variables such as temperature, pH, dissolved gases, and foam levels [15]. For the downstream processing, PAT implementation is quite limited due to the short operation times of the purification steps (i.e. chromatography steps) [12] and the lack of sensor options (pH, conductivity, absorbance, and pressure sensors do not actually measure the biomolecule's CQAs). Hence, several improvements in sensor technology, configuration, and robustness are still required for further PAT implementation and, subsequently, continuous processing [15].

One of the major CQAs during mAb production is protein aggregation, a common but poorly understood phenomenon [16]. Typically, protein aggregation is described by mechanisms in which individual molecules assemble to form stable complexes of two or more proteins [17]. Depending on the nature of bonds, aggregates can be formed from: (1) weak nonspecific bonds (such as Van der Waals, hydrophobic and electrostatic interactions), remaining unchanged in primary structure, or (2) covalent bonds (disulfide bonds). Protein aggregation can be irreversible, especially at later stages, containing high levels of proteins with a non-native conformation [18]. In the final formulation of the mAb biopharmaceutical, the presence of high molecular weight (HMW) species is highly undesirable since it might lead to an adverse immune response or a decrease in product efficacy [19]. Nevertheless, several processing parameters and environmental factors are known to influence aggregation, with some examples found in **Table 1.2**.

Table 1.2 – Examples of processing parameters and environmental factors known to contribute to protein aggregation.

Environment factors	Process parameters
Low pH (protein A chromatography and viral inactivation) [20]	Interaction with metal/glass surfaces [21]
High temperature [22]	Freeze–thawing / Freeze-drying [19]
High protein concentration [23]	Shear stress (induced from pumps) [24]
Salt type and concentration (of the buffer) [25]	Agitation (to homogenize solutions) [19, 26]

Therefore, the formation of these HMW species is unavoidable and expected during a continuous downstream process. Controlling their formation (and even possibly quantifying) is then crucial to have immediate feedback and process control. The measurement of aggregate formation must be immediate, with a time frame ranging from seconds until minutes. Working in a microfluidic environment seems a viable option to fulfil this requirement. Miniaturized sensors, placed after each downstream unit operation, are a powerful solution to speed up the analytical measurement. Short reaction times, small sample size (in the µL or nL-scale), portability, low cost, versatility in design, and potential for parallel operation are just some advantages provided by a miniaturized biosensor [25, 26]. Hence, by miniaturizing the analytical technique, the measurement can be extremely expedited to the necessary time range, to merely a few minutes. A miniaturized chip will work as an in/on-line detector, minimizing the volumes of sample required and proving immediate results in order to conceive a real-time PAT tool to monitor aggregate formation.

2.2. CONTINUOUS DOWNSTREAM PROCESSING OF BIOPRODUCTS (CODOBIO)

An expert consortium of nine industry partners, eight universities, one research organisation and a regulatory institution has developed a research and training programme to address the most urgent topics in continuous downstream processing. The CODOBIO project has the mission of delivering a new generation of highly-skilled and innovative Early Stage Researchers (ESRs) able to face the future transition challenges to a continuous biomanufacturing. The main objective is to tackle the major challenges in continuous downstream processing, being divided into three Working Packages (WP): (1) process control and modelling; (2) miniaturization, scale-

up and scale-down of unit operations and (3) process design and development of integrated continuous processes. A total of 15 projects were designed and divided into WPs and later assigned to each ESR.

Falling into WP1, process control and modelling, a project regarding the design of a microfluidic biosensor prototype for a fast in-line measurement of HMW species was developed. The main deliverables of this work were to examine analytics on a smaller scale in combination with miniaturization of operation units and the implementation of this PAT tool in a continuous downstream process. Thus, the worked developed in this project was focused on creating and developing this miniaturized PAT tool for aggregate detection. More information on the other projects and on the CODOBIO consortium can be found online [29].

2.3. Thesis Outline

Thus, the development of this real-time miniaturized PAT tool for the detection of HMW species is described across this PhD thesis (**Figure 1.3**). Resorting to fluorescent dyes (FDs) to produce a real-time measurement, a microfluidic mixing channel was designed, applied and then ultimately validated in an integrated process for the purification of mAbs.

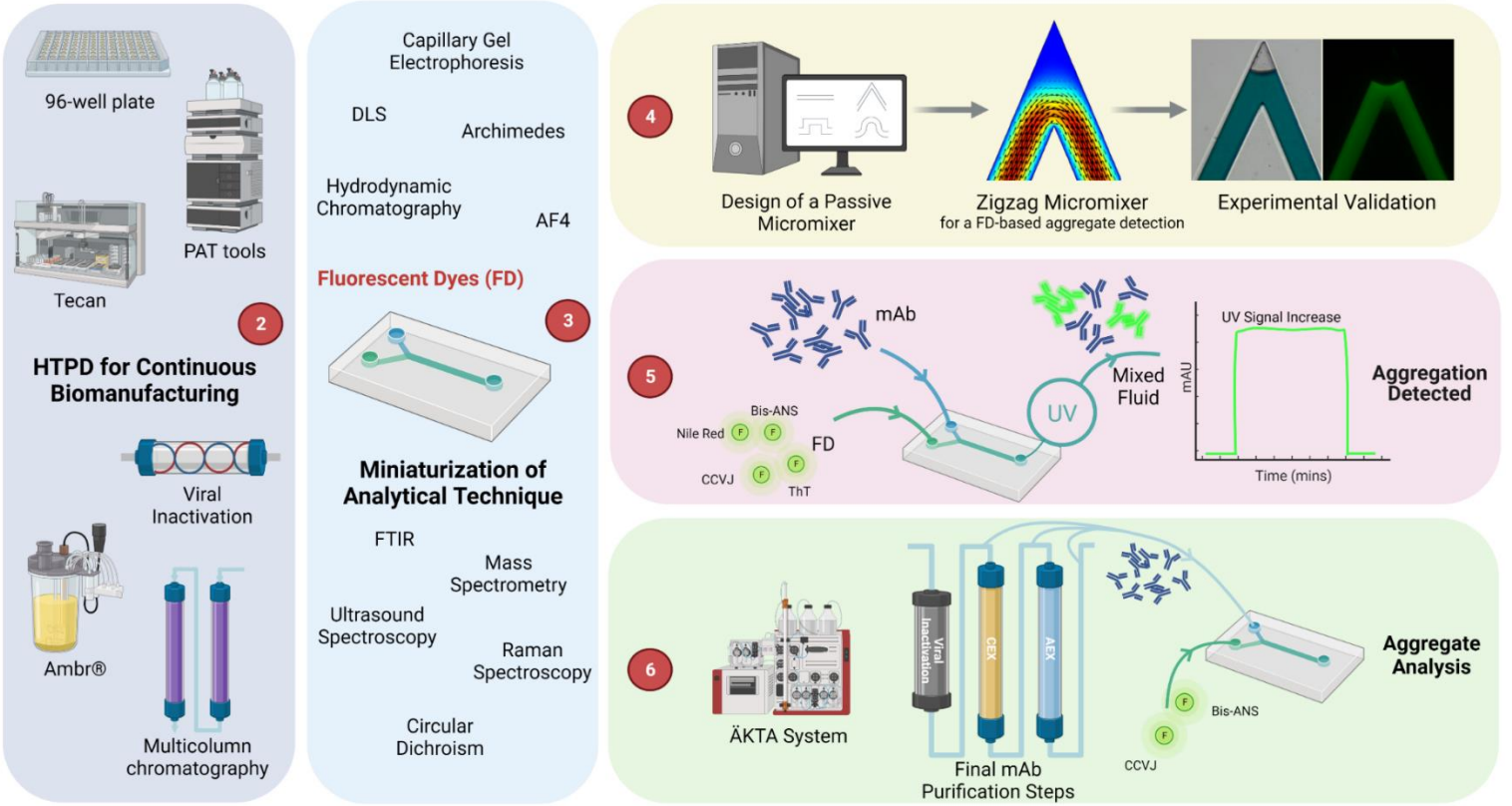

Figure 1.3 - Structural overview of this dissertation. Chapter numbers are highlighted in red.

Firstly, Chapter 1 briefly introduces the problem at hand, highlighting the scope and outline of this thesis.

In Chapter 2, an extensive literature review on the state-of-art of continuous biomanufacturing is performed. From data collected in a workshop on the 2019 Integrated Continuous Biomanufacturing (ICB) conference, academia and industry participants addressed the major gaps in high-throughput process development (HTPD), with the main needs and possible solutions to achieve an end-to-end ICB also discussed. The current HTPD state-of-the-art for several unit operations is discussed in detail, as well as the emerging technologies which can expedite the shift to ICB. One leading conclusion was the real necessity of creating analytical techniques which can provide real-time information of each step to gain knowledge and control over the overall process.

Thus, the proposed solution to create this real-time measurement for protein aggregation is to miniaturize the analytical technique. Due to the inherent short operation times, these miniaturized biosensors can be positioned in-line after each purification step to gather information on the biomanufacturing process. In Chapter 3, already well-established analytical methods, such as Dynamic Light Scattering and Raman spectroscopy, are extensively evaluated for the possibility of providing a real-time measurement of mAb aggregation. The miniaturization of each of these techniques is analysed, discussing the design and fabrication material of the microfluidic chip. A comparison between all analysed methods and the current techniques employed by the biopharmaceutical industry to detect protein aggregation is also performed. FDs was a promising solution encountered, being the chosen analytical technique to be miniaturized.

However, a major challenge when employing these FDs in a microfluidic chip is the mixing of both streams. Due to the presence of laminar flow, both fluids flow in parallel layers, with no disruption, and mixing is solely dominated by molecular diffusion, an inherently slow process. Passive mixing methods have been used to enhance the mixing efficiency by altering the structure or configuration of microfluidic channels. Therefore, in Chapter 4, a screening of possible geometries and, subsequently, its mixing efficiency was performed, resorting to a computational fluid dynamic (CFD) model. From all assessed configurations, a zigzag microchannel, with a total of 30 mixing units and a 45^0 angle, showed the highest mixing efficiency. This mixing efficiency was then experimentally demonstrated: first resorting to colour dyes, and then to a fluorescent tagged IgG molecule (FITC-IgG).

With the design of the micromixer defined, the next step was to validate the proposed PAT tool to actually detect aggregation, discussed in **Chapter 5**. First, a high-throughput (HT) screening of four well-known FDs was performed to assess the required concentration and emission wavelength. Then, resorting to a UV-Vis detector and each FD, the micromixer detected aggregation across differently induced mAb aggregation samples (such as temperature or low pH) by an increase of the UV signal. A final validation was then performed in an anion exchange (AEX) chromatographic operation for aggregate removal, implementing the microfluidic sensor in an ÄKTA™ unit.

Lastly, the implementation and validation of the developed PAT tool in an integrated continuous downstream process was achieved. In **Chapter 6**, the last steps of a mAb purification scheme, viral inactivation and two chromatographic polishing steps, were reproduced and integrated in an ÄKTA™ unit. A sample after each phase of the unit operation was directly sent to the microfluidic sensor, which was able to effectively detect aggregation under 10 minutes. Thus, a real-time measurement was achieved, fulfilling the research goal of this dissertation.

Finally, **Chapter 7** summarizes the work developed and the key findings of this dissertation, giving an outlook to future research.

2.4. REFERENCES

[1] Zahavi, D. and Weiner, L., Monoclonal Antibodies in Cancer Therapy. *Antibodies (Basel)* 2020, *9(3)*.

[2] Brummer, T., Ruck, T., Meuth, S.G., Zipp, F. and Bittner, S., Treatment approaches to patients with multiple sclerosis and coexisting autoimmune disorders. *Ther Adv Neurol Disord* 2021, *14*, 17562864211035542.

[3] Deb, P., Molla, M.M.A. and Saif-Ur-Rahman, K.M., An update to monoclonal antibody as therapeutic option against COVID-19. *Biosaf Health* 2021, *3(2)*, 87-91.

[4] Tsumoto, K., Isozaki, Y., Yagami, H. and Tomita, M., Future perspectives of therapeutic monoclonal antibodies. *Immunotherapy* 2019, *11(2)*, 119 - 27.

[5] Grilo, A.L. and Mantalaris, A., The Increasingly Human and Profitable Monoclonal Antibody Market. *Trends Biotechnol* 2019, *37(1)*, 9-16.

[6] Konstantinov, K.B. and Cooney, C.L., White Paper on Continuous Bioprocessing May 20–21 2014 Continuous Manufacturing Symposium. *Journal of Pharmaceutical Sciences* 2015, *104(3)*, 813-20.

[7] Rathore, A.S., Agarwal, H., Sharma, A.K., Pathak, M. and Muthukumar, S., Continuous processing for production of biopharmaceuticals. *Prep Biochem Biotechnol* 2015, *45(8)*, 836-49.

[8] Somasundaram, B., Pleitt, K., Shave, E., Baker, K. and Lua, L.H.L., Progression of continuous downstream processing of monoclonal antibodies: Current trends and challenges. *Biotechnol Bioeng* 2018, *115(12)*, 2893-907.

[9] Walther, J., Godawat, R., Hwang, C., Abe, Y., *et al.*, The business impact of an integrated continuous biomanufacturing platform for recombinant protein production. *J Biotechnol* 2015, *213*, 3-12.

[10] U.S. Department of Health and Human Services, FDA, CDER, CVM and ORA. PAT- A Framework for Innovative Pharmaceutical Development Manufacturing and Quality Assurance. 2004.

[11] Glassey, J., Gernaey, K.V., Clemens, C., Schulz, T.W., *et al.*, Process analytical technology (PAT) for biopharmaceuticals. *Biotechnol J* 2011, *6(4)*, 369-77.

[12] Read, E.K., Park, J.T., Shah, R.B., Riley, B.S., *et al.*, Process analytical technology (PAT) for biopharmaceutical products: Part I. concepts and applications. *Biotechnol Bioeng* 2010, *105(2)*, 276-84.

[13] Wasalathanthri, D.P., Rehmann, M.S., Song, Y., Gu, Y., *et al.*, Technology outlook for real-time quality attribute and process parameter monitoring in biopharmaceutical development—A review. *Biotechnology and Bioengineering* 2020, *117(10)*, 3182-98.

[14] Zydney, A.L., Perspectives on integrated continuous bioprocessing—opportunities and challenges. *Current Opinion in Chemical Engineering* 2015, *10*, 8-13.

[15] Fisher, A.C., Kamga, M.H., Agarabi, C., Brorson, K., *et al.*, The Current Scientific and Regulatory Landscape in Advancing Integrated Continuous Biopharmaceutical Manufacturing. *Trends Biotechnol* 2019, *37(3)*, 253-67.

[16] Bansal, R., Gupta, S. and Rathore, A.S., Analytical Platform for Monitoring Aggregation of Monoclonal Antibody Therapeutics. *Pharm Res* 2019, *36(11)*, 152.

[17] Roberts, C.J., Therapeutic protein aggregation: mechanisms, design, and control. *Trends Biotechnol* 2014, *32(7)*, 372-80.

[18] Le Basle, Y., Chennell, P., Tokhadze, N., Astier, A. and Sautou, V., Physicochemical Stability of Monoclonal Antibodies: A Review. *J Pharm Sci* 2020, *109(1)*, 169-90.

[19] Telikepalli, S.N., Kumru, O.S., Kalonia, C., Esfandiary, R., *et al.*, Structural characterization of IgG1 mAb aggregates and particles generated under various stress conditions. *J Pharm Sci* 2014, *103(3)*, 796-809.

[20] Walchli, R., Ressurreicao, M., Vogg, S., Feidl, F., *et al.*, Understanding mAb aggregation during low pH viral inactivation and subsequent neutralization. *Biotechnol Bioeng* 2020, *117(3)*, 687-700.

[21] Hawe, A., Kasper, J.C., Friess, W. and Jiskoot, W., Structural properties of monoclonal antibody aggregates induced by freeze-thawing and thermal stress. *Eur J Pharm Sci* 2009, *38(2)*, 79-87.

[22] Hoehne, M., Samuel, F., Dong, A., Wurth, C., *et al.*, Adsorption of monoclonal antibodies to glass microparticles. *J Pharm Sci* 2011, *100(1)*, 123-32.

[23] Neergaard, M.S., Nielsen, A.D., Parshad, H. and Van De Weert, M., Stability of monoclonal antibodies at high-concentration: head-to-head comparison of the IgG1 and IgG4 subclass. *J Pharm Sci* 2014, *103(1)*, 115-27.

[24] Thomas, C.R. and Geer, D., Effects of shear on proteins in solution. *Biotechnol Lett* 2011, *33(3)*, 443-56.

[25] Fesinmeyer, R.M., Hogan, S., Saluja, A., Brych, S.R., *et al.*, Effect of ions on agitation- and temperature-induced aggregation reactions of antibodies. *Pharm Res* 2009, *26(4)*, 903-13.

[26] Mahler, H.C., Muller, R., Friess, W., Delille, A. and Matheus, S., Induction and analysis of aggregates in a liquid IgG1-antibody formulation. *Eur J Pharm Biopharm* 2005, *59(3)*, 407-17.

[27] Kricka, L.J., Miniaturization of analytical systems. *Clinical Chemistry* 1998, *44*, 2008–14.

[28] Sia, S.K. and Whitesides, G.M., Microfluidic devices fabricated in poly(dimethylsiloxane) for biological studies. *Electrophoresis* 2003, *24(21)*, 3563-76.

[29] acib, (2019), Continuous Downstream Processing of Bioproducts (CODOBIO) (accessed in 15 February 2023), Available from https://www.codobio.eu/

Chapter 2

High Throughput Process Development for Integrated Continuous Biomanufacturing

Continuous manufacturing is an indicator of a maturing industry, as can be seen by the example of petrochemical industry. Patent expiry promotes a price competition between manufacturing companies, and more efficient and cheaper processes are needed to achieve lower production costs. Over the last decade, continuous biomanufacturing has had significant breakthroughs, with regulatory agencies encouraging industry to implement this processing mode. Process Development is resource and time consuming and, although it is increasingly becoming less expensive and faster through High-Throughput Process Development (HTPD) implementation, reliable HTPD technology for integrated and continuous biomanufacturing is still lacking and is considered to be an emerging field. Therefore, this paper aims to illustrate the major gaps in HTPD and to discuss the major needs and possible solutions to achieve an end-to-end Integrated Continuous Biomanufacturing (ICB), as discussed in the context of the 2019 ICB Conference. The current HTPD state-of-the-art for several unit operations is discussed, as well as the emerging technologies which will expedite a shift to a continuous biomanufacturing.

Published as: São Pedro, M. N., Silva, T. C., Patil, R., & Ottens, M. (2021), *White paper on high-throughput process development for integrated continuous biomanufacturing*, Biotechnology Bioengineering, 118, 3275–3286 (https://doi.org/10.1002/bit.27757)

2.1. INTRODUCTION

A possible solution to establish more efficient and flexible processes in the biopharmaceutical industry is to transition to continuous integrated manufacturing: an improvement in productivity, product quality and consistency can be achieved while drastically reducing the facility footprint and manufacturing costs [1-3]. Continuous bioprocessing utilizes a continuous flow of material through the various unit operations such that, at steady state, product of consistent quality is being produced as long as the operation runs [2].

Many manufacturing sectors, such as chemical, food and pharmaceutical have long adopted continuous manufacturing, but its implementation in biotechnology manufacturing, particularly of biotherapeutics, is still behind [2, 4]. However, Walther *et al.* [5] conducted an economic analysis into an integrated continuous biomanufacturing platform, and concluded that it would allow to reduce costs by 55% relative to conventional batch processing, demonstrating the promise of implementing a continuous bioprocess for the manufacturing of recombinant proteins. Therefore, there is a growing interest, from both academia and industrial researches, to develop continuous processing systems [6]. An example is the ongoing project Continuous Downstream Processing of Biologics - CODOBIO [7], a research program with the main goal of facing the future transition challenges to a continuous downstream process, implementing innovative integrated continuous manufacturing in the bio-industry.

The Integrated Continuous Biomanufacturing (ICB) conference aims to bring together academia and industry peers in order to shed some light on the recent advances and discoveries on bioprocesses, which could help to achieve the "holy grail" of a continuous end-to-end process and real time release. Within the fourth edition of the conference (ICB IV), held in Cape Cod (Massachusetts, USA) in 2019, a workshop entitled "High-Throughput Methodologies for ICB" brought together participants with different backgrounds (**Figure 2.1**). The workshop aimed to trigger the discussion on which are the perceived gaps in high-throughput (HT) technologies for process development, what are the current needs for ICB, the major problems and the correspondent expected solutions and what is currently being done in research to achieve this continuous biomanufacturing. With a total of 73 participants (from which the vast majority belonging to industry), the workshop aimed to collect relevant and up-to-date data on what is the view regarding the shift to continuous manufacturing in the biopharmaceutical realm, and what still needs to be done in order to put this

industry closer to this objective. The attendees were asked to split and mix with their peers from different background and affiliation. This aimed to achieve a more diverse discussion between the groups and promote a greater need for consensus when posting an answer. Overall, six out of the eight groups were mixed in terms of affiliation and a good mix of backgrounds was also possible to achieve (**Figure 2.1C**).

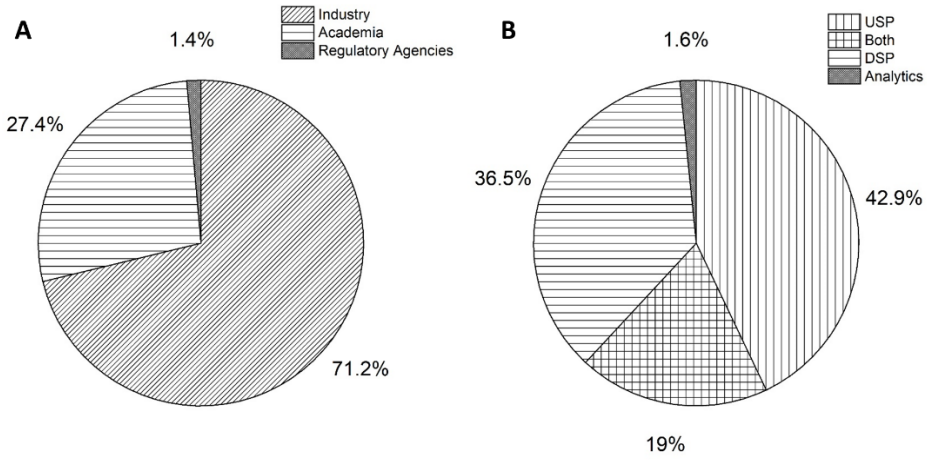

C

Groups	Industry	Academia	Regulatory Agencies	USP	DSP	Process Development	Analytics
1	6	4	-	5	2	2	1
2	6	3	1	2	4	3	-
3	4	5	-	*information not collected			
4	9	-	-	4	3	2	-
5	6	3	-	5	4	-	-
6	6	2	-	2	3	3	-
7	10	-	-	5	3	2	-
8	5	3	-	4	4	-	-

*Figure 2.1 - Workshop participants background: **A** – Area where the participants work in: Industry, Academia or Regulatory Agencies; **B** – Function/Department where the participants work in: USP, Upstream Processing; DSP, Downstream Processing; Process Development, which implicates both USP and DSP function; and Analytics. **C** – Descriptive constitution of each of the eight groups formed during the workshop, according to the area/function of each participant.*

Although current trends in the production of biopharmaceuticals are to gradually move from batch processes to integrated continuous processing strategies, in order to perform the process in a continuous mode, an integration of the different unit operations in one single production and purification train is the ultimate goal, adding to each unit operation the capacity of recycling streams and the ability to purge impurities as required by the process [2]. Furthermore, analytical techniques must provide real-time information of each biomanufacturing step in order to gain knowledge and control over the overall process. Therefore, this white paper will

discuss the major gaps in HTPD for the different unit operations, the integration problems present in a continuous manufacturing of biopharmaceuticals and the already available tools to overcome these challenges. By covering what is the state of the art for several established technologies, the paper aims to shed some light on the emerging tools for process development to enable and accelerate the shift to a continuous process.

2.2. Outcome of the Workshop

After identifying the state of the art in HTPD, it was possible to pinpoint the gaps in HTPD for continuous biomanufacturing. In Figure 2.2, the unit operations/system components perceived by the participants as having a major gap for high-throughput process development are presented: cell culture was unanimously identified by every group, followed by the filtration unit operation and the current analytical tools for a continuous process. Some groups also pointed out potential gaps regarding cell media development, viral inactivation, chromatography and other unit operations, such as centrifugation and aqueous two-phase extraction.

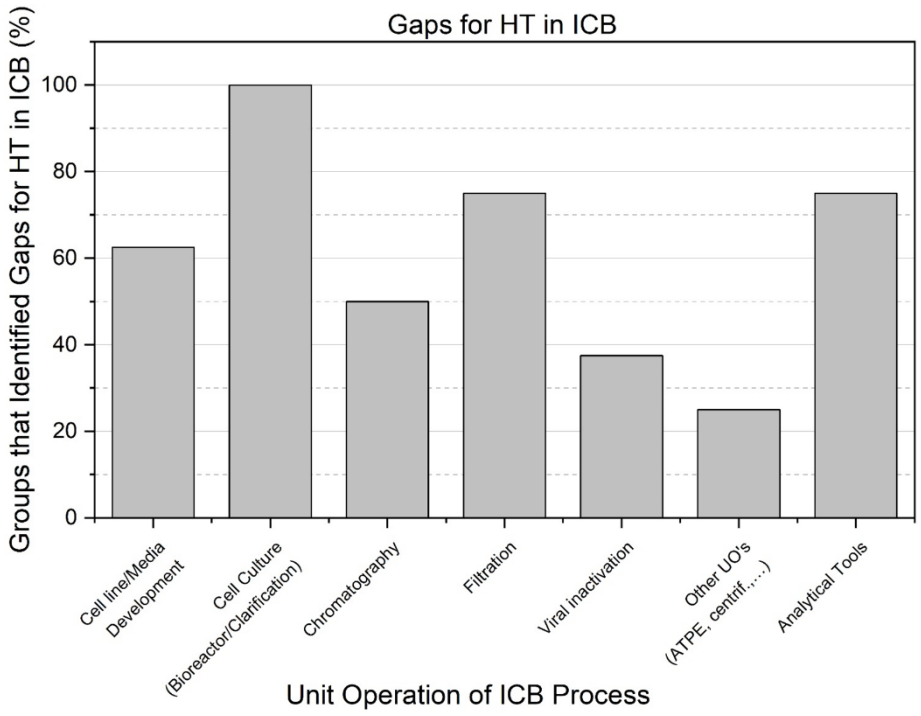

Figure 2.2 - Major gaps indicated for high-throughput development in ICB by the participants in the workshop.

Cell culture has had the industry's attention for several years, with higher titer producing strains being developed. There is already equipment available for the HTPD of cell culture, still such systems come at a high price, as will be discussed further, which make it to be perceived by all groups as being an area where a significant gap is present.

On the other hand, filtration has been an overlooked unit operation when it comes to HTPD. When many researchers focused efforts in the optimization of chromatography, most likely due to being one of the most expensive unit operations, filtration steps have stayed behind when it comes to HT alternatives. Although a batch filtration step can easily be implemented in a continuous process, the optimization of such step can become costly, as scale-down models are lacking, with a large investment to find optimal operating conditions needed. Therefore, there usually exists a compromise between oversizing the equipment or spending a considerable amount for the optimization of this unit operation. However, recent studies developed by Fernandez-Cerezo *et al.* [8] used a downscale method for a filtration unit resorting to using a combination of critical flow regime analysis, modelling and experimentation to predict the performance of a pilot-scale system, therefore showing a possible HT tool for future conditions studies in this unit operation.

Regarding the analytical tools needed for implementation in a continuous process, the major gaps indicated are related to the quantity of sample and different techniques necessary to obtain information on the overall process. Furthermore, there are still great limitations in the available HT analytical tools used in ICB, highlighted by the limited number of techniques which were able to be integrated in HT platforms. A possible explanation for this limitation is related to the lengthy analysis times of each technique, which can make it difficult to employ for process monitoring and control. The current trend to tackle these analytical shortcomings is the creation of at-line sensors, which can provide a real-time measurement and data on a continuous process, titled Process Analytical Technology (PAT), and will be further discussed in this paper.

2.3. State-of-art in Continuous Biomanufacturing

The workshop participants were tasked to come up with HT technologies that are currently in use in process development for continuous biomanufacturing. Although some unit operations got more attention than others, the main goal of this activity was to understand what are the mainly used equipment and tools involved in the

development of processes for the desired successful shift to a continuous operation. The main tools already in place are the automated systems for liquid-handling, where there is the possibility to use tailored equipment for a specific unit operation or an equipment with a broader capability that can have minor adaptions for different uses. In **Table 2.1**, the state of the art of HTPD tools for the development of different unit operations are summarized.

The use of liquid-handling stations for the determination of best operating conditions for cell media development and antibody purification has gained popularity over the past years [9]. The work developed by Schmidt *et al.* [10] shows an improvement of previous studies where a platform for the purification of an antibody in an automated two-step chromatography purification was developed. The HT system showed limitations in the flow rate that could be used in the RoboColumns, which affected the value for the Dynamic Binding Capacity (DBC) that could be obtained, but the results were comparable to the previously used ÄKTA™ systems. This platform process allows for the purification of hundreds of monoclonal antibodies per week, even at low feed concentrations.

In terms of available HTPD tools for viral inactivation and viral clearance, even though the participants indicated to be a considerable gap in development, recent studies have been published demonstrating the potential of developing a virus filter micro-scale HTPD model. Tang *et al.* [11] used, in combination with an automated liquid handling system, a 96-well filter plate to assess its suitability to be a novel micro-scale HTPD scale-down model. With these types of tools, HT virus filtration optimization is now an option, enabling rapid process development for the continuous biomanufacturing. Additionally, in order to make this important step continuous, several lab-scale models of viral inactivation system have been simulated, designed and built: for example, Gillespie *et al.* [12] tested multiple incubation chamber designs to allow narrow residence time distributions; whereas Parker *et al.* [13] used a comprehensive Computational Fluid Dynamics (CFD) model to create a laminar flow tubular reactor.

Table 2.1 - State of the art in the integrated continuous biomanufacturing field; (*) Mainly a description of what is being done in the scope of ICB and not completely related to HT; (**) Few groups answered this question: either they had some struggles to find an answer or didn't consider this technology to be a bottleneck.

Technology	Answers	References from literature
Cell Line / Media Development	Ambr® 15/250/P	[47, 59]
	Liquid Handling Systems (Tecan)	[60]
	Beacon®	[61]
	Spin Tubes	[62]
Cell culture (Bioreactor)	Ambr® 15/250/P	[47, 59]
	Small Scale Bioreactors	[63]
Cell culture (Clarification) (*)	Pendotech	[64, 65]
	Filtration Skids	[66]
	Acoustic Wave	[67, 68]
	ATF/TFF	[65, 66]
	Centrifugation	[69, 70]
Chromatography	Tecan	[71, 72]
	Predictor Plates	[73]
	RoboColumns	[10, 74]
	Mechanistic Understanding using HT	[30, 31, 75]
	ÄKTA™	[74]
	Multi Column Chromatography (MCC)	[76]
Filtration (*) (**)	SPTFF	[8, 77]
	UF Membranes	[78]
	96-Well Plate	[11]
Viral inactivation (*) (**)	Low pH/Mixing	[12, 13, 79, 80]
	Solvents/Detergents	[81, 82]
	Filters	[11, 83]
	Temperature	[12]
	Purification Steps	[40]
	Tubular Reactor	[12, 13, 80]
	Two Chambers (not continuous)	[40]
Analytical Tools (*) (**)	UV	[25, 84]
	pH	[12, 85]
	Conductivity	[85]
	Raman Spectroscopy	[23, 86, 87]
	NIR/MIR Spectroscopy	[88-91]
	MALS	[92, 93]
	Online LC	[19, 94, 95]
	Mass Spectrometry	[24, 96, 97]

2.4. Current Needs in the Integrated Continuous Bioprocessing

From the information gathered during the workshop, the major challenges pointed out by the participants in HTPD for the implementation of continuous bioprocessing are presented in Table 2.2. Furthermore, it was requested to the participants to propose possible solutions for each of the challenges discussed. Modelling and micro/nanofluidics were the main suggestions for the fields to further invest/prioritize to make an easier and smoother transition to continuous biomanufacturing. These proposed solutions and other current needs in ICB will be further discussed, with a particular focus given to PAT tools and unit operation connection.

*Table 2.2 - **A** - Major problems indicated by the participants of the workshop, with the proposed solutions/fields to invest/prioritize for ICB process development; **B** - Summary of the suggested tools by the participants (only six groups answered this question) as solutions for current gaps/problems with HTPD in ICB.*

A

Major Problem	Suggested Solution
Scale Down of Filtration Processes	Microfluidics
USP-DSP Integration	Microfluidics Modelling
Low-Throughput Cell Line and Media Development	Integrate robotics into existing systems
Cell Culture Development (bioreactor/cell retention device) is not mechanistic	Big Data Analysis / Smart HTPD (Artificial Intelligence / Mechanistic Modelling)
Process Development for Cell Culture	Microfluidics
Scability of Mini-Columns (done in batch mode)	Modelling
Integration of Chromatographic Steps	Modelling

B

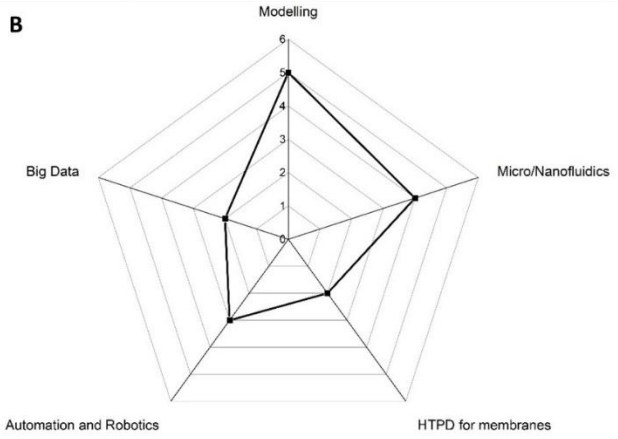

2.4.1. Process Analytical Technology (PAT)

PAT was defined as "a system for designing, analysing, and controlling manufacturing through timely measurements (i.e., during processing) of critical quality and performance attributes of raw and in-process materials and processes, with the goal of ensuring final product quality" [14]. The ultimate goal of implementing PAT in the biopharmaceutical industry is to design and develop well-understood processes that will reliably ensure a predefined quality in the final product by either monitoring the raw material or in-process product attributes in real-time to control the process, the critical quality attributes (CQAs) [15, 16]. The clear process control and understanding provided by the PAT framework supports as well the Quality by Design (QbD) approach adopted by the biopharmaceutical industry. QbD was defined as "a systematic approach to development that begins with predefined objectives and emphasizes product and process understanding and process control, based on sound science and quality risk management" [17]. Hence, PAT implementation will aid this systematic process development method, QbD, by providing a better understanding of the products and design processes that will ensure consistent product quality.

The crucial element for PAT applications in a continuous process is to be able to gather CQA information for the process and elicit a timely response to facilitate control. It is necessary for the analytical measurements to be available in the time-frame necessary to facilitate real-time decision making [15]. Additionally, to easily implement a PAT tool, the cost required for the instrumentation should not be high, at least until it does not drastically increase the biopharmaceutical production cost. Furthermore, the chosen analytical technique has to be precise, accurate and robust [18]. Although a continuous process has a lot of gain from PAT implementation, these types of tools have been fairly unexplored [15, 19] and for the advancement of continuous processes, important improvements in sensor technology, configuration, and robustness are still required [20].

Regarding the upstream processing, classical process sensors provide information on process variables such as temperature, pH, dissolved gases, and foam levels [20]. However, more robust techniques, involving spectrometric sensors, have been successfully implemented for process monitoring. For example, near infrared (NIR) spectroscopy has been most extensively studied to determine the concentration of individual components in cell culture broth, as demonstrated by Arnold *et al.* [21]. Furthermore, Raman spectroscopy can be used not only to analyse broth component profiles as well as to monitor structural/chemical changes in proteins, of particular

interest to on-line monitor aggregate formation [22] or quality attributes such as glycosylation [23]. Recently, liquid chromatography-mass spectrometry (LC-MS) based multiattribute methods (MAM) has emerged as an important PAT, allowing for a simultaneous monitoring of the product quality attributes such as glycan profile, charge variants, and purity of biotherapeutics [17]. By developing a platform with the collection of cell-free samples from bioreactors, followed by automated HT purification using an automated liquid handling system, Dong *et al.* [24] demonstrated that it was possible to produce a "near-real-time" measurement, laying out a solid foundation towards using this technique to monitor multiple CQAs during the entire biomanufacturing process.

For the downstream processing, PAT implementation is still fairly limited due to, in part, a lack of sensor options: pH, conductivity, absorbance and pressure sensors do not actually measure quality attributes of the biomolecule, such as protein aggregation. However, Kamga *et al.* [25] employed multiwave UV spectra to effectively determine the concentration of individual components in a protein mixture, accurately predicting aggregate concentration relative to the protein of interest. Additionally, for the chromatography steps, implementing PAT can be challenging because of the typical short process times of these unit operations [15]. Sharma *et al.* [19] demonstrated that, with on-line analytical liquid chromatography, continuous monitoring of the chromatography step for aggregate peaks can be achieved. An on-line HPLC system was used to investigate the real-time pooling of a process chromatography column and it was programmed to stop collecting when the aggregate peak starts, showing the feasibility of using PAT in order to facilitate real-time decisions for column pooling based on product quality attributes.

Therefore, in a continuous process, a PAT tool must provide decisive information for subsequent process steps on-line, making continuity of processing possible [18]. In the future, the development and implementation of these PAT will allow for the design of a manufacturing process that will deliver a consistent, well-defined quality product and improve process efficiency. Foreseeable challenges include implementing non-invasive process monitoring techniques and incorporating advanced sensors into automated process control strategies [20].

2.4.2. Data Collection/Modelling

The biological processes in the biotechnology industry present many challenges and are usually, if not always, less straightforward than in other industries. The complexity of the operations, especially fermentation, drove the industry to a trial-and-error

mode of optimization for years. However, in recent years with the application of QbD and PAT initiatives [26, 27], there has been a greater push for better understanding of the process. This has empowered scientists and engineers to have greater knowledge and details of each operation and not treat processes purely as black boxes.

The ability to translate a process, whether it is a relatively complex process, such as a fermentation, or a simpler process, such as a mixing tank, into a mathematical model has not only allowed a greater process understanding but also a reduction in time and experiments needed for optimization [28, 29]. Mechanistic models (MM) aim to accurately describe the physico-chemical phenomena of the system to be described, and several examples of such models have been published for bioprocesses [30-33]. Besides models that are purely mechanistic, hybrid approaches using MM and machine learning, like Artificial Neural Networks (ANNs), can help to ease up the computational load on the computer, e.g. by using data sets for the determination of certain parameters and then use these as input to the models. This accelerates the process development and provides faster results, as has been shown in literature, for estimation of process parameters [34] and optimization of full downstream processes [35]. Once such models are tuned and trained, the output of these computations will provide valuable insight on the processes. It is clear that models are of great importance for the leap into integrated continuous biomanufacturing, both in the process development stage and also once such processes are implemented in the production facilities. Modelling cannot, however, be completely detached from the experimental work and data. It needs data to estimate parameters, to train models and ultimately to validate them. Moreover, mathematical models are important for the implementation and realization of much needed control strategies, which are crucial for ensuring the proper functioning of such a complex production train.

The use of models is now widely accepted by industry and is certainly a critical feature of the future continuous processes. The ability to make decisions on the fly depending on unexpected changes to the process based on an accurately described model is something the industry requires. This also raises the need for a reliable and accurate data collection. Coupled to increasingly improved sensors, there is a great need to have very fast and accurate analytics in order to not only collect data on the process's behaviour in order for fast action to take place, but also to be able to monitor and control the CQAs and maintain the final product quality. Considering all the unit operations and processes taking place in a production facility, the amount of data generated at once can be overwhelming. While this generation of large amounts of

data is of paramount importance for the process understanding and monitoring, automation of the analyses of the data is crucial [36]. The integrated continuous biomanufacturing initiatives are longing for ways to accommodate and make good use of all the generated data, whether it is destined to process control, process overview or process development.

2.4.3. Upstream/Downstream Processing Connection (& Unit Operations)

For a truly integrated continuous biomanufacturing, the uninterrupted connection of continuous unit operations (upstream and downstream) is necessary, with no or minimal isolated intermediate or hold steps occurring between them.

Several examples of integrating a continuous upstream process with immediate capture have been established [37, 38], with the use of perfusion culture to continuously remove media and extracellular material from the bioreactor. A major challenge with integrating both processes is synchronizing the upstream perfusion flow rate with the downstream purification flow rate [20]. Synchronized control systems between upstream and downstream systems are also lacking. Therefore, a deviation in the upstream process will not be detected by downstream systems (feedforward control) or vice versa (feedback control). This type of system needs to be developed and implemented since several upstream parameters can impact subsequent downstream operations. Karst *et al.* [38] demonstrated the possibility of implementing feedback control with the installation of an at-line HPLC to provide titer data on bioreactor harvest to modulate the operating conditions of the capture step and regulate the continuous volumetric flow rate by using control loops.

While continuous upstream bioprocessing is reasonably well established, the integration of a full continuous downstream processing is still a developing field. For a continuous capture and polishing chromatography, two main systems can be applied: periodic counter-current chromatography (PCC) and simulated moving bed (SMB) chromatography. In a truly integrated continuous chromatography platform, process synchronization can be achieved by enforcing the residence time in a column to exceed the successive column steps. To ensure that poor quality eluent material from one column is not pooled with material to next functioning column, real-time monitoring and feedback control is necessary. The pooling between columns might also introduce the risk of cross-contamination, which this feedback control strategy might be able to detect and divert the effluent away from the second column [20]. At a small scale, the connection between different chromatography columns and an

ultrafiltration unit for the purification of a recombinant protein was developed by Gomis-Fons *et al.* [39]. An external controller, Orbit, was used to make the system automated and open and closed-loop control strategies were applied: UV was monitored in-line and used for automatic product pooling based on cut-off absorbance levels, for example. Furthermore, in an integrated continuous downstream process, a significant reduction in consumable needs, such as chromatography media and buffer consumption, will lead to a drastic reduction in operating and costs. Gjoka *et al.* [40] converted four purification unit operations into a continuous process, reducing the resin volume and buffer required by more than 95% and 44% compared to the corresponding batch process, respectively, and significantly decreasing consumables consumption.

Therefore, a fully integrated continuous process has potential to improve quality, cost, speed, and flexibility, with the most urgent challenge to be tackled being the creation of a global monitoring and control strategy for the entire biomanufacturing process. This would entail not only the monitoring and control of continuous measurements at all inlet and outlet streams (PAT framework), but also a realistic feedback and feedforward control strategy to ensure the final product quality. Thus far, to the author's knowledge, a complete end-to-end integration in manufacturing processes has still to be reported. However, Godawat *et al.* [41] was able to combined a perfusion bioreactor with two periodic PCC units for initial capture and successive ion-exchange steps, showing it is feasible to fully create and integrate an end-to-end continuous bioprocessing platform. More recently, Coolbaugh *et al.* [42] have demonstrated such end-to-end continuous processes are scalable by showing a successful proof-of-concept at pilot-scale.

2.4.4. Other Needs

The aforementioned needs represent three big realms where further development is needed. However, there are also some needs that are missing and others that despite not being totally missing still lack the practicality and/or affordability in order to be reliable solutions. The increased democratization of High-Throughput Screening (HTS) has led facilities around the world to more automated labs and miniaturized assays.

The use of automated liquid-handling systems has long been established as the standard for HTPD in downstream (mainly chromatography), as methods for the determination of adsorption isotherms and even full chromatographic runs have been described [43-46]. The use of such equipment allows for the automation of the assays

while keeping the used volumes low, yielding a faster and more cost-effective analysis. For upstream, there have been solutions for HTPD, however these usually come with a very high price tag such as the Ambr® systems [47], which can discourage scientists and companies from investing. Industry is therefore calling for affordable alternatives and sees in microfluidics a good opportunity to fill this need. When it comes to cell line development, the current state-of-the-art for companies without the Ambr® system is to take the better performing strains in batch mode and then test it in perfusion mode. There is therefore a need for deeper understanding on cell biology which will ultimately lead to the development of better cell lines at affordable prices, and microfluidics steps up to offer that [48].

Microfluidics has already shown to be a powerful scale-down model of equipment capable of mimicking several unit operations with the advantage of using less sample volume and achieving faster assays. These devices are still paving their way into the repertoire of process development but have already shown promising results for different unit operations such as crystallization [49], chromatography [50], cell culture [51], aqueous two-phase systems [52], biocatalysis [53] and as a promising scale-down model for HTS equipment, where parallel assays at a manifold volume and time reduction has been previously demonstrated [54]. However, filtration have lacked a scale-down model that would allow for HTPD of the specific unit operations. Membrane filtration is also not widely used in microfluidics, with both inertial and membrane filtration being reported as alternatives [55, 56]. The adaption of liquid-handling stations to the HTPD of such unit operation is still in very early stages. Filtration process development usually needs a large amount of materials and time-consuming work. The use of a HTS equipment for such system emphasizes on reducing reagent consumption in process development while avoiding the oversizing of equipment, consequence of a poorer process knowledge [11].

2.5. Conclusion

The change to continuous processing is a natural path for a maturing industry, and biopharmaceutical industries are following it, with technological advancements empowering this shift more and more. The advantages of this technology are great and well demonstrated, and it has been evidenced that it allows for process cost reductions at different scales, even when compared to the most established batch processing modes and different production scales [57].

Continuous processing allows, in general, for more efficient processes while reducing the footprint. Increasing the volumetric flow translates into a smaller increase in equipment and consumables cost for continuous processing than for what is observed for batch processes, due to a more efficient use of equipment. The counterpart of continuous bioprocessing is the increased need for fast analytics and control, that can provide real-time responses for fluctuations in operational conditions in order to guarantee product quality.

Although the technological breakthroughs have been immense over the past 20 years, we can understand that academia and industry are eager for better processing technologies. From the workshop outcome it is possible to conclude that although there are plenty options for process development and optimization, the room for improvement is still quite large, either to have new technologies or to find a way to cut down the prices of existing technologies in order to democratize process development. Among the tools perceived as the most promising to fulfil current gaps in ICB are modelling and micro/nanofluidics. This goes in accordance with current demands of regulatory agencies translated in PAT and QbD initiatives, where a higher process understanding is in order and a control of the final product quality is achieved, reducing the product variance in meeting CQA's.

Recent advances in both upstream and downstream processing research allowed to achieve competitive unit operations running in continuous mode, allowing these new processes to outperform the previously established ones. As the upstream and downstream processing have been developed separately throughout the years, the challenge now relies on integrating all these continuous unit operations into a continuous end-to-end manufacturing process [58]. The integration of software and hardware is important to achieve a fully continuous process, as well as process control, both feedforward and feedback, so that faster decisions are made according to what is happening in other unit operations. The further development of PAT and a synchronization of control systems will be the key enablers of the shift to an end-to-end continuous process in the biopharmaceutical industry [20].

Reducing the time to market usually hinders the implementation of a continuous process, as it is easier to "play safe" and assure that the "race is won". Biosimilars can, however, take advantage of the patent expiry and bet on such processing mode, aiming to achieve a more efficient and less expensive process allowing the biosimilars producing companies to compete with major players.

2.6. REFERENCES

[1] Somasundaram, B., Pleitt, K., Shave, E., Baker, K. and Lua, L.H.L., Progression of continuous downstream processing of monoclonal antibodies: Current trends and challenges. Biotechnol Bioeng 2018, 115(12), 2893-907.

[2] Rathore, A.S., Agarwal, H., Sharma, A.K., Pathak, M. and Muthukumar, S., Continuous processing for production of biopharmaceuticals. Prep Biochem Biotechnol 2015, 45(8), 836-49.

[3] Shukla, A.A., Wolfe, L.S., Mostafa, S.S. and Norman, C., Evolving trends in mAb production processes. Bioeng Transl Med 2017, 2(1), 58-69.

[4] Zydney, A.L., Continuous downstream processing for high value biological products: A Review. Biotechnol Bioeng 2016, 113(3), 465-75.

[5] Walther, J., Godawat, R., Hwang, C., Abe, Y., *et al.*, The business impact of an integrated continuous biomanufacturing platform for recombinant protein production. J Biotechnol 2015, 213, 3-12.

[6] Konstantinov, K.B. and Cooney, C.L., White paper on continuous bioprocessing. May 20-21, 2014 Continuous Manufacturing Symposium. J Pharm Sci 2015, 104(3), 813-20.

[7] CODOBIO, Continuous Downstream Processing of Biologics. https://wwwcodobioeu/2018 – 2022.

[8] Fernandez-Cerezo, L., Rayat, A., Chatel, A., Pollard, J.M., *et al.*, An ultra scale-down method to investigate monoclonal antibody processing during tangential flow filtration using ultrafiltration membranes. Biotechnol Bioeng 2019, 116(3), 581-90.

[9] Treier, K., Hansen, S., Richter, C., Diederich, P., *et al.*, High-throughput methods for miniaturization and automation of monoclonal antibody purification processes. Biotechnol Prog 2012, 28(3), 723-32.

[10] Schmidt, P.M., Abdo, M., Butcher, R.E., Yap, M.-Y., *et al.*, A robust robotic high-throughput antibody purification platform. Journal of Chromatography A 2016, 1455, 9-19.

[11] Tang, A., Ramos, I., Newell, K. and Stewart, K.D., A novel high-throughput process development screening tool for virus filtration. Journal of Membrane Science 2020, 611.

[12] Gillespie, C., Holstein, M., Mullin, L., Cotoni, K., *et al.*, Continuous In-Line Virus Inactivation for Next Generation Bioprocessing. Biotechnol J 2019, 14(2), e1700718.

[13] Parker, S.A., Amarikwa, L., Vehar, K., Orozco, R., *et al.*, Design of a novel continuous flow reactor for low pH viral inactivation. Biotechnol Bioeng 2018, 115(3), 606-16.

[14] U.S. Department of Health and Human Services, F.a.D.A.F., Center for Drug Evaluation and Research (CDER), Center for Veterinary Medicine (CVM), Office of Regulatory Affairs (ORA). PAT- A Framework for Innovative Pharmaceutical Development Manufacturing and Quality Assurance. 2004.

[15] Read, E.K., Park, J.T., Shah, R.B., Riley, B.S., *et al.*, Process analytical technology (PAT) for biopharmaceutical products: Part I. concepts and applications. Biotechnol Bioeng 2010, 105(2), 276-84.

[16] Glassey, J., Gernaey, K.V., Clemens, C., Schulz, T.W., *et al.*, Process analytical technology (PAT) for biopharmaceuticals. Biotechnol J 2011, 6(4), 369-77.

[17] Wasalathanthri, D.P., Rehmann, M.S., Song, Y., Gu, Y., *et al.*, Technology outlook for real-time quality attribute and process parameter monitoring in biopharmaceutical development-A review. Biotechnol Bioeng 2020, 117(10), 3182-98.

[18] Mandenius, C.-F. and Gustavsson, R., Mini-review: soft sensors as means for PAT in the manufacture of bio-therapeutics. Journal of Chemical Technology & Biotechnology 2015, 90(2), 215-27.

[19] Sharma, A., Chilin, D. and Rathore, A.S., Applying Process Analytical Technology to Biotech Unit Operations. BioPharm International 2006, 19(8).

[20] Fisher, A.C., Kamga, M.H., Agarabi, C., Brorson, K., *et al.*, The Current Scientific and Regulatory Landscape in Advancing Integrated Continuous Biopharmaceutical Manufacturing. Trends Biotechnol 2019, 37(3), 253-67.

[21] Arnold, S.A., Gaensakoo, R., Harvey, L.M. and McNeil, B., Use of at-line and in-situ near-infrared spectroscopy to monitor biomass in an industrial fed-batch Escherichia coli process. Biotechnol Bioeng 2002, 80(4), 405-13.

[22] Gryniewicz, C.M. and Kauffman, J.F., Multivariate calibration of covalent aggregate fraction to the raman spectrum of regular human insulin. J Pharm Sci 2008, 97(9), 3727-34.

[23] Li, M.Y., Ebel, B., Paris, C., Chauchard, F., *et al.*, Real-time monitoring of antibody glycosylation site occupancy by in situ Raman spectroscopy during bioreactor CHO cell cultures. Biotechnol Prog 2018, 34(2), 486-93.

[24] Dong, J., Migliore, N., Mehrman, S.J., Cunningham, J., *et al.*, High-Throughput, Automated Protein A Purification Platform with Multiattribute LC-MS Analysis for Advanced Cell Culture Process Monitoring. Anal Chem 2016, 88(17), 8673-9.

[25] Kamga, M.H., Woo Lee, H., Liu, J. and Yoon, S., Quantification of protein mixture in chromatographic separation using multi-wavelength UV spectra. Biotechnol Prog 2013, 29(3), 664-71.

[26] Rathore, A.S., Roadmap for implementation of quality by design (QbD) for biotechnology products. Trends in biotechnology 2009, 27(9), 546-53.

[27] U.S. Department of Health and Human Services, F.a.D.A.F., Center for Drug Evaluation and Research (CDER), Center for Veterinary Medicine (CVM), Office of Regulatory Affairs (ORA). Guidance for Industry: Process Validation: General Principles and Practices. 2011.

[28] Nfor, B.K., Ahamed, T., van Dedem, G.W., Verhaert, P.D., *et al.*, Model-based rational methodology for protein purification process synthesis. Chemical Engineering Science 2013, 89, 185-95.

[29] Chhatre, S., Farid, S.S., Coffman, J., Bird, P., *et al.*, How implementation of quality by design and advances in biochemical engineering are enabling efficient bioprocess development and manufacture. Journal of Chemical Technology & Biotechnology 2011, 86(9), 1125-9.

[30] Nfor, B.K., Ripić, J., van der Padt, A., Jacobs, M. and Ottens, M., Model-based high-throughput process development for chromatographic whey proteins separation. Biotechnology journal 2012, 7(10), 1221-32.

[31] Kumar, V., Leweke, S., von Lieres, E. and Rathore, A.S., Mechanistic modeling of ion-exchange process chromatography of charge variants of monoclonal antibody products. Journal of Chromatography A 2015, 1426, 140-53.

[32] Hebbi, V., Roy, S., Rathore, A.S. and Shukla, A., Modeling and prediction of excipient and pH drifts during ultrafiltration/diafiltration of monoclonal antibody biotherapeutic for high concentration formulations. Separation and Purification Technology 2020, 238, 116392.

[33] Yahia, B.B., Malphettes, L. and Heinzle, E., Macroscopic modeling of mammalian cell growth and metabolism. Applied microbiology and biotechnology 2015, 99(17), 7009-24.

[34] Wang, G., Briskot, T., Hahn, T., Baumann, P. and Hubbuch, J., Estimation of adsorption isotherm and mass transfer parameters in protein chromatography using artificial neural networks. Journal of Chromatography A 2017, 1487, 211-7.

[35] Pirrung, S.M., van der Wielen, L.A., van Beckhoven, R.F., van de Sandt, E.J., *et al.*, Optimization of biopharmaceutical downstream processes supported by mechanistic models and artificial neural networks. Biotechnology progress 2017, 33(3), 696-707.

[36] Oliveira, A.L., Biotechnology, big data and artificial intelligence. Biotechnology journal 2019, 14(8), 1800613.

[37] Kamga, M.H., Cattaneo, M. and Yoon, S., Integrated continuous biomanufacturing platform with ATF perfusion and one column chromatography operation for optimum resin utilization and productivity. Prep Biochem Biotechnol 2018, 48(5), 383-90.

[38] Karst, D.J., Steinebach, F., Soos, M. and Morbidelli, M., Process performance and product quality in an integrated continuous antibody production process. Biotechnol Bioeng 2017, 114(2), 298-307.

[39] Gomis-Fons, J., Lofgren, A., Andersson, N., Nilsson, B., *et al.*, Integration of a complete downstream process for the automated lab-scale production of a recombinant protein. J Biotechnol 2019, 301, 45-51.

[40] Gjoka, X., Gantier, R. and Schofield, M., Transfer of a three step mAb chromatography process from batch to continuous: Optimizing productivity to minimize consumable requirements. J Biotechnol 2017, 242, 11-8.

[41] Godawat, R., Konstantinov, K., Rohani, M. and Warikoo, V., End-to-end integrated fully continuous production of recombinant monoclonal antibodies. J Biotechnol 2015, 213, 13-9.

[42] Coolbaugh, M.J., Varner, C.T., Vetter, T.A., Davenport, E.K., *et al.*, Pilot-scale demonstration of an end-to-end integrated and continuous biomanufacturing process. Biotechnol Bioeng 2021.

[43] Wiendahl, M., Schulze Wierling, P., Nielsen, J., Fomsgaard Christensen, D., *et al.*, High Throughput Screening for the Design and Optimization of Chromatographic Processes – Miniaturization, Automation and Parallelization of Breakthrough and Elution Studies. Chemical Engineering & Technology 2008, 31(6), 893-903.

[44] Nfor, B.K., Noverraz, M., Chilamkurthi, S., Verhaert, P.D., *et al.*, High-throughput isotherm determination and thermodynamic modeling of protein adsorption on mixed mode adsorbents. J Chromatogr A 2010, 1217(44), 6829-50.

[45] Kiesewetter, A., Menstell, P., Peeck, L.H. and Stein, A., Development of pseudo-linear gradient elution for high-throughput resin selectivity screening in RoboColumn® Format. Biotechnology progress 2016, 32(6), 1503-19.

[46] Evans, S.T., Stewart, K.D., Afdahl, C., Patel, R. and Newell, K.J., Optimization of a micro-scale, high throughput process development tool and the demonstration of comparable process performance and product quality with biopharmaceutical manufacturing processes. Journal of Chromatography A 2017, 1506, 73-81.

[47] Xu, P., Clark, C., Ryder, T., Sparks, C., *et al.*, Characterization of TAP Ambr 250 disposable bioreactors, as a reliable scale-down model for biologics process development. Biotechnology progress 2017, 33(2), 478-89.

[48] Kwon, T., Prentice, H., De Oliveira, J., Madziva, N., *et al.*, Microfluidic cell retention device for perfusion of mammalian suspension culture. Scientific reports 2017, 7(1), 1-11.

[49] Li, L. and Ismagilov, R.F., Protein crystallization using microfluidic technologies based on valves, droplets, and SlipChip. 2010.

[50] Pinto, I.F., Santos, D., Soares, R., Aires-Barros, M., *et al.*, A regenerable microfluidic device with integrated valves and thin-film photodiodes for rapid optimization of chromatography conditions. Sensors and Actuators B: Chemical 2018, 255, 3636-46.

[51] Mehling, M. and Tay, S., Microfluidic cell culture. Current opinion in Biotechnology 2014, 25, 95-102.

[52] Silva, D., Azevedo, A., Fernandes, P., Chu, V., *et al.*, Determination of aqueous two phase system binodal curves using a microfluidic device. Journal of Chromatography A 2014, 1370, 115-20.

[53] Zhu, Y., Chen, Q., Shao, L., Jia, Y. and Zhang, X., Microfluidic immobilized enzyme reactors for continuous biocatalysis. Reaction Chemistry & Engineering 2020, 5(1), 9-32.

[54] Rho, H.S., Hanke, A.T., Ottens, M. and Gardeniers, H., A microfluidic device for the batch adsorption of a protein on adsorbent particles. Analyst 2017, 142(19), 3656-65.

[55] Bhagat, A.A.S., Kuntaegowdanahalli, S.S. and Papautsky, I., Inertial microfluidics for continuous particle filtration and extraction. Microfluidics and Nanofluidics 2008, 7(2), 217-26.

[56] Chen, X. and Shen, J., Review of membranes in microfluidics. Journal of Chemical Technology & Biotechnology 2017, 92(2), 271-82.

[57] Hummel, J., Pagkaliwangan, M., Gjoka, X., Davidovits, T., *et al.*, Modeling the downstream processing of monoclonal antibodies reveals cost advantages for continuous methods for a broad range of manufacturing scales. 2019, 14(2), 1700665.

[58] Gronemeyer, P., Thiess, H., Zobel-Roos, S., Ditz, R., *et al.*, Integration of Upstream and Downstream in Continuous Biomanufacturing. 2017, 481-510.

[59] Sandner, V., Pybus, L.P., McCreath, G. and Glassey, J., Scale-Down Model Development in ambr systems: An Industrial Perspective. Biotechnology journal 2019, 14(4), 1700766.

[60] Shi, S., Condon, R.G., Deng, L., Saunders, J., *et al.*, A high-throughput automated platform for the development of manufacturing cell lines for protein therapeutics. JoVE (Journal of Visualized Experiments) 2011, (55), e3010.

[61] Le, K., Tan, C., Le, H., Tat, J., *et al.*, Assuring Clonality on the Beacon Digital Cell Line Development Platform. Biotechnology Journal 2020, 15(1), 1900247.

[62] Strnad, J., Brinc, M., Spudić, V., Jelnikar, N., *et al.*, Optimization of cultivation conditions in spin tubes for Chinese hamster ovary cells producing erythropoietin and the comparison of glycosylation patterns in different cultivation vessels. Biotechnology progress 2010, 26(3), 653-63.

[63] Schwarz, H., Zhang, Y., Zhan, C., Malm, M., *et al.*, Small-scale bioreactor supports high density HEK293 cell perfusion culture for the production of recombinant Erythropoietin. Journal of Biotechnology 2020, 309, 44-52.

[64] Fedorenko, D., Dutta, A.K., Tan, J., Walko, J., *et al.*, Improved protein A resin for antibody capture in a continuous countercurrent tangential chromatography system. Biotechnol Bioeng 2020, 117(3), 646-53.

[65] Pinto, N.D.S., Napoli, W.N. and Brower, M., Impact of micro and macroporous TFF membranes on product sieving and chromatography loading for perfusion cell culture. Biotechnol Bioeng 2020, 117(1), 117-24.

[66] Arunkumar, A., Singh, N., Peck, M., Borys, M.C. and Li, Z.J., Investigation of single-pass tangential flow filtration (SPTFF) as an inline concentration step for cell culture harvest. Journal of Membrane Science 2017, 524, 20-32.

[67] Baptista, R.P., Fluri, D.A. and Zandstra, P.W., High density continuous production of murine pluripotent cells in an acoustic perfused bioreactor at different oxygen concentrations. Biotechnol Bioeng 2013, 110(2), 648-55.

[68] Granicher, G., Coronel, J., Trampler, F., Jordan, I., *et al.*, Performance of an acoustic settler versus a hollow fiber-based ATF technology for influenza virus production in perfusion. Appl Microbiol Biotechnol 2020, 104(11), 4877-88.

[69] Tait, A.S., Aucamp, J.P., Bugeon, A. and Hoare, M., Ultra scale-down prediction using microwell technology of the industrial scale clarification characteristics by centrifugation of mammalian cell broths. Biotechnol Bioeng 2009, 104(2), 321-31.

[70] Hogwood, C.E., Tait, A.S., Koloteva-Levine, N., Bracewell, D.G. and Smales, C.M., The dynamics of the CHO host cell protein profile during clarification and protein A capture in a platform antibody purification process. Biotechnol Bioeng 2013, 110(1), 240-51.

[71] McDonald, P., Tran, B., Williams, C.R., Wong, M., *et al.*, The rapid identification of elution conditions for therapeutic antibodies from cation-exchange chromatography resins using high-throughput screening. Journal of Chromatography A 2016, 1433, 66-74.

[72] Sisodiya, V.N., Lequieu, J., Rodriguez, M., McDonald, P. and Lazzareschi, K.P., Studying host cell protein interactions with monoclonal antibodies using high throughput protein A chromatography. Biotechnology Journal 2012, 7(10), 1233-41.

[73] Bergander, T., Nilsson-Välimaa, K., Öberg, K. and Lacki, K.M., High-throughput process development: determination of dynamic binding capacity using microtiter filter plates filled with chromatography resin. Biotechnology progress 2008, 24(3), 632-9.

[74] Keller, W.R., Evans, S.T., Ferreira, G., Robbins, D. and Cramer, S.M., Use of MiniColumns for linear isotherm parameter estimation and prediction of benchtop column performance. Journal of chromatography A 2015, 1418, 94-102.

[75] Pirrung, S.M., Parruca da Cruz, D., Hanke, A.T., Berends, C., *et al.*, Chromatographic parameter determination for complex biological feedstocks. Biotechnology progress 2018, 34(4), 1006-18.

[76] Gjoka, X., Rogler, K., Martino, R.A., Gantier, R. and Schofield, M., A straightforward methodology for designing continuous monoclonal antibody capture multi-column chromatography processes. Journal of Chromatography A 2015, 1416, 38-46.

[77] Clutterbuck, A., Beckett, P., Lorenzi, R., Sengler, F., *et al.*, Single-Pass Tangential Flow Filtration (SPTFF) in Continuous Biomanufacturing. Continuous Biomanufacturing: Innovative Technologies and Methods 2017, 423-56.

[78] Baek, Y., Singh, N., Arunkumar, A., Borys, M., *et al.*, Ultrafiltration behavior of monoclonal antibodies and Fc-fusion proteins: Effects of physical properties. Biotechnology and bioengineering 2017, 114(9), 2057-65.

[79] David, L., Maiser, B., Lobedann, M., Schwan, P., *et al.*, Virus study for continuous low pH viral inactivation inside a coiled flow inverter. Biotechnol Bioeng 2019, 116(4), 857-69.

[80] Orozco, R., Godfrey, S., Coffman, J., Amarikwa, L., *et al.*, Design, construction, and optimization of a novel, modular, and scalable incubation chamber for continuous viral inactivation. Biotechnol Prog 2017, 33(4), 954-65.

[81] Lofgren, A.L., Fons, J.G., Andersson, N., Nilsson, B., *et al.*, An integrated continuous downstream process with real-time control: A case study with periodic countercurrent chromatography and continuous virus inactivation. 2020.

[82] Martins, D.L., Sencar, J., Hammerschmidt, N., Tille, B., *et al.*, Continuous Solvent/Detergent Virus Inactivation Using a Packed-Bed Reactor. Biotechnol J 2019, 14(8), e1800646.

[83] Lute, S., Kozaili, J., Johnson, S., Kobayashi, K. and Strauss, D., Development of small-scale models to understand the impact of continuous downstream bioprocessing on integrated virus filtration. Biotechnol Prog 2020, 36(3), e2962.

[84] Li, S.W., Song, H.P. and Leng, Y., Rapid determination of lovastatin in the fermentation broth of Aspergillus terreus using dual-wavelength UV spectrophotometry. Pharm Biol 2014, 52(1), 129-35.

[85] Zelger, M., Pan, S., Jungbauer, A. and Hahn, R., Real-time monitoring of protein precipitation in a tubular reactor for continuous bioprocessing. Process Biochemistry 2016, 51(10), 1610-21.

[86] Kornecki, M. and Strube, J., Process Analytical Technology for Advanced Process Control in Biologics Manufacturing with the Aid of Macroscopic Kinetic Modeling. Bioengineering (Basel) 2018, 5(1).

[87] Nagy, B., Farkas, A., Gyurkes, M., Komaromy-Hiller, S., *et al.*, In-line Raman spectroscopic monitoring and feedback control of a continuous twin-screw pharmaceutical powder blending and tableting process. Int J Pharm 2017, 530(1-2), 21-9.

[88] Thakur, G., Hebbi, V. and Rathore, A.S., An NIR-based PAT approach for real-time control of loading in Protein A chromatography in continuous manufacturing of monoclonal antibodies. Biotechnol Bioeng 2020, 117(3), 673-86.

[89] Thakur, G., Thori, S. and Rathore, A.S., Implementing PAT for single-pass tangential flow ultrafiltration for continuous manufacturing of monoclonal antibodies. Journal of Membrane Science 2020, 613.

[90] Capito, F., Skudas, R., Kolmar, H. and Stanislawski, B., Host cell protein quantification by Fourier transform mid infrared spectroscopy (FT-MIR). Biotechnol Bioeng 2013, 110(1), 252-9.

[91] Capito, F., Zimmer, A. and Skudas, R., Mid-infrared spectroscopy-based analysis of mammalian cell culture parameters. Biotechnol Prog 2015, 31(2), 578-84.

[92] Patel, B.A., Gospodarek, A., Larkin, M., Kenrick, S.A., *et al.*, Multi-angle light scattering as a process analytical technology measuring real-time molecular weight for downstream process control. MAbs 2018, 10(7), 945-50.

[93] Sauer, D.G., Melcher, M., Mosor, M., Walch, N., *et al.*, Real-time monitoring and model-based prediction of purity and quantity during a chromatographic capture of fibroblast growth factor 2. Biotechnol Bioeng 2019, 116(8), 1999-2009.

[94] Rathore, A.S., Wood, R., Sharma, A. and Dermawan, S., Case study and application of process analytical technology (PAT) towards bioprocessing: II. Use of ultra-performance liquid chromatography (UPLC) for making real-time pooling decisions for process chromatography. Biotechnol Bioeng 2008, 101(6), 1366-74.

[95] Rathore, A.S., Yu, M., Yeboah, S. and Sharma, A., Case study and application of process analytical technology (PAT) towards bioprocessing: use of on-line high-performance liquid chromatography (HPLC) for making real-time pooling decisions for process chromatography. Biotechnol Bioeng 2008, 100(2), 306-16.

[96] Steinhoff, R.F., Karst, D.J., Steinebach, F., Kopp, M.R., *et al.*, Microarray-based MALDI-TOF mass spectrometry enables monitoring of monoclonal antibody production in batch and perfusion cell cultures. Methods 2016, 104, 33-40.

[97] Liu, Y., Fernandez, J., Pu, Z., Zhang, H., *et al.*, Simultaneous Monitoring and Comparison of Multiple Product Quality Attributes for Cell Culture Processes at Different Scales Using a LC/MS/MS Based Multi-Attribute Method. J Pharm Sci 2020, 109(11), 3319-29.

Chapter 3

Process Analytical Technique Miniaturization for mAb Aggregate Detection in Continuous Downstream Processing

The transition to continuous biomanufacturing is considered the next step to reduce costs and improve process robustness in the biopharmaceutical industry, while also improving productivity and product quality. The platform production process for monoclonal antibodies (mAbs) is eligible for continuous processing to lower manufacturing costs due to patent expiration and subsequent growing competition. One of the critical quality attributes (CQAs) of interest during mAb purification is aggregate formation, with several processing parameters and environmental factors known to influence antibody aggregation. Therefore, a real-time measurement to monitor aggregate formation is crucial to have immediate feedback and process control and to achieve a continuous downstream processing. Miniaturized biosensors as in-line process analytical technology (PAT) tool could play a pivotal role to facilitate the transition to continuous manufacturing. In this review, miniaturization of already well-established methods to detect protein aggregation, such as Dynamic Light Scattering, Raman Spectroscopy and Circular Dichroism, will be extensively evaluated for the possibility of providing a real-time measurement on mAb aggregation. The method evaluation presented in this review shows which limitations of each analytical method still need to be addressed and provides application examples of each technique for mAb aggregate characterization. Additionally, challenges related miniaturization are also addressed, such as the design of the microfluidic chip and the microfabrication material. The evaluation provided in this review shows why the development of microfluidic biosensors is considered the key for real-time measurement of mAb aggregates and how it can contribute to the transition to a continuous processing.

Published as: São Pedro, M.N., Klijn, M.E., Eppink, M.H. and Ottens, M. (2022), *Process analytical technique (PAT) miniaturization for monoclonal antibody aggregate detection in continuous downstream processing*, J Chem Technol Biotechnol, 97, 2347-2364 (https://doi.org/10.1002/jctb.6920)

3.1. INTRODUCTION

Continuous manufacturing has been applied in many different industries, such as the chemical [1], food [2], and pharmaceutical [3, 4] industries. However, the implementation of continuous manufacturing in the biotechnological industry is still awaited, particularly in the field of biotherapeutics [5-7]. Continuous bioprocessing utilizes a continuous flow of material through the various unit operations such that, at a steady state, product of consistent quality is being produced as long as the operation runs. This processing mode allows for production at a smaller scale, resulting in lower capital cost, higher process automation, and lower labour cost [5]. In addition to lower manufacturing costs, benefits of switching from a batch to a continuous process include an improvement in productivity, product quality and consistency, while drastically reducing the environmental footprint [5, 8, 9]. Considering all the advantages of continuous biomanufacturing, regulatory agencies are eager to implement this type of processing. The development of the FDA strategic plans, Quality by Design (QbD) initiative, the guideline on Real Time Release Testing (RTRT), ICH Q13 Guideline and Process Analytical Technology (PAT) framework encourage this continuous biomanufacturing [10-13].

The biomanufacturing process of monoclonal antibodies (mAbs), an important therapeutic agent in the treatment of several diseases such as cancers and autoimmune disorders [14], has received major focus in the last years. Due to patent expiration and rise of biosimilars, the biopharmaceutical industry aims to lower mAb manufacturing cost [15, 16]. Thus, several biopharmaceutical companies are currently exploring the economy of continuous processes [7, 17]. For example, Walther *et al.* [18] conducted an economic analysis into an integrated continuous biomanufacturing platform with mAb production in the business portfolio, and concluded that it would allow to reduce costs by 55% relative to conventional batch processing [18]. Additionally, advances in upstream processing (e.g. improved expression levels) of these biopharmaceuticals created bottlenecks in the purification process of mAbs, which are limiting production efficiency [8]. A possible solution is implementing a continuous downstream processing, as long as the final mAb characteristics do not suffer any impact [19].

However, to perform the entire process in a continuous mode, all the unit operations need to be fully integrated and controlled [5]. Therefore, there is a critical need for development of real-time PAT tools that are capable of identifying changes in product critical quality attributes (CQAs), such as product aggregation and glycosylation

patterns. PAT needs to be integrated with appropriate global process control strategies to ensure that the continuous process remains within the defined specifications. This includes the management of process interruptions when impurities arise or, at least, adjustments in operating conditions based on the information collected [17].

An important CQA in the production scheme of mAbs is protein aggregation, a recurrent and poorly-understood phenomenon [20]. The formation of aggregates may lead to an increase in adverse immune responses or a decrease in efficacy of the biopharmaceutical.[21] In general, aggregation of proteins is often described by mechanisms where molecules assemble into stable complexes of two or more proteins, often held together by strong non-covalent contacts [22-24]. Several environmental factors and process parameters are known to induce protein aggregate formation. Environment factors, like low pH during chromatographic and viral inactivation steps [25-27], high temperature [28-30], or increase in protein concentration [31, 32], have been experimentally demonstrated to cause mAb aggregation. For example, mAbs are suspended in various buffer solutions that, depending on the type and concentration of the salt, and the charged groups of the protein, might have a destabilizing influence on the protein structure [33-35]. Process parameters, such as freeze–thawing and freeze-drying processes [21, 28], interaction with metal and glass surfaces [36, 37], shear stress induce from pumps [38, 39] or agitation [21, 40], have been also proven to be contributors to mAb aggregation. More specifically, the use of pumps or the agitation used for homogenising solutions (e.g. buffers added to adjust pH) creates a gas/liquid interface at which aggregation predominantly occurs [33, 38, 40]. For more information on how the environmental conditions and process parameters used for the purification of biomolecules can induce unwanted aggregation, several reviews are recommended [33, 41-43] and will not be further discussed here. Thus, the formation of aggregates is inevitable during continuous downstream processing but controlling (and even reducing) aggregate levels can be achieved by resorting to a real-time PAT tool. Protein aggregates are heterogeneous in size, morphology, and other physicochemical properties and can be categorized based on [41]:

- the type of bond, with noncovalent aggregates (such as weak electrostatic forces) [44] or covalent aggregates (caused by disulfide bridges) [45, 46];
- the reversibility: reversible [47, 48] versus irreversible [49] aggregates;
- size [40, 50];

- or the protein conformation: aggregates with predominantly native structure or predominantly non-native structure (such as partially unfolded multimeric species [50-52] and fibrillar aggregates [53-55]).

This review will solely focus on the size of these aggregates, which are classified into small soluble aggregates (oligomers such as dimers, trimers, tetramers, etc.), with the size ranging from 10 to 100 nm; insoluble aggregates/subvisible particles, from 100 nm to 100 µm; and, visible particles, for aggregates with a size larger than 100 µm [33, 41]. Insoluble aggregates are of great concern in the final formulation as it has been reported to cause immunogenicity [56, 57]. This is reflected in regulatory guidelines provided by the United States Pharmacopeia (USP) and the European Pharmacopeia (EP), which state that all injectable solutions need to be "practically/essentially free" of these type of particles. Regulatory agencies also defined the maximum numbers of subvisible particles allowed in the final formulation: the number of particulates over 10 µm is ≤6000 per container, while the number of particulates over 25 µm is ≤600 per container [58]. These criteria were focused on particles originating from external sources and not specifically defined for proteinaceous particles. Additionally, only relatively large particles are considered, dismissing the more abundant smaller particles (between 10 nm and 10 µm) [58].

Furthermore, a major challenge for the analysis of mAb aggregates is that no single analytical method exists to cover the entire size range or type of aggregates which may appear [59], as can be observed in **Figure 3.1**. Each analytical method not only has its specific advantages but also its inherent limitations, such as the possibility of creating unrepresentative measurements through sample preparation by inducing or destroying the aggregates [41]. Moreover, during formulation, mAbs are produced at relatively high concentrations, but only a small fraction of the total population of molecules will form aggregates. Thus, aggregate detection must be able to identify a small amount of aggregates against the background of folded mAb monomers [60]. Furthermore, quantification and characterization of each different type of aggregates is often not possible due to the heterogeneity of aggregates, both in quantity and quality, such as size, shape, and morphology [41, 61].

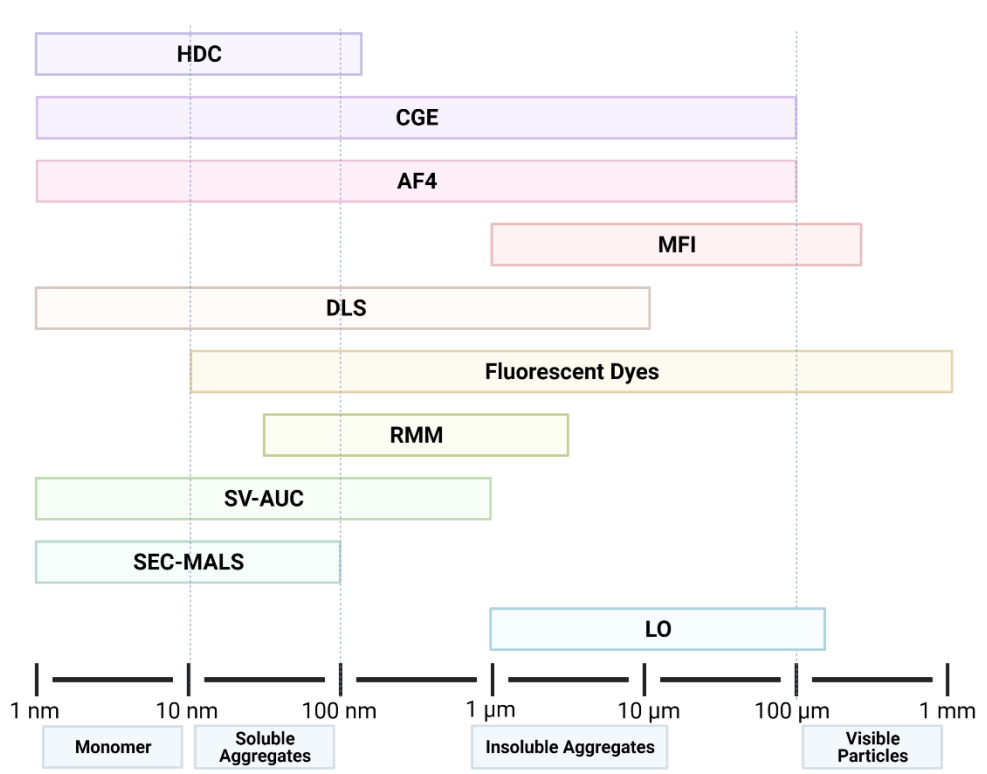

Figure 3.1 - Schematic representation of the approximate range of protein sizes, in terms of diameter, of various analytical methods discussed in this review: Hydrodynamic Chromatography (HDC), Capillary Gel Electrophoresis (CGE), Asymmetrical Flow Field-Flow Fractionation (AF4), Micro-Flow Imaging (MFI), Dynamic Light Scattering (DLS), Resonant Mass Measurement (RMM), Sedimentation Velocity Analytical Ultracentrifugation (SV-AUC), Size-Exclusion Chromatography combined with Multi-Angle Light Scattering (SEC-MALS) and Light Obscuration (LO).

Hence, there is a demand for a PAT tool capable to detect and quantify aggregate formation for the implementation of continuous processing. Ideally, this PAT tool has to produce a real-time measurement, within seconds to a few minutes, to facilitate decision making and control of the process [62]. Miniaturized sensors can be a powerful solution to speed up the analytical measurements of CQAs. Employing a microfluidic environment not only results in shorter reaction times, but also leads to small sample volumes (µL or nL-scale), portability, lower cost, design versatility, potential for parallel operation, and for integration with other miniaturized devices [63]. Moreover, a micro-miniature device allows for power needs and consumable reagents reduction, while offering the possibility of high-throughput testing [64].

In this review, the creation of a miniaturized PAT tool for detection, and possibly quantification, of protein aggregates in a continuous mAb purification process is explored. First, requirements for the implementation of a PAT tool in a continuous process are discussed, as well as the current analytical techniques employed by the biopharmaceutical industry for aggregation studies. Subsequently, design constraints necessary to develop miniaturized analytical techniques are examined and a thorough evaluation of established analytical techniques for mAb aggregation detection is provided. The last section of this review addresses additional challenges in the PAT development and implementation to facilitate the transition towards a continuous biomanufacturing.

3.2. Current Analytical Techniques

The current analytical methods employed to assess and quantify protein aggregate formation in the biopharmaceutical industry are size-exclusion chromatography combined with multi-angle light scattering (SEC-MALS), sedimentation velocity analytical ultracentrifugation (SV-AUC), and light obscuration (LO). Although SEC-MALS and SV-AUC are considered sensitive and allow aggregate quantification, both techniques are time-consuming, require highly specialized operators and costly equipment [41, 65]. More specifically, for SEC, the stationary phase can interact with the protein aggregates and reduce mass recovery from the column, thereby compromising the accuracy of aggregate quantification [66, 67]. The estimation of aggregates by means of SEC is compromised since proteins will be diluted in the mobile phase, which can dissociate the aggregates. Higher molecular weight (MW) species (such as subvisible particles) will not pass through the frit and therefore not enter the column [67, 68]. Due to the short length of the column, SEC has a limited separation ability, making the full separation of oligomeric forms difficult [69]. Additionally, molar mass calculations for large aggregates can be inaccurate as detection of large aggregates results in an intense light scattering signal despite a low concentration [68, 69]. SV-AUC is the golden standard in biopharmaceutical characterization due to the wide range of sample concentrations and the sensitivity to small fractions of aggregates [70]. However, the quantification of protein aggregates depends on the equipment and analysis variables controlled by the operator, leading to large and poorly understood variability between different measurements [67, 71, 72]. Furthermore, precision and limit of detection/quantification of SV-AUC is considered lower than for SEC [41, 73]. LO allows to count individual subvisible particles by size from approximately 1 to 150 µm, depending on the probe used [41].

Therefore, LO was the preferred method by the USP and EP regulatory agencies to define the maximum numbers of particles allowed in the final biopharmaceutical formulation [58]. Nevertheless, LO presents severe weaknesses related to limit of detection and false negative results if the particle's transparency is too high and therefore not detectable by the instrument. Moreover, LO cannot differentiate between protein aggregates, particles from extraneous source, and air bubbles [41, 58, 74]. Hence, the development of highly sensitive and robust analytical techniques which are able to detect the entire size range of aggregates is crucial for the development of a continuous mAb manufacturing platform.

3.3. Design Constraints for the Miniaturization of a PAT Tool for Continuous Biomanufacturing

PAT was defined as "a system for designing, analysing, and controlling manufacturing through timely measurements (i.e., during processing) of critical quality and performance attributes of raw and in-process materials and processes, with the goal of ensuring final product quality" [11]. The ultimate goal of implementing PAT in the biopharmaceutical industry is to design and develop well-understood processes that will reliably ensure a predefined quality in the final product by either real-time monitoring the raw material or in-process product attributes to control the process [62, 75, 76]. Biopharmaceutical quality is then built into the process, rather than being tested before the release of the product final form [62]. The efforts made to implement QbD approaches and the development of PAT tools has put a focus on analytical method development, frequently titled Analytical QbD (AQbD). With the integration of QbD principles, the analytical methods developed will be far more robust, sensitive, and cost-efficient [77]. A possible solution, as previously discussed, is to miniaturize the analytical method.

Several PAT applications can be defined: at-line, on-line, in-line, and off-line, as illustrated in **Figure 3.2** [62, 75, 78-80]. Although biomanufacturing processes, especially continuous processing, have a lot of gain from PAT implementation, these types of tools have been fairly unexplored for aggregation detection [62, 81, 82]. Though all steps in a continuous process would directly benefit from aggregate detection PAT tools, the crucial steps to obtain aggregate information would be after the Protein A chromatography / viral inactivation, between and after the polishing steps, and after the ultrafiltration step (indicated in **Figure 3.3**). During the Protein A chromatography and the viral inactivation steps, mAbs are exposed to low pH conditions, which might cause structural changes [33]. Polishing steps, such as cation-

and anion-exchange chromatography, are performed to eliminate impurities, including aggregates. Thus, a PAT tool placed between and after the two unit operations will inform if these aggregates are eliminated from the product stream. Ultrafiltration is used for the concentration and to obtain final formulation of the mAb. Here, mAbs will be exposed to physical stress due to pumping, which may induce aggregate formation [33].

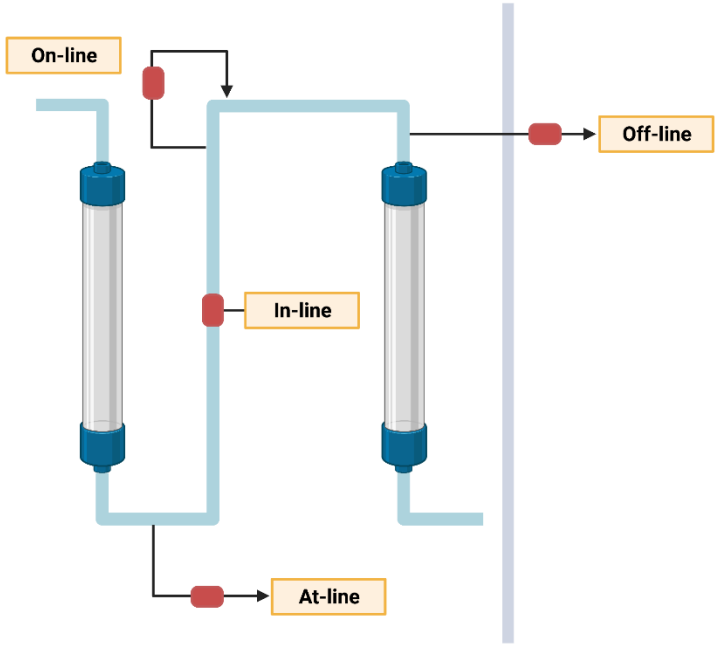

Figure 3.2 - Schematic representation of different PAT applications in a continuous chromatographic set-up: at-line, where the sample is removed and analysed close to the process stream, with the laboratory analysis at the biomanufacturing site; on-line, where the sample is removed from the process stream, analysed and returned to the original process stream after the measurement; in-line, where the sample is not removed, but analysed in situ (the process stream may be disturbed, for example, a probe may be inserted); and off-line, where the sample is removed and analysed away from the original process stream, at a separate site [62, 75, 78-80].

The crucial element for PAT application in a continuous downstream process is to gather real-time information for process control [75, 82]. However, especially for the chromatography steps, implementing PAT can be challenging because of the typical short process times (in the time frame of minutes) [62]. Rathore *et al.* [83] demonstrated that, with on-line analytical liquid chromatography (with the measurement performed in 10 minutes), continuous monitoring of the chromatography step for aggregate peaks can be achieved. An on-line HPLC system was programmed to investigate the real-time pooling of an eluting product during a

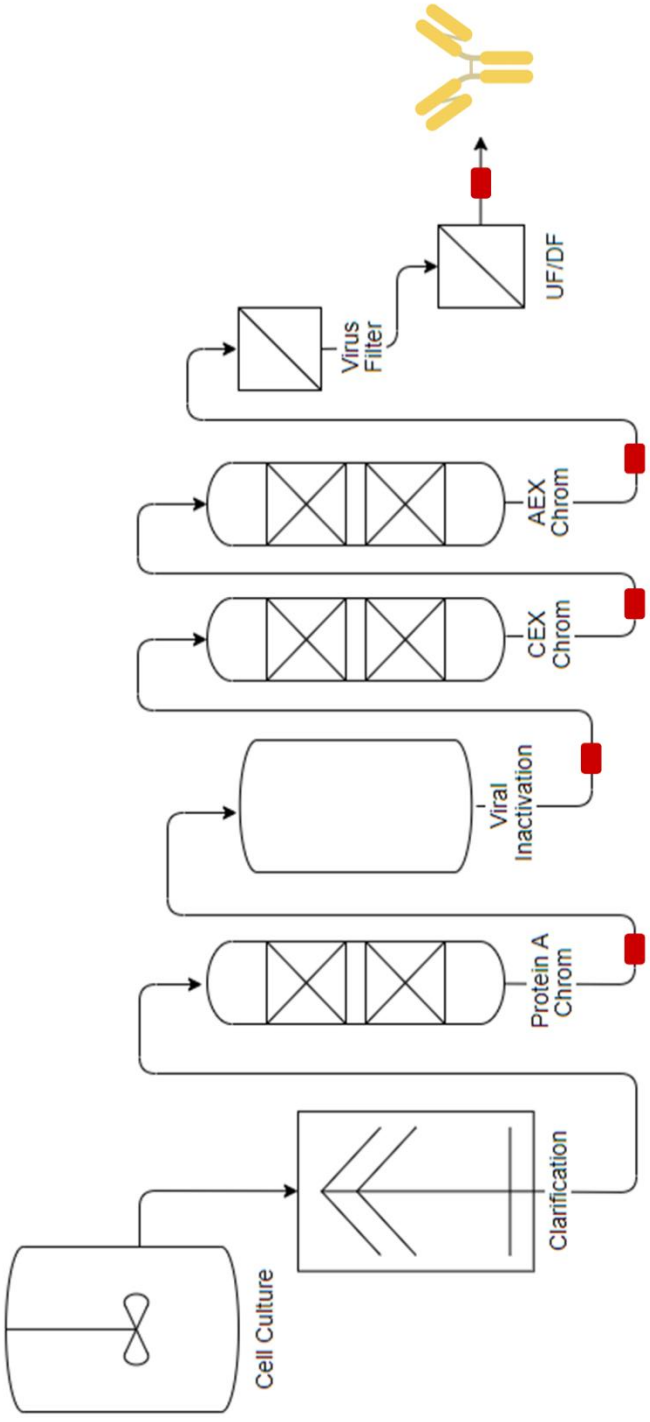

Figure 3.3 - A typical mAb purification platform process: the first step is cell culture to produce the biopharmaceutical, followed by an initial clarification to remove the cells. Then, the downstream process begins, with a capture step, Protein A chromatography, followed by a viral inactivation step and two polishing steps, cation- (CEX) and anion-exchange (AEX) chromatography. An additional virus retentive filtration step is subsequent and finally, an ultrafiltration/diafiltration (UF/DF) step to formulate and concentrate the product. Regarding a PAT sensor for the detection of aggregates, all the aforementioned steps would benefit in the implementation of this tool but the crucial steps where more information could be retrieved are marked in red: after the Protein A chromatography / viral inactivation step, between and after the two chromatographic polishing steps and the final UF/DF step.

process chromatography step and stopped collecting when the aggregate peak starts, showing the feasibility of using PAT to facilitate real-time decisions for column pooling based on CQAs [83]. Due to the inherent short reaction times provided by the miniaturization of the analytical technique, the much-needed real-time detection can be achieved, delivering immediate information to regulate manufacturing conditions.

To evaluate an analytical technique's potential as a real-time miniaturized PAT tool, several constraints must be met. This includes the minimization of measurement time frame within the range of seconds to a few minutes. To reach this time frame, the technique should require minimal to no sample preparation. Furthermore, the measurement should be preferably in-line, that is, the stream should be analysed in situ. On-line and at-line measurements can also be applied as long as the result obtained is within the necessary time frame. Another important requirement is that the analytical technique should cover the broadest size range of aggregates which can arise, ranging from the dimers to larger visible particles. If possible, the chosen method should be able to not only detect the formation of high MW species, but also to distinguish and quantify the different type of aggregates. The analytical technique should have high sensitivity to detect even low aggregate levels in the continuous process, and robustness to provide reproducible measurements [84]. Finally, other significant conditions to consider is the overall cost of the technique, and operation simplicity of the microfluidic chip, where additional training of operators is minimized.

Taking into account the design constraints, several analytical techniques were evaluated for a possible miniaturization for the detection of mAb aggregates. A few analytical techniques that are able to provide a real-time measurement for mAb aggregate detection were excluded, as the technique could not be miniaturized. For example, Micro-Flow Imaging (MFI) is a widely applied analytical technique to detect and characterize mAb aggregates [20, 85-88]. MFI is a flow microscopy technology, where bright field images are captured in successive frames as a continuous sample stream passes through a flow cell [89]. MFI is more sensitive with regard to the detection of visible particles compared to other techniques and offers a better differentiation between the various sub populations having different shapes via imaging filters [88-90]. For example, Kalonia *et al.* [85] developed an accurate method to calculate the mass of visible protein particles using particle number and size data obtained from MFI, which was evaluated with stressed IgG solutions. However, the equipment employed for this technique, a flow cell and a camera with high

magnification [89], cannot be miniaturized or the measurement itself cannot be performed within a microfluidic chip. Similarly, LO also requires a non-miniaturizable flow cell to perform the measurement [74]. Therefore, MFI and LO will not be further explored in this review. A summary of the considered analytical techniques and their characteristics can be found in **Table 3.1**. In the next section, a more in-depth explanation is provided for each evaluated technique with regard to the creation of a miniaturized PAT tool.

3.4. MINIATURIZABLE ANALYTICAL TECHNIQUES

This section provides a detailed examination of all the evaluated analytical techniques, where inherent characteristics and drawbacks for miniaturization are considered. Previous reported examples on how the respective analytical method is applied for the detection of aggregates are also presented. These techniques were divided into two categories according to the principle of aggregate detection: techniques which detect aggregates according to changes in the MW of the mAb monomer (colloidal stability) and the techniques which assess differences in the mAb monomer structure (conformational stability). Essentially, colloidal stability relates to protein's ability to stay in a monomeric state and is influenced by protein-protein interactions (depending on the particles distance), forming small soluble aggregates. On the other hand, conformational stability is related to 3D-structural changes of the protein's native form, where the analytical technique measures conformational alterations in the denatured state (or an intermediate state) of the protein [91, 92].

Table 3.1 - A summary of the analytical techniques discussed in this review, considering the size range, simplicity, in-line measurement, robustness, sensitivity, time, sample preparation, quantification of the aggregates, cost and the possible miniaturization of each technique for its implementation as a PAT tool for the detection of mAb aggregates in a continuous downstream process. ● – Low, ●● – Medium and ●●● – High.

Techniques	Size Range	Simplicity	In-line Measurement	Robustness	Sensitivity	Time	Sample Preparation	Quantification of the Aggregates	Cost	Possible Miniaturization
Study of the Aggregates on a Size Level										
Size Exclusion Chromatography with Multi-Angle Light Scattering (SEC-MALS)	1 - 100 nm	●●	Yes	●●●	Medium	Slow [41]	Concentrated sample	Yes (soluble aggregates)	High	No
Analytical Ultracentrifu-gation (AUC)	1 nm - 1 µm	●	No	●	High [41]	Slow [41]	None to Minimal (dilution for high protein concentrations)	Yes	High	No
Light Obscuration (LO)	1 µm - 150 µm	●●●	Yes	●●	Low [41]	Immediate (few seconds)	Necessity of sample dilution	Yes	Low	No
Fluorescent dyes	10 nm - 1000 µm	●●●	No	●●●	High [61]	Immediate (few seconds) [61]	Concentrated sample	Possible	Low	[99, 102-111]
Dynamic Light Scattering (DLS)	1 nm - 10 µm	●●	Yes	●	Poor (for very low aggregates levels)	Rapid (few minutes) [41]	None to Minimal (dilution for high protein concentrations)	Not suitable	Low	[122-124]
Micro-Flow Imaging (MFI)	1 - 400 µm	●●●	Yes	●	Poor [89]	Rapid	Necessity of sample dilution	Not suitable	Low	No
Asymmetrical Flow Field-Flow Fractioning (AF_4)	1 nm - 100 µm	●●	Yes	●●●	Medium	Slow [131]	None to Minimal (dilution for high protein concentrations)	Yes (soluble aggregates)	Medium/ High	[131-134]

Table 3.1 (continuation) - A summary of the analytical techniques discussed in this review, considering the size range, simplicity, in-line measurement, robustness, sensitivity, time, sample preparation, quantification of the aggregates, cost and the possible miniaturization of each technique for its implementation as a PAT tool for the detection of mAb aggregates in a continuous downstream process. ● – Low, ●● – Medium and ●●● – High.

Techniques	Size Range	Simplicity	In-line Measurement	Robustness	Sensitivity	Time	Sample Preparation	Quantification of the Aggregates	Cost	Possible Miniaturization
Capillary Electrophoresis (CGE)	1 nm - 100 µm	●●●	Yes	●	Low	Rapid	None to Minimal (dilution for high protein concentrations)	Yes (soluble aggregates)	Low	[140-143]
Hydrodynamic Chromatography (HDC)	0.7 - 110 nm	●●●	Yes	●	Low	Immediate	None to Minimal	Yes (soluble aggregates)	Low	[114]
Resonant Mass Measurement (RMM)	50 nm – 5 µm	●●	Yes	●●●	Medium [145]	Rapid (few minutes) [145]	None to Minimal	Yes	Medium	Already performed in a microchannel [144]
Study of the Aggregates on a Structural Level										
Fourier-transform Infrared Spectroscopy (FTIR)	X	●	Yes	●●●	Medium [41]	Medium [41]	Minimal	Not suitable	Low	[151, 152]
Native Mass Spectrometry		●	Yes	●●●	High [69]	Rapid	None	Yes	High	[160, 162, 188, 189]
Ultrasound		●●	Yes	●●	Medium	Rapid [117]	None	Possible	Low	[171]
Circular Dichroism (CD)		●●●	Yes	●	Poor [41]	Rapid [184]	Minimal	Not suitable	Low	[186, 187]
Raman Spectroscopy		●	Yes	●●●	Medium [172]	Rapid [41]	Concentrated sample	Not suitable	Low	[179-181]

3.4.1. Study of Aggregation: Colloidal Stability

3.4.1.1. Fluorescent Dyes

One common route for the formation of protein aggregates is through interactions of exposed hydrophobic areas. Fluorescence probes that are sensitive to the hydrophobicity of the surrounding environment, such as anilinonaphthalene-1-sulfonate (ANS), 4-4-bis-1-phenylamino-8-naphthalene sulfonate (Bis-ANS), Nile Red, and SYPRO Orange, can be used to study this phenomenon [61, 93, 94]. In the presence of hydrophobic unfolded protein structures, the dye's fluorescence will strongly increase compared to the intensity in the presence of the native monomeric mAb form [93], providing an immediate and straightforward result. However, ANS-based probes have been shown to bind to some proteins through electrostatic as well as hydrophobic interactions, which can interfere with protein folding and unfolding pathways. Additionally, Nile Red is highly sensitive to pH and to buffer type, which can impair signal detection [93]. A novel class of fluorescent molecular rotors, such as Proteostat, Thioflavin T (ThT), 9-(2,2-Dicyanovinyl)julolidine (DCVJ) and 9-(2-Carboxy-2-cyanovinyl)julolidine (CCVJ), recently emerged as possible alternatives to the classic fluorescence probes. These novel fluorescent molecular rotors are mainly sensitive to changes in the viscosity of the environment and less to polarity [95, 96]. The molecular rotors rotate freely in solution, but changes in the micro-environment will restrict the dye's movement, resulting in fluorescence emission [96]. For example, ThT will give information on aggregation due to the presence of β-sheet structures in a protein's structure since ThT binding is linked to the presence of this structural motif in fibrils and in amyloid formation, allowing to dissect its aggregation mechanism [97, 98]. A summary of the application of these fluorescent dyes, sensitive to the environment's hydrophobicity and viscosity, for the detection of mAb aggregates, can be found in **Table 3.2**. Additionally, these dyes can be used in combination with other analytical techniques to develop an online fluorescent dye detection method, such as high-pressure size exclusion chromatography (HP–SEC) and asymmetrical flow field-flow fractionation (AF_4), as demonstrated by Hawe *et al.* [30]. This online fluorescent dye detection for HP–SEC or AF_4 is a viable method to detect both aggregation and structural changes of both monomeric and aggregated mAbs [30, 95].

*Table 3.2 - A summary of the available fluorescent dyes, sensitive to hydrophobicity and viscosity of the environment, which are applied for the detection of mAb aggregates. The excitation and emission wavelength, the type of mAb aggregates and the concentration ranges used are also described. *The manufacturer of these dyes do not specify the molar concentration of the product. SYPRO Orange dye is commercially supplied in 100%(v/v) dimethyl sulfoxide (DMSO) at 5000x the final working concentration, being diluted to achieve a 2x/1x SYPRO Orange final concentration. Proteostat dye is commercially supplied in 100%(v/v) DMSO at 1000x the final working concentration, being diluted to achieve a 1x Proteostat final concentration.*

Fluorescent Dye	Excitation Wavelength (nm)	Emission Wavelength (nm)	Type of mAb aggregates	Concentration Range (μM)	Reference
Bis-ANS	385 – 400	470-530	Oligomers (Dimers, Trimers)	1-5	[30, 95, 190, 191]
ANS	350 - 380	505	Oligomers (Dimers, Trimers)	25 - 100	[88, 97, 191, 192]
Nile Red	540 - 580	580-660	Insoluble Aggregates and Visible Particles	100	[121, 190, 193]
SYPRO Orange	485 - 495	550 - 700	Oligomers, Insoluble Aggregates and Visible Particles	1x-5x*	[93, 96, 190, 194, 195]
Thioflavin T	415 - 450	480 - 600	Oligomers (high order) and Insoluble Aggregates	2-50	[96, 97, 190, 191, 193, 196]
Proteostat	448 - 530	560 - 700	Oligomers, Insoluble Aggregates and Visible Particles	1x* - 3	[96, 195]
DCVJ	450	470 - 530	Oligomers and Insoluble Aggregates	5 - 100	[95, 190, 194]
CCVJ	435	450 - 650	Oligomers and Insoluble Aggregates	5	[95]

However, employing fluorescent dyes requires mixing the dyes with the sample. Microfluidic systems operate in a laminar flow regime, which complicates mixing of the sample with the fluorescent dye [99]. Mixing efficiency can be achieved with microfluidic structures by inducing chaotic advection or increasing the contact area of fluidic layers. Mixing within microfluidics can be separated into two main categories, namely passive and active mixing [100, 101]. Passive mixing is achieved by altering the structure or configuration of microfluidic channels and is incorporated into the system during microfabrication. For example, using distinct zigzag angles [102], different zigzag [103] or serpentines configurations [104], slanted wells [105] or obstructions [106] in the middle of the channel are considered passive methods. The major advantage of applying passive mixing is relatively simple fabrication and operation, as moving parts are not necessary, meaning that it is not externally controlled by users [99]. On the other hand, active mixers are activated by the user and apply external forces for stirring or agitating the fluid flow [100]. This controllable mixing may be carried out using pressure gradients, electrical voltages across the fluid, or integrated mixing elements like stirring bars [99, 107]. Microstirrers [108], acoustic waves [109], flow pulsation [110] or thermal enhancement [111] fall into this category. Even though active micromixers can reach higher mixing efficiency compared to passive mixing, the integration of peripheral devices for external power source and the complex and expensive fabrication process are severe limitations for practical applications. Furthermore, active micromixers can produce high temperature gradients, which can potentially influence mAb stability. Therefore, active mixers are not an ideal solution for biological applications [101]. For more information related to mixing in a microfluidic chip, the following reviews are advised to be consulted [99-101, 112].

Thus, due to several commercially available fluorescent dyes and recent advances in microfluidic design and fabrication, the use of fluorescent dyes in a miniaturized chip can be a reliable solution for the development of a real-time measure of the level of aggregation in a continuous process. Nevertheless, fluorescent dyes do not allow for the quantification and differentiation of the type of mAb aggregates, which might limit its implementation as a broadly applicable PAT tool.

3.4.1.2. Hydrodynamic Chromatography

Hydrodynamic Chromatography (HDC) provides a fast and efficient analysis as it is based on the effect of the flow profile on an analyte carried through a tube of comparable size and does not involve mass transfer. In HDC, larger molecules or

particles are transported faster than smaller ones in a narrow channel (effective size ≤1 μm) with a laminar flow, as they cannot fully access slow-flow regions near the conduit walls [113]. A schematic representation of this process is shown in **Figure 3.4**.

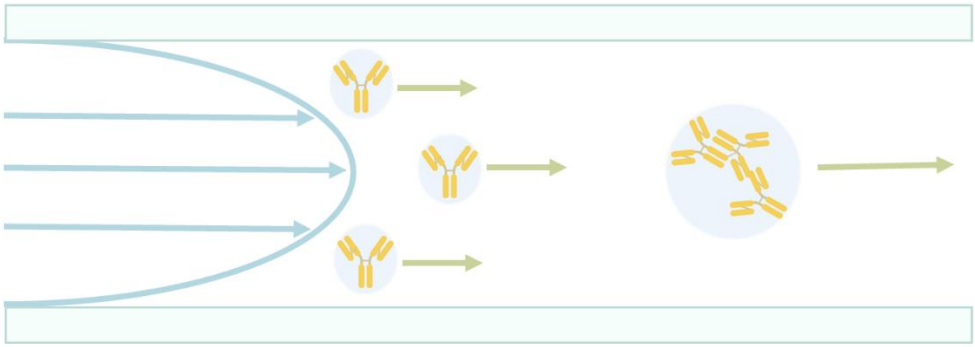

***Figure 3.4** - Physical principle of HDC separation: in a laminar flow regime, larger particles, such as mAb aggregates, are transported faster than smaller ones, mAb monomer, as these HMW species cannot fully access slow-flow regions near the conduit walls. As such, the aggregates remain near the centre of the flow profile where they preferentially experience faster streamlines.*

To miniaturize this technique, some constraints need to be taken into account upon the design of this chip: a long separation channel with a flat channel fluidic is required, with a large aspect ratio to increase the detection sensitivity (1 μm deep, 1000 μm wide and 8 cm long, for example), as demonstrated by Chmela *et al.* [114]. This method presents three main advantages, namely (1) high separation efficiency due to the microfluidic integration, (2) fast analysis, with the separation occurring in 3 minutes, and (3) provides a size range from 0.7 to 110 nm (soluble and insoluble aggregates).[114] From the same research group, Blom *et al.* [115] used a similar planar chip configuration to separate a biopolymer mixture, ranging from 26 to 155 nm of size, within 70 seconds [115].

Despite the desirable characteristics for PAT implementation, the detection of mAb aggregates by means of HDC is not yet demonstrated and validated. Moreover, this technique only allows for the separation of molecules according to size, thus the detection of the monomer or aggregates in the end of the channel must be performed resorting to other analytical techniques. However, HDC has been coupled to a multiplicity of detection methods, such as UV or a light scattering technique, being able to provide information on the particles' MW, shape and structure [113, 115].

3.4.1.3. Light Scattering Technique – Dynamic Light Scattering

Light scattering is employed to detect and characterize soluble aggregates, with a size range from 1 nm to 5 µm [116]. Several types of light scattering methods are available, and, as an example, this review will focus on the dynamic light scattering (DLS). DLS has been chosen based on the employment frequency in published aggregation studies and miniaturization experiments. DLS captures the Brownian motion of dispersed particles, which can be related to its hydrodynamic radius by the Stokes-Einstein equation [41]. DLS does not require sample preparation and allows for fast (few minutes) and high-throughput measurement [41, 117]. Despite presenting several advantages for implementation in a continuous process, DLS lacks sensitivity, especially for low aggregate levels [41, 117]. Additionally, in a continuous downstream process, the mAb solution will be highly concentrated. The high protein concentration can lead to the loss of light scattering intensity due to multiple scattering effects, making this technique only applicable as a semi-quantitative measurement [116]. However, the sensitivity of the technique can increase for a larger particle size due to the higher scattering intensity of larger particles, which is beneficial for detecting even the slightest quantity of large aggregate molecules [118].

Regarding the use of DLS for mAb aggregate detection, a multitude of studies have been published employing this analytical tool for characterization of these type of species [97, 118-121]. For example, Ahrer *et al.* [120] showed the ability of DLS to detect small traces of aggregates in IgG samples from different process steps without sample preparation [120]. Similarly, Arosio *et al.* [97] followed the aggregation kinetics in situ for IgG monomers and oligomers, characterizing and studying the stability of three different antibodies [97].

To perform DLS measurements in a microfluidic chip, Destremaut *et al.* [122] used small flow rates (and thus shear rates) in a tall microchannel fabricated in polydimethylsiloxane (PDMS) and glass. Dimensions for such a microchannel were 3 mm long, 500 mm wide and 700 mm high. However, to perform a DLS measurement, a specific external set-up still needs to be operated. This set-up is depicted in **Figure 3.5**. The set-up included a laser beam directed through the microfluidic device, with the alignment of the incident wave vector (k_i) of the laser orthogonal to the microfluidic chip and spatial filters collecting the scattered electric field. The measurement time of this miniaturized DLS device is approximately 300 milliseconds, depending on the employed flow rate [122]. Even though a fast and continuous measurement can be obtained with this configuration, the external set-up and the

alignment required complicate the implementation of DLS. Therefore, Chastek and co-workers integrated an online fiber optic DLS into the microfluidic chip, making the laser and detector fiber optic probes in direct contact with the sample. Thus, typical problems associated with laser alignment and light refraction are minimized as the multiple scattering is reduced [123, 124].

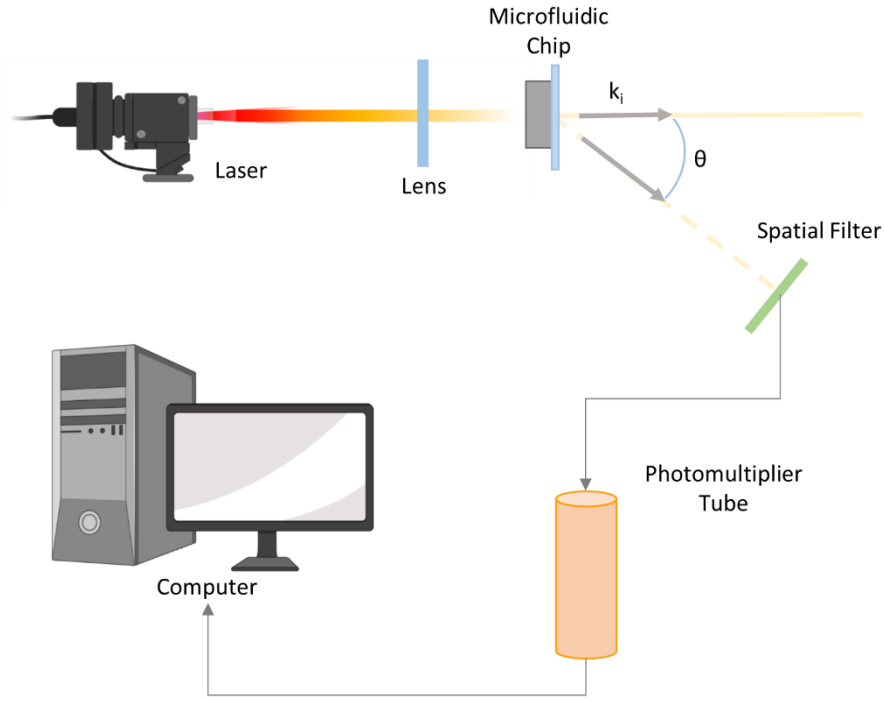

Figure 3.5 - A simplified external set-up necessary to perform DLS in a microfluidic chip. A laser beam is directed through the microfluidic chip, and focussed inside the channel through the lens. Alignment of the incident beam is performed to have the incident wave vector k_i orthogonal to the chip. The spatial filter collects the electric field scattered at the angle θ by the sample in the microchannel. The collected scattered light is then directed to the photomultiplier tube, and the information is then sent to a computer [122].

The two aforementioned examples demonstrate that DLS is a promising on-line PAT tool to study mAb aggregation in real-time in a continuous process. Nevertheless, DLS cannot be completely miniaturized as it requires external hardware, such as a laser source and scattered light detectors.

3.4.1.4. Asymmetrical Flow Field-Flow Fractioning

Field-flow fractioning (FFF) is a separation method able to set apart molecules ranging from the lowest nm-range over to a two-digit mm-range with high resolution. Separation is performed inside a narrow ribbon-like channel, with the typical

dimensions of approximately 50 cm in length, 2 cm in width, and between 50 and 500 mm in height. A carrier liquid is pumped through the channel, establishing a parabolic laminar flow profile that forces the sample towards the outlet. An external field is applied perpendicular to the direction of the carrier liquid flow, resulting in the sample components to accumulate at one of the channel walls, the so-called accumulation wall [125]. Variations of this technique have been developed over the years, varying the type of field applied during separation, such as sedimentation, thermal, and electrical changes [125]. The variant employing a hydrodynamic field to induce separation, the flow field-flow fractionation, is considered a well-established technique for the analysis of biomolecules [126]. A second stream of the carrier liquid is pumped in vertical direction to the axial flow stream. For asymmetrical flow field-flow fractioning (AF_4) there is only one permeable wall, which means the carrier liquid can leave the channel solely via the accumulation wall to generate a cross-flow [125].

In AF_4, retention is inversely proportional to the hydrodynamic diffusion coefficient of the analyte and, consequently, to its molecular weight. AF_4 is suitable for protein aggregate characterization, as it is selective and mechanical and shear stress are minimized by the absence of a stationary phase [121, 127-130]. For example, Hawe *et al.* [127] developed an AF_4 method for the analysis of protein aggregates in the size range of 10 nm up to 1000 nm and used this method to evaluate aggregation in heat-stressed IgG formulations. A better separation and recovery was achieved with AF_4 when compared to high-performance SEC, proving that AF_4 is a valuable method for quantification of submicron protein aggregates [127]. However, Bria *et al.* [128] investigated the impact of AF_4 on protein aggregate species by studying stability of two different IgG molecules as a function of different carrier liquids, shear stress (related to sample injection), and sample dilution during separation. The results showed that the employed conditions will influence aggregate formation and detection. Nevertheless, the dilution during AF_4 separation is significantly lower than in SEC, with dilution occurring mainly at the channel outlet and not during the separation. This make AF_4 a powerful alternative for SEC, as long as the AF_4 retention theory is used to understand the impacts of dilution on analytes [128].

Although AF_4 presents many advantages as a separation technique for aggregate detection, its adoption has been limited. This is mainly due to the large footprint of available separation cartridges, extended analysis times, and solvent consumption [131]. Miniaturization of this analytical method can address these issues, with the simplification of the AF_4 cartridge, reduction of reagent consumption and analysis

time. Several miniaturization approaches have already been reported [131-134]. Muller *et al.* [131] described the fabrication and characterization of miniaturized AF4 cartridges and evaluated the separation performance using gold and silver nanoparticle standards. The obtained separation performance was comparable to or even better than a normal macroscopic AF4 cartridge, where high sensitivity and improved signal to noise ratio was achieved. This was mainly due to a reduced sample dilution and, consequently, a minimal band dispersion. However, the implementation of a miniaturized AF4 method as PAT tool in a continuous process is still a major challenge. Even though a reliable separation and a real-time measurement can be achieved, this technique only allows for the separation of molecules. Thus, similar to HDC, aggregate detection relies on other analytical techniques, such as MALS. Additionally, this type of miniaturized cartridges still needs to be explored for the specific case of mAb aggregates, which are smaller particles than the nanoparticles and molecules experimentally tested [131, 132].

3.4.1.5. Capillary Gel Electrophoresis

Capillary gel electrophoresis (CGE) separates proteins according to their size in a fused-silica capillary with the advantages of automation, higher precision, and increased throughput when compared to other electrophoresis techniques, such as sodium dodecyl sulfate-polyacrylamide gel electrophoresis (SDS-PAGE). The band detection is based on UV or fluorescence, with the molecules being pre-labelled with a fluorescent dye, resulting in an easier and more accurate quantification [135, 136]. Coupling this technique with mass spectrometry (CGE-MS) can overcome limitations of optical detections and provide further structural information [136]. CGE can be performed under both non-reducing and reducing conditions to characterize the size heterogeneity of the intact mAb [135, 136]. Therefore, CGE has been widely used for high resolution separation and quantification of mAb aggregates and fragments to ensure the quality of mAb therapeutics [136-139]. For instance, Rouby *et al.* [139] employed CGE, among other techniques, to study the nature and structure of aggregates species present in an unstressed formulated mAb.

The miniaturization of CGE has been developed since the 90's, due to the need for a high-throughput analysis while maintaining resolution and efficiency [140-143]. More recently, especially for mAb analysis, this miniaturization has been recognized as a valuable alternative [137]. Smith *et al.* [143] used a commercially available chip to develop and validated a microfluidic CGE method to study biopharmaceuticals size variants and purity in reducing and non-reducing conditions. Evaluation parameters

such as specificity, accuracy, reproducibility, and limit of detection/quantification were assessed. The microfluidic CGE platform enabled a rapid testing for product development support, due to the inherent high throughput characteristics [143]. Therefore, as CGE is already a well-established and validated technique used in biopharmaceutical industry for the detection of mAb aggregates, microfluidic CGE can easily be implemented as a PAT tool in a continuous process, allowing for a fast and robust measurement of aggregation levels.

3.4.1.6. Resonant Mass Measurement (Archimedes)

Resonant mass measurement (RMM) allows size particle analysis based on the Archimedes principle: any object submerged in a fluid is acted upon by an upward buoyant force, for which the magnitude is equal to the weight of the fluid displaced by the object [74, 144]. The Archimedes system (Malvern Instruments, Malvern, UK) is the first and, until now, the only RMM instrument available [74] and has been largely employed in research and development of biopharmaceuticals. The sample solution to be studied is flushed through a microchannel inside a resonating cantilever (called suspended microchannel resonator (SMR)), which changes its frequency depending on the mass of the particles passing the channel [145]. With a size range from about 50 nm up to 5 µm, depending on the sensor [144, 145], RMM can analyse the subvisible range. Nevertheless, possible drawbacks of RMM are the tendency of protein aggregates to stick to and clog the sensor microchannels. Thus, intermediate cleaning procedures (with detergents or bleach) and regular cleanliness checks are necessary between measurements, which prevents a faster analysis and complicates the process procedure [74].

Published studies employing on RMM are still scarce, especially for the detection of mAb aggregates. However, Weinbuch *et al.* [145] used RMM and MFI as orthogonal methods to analyze protein particles and silicone oil droplets, covering the submicron and micron size range. RMM showed a highly accurate discrimination in the size range from 0.5 to 2 µm, as long as a sufficient number of particles (>50 particles) was counted [145]. Panchal *et al.* [144] compared RMM to DLS by measuring, among other solutions, low and high-concentrated aggregated IgG samples (5 and 100 mg.mL-1, respectively). The RMM limit of detection was determined for the IgG samples of ~150 nm. Additionally, the authors showed that RMM did not accurately measure the particle size distribution due to the small volume tested. However, by testing multiple samples and perform longer analysis times, this limitation can be surpassed [144].

Since RMM measurement is already performed in a microfluidic channel, further improvements for the its implementation should focus on increasing the limit of detection, especially for samples with high particle quantities, the life span of the sensor [74], and to add a temperature control to inhibit further aggregation [144]. Moreover, additional experimental studies for the detection and quantification of aggregation still need to be performed to gain a better understanding of the RMM potential and possible limitations.

3.4.2. Study of the Aggregates: Conformational Stability

3.4.2.1. Fourier-transform Infrared Spectroscopy

Fourier-transform infrared (FTIR) spectroscopy provides information on the secondary structure of a protein by characterizing the amide I, amide II, and amide III bands, and, consequently, any possible conformational changes that occur [146]. The evolution in IR instrumentation resulted in a straightforward data collection within seconds, enabling real-time monitoring [147, 148]. Several studies employed FTIR spectroscopy for the detection and quantification of mAb aggregates as well as protein stability tests [88, 147, 149, 150]. More specifically, this analytical technique was already employed as an at-line measurement in a downstream process by Capito *et al.* [147]. At laboratory scale, FTIR was used to quantify the aggregation levels in different unit operations. The authors demonstrated that FTIR cannot be fully applicable for all processing steps, as it is only suitable for processing steps that result in higher aggregate formation (filtration and low pH virus inactivation) [147].

A severe drawback for the miniaturization of this technique is that materials used for the fabrication of the microfluidic device, such as polymers (PDMS, more specifically), will strongly absorb the mid-IR radiation [151]. A possible solution, demonstrated by Birarda *et al.* [152], would be to fabricate the device in transparent calcium fluoride (CaF2) [152]. Another solution was presented by Srisa-Art *et al.* [151], where an alternative fabrication method was used to minimize the thickness of PDMS. The FTIR measurements would be performed in the optically thin PDMS microchannel layer and a supportive layer was incorporated in the device for handling and connections [151]. In addition to the issues related to the microfluidic chip materials, performing FTIR spectroscopy in a microfluidic chip requires an external hardware set-up built around the chip to collect the signal. Since IR spectroscopy is already applied as a PAT tool for real-time control of the protein A chromatography protein loading and the output concentration of an ultrafiltration step in a continuous process [153, 154], FTIR spectroscopy miniaturization might bring the needed optimization. To advance FTIR

spectroscopy for real-time PAT purposes, further research should focus on instrumentation and data collection to increase accuracy and limit of detection for aggregate quantification [146, 147].

3.4.2.2. Mass Spectrometry

Mass spectrometry (MS) is considered one of the most powerful analytical techniques due to its high sensitivity, accuracy, and high-throughput capabilities. MS provides structural information by measuring the mass-to-charge ratio (m/z) values of the charged molecules. Three elements are required to perform MS, namely (1) a ionization source, (2), a mass analyzer, and (3) a detector [155]. For the ionization source, two options are able to ionize sample molecules with minimal fragmentation. The first one is electrospray ionization (ESI), where the sample is infused through the electrospray emitter, usually in a needle-shaped structure. The second option is matrix-assisted laser desorption/ionization (MALDI), where the sample is co-crystallized with a matrix and pulses of UV laser are used to vaporize the matrix and liberate the molecules as gaseous ions [156].

In terms of employing MS for the detection of aggregates, the hyphenation of this technique with non-denaturing liquid chromatographic (LC) modes (ion exchange (IEX), SEC and hydrophobic interaction chromatography (HIC)) has attracted attention in the last years [157]. Ehkirch *et al.* [158] proposed a multidimensional analytical approach combining on-line SEC to ion mobility and mass spectrometry (IM-MS) for structural characterization of mAb size variants under native conditions [158]. Toth *et al.* [159] used Hydrogen Exchange Mass Spectrometry (HX-MS) to study the stability of an IgG4 mAb and comparing the data obtained with other orthogonal techniques, such as SEC and MFI. The authors demonstrated that HX-MS can be set up as a methodology to screen formulation excipients for their ability to physically stabilize mAbs [159].

The coupling of microfluidic chips to MS can greatly improve the implementation of this technique and expand the MS analysis for applications requiring fast measurement time and enhance sensitivity [156]. Various ionization sources and mass analyzers have been developed, with the most common approach being the miniaturization of ESI and its integration with various separation and sampling units. Redman *et al.* [160] developed a microfluidic chip incorporating CE with ESI to analyze a lysine-linked antibody drug conjugate for possible post translational modifications and drug load variants [160]. More recently, nanoelectrospray has become the most

widely exploited ionization method, a modification of ESI that enables reduction in the applicable flow rates and increase in detection sensitivity. Additionally, nanospray emitters are easily fabricated and allow a straightforward coupling to microfluidic separation devices due to the use of equal flow rates [161]. Yin *et al.* [162] developed a microfluidic chip composed by an integrated LC column, a sample enrichment column and a nanoelectrospray tip for analysis of proteins, demonstrating the potential of microfluidic MS to be incorporated with other separation techniques in a chip [162].

Thus, a MS microfluidic chip could be a viable option as a PAT tool for implementation in a continuous process to detect mAb aggregates. Several examples can be found where direct analysis in real-time MS (DART-MS) was used as a PAT tool for monitoring processes [163, 164]. Important to mention is that the detector component of MS cannot be miniaturized, so an external set-up to collect the ions still needs to be utilized. This external set-up can be an obstacle for its implementation within the biopharmaceutical industry due to the overall cost of the equipment. By comparing the instrumentation costs with the other discussed analytical techniques, MS might not be as affordable. Further improvements should focus on the ease of operating such equipment and on data treatment to extract relevant information for its implementation as a miniaturized PAT tool.

3.4.2.3. Ultrasound Spectroscopy

Ultrasound spectroscopy (US) presents the greatest potential for process control from all the presented analytical techniques for the detection of structural changes. US is considered a relatively rapid technique, with minimal sample preparation, and showed to detect changes as a result of aggregation and conformational instability of proteins. Moreover, US is a non-invasive technique that can be performed in-line, readily applicable as a PAT tool for monitoring and control [117, 165]. The physical principle of US lies in the compression and decompression of the sample medium caused when ultrasonic waves pass through a sample. This (de)compression leads to change in distance between particles and molecules in the sample, which in turn represents intermolecular attraction and repulsion [166, 167]. Thus, the analysis of aggregate formation by the sound scattering properties of the dispersed particles should be, in theory, possible [41]. However, changes detected by other analytical techniques can be assigned to definitive structural changes to a protein, whereas, for ultrasound, this is not currently possible. Further work is required to understand what aspects of a protein's structure can be monitored by US [117]. Furthermore, although

US has been used to investigate aggregation of various biomolecules, such as red blood cells [168, 169] and amyloidogenic proteins (insulin) [170], currently there are no studies reporting the detection of mAb aggregates in solution.

Although much effort still needs to be done to understand and validate this analytical method, a miniaturized chip for US has already been developed. Agrawal *et al.* [171] were the first to report on the development of a microfluidic device using continuous wave broadband US. This miniaturized device consisted of a set of ultrasound transducers integrated throughout a microfluidic channel and was validated by measuring various concentrations of glucose-water solutions [171]. Since US displays numerous advantages compared to other analytical techniques, the further development of US microfluidic chips can assist to a better understanding of the method itself and the results obtained.

3.4.2.4. Raman Spectroscopy

Raman Spectroscopy (RS) measures the inelastic scattering of light from molecules when excited by a monochromatic light source. While the majority of scattered photons are scattered without any change in energy, a small fraction will be scattered at a different energy from that of the incident light (Raman scattering). This difference in scattered frequencies, the Raman shift, is characteristic to a chemical bond, resulting in a unique spectrum for each molecule. Thus, RS is able to provide dynamic information about secondary structure, tertiary structure, and aggregation mechanisms [172]. RS is robust, non-destructive, and sample preparation is not required. Raman scattering can provide simultaneous real-time information about multiple components and molecules, making it ideal for on-line monitoring of a process [22, 173, 174]. Nonetheless, this technique presents significant drawbacks. For example, the Raman effect is an inherently weak process, with only 1 out of 106-108 photons being scattered this way [172, 175]. Additionally, fluorescence is also a well-known limitation of RS and the laser heat may induce changes in the sample [117, 172]. Therefore, significant technological advances have been achieved in recent years with regard of RS instrumentation, ranging from the efficiency and variety of sensors and low noise detectors [172].

RS is a well-established PAT tool in the upstream production of mAbs, where it is widely used as an in-line measurement to perform a real-time control of multiple attributes in a cell culture bioreactor, such as consumption of nutrients and the production of metabolic waste products [173, 174, 176]. However, regarding the downstream processing of mAbs, RS has remained fairly unexplored, especially for the

detection of mAb aggregates. Zhang *et al.* [177] presented a method combining RS with a multivariate analysis which could differentiate between aggregation levels in mAb samples [177], demonstrating the feasibility of using this technique for the detection of aggregates. Additionally, McAvan *et al.* [178] demonstrated, for the first time, the ability of RS to differentiate between degraded samples of IgG4 with differing fragmentation and mixed aggregate species [178].

In recent years, a great effort has been placed in the miniaturization of this technique to solve limitations regarding the intrinsically weak scattering signal [175]. For example, Ashok *et al.* [179] developed a novel Raman spectroscopic detection scheme: Waveguide Confined Raman Spectroscopy (WCRS). A major limitation of the implementation of WCRS at the micro-scale is that the weak Raman signal can be overwhelmed by a strong spectral background from the material in which the microfluidic chip is fabricated. Thus, to fabricate this microfluidic structure, it is crucial to minimize the interference of the background. This can be achieved by embedding fibers throughout the chip's geometry, confining the Raman excitation and collection region and ensuring maximum Raman signal collection [179]. Another approach to enhance the weak Raman signal is bringing the target molecules into the proximity of metallic nanostructures, denominated surface-enhanced Raman spectroscopy (SERS) [175]. Zhou *et al.* [180] created a SERS microfluidic platform that was fabricated in PDMS and containing gold nanoparticles. This microfluidic SERS platform was able to detect bovine serum albumin, down to a picomolar level. Choi *et al.* [181] fabricated a microfluidic device using gold nanoparticles-based SERS-active substrate to study the aggregation of an amyloid beta peptide. This microfluidic device was sensitive enough to detect the aggregates at concentrations much lower (from 10 fM up to 1 μM) than the limit of detection of existing instrumentation [181]. Therefore, the miniaturization RS can be the driving force to implement RS as a downstream PAT tool since it will allow for a more sensitive and accurate measurement of the intrinsically weak Raman signal.

3.4.2.5. Circular Dichroism

Circular Dichroism (CD) is a light absorption spectroscopy method based on the difference in absorbance of left and right-circularly polarized light. Optically active chiral molecules, such as proteins, will preferentially absorb one direction of the circularly polarized light. CD has been widely used to analyse the secondary structure of optically active biomacromolecules [182]. Even though CD does not provide information on the secondary structure of specific residues, the method has the

advantage that the measurement is sensitive (≤20 µg of protein sample [183]) and can be collected real-time and in situ for the monitoring of molecular aggregation [182].

In the past years, numerous publications have used CD as an orthogonal method to study and characterize mAb aggregation [88, 97, 121, 184, 185]. Furthermore, Joshi *et al.* [184] employed this analytical method as a high-throughput screening tool for examining mAb stability in various buffers, proving that CD is a reliable method for rapid monitoring of mAb conformational changes.

Regarding the miniaturization of CD, a major challenge was the incompatibility of conventional materials used in the fabrication of these devices, such as PDMS, with the far UV measurement needed in CD [186]. Kane *et al.* [187] reported a microfluidic chip employing synchrotron radiation circular dichroism (SRCD), where an intense light source is used for these measurements to study protein refolding kinetics of cytochrome C. The used mixing devices were made of fused silica with the beam light focused on a masked slit [187]. Bortolini *et al.* [186] try to overcome the polymer incompatibility problem by using conventional PDMS-based soft lithography to fabricate the CD microfluidic chip. The authors studied two architectures with measurement chambers of different height, to allow a SRCD measurement within the chip. Heterogeneous protein mixtures were used to validate the chips. By taking advantage of the laminar flow properties inherent to microfluidic devices, these complex mixtures were separated into well-resolved size-dependent fractions, using an H-filter configuration. This design allows for a more accurate and sensitive measurement per component of the mixture since only average spectroscopic features can be resolved [186]. Thus, with these promising breakthroughs, an affordable CD microfluidic chip can be developed. This affordable chip can be used to obtain further understanding of the results acquired by CD and push its implementation as an accurate and reliable PAT tool for the detection of mAb aggregates.

3.4.3. Comparison of the Colloidal and Conformational Stability Methods

The miniaturization of colloidal methods, where aggregation is detected according to changes in the mAb monomer size, can be considered less complex to implement compared to conformation stability methods. In general, the design of the microfluidic chip is rather modest, with a single channel used to separate the particles (HDC, AF_4, and CGE). An external set-up is not necessary, except for DLS, where a laser beam, lenses, and spatial filters are required to perform the measurement. Many

of the techniques can be miniaturized using affordable fabrication material resulting in a lower overall cost. An example of a miniaturized colloidal stability method being employed is RMM, where the sample measurement is performed in a microchannel [144]. The simplicity and affordability of miniaturized device of colloidal methods might be the ideal solution for PAT implementation in a continuous downstream processing. However, the sensitivity to detect low aggregate levels and the robustness are inferior when compared to conformational stability methods. Additionally, none of the analytical methods discussed can completely cover the entire size range of aggregates which might be formed during a continuous process. The quantification of the aggregates resorting to the majority of the colloidal methods will also be possible, but only for the soluble aggregates.

Conformational stability methods will allow for an in-line measurement with minimal sample preparation and present overall better sensitivity and robustness. These characteristics make conformational stability methods a better fit for process control. However, the design of the microfluidic chip will be more complex and an external set-up will be required to complete the measurement. Even though several efforts have been employed in the design and fabrication of these devices in affordable polymers, the overall cost is higher when compared to colloidal stability methods. Further advances in the design, the fabrication material, and the necessary external set-up are then still required to obtain a competitive alternative.

Even though the miniaturization of a PAT tool speeds up the analytical measurement, not all miniaturized devices can be easily implemented in a continuous process. By performing the measurement in a microfluidic chip, the PAT tools are transformed from in-line to on-line applications, with a reduced flow stream split from the main stream sending a sample to the microfluidic device. Although the aggregation measurement is preferred to be in-line, on-line and at-line measurements can also be applied if the result are achieved within the necessary time frame. From the analytical techniques discussed, only the slow methods, like AF_4, will not fit for on-line control. Analytical techniques that provide immediate results will be ideal for process control, such as HDC and fluorescent dyes. In particular, a microfluidic device employing fluorescent dyes for aggregate detection will work at-line since the split stream cannot return to the main stream. However, the time range to perform this technique is minor, with the measurement taking place within seconds [61], making fluorescent dyes a viable alternative for miniaturization.

3.5. Additional Future Challenges for PAT Implementation

A major challenge towards the transition of an integrated and continuous mAb production is the development of real-time and in-process analytics for the detection of high MW species [82]. The particle size of these aggregates can range from several nanometres to micrometres, making it impossible for any analytical method to offer accurate, qualitative, and quantitative characterization over the complete size range. A possible solution could be the combination of multiple orthogonal analytical techniques in a single microfluidic chip, thereby covering a broad size range of aggregates. At the lab-scale, Bansal *et al.* [116] combined three analytical tools to characterize and quantify aggregates over the complete size spectrum (1 nm to 300 µm) [116]. However, combining two or more different techniques in a microfluidic chip, the complexity of fabrication, handling, and instrumentation set-up drastically increases. Yet, the increase in complexity when performing the measurement will be balanced out if more relevant information can be collected. Another benefit of combining different techniques is the ability to overcome inherent limitations. For example, by combining HDC, a separation method, with DLS, a light detection technique, the accuracy of molecular weight determination will increase since one of the drawbacks of using DLS for mAb aggregate detection is low sensitivity.

The implementation of the PAT framework is often accompanied by the application of multivariate mathematical approaches to better understand and extract relevant information from large quantities of multivariate measurements or raw data [146]. Infrared, ultrasound, CD, and Raman spectroscopy are attractive methods to implement as a PAT tool, as these analytical techniques rapidly and non-destructively provide chemical and physical information. However, the use of the appropriate data analytical procedures is essential to extract the maximum amount of information from a spectra. Multivariate data analysis (MVDA), such as partial-least squares and principal components analysis, are commonly used methods in pharmaceutical and bioprocessing to create soft sensors. Biological therapeutics, such as mAbs, often show only subtle changes or structural rearrangements as a result of the aggregation mechanism, which are difficult to detect in a large molecules and interpret in a spectrum. By using MVDA, these subtle structural differences can be drawn out, as shown by McAvan *et al.* [178]. Therefore, in addition to instrumentation and limit of detection of each analytical technique, data collecting and handling needs to be addressed.

3.6. CONCLUSION

MAbs are currently produced almost entirely using batch operations. Recent advances in downstream processing technology for the purification of these molecules have created significant opportunities for the realization of fully integrated continuous processes. Continuous processing could provide unique opportunities for the production and delivery of low-cost mAbs. One of the major challenges for the transition towards continuous processes is the implementation of PAT tools that provide information on the status of the process, especially on the formation of aggregates. The ability to measure CQAs makes it possible to have immediate feedback on process performance. This could help significantly improve the implementation of continuous bioprocessing by allowing proactive decision-making based on real-time process data. Real-time measurement of CQAs will be beneficial in all types of processes (batch or semi-continuous). Although batch processes are more flexible in terms of the measurement time range, up to few minutes, the real-time PAT tools developed for continuous processes could easily be implemented. Thus, the development of real-time in-process analytics plays a central role in ensuring product quality. By miniaturizing the already well-established analytical techniques for the detection of mAb aggregates, an attractive solution for the creation of a PAT tool can be achieved. A microfluidic chip will speed up the measurement, allowing to gain control over the manufacturing process. Advances in design and fabrication of these micro devices are still necessary, especially for the conformational stability methods. Here, the focus should be on reducing the fabrication material costs and simplify the design and equipment set-up.

3.7. REFERENCES

[1] Calabrese, G.S. and Pissavini, S., From batch to continuous flow processing in chemicals manufacturing. AIChE Journal 2011, 57(4), 828-34.

[2] Moreno-González, M., Keulen, D., Gomis-Fons, J., Gomez, G.L., *et al.*, Continuous adsorption in food industry: The recovery of sinapic acid from rapeseed meal extract. Separation and Purification Technology 2021, 254.

[3] Roggo, Y., Pauli, V., Jelsch, M., Pellegatti, L., *et al.*, Continuous manufacturing process monitoring of pharmaceutical solid dosage form: A case study. J Pharm Biomed Anal 2020, 179, 112971.

[4] Burcham, C.L., Florence, A.J. and Johnson, M.D., Continuous Manufacturing in Pharmaceutical Process Development and Manufacturing. Annu Rev Chem Biomol Eng 2018, 9, 253-81.

[5] Rathore, A.S., Agarwal, H., Sharma, A.K., Pathak, M. and Muthukumar, S., Continuous processing for production of biopharmaceuticals. Prep Biochem Biotechnol 2015, 45(8), 836-49.

[6] Zydney, A.L., Continuous downstream processing for high value biological products: A Review. Biotechnol Bioeng 2016, 113(3), 465-75.

[7] Jungbauer, A., Continuous downstream processing of biopharmaceuticals. Trends Biotechnol 2013, 31(8), 479-92.

[8] Somasundaram, B., Pleitt, K., Shave, E., Baker, K. and Lua, L.H.L., Progression of continuous downstream processing of monoclonal antibodies: Current trends and challenges. Biotechnol Bioeng 2018, 115(12), 2893-907.

[9] Shukla, A.A., Wolfe, L.S., Mostafa, S.S. and Norman, C., Evolving trends in mAb production processes. Bioeng Transl Med 2017, 2(1), 58-69.

[10] Pollock, J., Coffman, J., Ho, S.V. and Farid, S.S., Integrated continuous bioprocessing: Economic, operational, and environmental feasibility for clinical and commercial antibody manufacture. Biotechnol Prog 2017, 33(4), 854-66.

[11] U.S. Department of Health and Human Services, FDA, CDER, CVM and ORA. PAT-A Framework for Innovative Pharmaceutical Development Manufacturing and Quality Assurance. 2004.

[12] Guideline ICH Q13 - Continuous Manufaturing of Drug Substances and Drug Products, (2021).

[13] EMA, Guideline on Real Time Release Testing (formerly Guideline on Parametric Release) Europeans Medicines Agency, Committee for Medicinal Products for Human Use 2012.

[14] Azevedo, A.M., Rosa, P.A., Ferreira, I.F., de Vries, J., *et al.*, Downstream processing of human antibodies integrating an extraction capture step and cation exchange chromatography. J Chromatogr B Analyt Technol Biomed Life Sci 2009, 877(1-2), 50-8.

[15] Grilo, A.L. and Mantalaris, A., The Increasingly Human and Profitable Monoclonal Antibody Market. Trends Biotechnol 2019, 37(1), 9-16.

[16] Konstantinov, K.B. and Cooney, C.L., White paper on continuous bioprocessing. May 20-21, 2014 Continuous Manufacturing Symposium. J Pharm Sci 2015, 104(3), 813-20.

[17] Zydney, A.L., Perspectives on integrated continuous bioprocessing—opportunities and challenges. Current Opinion in Chemical Engineering 2015, 10, 8-13.

[18] Walther, J., Godawat, R., Hwang, C., Abe, Y., *et al.*, The business impact of an integrated continuous biomanufacturing platform for recombinant protein production. J Biotechnol 2015, 213, 3-12.

[19] David, L., Schwan, P., Lobedann, M., Borchert, S.O., *et al.*, Side-by-side comparability of batch and continuous downstream for the production of monoclonal antibodies. Biotechnol Bioeng 2020, 117(4), 1024-36.

[20] Bansal, R., Gupta, S. and Rathore, A.S., Analytical Platform for Monitoring Aggregation of Monoclonal Antibody Therapeutics. Pharmaceutical Research 2019, 36(11).

[21] Telikepalli, S.N., Kumru, O.S., Kalonia, C., Esfandiary, R., *et al.*, Structural characterization of IgG1 mAb aggregates and particles generated under various stress conditions. J Pharm Sci 2014, 103(3), 796-809.

[22] Gomez de la Cuesta, R., Goodacre, R. and Ashton, L., Monitoring antibody aggregation in early drug development using Raman spectroscopy and perturbation-correlation moving windows. Anal Chem 2014, 86(22), 11133-40.

[23] Remmele, R.L., Bee, J.S., Phillips, J.J., Mo, W.D., *et al.* Characterization of Monoclonal Antibody Aggregates and Emerging Technologies. State-of-the-Art and Emerging Technologies for Therapeutic Monoclonal Antibody Characterization Volume 3 Defining the Next Generation of Analytical and Biophysical Techniques. ACS Symposium Series2015. p. 113-58.

[24] Roberts, C.J., Therapeutic protein aggregation: mechanisms, design, and control. Trends Biotechnol 2014, 32(7), 372-80.

[25] Kukrer, B., Filipe, V., van Duijn, E., Kasper, P.T., *et al.*, Mass spectrometric analysis of intact human monoclonal antibody aggregates fractionated by size-exclusion chromatography. Pharm Res 2010, 27(10), 2197-204.

[26] Paul, R., Graff-Meyer, A., Stahlberg, H., Lauer, M.E., *et al.*, Structure and function of purified monoclonal antibody dimers induced by different stress conditions. Pharm Res 2012, 29(8), 2047-59.

[27] Walchli, R., Ressurreicao, M., Vogg, S., Feidl, F., *et al.*, Understanding mAb aggregation during low pH viral inactivation and subsequent neutralization. Biotechnol Bioeng 2020, 117(3), 687-700.

[28] Hawe, A., Kasper, J.C., Friess, W. and Jiskoot, W., Structural properties of monoclonal antibody aggregates induced by freeze-thawing and thermal stress. Eur J Pharm Sci 2009, 38(2), 79-87.

[29] Kalonia, C., Toprani, V., Toth, R., Wahome, N., *et al.*, Effects of Protein Conformation, Apparent Solubility, and Protein-Protein Interactions on the Rates and Mechanisms of Aggregation for an IgG1 Monoclonal Antibody. J Phys Chem B 2016, 120(29), 7062-75.

[30] Hawe, A., Friess, W., Sutter, M. and Jiskoot, W., Online fluorescent dye detection method for the characterization of immunoglobulin G aggregation by size exclusion chromatography and asymmetrical flow field flow fractionation. Anal Biochem 2008, 378(2), 115-22.

[31] Schermeyer, M.T., Woll, A.K., Kokke, B., Eppink, M. and Hubbuch, J., Characterization of highly concentrated antibody solution - A toolbox for the description of protein long-term solution stability. MAbs 2017, 9(7), 1169-85.

[32] Neergaard, M.S., Nielsen, A.D., Parshad, H. and Van De Weert, M., Stability of monoclonal antibodies at high-concentration: head-to-head comparison of the IgG1 and IgG4 subclass. J Pharm Sci 2014, 103(1), 115-27.

[33] Vazquez-Rey, M. and Lang, D.A., Aggregates in monoclonal antibody manufacturing processes. Biotechnol Bioeng 2011, 108(7), 1494-508.

[34] Fesinmeyer, R.M., Hogan, S., Saluja, A., Brych, S.R., *et al.*, Effect of ions on agitation- and temperature-induced aggregation reactions of antibodies. Pharm Res 2009, 26(4), 903-13.

[35] Singla, A., Bansal, R., Joshi, V. and Rathore, A.S., Aggregation Kinetics for IgG1-Based Monoclonal Antibody Therapeutics. AAPS J 2016, 18(3), 689-702.

[36] Hoehne, M., Samuel, F., Dong, A., Wurth, C., *et al.*, Adsorption of monoclonal antibodies to glass microparticles. J Pharm Sci 2011, 100(1), 123-32.

[37] Luo, Y., Ronk, M., Joubert, M.K., Semin, D. and Nashed-Samuel, Y., Determination of interactions between antibody biotherapeutics and copper by size exclusion chromatography (SEC) coupled with inductively coupled plasma mass spectrometry (ICP/MS). Anal Chim Acta 2019, 1079, 252-9.

[38] Biddlecombe, J.G., Craig, A.V., Zhang, H., Uddin, S., *et al.*, Determining Antibody Stability: Creation of Solid-Liquid Interfacial Effects within a High Shear Environment. Biotechnology Progress 2007, 23, 218-1222.

[39] Thomas, C.R. and Geer, D., Effects of shear on proteins in solution. Biotechnol Lett 2011, 33(3), 443-56.

[40] Mahler, H.C., Muller, R., Friess, W., Delille, A. and Matheus, S., Induction and analysis of aggregates in a liquid IgG1-antibody formulation. Eur J Pharm Biopharm 2005, 59(3), 407-17.

[41] Mahler, H.C., Friess, W., Grauschopf, U. and Kiese, S., Protein aggregation: pathways, induction factors and analysis. J Pharm Sci 2009, 98(9), 2909-34.

[42] Carpenter, J.F., Randolph, T.W., Jiskoot, W., Crommelin, D.J., *et al.*, Overlooking subvisible particles in therapeutic protein products: gaps that may compromise product quality. J Pharm Sci 2009, 98(4), 1201-5.

[43] Das, T.K., Narhi, L.O., Sreedhara, A., Menzen, T., *et al.*, Stress Factors in mAb Drug Substance Production Processes: Critical Assessment of Impact on Product Quality and Control Strategy. J Pharm Sci 2020, 109(1), 116-33.

[44] Moore, J.M., Patapoff, T.W. and Cromwell, M.E., Kinetics and thermodynamics of dimer formation and dissociation for a recombinant humanized monoclonal antibody to vascular endothelial growth factor. Biochemistry 1999, 38(42), 13960-7.

[45] Cromwell, M.E., Hilario, E. and Jacobson, F., Protein aggregation and bioprocessing. AAPS J 2006, 8(3), E572-9.

[46] Andya, J.D., Hsu, C.C. and Shire, S.J., Mechanisms of aggregate formation and carbohydrate excipient stabilization of lyophilized humanized monoclonal antibody formulations. AAPS PharmSci 2003, 5(2), E10.

[47] Arakawa, T., Prestrelski, S.J., Kenney, W.C. and Carpenter, J.F., Factors affecting short-term and long-term stabilities of proteins. Adv Drug Deliv Rev 2001, 46(1-3), 307-26.

[48] Arakawa, T. and Timasheff, S.N., The stabilization of proteins by osmolytes. Biophys J 1985, 47(3), 411-4.

[49] Kendrick, B.S., Cleland, J.L., Lam, X., Nguyen, T., *et al.*, Aggregation of recombinant human interferon gamma: kinetics and structural transitions. J Pharm Sci 1998, 87(9), 1069-76.

[50] Wang, W., Instability, stabilization, and formulation of liquid protein pharmaceuticals. Int J Pharm 1999, 185(2), 129-88.

[51] Kelly, J.W., The alternative conformations of amyloidogenic proteins and their multi-step assembly pathways. Curr Opin Struct Biol 1998, 8(1), 101-6.

[52] Marcon, G., Plakoutsi, G. and Chiti, F., Protein aggregation starting from the native globular state. Methods Enzymol 2006, 413, 75-91.

[53] Holm, N.K., Jespersen, S.K., Thomassen, L.V., Wolff, T.Y., *et al.*, Aggregation and fibrillation of bovine serum albumin. Biochim Biophys Acta 2007, 1774(9), 1128-38.

[54] Johansson, J., Amyloid fibrils. FEBS J 2005, 272(23), 5941.

[55] Makin, O.S. and Serpell, L.C., Structures for amyloid fibrils. FEBS J 2005, 272(23), 5950-61.

[56] van Beers, M.M. and Bardor, M., Minimizing immunogenicity of biopharmaceuticals by controlling critical quality attributes of proteins. Biotechnol J 2012, 7(12), 1473-84.

[57] Hamrang, Z., Rattray, N.J. and Pluen, A., Proteins behaving badly: emerging technologies in profiling biopharmaceutical aggregation. Trends Biotechnol 2013, 31(8), 448-58.

[58] den Engelsman, J., Garidel, P., Smulders, R., Koll, H., *et al.*, Strategies for the assessment of protein aggregates in pharmaceutical biotech product development. Pharm Res 2011, 28(4), 920-33.

[59] Philo, J.S., Is any measurement method optimal for all aggregate sizes and types? AAPS J 2006, 8(3), E564-71.

[60] Gabrielson, J.P., Brader, M.L., Pekar, A.H., Mathis, K.B., *et al.*, Quantitation of aggregate levels in a recombinant humanized monoclonal antibody formulation by size-exclusion chromatography, asymmetrical flow field flow fractionation, and sedimentation velocity. J Pharm Sci 2007, 96(2), 268-79.

[61] Paul, A.J., Bickel, F., Rohm, M., Hospach, L., *et al.*, High-throughput analysis of sub-visible mAb aggregate particles using automated fluorescence microscopy imaging. Anal Bioanal Chem 2017, 409(17), 4149-56.

[62] Rathore, A.S., Bhambure, R. and Ghare, V., Process analytical technology (PAT) for biopharmaceutical products. Anal Bioanal Chem 2010, 398(1), 137-54.

[63] Sia, S.K. and Whitesides, G.M., Microfluidic devices fabricated in poly(dimethylsiloxane) for biological studies. Electrophoresis 2003, 24(21), 3563-76.

[64] Kricka, L.J., Miniaturization of analytical systems. Clin Chem 1998, 44(9), 2008-14.

[65] Lebowitz, J., Lewis, M.S. and Schuck, P., Modern analytical ultracentrifugation in protein science: a tutorial review. Protein Sci 2002, 11(9), 2067-79.

[66] Yumioka, R., Sato, H., Tomizawa, H., Yamasaki, Y. and Ejima, D., Mobile phase containing arginine provides more reliable SEC condition for aggregation analysis. J Pharm Sci 2010, 99(2), 618-20.

[67] Gandhi, A.V., Pothecary, M.R., Bain, D.L. and Carpenter, J.F., Some Lessons Learned From a Comparison Between Sedimentation Velocity Analytical Ultracentrifugation and Size Exclusion Chromatography to Characterize and Quantify Protein Aggregates. J Pharm Sci 2017, 106(8), 2178-86.

[68] Carpenter, J.F., Randolph, T.W., Jiskoot, W., Crommelin, D.J., *et al.*, Potential inaccurate quantitation and sizing of protein aggregates by size exclusion chromatography: essential need to use orthogonal methods to assure the quality of therapeutic protein products. J Pharm Sci 2010, 99(5), 2200-8.

[69] Amartely, H., Avraham, O., Friedler, A., Livnah, O. and Lebendiker, M., Coupling Multi Angle Light Scattering to Ion Exchange chromatography (IEX-MALS) for protein characterization. Sci Rep 2018, 8(1), 6907.

[70] Berkowitz, S.A., Role of analytical ultracentrifugation in assessing the aggregation of protein biopharmaceuticals. AAPS J 2006, 8(3), E590-605.

[71] Arthur, K.K., Gabrielson, J.P., Kendrick, B.S. and Stoner, M.R., Detection of protein aggregates by sedimentation velocity analytical ultracentrifugation (SV-AUC): sources of variability and their relative importance. J Pharm Sci 2009, 98(10), 3522-39.

[72] Gabrielson, J.P. and Arthur, K.K., Measuring low levels of protein aggregation by sedimentation velocity. Methods 2011, 54(1), 83-91.

[73] Gabrielson, J.P., Randolph, T.W., Kendrick, B.S. and Stoner, M.R., Sedimentation velocity analytical ultracentrifugation and SEDFIT/c(s): limits of quantitation for a monoclonal antibody system. Anal Biochem 2007, 361(1), 24-30.

[74] Hawe, A., Weinbuch, D., Zölls, S., Reichel, A. and Carpenter, J.F. Submicrometer, micrometer and visible particle analysis in biopharmaceutical research and development. Biophysical Characterization of Proteins in Developing Biopharmaceuticals2020. p. 285-310.

[75] Read, E.K., Park, J.T., Shah, R.B., Riley, B.S., *et al.*, Process analytical technology (PAT) for biopharmaceutical products: Part I. concepts and applications. Biotechnol Bioeng 2010, 105(2), 276-84.

[76] Glassey, J., Gernaey, K.V., Clemens, C., Schulz, T.W., *et al.*, Process analytical technology (PAT) for biopharmaceuticals. Biotechnol J 2011, 6(4), 369-77.

[77] Beg, S., Haneef, J., Rahman, M., Peraman, R., *et al.* Introduction to analytical quality by design. Handbook of Analytical Quality by Design2021. p. 1-14.

[78] Read, E.K., Shah, R.B., Riley, B.S., Park, J.T., *et al.*, Process analytical technology (PAT) for biopharmaceutical products: Part II. Concepts and applications. Biotechnol Bioeng 2010, 105(2), 285-95.

[79] Yu, L.X., Lionberger, R.A., Raw, A.S., D'Costa, R., *et al.*, Applications of process analytical technology to crystallization processes. Adv Drug Deliv Rev 2004, 56(3), 349-69.

[80] Chew, W. and Sharratt, P., Trends in process analytical technology. Analytical Methods 2010, 2(10).

[81] Sharma, A., Chilin, D. and Rathore, A.S., Applying Process Analytical Technology to Biotech Unit Operations. BioPharm International 2006, 19(8).

[82] Sao Pedro, M.N., Silva, T.C., Patil, R. and Ottens, M., White Paper on High Throughput Process Development for Integrated Continuous Biomanufacturing. Biotechnol Bioeng 2021.

[83] Rathore, A.S., Yu, M., Yeboah, S. and Sharma, A., Case study and application of process analytical technology (PAT) towards bioprocessing: use of on-line high-performance liquid chromatography (HPLC) for making real-time pooling decisions for process chromatography. Biotechnol Bioeng 2008, 100(2), 306-16.

[84] Mandenius, C.-F. and Gustavsson, R., Mini-review: soft sensors as means for PAT in the manufacture of bio-therapeutics. Journal of Chemical Technology & Biotechnology 2015, 90(2), 215-27.

[85] Kalonia, C., Kumru, O.S., Prajapati, I., Mathaes, R., *et al.*, Calculating the mass of subvisible protein particles with improved accuracy using microflow imaging data. J Pharm Sci 2015, 104(2), 536-47.

[86] Barnard, J.G., Singh, S., Randolph, T.W. and Carpenter, J.F., Subvisible particle counting provides a sensitive method of detecting and quantifying aggregation of monoclonal antibody caused by freeze-thawing: insights into the roles of particles in the protein aggregation pathway. J Pharm Sci 2011, 100(2), 492-503.

[87] Wuchner, K., Buchler, J., Spycher, R., Dalmonte, P. and Volkin, D.B., Development of a microflow digital imaging assay to characterize protein particulates during storage of a high concentration IgG1 monoclonal antibody formulation. J Pharm Sci 2010, 99(8), 3343-61.

[88] Bickel, F., Herold, E.M., Signes, A., Romeijn, S., *et al.*, Reversible NaCl-induced aggregation of a monoclonal antibody at low pH: Characterization of aggregates and factors affecting aggregation. Eur J Pharm Biopharm 2016, 107, 310-20.

[89] Sharma, D.K., King, D., Oma, P. and Merchant, C., Micro-flow imaging: flow microscopy applied to sub-visible particulate analysis in protein formulations. AAPS J 2010, 12(3), 455-64.

[90] Zolls, S., Weinbuch, D., Wiggenhorn, M., Winter, G., *et al.*, Flow imaging microscopy for protein particle analysis--a comparative evaluation of four different analytical instruments. AAPS J 2013, 15(4), 1200-11.

[91] Filipe, V., Hawe, A., Carpenter, J.F. and Jiskoot, W., Analytical approaches to assess the degradation of therapeutic proteins. TrAC Trends in Analytical Chemistry 2013, 49, 118-25.

[92] Oyama, H., Koga, H., Tadokoro, T., Maenaka, K., *et al.*, Relation of Colloidal and Conformational Stabilities to Aggregate Formation in a Monoclonal Antibody. J Pharm Sci 2020, 109(1), 308-15.

[93] He, F., Phan, D.H., Hogan, S., Bailey, R., *et al.*, Detection of IgG aggregation by a high throughput method based on extrinsic fluorescence. J Pharm Sci 2010, 99(6), 2598-608.

[94] Paul, A.J., Schwab, K., Prokoph, N., Haas, E., *et al.*, Fluorescence dye-based detection of mAb aggregates in CHO culture supernatants. Anal Bioanal Chem 2015, 407(16), 4849-56.

[95] Hawe, A., Filipe, V. and Jiskoot, W., Fluorescent molecular rotors as dyes to characterize polysorbate-containing IgG formulations. Pharm Res 2010, 27(2), 314-26.

[96] Oshinbolu, S., Shah, R., Finka, G., Molloy, M., *et al.*, Evaluation of fluorescent dyes to measure protein aggregation within mammalian cell culture supernatants. J Chem Technol Biotechnol 2018, 93(3), 909-17.

[97] Arosio, P., Rima, S. and Morbidelli, M., Aggregation mechanism of an IgG2 and two IgG1 monoclonal antibodies at low pH: from oligomers to larger aggregates. Pharm Res 2013, 30(3), 641-54.

[98] Biancalana, M. and Koide, S., Molecular mechanism of Thioflavin-T binding to amyloid fibrils. Biochim Biophys Acta 2010, 1804(7), 1405-12.

[99] Ward, K. and Fan, Z.H., Mixing in microfluidic devices and enhancement methods. J Micromech Microeng 2015, 25(9).

[100] Lee, C.Y., Chang, C.L., Wang, Y.N. and Fu, L.M., Microfluidic mixing: a review. Int J Mol Sci 2011, 12(5), 3263-87.

[101] Capretto, L., Cheng, W., Hill, M. and Zhang, X., Micromixing within microfluidic devices. Top Curr Chem 2011, 304, 27-68.

[102] Tsai, C.D. and Lin, X.Y., Experimental Study on Microfluidic Mixing with Different Zigzag Angles. Micromachines (Basel) 2019, 10(9).

[103] Mengeaud, V., Josserand, J. and Girault, H.H., Mixing processes in a zigzag microchannel: finite element simulations and optical study. Anal Chem 2002, 74(16), 4279-86.

[104] Rhoades, T., Kothapalli, C.R. and Fodor, P.S., Mixing Optimization in Grooved Serpentine Microchannels. Micromachines (Basel) 2020, 11(1).

[105] Johnson, T.J., Ross, D. and Locascio, L.E., Rapid microfluidic mixing. Anal Chem 2002, 74(1), 45-51.

[106] Alam, A., Afzal, A. and Kim, K.-Y., Mixing performance of a planar micromixer with circular obstructions in a curved microchannel. Chemical Engineering Research and Design 2014, 92(3), 423-34.

[107] Liang-Hsuan, L., Kee Suk, R. and Chang, L., A magnetic microstirrer and array for microfluidic mixing. Journal of Microelectromechanical Systems 2002, 11(5), 462-9.

[108] Mensing, G.A., Pearce, T.M., Graham, M.D. and Beebe, D.J., An externally driven magnetic microstirrer. Philos Trans A Math Phys Eng Sci 2004, 362(1818), 1059-68.

[109] Petkovic-Duran, K., Manasseh, R., Zhu, Y. and Ooi, A., Chaotic micromixing in open wells using audio-frequency acoustic microstreaming. Biotechniques 2009, 47(4), 827-34.

[110] Balasuriya, S., Optimal frequency for microfluidic mixing across a fluid interface. Phys Rev Lett 2010, 105(6), 064501.

[111] Kim, S.J., Wang, F., Burns, M.A. and Kurabayashi, K., Temperature-programmed natural convection for micromixing and biochemical reaction in a single microfluidic chamber. Anal Chem 2009, 81(11), 4510-6.

[112] Jeong, G.S., Chung, S., Kim, C.B. and Lee, S.H., Applications of micromixing technology. Analyst 2010, 135(3), 460-73.

[113] Striegel, A.M. and Brewer, A.K., Hydrodynamic chromatography. Annu Rev Anal Chem (Palo Alto Calif) 2012, 5, 15-34.

[114] Chmela, E., Tijssen, R., Blom, M.T., Gardeniers, H.J. and van den Berg, A., A chip system for size separation of macromolecules and particles by hydrodynamic chromatography. Anal Chem 2002, 74(14), 3470-5.

[115] Blom, M.T., Chmela, E., Oosterbroek, R.E., Tijssen, R. and Van den Berg, A., On-Chip Hydrodynamic Chromatography Separation and Detection of Nanoparticles and Biomolecules. Analytical Chemistry 2003, 75(24), 6761-8.

[116] Bansal, R., Gupta, S. and Rathore, A.S., Analytical Platform for Monitoring Aggregation of Monoclonal Antibody Therapeutics. Pharm Res 2019, 36(11), 152.

[117] Flatman, S., Alam, I., Gerard, J. and Mussa, N., Process analytics for purification of monoclonal antibodies. J Chromatogr B Analyt Technol Biomed Life Sci 2007, 848(1), 79-87.

[118] Ahrer, K., Buchacher, A., Iberer, G. and Jungbauer, A., Thermodynamic stability and formation of aggregates of human immunoglobulin G characterised by differential scanning calorimetry and dynamic light scattering. J Biochem Biophys Methods 2006, 66(1-3), 73-86.

[119] Nobbmann, U., Connah, M., Fish, B., Varley, P., *et al.*, Dynamic light scattering as a relative tool for assessing the molecular integrity and stability of monoclonal antibodies. Biotechnol Genet Eng Rev 2007, 24, 117-28.

[120] Ahrer, K., Buchacher, A., Iberer, G., Josic, D. and Jungbauer, A., Analysis of aggregates of human immunoglobulin G using size-exclusion chromatography, static and dynamic light scattering. Journal of Chromatography A 2003, 1009(1-2), 89-96.

[121] Demeule, B., Lawrence, M.J., Drake, A.F., Gurny, R. and Arvinte, T., Characterization of protein aggregation: the case of a therapeutic immunoglobulin. Biochim Biophys Acta 2007, 1774(1), 146-53.

[122] Destremaut, F., Salmon, J.B., Qi, L. and Chapel, J.P., Microfluidics with on-line dynamic light scattering for size measurements. Lab Chip 2009, 9(22), 3289-96.

[123] Chastek, T.Q., Beers, K.L. and Amis, E.J., Miniaturized dynamic light scattering instrumentation for use in microfluidic applications. Rev Sci Instrum 2007, 78(7), 072201.

[124] Chastek, T.Q., Iida, K., Amis, E.J., Fasolka, M.J. and Beers, K.L., A microfluidic platform for integrated synthesis and dynamic light scattering measurement of block copolymer micelles. Lab Chip 2008, 8(6), 950-7.

[125] Fraunhofer, W. and Winter, G., The use of asymmetrical flow field-flow fractionation in pharmaceutics and biopharmaceutics. Eur J Pharm Biopharm 2004, 58(2), 369-83.

[126] Reschiglian, P., Roda, B., Zattoni, A., Tanase, M., *et al.*, Hollow-fiber flow field-flow fractionation with multi-angle laser scattering detection for aggregation studies of therapeutic proteins. Anal Bioanal Chem 2014, 406(6), 1619-27.

[127] Hawe, A., Romeijn, S., Filipe, V. and Jiskoot, W., Asymmetrical flow field-flow fractionation method for the analysis of submicron protein aggregates. J Pharm Sci 2012, 101(11), 4129-39.

[128] Bria, C.R. and Williams, S.K., Impact of asymmetrical flow field-flow fractionation on protein aggregates stability. J Chromatogr A 2016, 1465, 155-64.

[129] Runyon, J.R., Nilsson, L., Alftren, J. and Bergenstahl, B., Characterization of oat proteins and aggregates using asymmetric flow field-flow fractionation. Anal Bioanal Chem 2013, 405(21), 6649-55.

[130] Ma, D., Martin, N., Tribet, C. and Winnik, F.M., Quantitative characterization by asymmetrical flow field-flow fractionation of IgG thermal aggregation with and without polymer protective agents. Anal Bioanal Chem 2014, 406(29), 7539-47.

[131] Muller, D., Cattaneo, S., Meier, F., Welz, R. and de Mello, A.J., Nanoparticle separation with a miniaturized asymmetrical flow field-flow fractionation cartridge. Front Chem 2015, 3, 45.

[132] Yohannes, G., Sneck, M., Varjo, S.J., Jussila, M., *et al.*, Miniaturization of asymmetrical flow field-flow fractionation and application to studies on lipoprotein aggregation and fusion. Anal Biochem 2006, 354(2), 255-65.

[133] Kim, K.H. and Moon, M.H., Development of a multilane channel system for nongel-based two-dimensional protein separations using isoelectric focusing and asymmetrical flow field-flow fractionation. Anal Chem 2009, 81(4), 1715-21.

[134] Kang, D. and Moon, M.H., Miniaturization of frit inlet asymmetrical flow field-flow fractionation. Anal Chem 2004, 76(13), 3851-5.

[135] Wang, D., Nowak, C., Mason, B., Katiyar, A. and Liu, H., Analytical artifacts in characterization of recombinant monoclonal antibody therapeutics. J Pharm Biomed Anal 2020, 183, 113131.

[136] Wang, W.H., Cheung-Lau, J., Chen, Y., Lewis, M. and Tang, Q.M., Specific and high-resolution identification of monoclonal antibody fragments detected by capillary electrophoresis-sodium dodecyl sulfate using reversed-phase HPLC with top-down mass spectrometry analysis. MAbs 2019, 11(7), 1233-44.

[137] Lechner, A., Giorgetti, J., Gahoual, R., Beck, A., *et al.*, Insights from capillary electrophoresis approaches for characterization of monoclonal antibodies and antibody drug conjugates in the period 2016-2018. J Chromatogr B Analyt Technol Biomed Life Sci 2019, 1122-1123, 1-17.

[138] Molina, P., Schick, A.J., 3rd, Welch, L., Niedringhaus, T., *et al.*, Using differential scanning calorimetry for the development of non-reduced capillary electrophoresis sodium dodecyl sulfate methods for monoclonal antibodies. Anal Biochem 2020, 609, 113948.

[139] Rouby, G., Tran, N.T., Leblanc, Y., Taverna, M. and Bihoreau, N., Investigation of monoclonal antibody dimers in a final formulated drug by separation techniques coupled to native mass spectrometry. MAbs 2020, 12(1), e1781743.

[140] Jacobson, S.C., Hergenroder, R., Koutny, L.B. and Ramsey, J.M., High-Speed Separations on a Microchip. Analytical Chemistry 1994, 66(7), 1114 - 8.

[141] Yao, S., Anex, D.S., Caldwell, W.B., Arnold, D.W., *et al.*, SDS capillary gel electrophoresis of proteins in microfabricated channels. PNAS 1999, 96, 5372 - 7.

[142] Dolnik, V., Liu, C. and Jovanovich, S., Capillary Electrophoresis on Microchip. Electrophoresis 2001, 21, 41 - 54.

[143] Smith, M.T., Zhang, S., Adams, T., DiPaolo, B. and Dally, J., Establishment and validation of a microfluidic capillary gel electrophoresis platform method for purity analysis of therapeutic monoclonal antibodies. Electrophoresis 2017, 38(9-10), 1353-65.

[144] Panchal, J., Kotarek, J., Marszal, E. and Topp, E.M., Analyzing subvisible particles in protein drug products: a comparison of dynamic light scattering (DLS) and resonant mass measurement (RMM). AAPS J 2014, 16(3), 440-51.

[145] Weinbuch, D., Zolls, S., Wiggenhorn, M., Friess, W., *et al.*, Micro-flow imaging and resonant mass measurement (Archimedes)--complementary methods to quantitatively differentiate protein particles and silicone oil droplets. J Pharm Sci 2013, 102(7), 2152-65.

[146] Rudt, M., Briskot, T. and Hubbuch, J., Advances in downstream processing of biologics - Spectroscopy: An emerging process analytical technology. J Chromatogr A 2017, 1490, 2-9.

[147] Capito, F., Zimmer, A. and Skudas, R., Mid-infrared spectroscopy-based analysis of mammalian cell culture parameters. Biotechnol Prog 2015, 31(2), 578-84.

[148] Manning, M.C., Use of infrared spectroscopy to monitor protein structure and stability. Expert Review of Proteomics 2005, 2(5), 731 - 43.

[149] Matheus, S., Mahler, H.C. and Friess, W., A critical evaluation of Tm(FTIR) measurements of high-concentration IgG1 antibody formulations as a formulation development tool. Pharm Res 2006, 23(7), 1617-27.

[150] Boulet-Audet, M., Byrne, B. and Kazarian, S.G., High-throughput thermal stability analysis of a monoclonal antibody by attenuated total reflection FT-IR spectroscopic imaging. Anal Chem 2014, 86(19), 9786-93.

[151] Srisa-Art, M. and Furutani, Y., Simple and Rapid Fabrication of PDMS Microfluidic Devices Compatible with FTIR Microspectroscopy. Bulletin of the Chemical Society of Japan 2016, 89(2), 195-202.

[152] Birarda, G., Grenci, G., Businaro, L., Marmiroli, B., *et al.*, Fabrication of a microfluidic platform for investigating dynamic biochemical processes in living samples by FTIR microspectroscopy. Microelectronic Engineering 2010, 87(5-8), 806-9.

[153] Thakur, G., Hebbi, V. and Rathore, A.S., An NIR-based PAT approach for real-time control of loading in Protein A chromatography in continuous manufacturing of monoclonal antibodies. Biotechnol Bioeng 2020, 117(3), 673-86.

[154] Thakur, G., Thori, S. and Rathore, A.S., Implementing PAT for single-pass tangential flow ultrafiltration for continuous manufacturing of monoclonal antibodies. Journal of Membrane Science 2020, 613.

[155] Awad, H., Khamis, M.M. and El-Aneed, A., Mass Spectrometry, Review of the Basics: Ionization. Applied Spectroscopy Reviews 2014, 50(2), 158-75.

[156] Feng, X., Liu, B.F., Li, J. and Liu, X., Advances in coupling microfluidic chips to mass spectrometry. Mass Spectrom Rev 2015, 34(5), 535-57.

[157] Farsang, E., Guillarme, D., Veuthey, J.L., Beck, A., *et al.*, Coupling non-denaturing chromatography to mass spectrometry for the characterization of monoclonal antibodies and related products. J Pharm Biomed Anal 2020, 185, 113207.

[158] Ehkirch, A., Goyon, A., Hernandez-Alba, O., Rouviere, F., *et al.*, A Novel Online Four-Dimensional SECxSEC-IMxMS Methodology for Characterization of Monoclonal Antibody Size Variants. Anal Chem 2018, 90(23), 13929-37.

[159] Toth, R.T.t., Pace, S.E., Mills, B.J., Joshi, S.B., *et al.*, Evaluation of Hydrogen Exchange Mass Spectrometry as a Stability-Indicating Method for Formulation Excipient Screening for an IgG4 Monoclonal Antibody. J Pharm Sci 2018, 107(4), 1009-19.

[160] Redman, E.A., Mellors, J.S., Starkey, J.A. and Ramsey, J.M., Characterization of Intact Antibody Drug Conjugate Variants Using Microfluidic Capillary Electrophoresis-Mass Spectrometry. Anal Chem 2016, 88(4), 2220-6.

[161] Sikanen, T., Franssila, S., Kauppila, T.J., Kostiainen, R., *et al.*, Microchip technology in mass spectrometry. Mass Spectrom Rev 2010, 29(3), 351-91.

[162] Yin, H., Killeen, K., Brennen, R., Sobek, D., *et al.*, Microfluidic Chip for Peptide Analysis with an Integrated HPLC Column, Sample Enrichment Column, and Nanoelectrospray Tip. Analytical Chemistry 2005, 77(2), 527 - 33.

[163] Yan, B., Chen, T., Xu, Z. and Qu, H., Rapid process development of chromatographic process using direct analysis in real time mass spectrometry as a process analytical technology tool. J Pharm Biomed Anal 2014, 94, 106-10.

[164] Wang, L., Zeng, S., Chen, T. and Qu, H., Direct analysis in real time mass spectrometry, a process analytical technology tool for real-time process monitoring in botanical drug manufacturing. J Pharm Biomed Anal 2014, 91, 202-9.

[165] Forrester, D.M., Huang, J. and Pinfield, V.J., Characterisation of colloidal dispersions using ultrasound spectroscopy and multiple-scattering theory inclusive of shear-wave effects. Chemical Engineering Research and Design 2016, 114, 69-78.

[166] Sarvazyan, A.P., Ultrasonic velocimetry of biological compounds. Annu Rev Biophys Biophys Chem 1991, 20, 321-42.

[167] Józefczak, A., Study of low concentrated ionic ferrrofluid stability in magnetic field by ultrasound spectroscopy. Journal of Magnetism and Magnetic Materials 2009, 321(14), 2225-31.

[168] Strohm, E.M., Berndl, E.S. and Kolios, M.C., Probing red blood cell morphology using high-frequency photoacoustics. Biophys J 2013, 105(1), 59-67.

[169] Hysi, E., Saha, R.K. and Kolios, M.C., Photoacoustic ultrasound spectroscopy for assessing red blood cell aggregation and oxygenation. J Biomed Opt 2012, 17(12), 125006.

[170] Smirnovas, V. and Winter, R., Revealing different aggregation pathways of amyloidogenic proteins by ultrasound velocimetry. Biophys J 2008, 94(8), 3241-6.

[171] Agrawal, M. and Seshia, A., A microfluidic platform for glucose sensing using Broadband Ultrasound Spectroscopy. IEEE 2016.

[172] Ettah, I. and Ashton, L., Engaging with Raman Spectroscopy to Investigate Antibody Aggregation. Antibodies (Basel) 2018, 7(3).

[173] Esmonde-White, K.A., Cuellar, M., Uerpmann, C., Lenain, B. and Lewis, I.R., Raman spectroscopy as a process analytical technology for pharmaceutical manufacturing and bioprocessing. Anal Bioanal Chem 2017, 409(3), 637-49.

[174] Baradez, M.O., Biziato, D., Hassan, E. and Marshall, D., Application of Raman Spectroscopy and Univariate Modelling As a Process Analytical Technology for Cell Therapy Bioprocessing. Front Med (Lausanne) 2018, 5, 47.

[175] Jahn, I.J., Zukovskaja, O., Zheng, X.S., Weber, K., *et al.*, Surface-enhanced Raman spectroscopy and microfluidic platforms: challenges, solutions and potential applications. Analyst 2017, 142(7), 1022-47.

[176] Abu-Absi, N.R., Kenty, B.M., Cuellar, M.E., Borys, M.C., *et al.*, Real time monitoring of multiple parameters in mammalian cell culture bioreactors using an in-line Raman spectroscopy probe. Biotechnol Bioeng 2011, 108(5), 1215-21.

[177] Zhang, C., Springall, J.S., Wang, X. and Barman, I., Rapid, quantitative determination of aggregation and particle formation for antibody drug conjugate therapeutics with label-free Raman spectroscopy. Anal Chim Acta 2019, 1081, 138-45.

[178] McAvan, B.S., Bowsher, L.A., Powell, T., O'Hara, J.F., *et al.*, Raman Spectroscopy to Monitor Post-Translational Modifications and Degradation in Monoclonal Antibody Therapeutics. Anal Chem 2020, 92(15), 10381-9.

[179] Ashok, P.C., Singh, G.P., Rendall, H.A., Krauss, T.F. and Dholakia, K., Waveguide confined Raman spectroscopy for microfluidic interrogation. Lab Chip 2011, 11(7), 1262-70.

[180] Zhou, J., Ren, K., Zhao, Y., Dai, W. and Wu, H., Convenient formation of nanoparticle aggregates on microfluidic chips for highly sensitive SERS detection of biomolecules. Anal Bioanal Chem 2012, 402(4), 1601-9.

[181] Choi, I., Huh, Y.S. and Erickson, D., Ultra-sensitive, label-free probing of the conformational characteristics of amyloid beta aggregates with a SERS active nanofluidic device. Microfluidics and Nanofluidics 2011, 12(1-4), 663-9.

[182] Zhang, H., Zheng, X., Kwok, R.T.K., Wang, J., *et al.*, In situ monitoring of molecular aggregation using circular dichroism. Nat Commun 2018, 9(1), 4961.

[183] Greenfield, N.J., Using circular dichroism spectra to estimate protein secondary structure. Nat Protoc 2006, 1(6), 2876-90.

[184] Joshi, V., Shivach, T., Yadav, N. and Rathore, A.S., Circular dichroism spectroscopy as a tool for monitoring aggregation in monoclonal antibody therapeutics. Anal Chem 2014, 86(23), 11606-13.

[185] Narvekar, A., Gawali, S.L., Hassan, P.A., Jain, R. and Dandekar, P., pH dependent aggregation and conformation changes of rituximab using SAXS and its comparison with the standard regulatory approach of biophysical characterization. Int J Biol Macromol 2020, 164, 3084-97.

[186] Bortolini, C., Kartanas, T., Copic, D., Condado Morales, I., *et al.*, Resolving protein mixtures using microfluidic diffusional sizing combined with synchrotron radiation circular dichroism. Lab Chip 2018, 19(1), 50-8.

[187] Kane, A.S., Hoffmann, A., Baumgartel, P., Seckler, R., *et al.*, Microfluidic Mixers for the Investigation of Rapid Protein Folding Kinetics Using Synchrotron Radiation Circular Dichroism Spectroscopy. Analytical Chemistry 2008, 80(24), 9534 - 41.

[188] Sun, X., Kelly, R.T., Tang, K. and Smith, R.D., Membrane-based emitter for coupling microfluidics with ultrasensitive nanoelectrospray ionization-mass spectrometry. Anal Chem 2011, 83(14), 5797-803.

[189] Hoffmann, P., Hausig, U., Schulze, P. and Belder, D., Microfluidic glass chips with an integrated nanospray emitter for coupling to a mass spectrometer. Angew Chem Int Ed Engl 2007, 46(26), 4913-6.

[190] Li, Y., Mach, H. and Blue, J.T., High throughput formulation screening for global aggregation behaviors of three monoclonal antibodies. J Pharm Sci 2011, 100(6), 2120-35.

[191] Schwab, K. and Hesse, F., Estimating Extrinsic Dyes for Fluorometric Online Monitoring of Antibody Aggregation in CHO Fed-Batch Cultivations. Bioengineering (Basel) 2017, 4(3).

[192] Kayser, V., Chennamsetty, N., Voynov, V., Helk, B. and Trout, B.L., Conformational stability and aggregation of therapeutic monoclonal antibodies studied with ANS and Thioflavin T binding. MAbs 2011, 3(4), 408-11.

[193] Demeule, B., Gurny, R. and Arvinte, T., Detection and characterization of protein aggregates by fluorescence microscopy. Int J Pharm 2007, 329(1-2), 37-45.

[194] Menzen, T. and Friess, W., High-Throughput Melting-Temperature Analysis of a Monoclonal Antibody by Differential Scanning Fluorimetry in the Presence of Surfactants. Journal of Pharmaceutical Sciences 2013, 102(2), 415-28.

[195] McClure, S.M., Ahl, P.L. and Blue, J.T., High Throughput Differential Scanning Fluorimetry (DSF) Formulation Screening with Complementary Dyes to Assess Protein Unfolding and Aggregation in Presence of Surfactants. Pharm Res 2018, 35(4), 81.

[196] Kayser, V., Chennamsetty, N., Voynov, V., Helk, B., *et al.*, A screening tool for therapeutic monoclonal antibodies: Identifying the most stable protein and its best formulation based on thioflavin T binding. Biotechnol J 2012, 7(1), 127-32.

Chapter 4

Design of a Microfluidic Mixer Channel: First Steps into Creating a Fluorescent Dye-based Biosensor for mAb Aggregate Detection

A major challenge in the transition to continuous biomanufacturing is the lack of process analytical technology (PAT) tools which are able to collect real-time information on the process and elicit a response to facilitate control. One of the critical quality attributes (CQAs) of interest during monoclonal antibodies production is aggregate formation. The development of a real-time PAT tool to monitor aggregate formation is then crucial to have immediate feedback and process control. Miniaturized sensors placed after each unit operation can be a powerful solution to speed up an analytical measurement due to their characteristic short reaction time. In this work, a micromixer structure capable of mixing two streams is presented, to be employed in the detection of mAb aggregates using fluorescent dyes. Computational fluid dynamics (CFD) simulations were used to compare the mixing performance of a series of proposed designs. A final design of a zigzag microchannel with 45^0 angle was reached and this structure was subsequently fabricated and experimentally validated with colour dyes and, later, with a FITC-IgG molecule. The designed zigzag micromixer presents a mixing index of around 90%, obtained in less than 30 seconds. Therefore, a micromixer channel capable of a fast and efficient mixing is hereby demonstrated, to be used as a real-time PAT tool for a fluorescence based detection of protein aggregation.

Published as: São Pedro, M. N., Santos, M.S., Eppink M.H.M., & Ottens, M. (2022), *Design of a microfluidic mixer channel: First steps into creating a fluorescent dye-based biosensor for mAb aggregate detection*, Biotechnology Journal, 18, e2200332 (https://doi.org/10.1002/biot.202200332)

4.1. INTRODUCTION

In recent years, the biopharmaceutical industry has demonstrated a growing interest in implementing continuous biomanufacturing, especially for the production of monoclonal antibodies (mAbs) [1, 2]. The expiration of mAb patents held by the biopharmaceutical companies and, subsequently, the rise of biosimilars has led to the need of reducing manufacturing costs [1, 2]. However, A major challenge which still needs to be tackled to implement continuous bioprocessing is the development of process analytical technologies (PAT) [3]. By creating at-line sensors which can provide a real-time measurement of product critical quality attributes (CQAs), PAT will provide control within a continuous process and elicit a timely response [1]. To perform an entire process in a continuous mode, all the unit operations need to be fully integrated and controlled. Analytical techniques implemented must then provide real-time information of each unit operation to gain control and elicit a timely response [1, 4]. The implementation of PAT has the potential to tackle these analytical shortcomings by creating at-line sensors which can provide a real-time measurement of product critical quality attributes (CQAs) [1]. Product aggregation, a poorly understood phenomenon, is considered a critical CQA in the manufacturing of mAbs. In the final formulation of the biopharmaceutical, aggregates may lead to an increase in adverse immune response or a decrease in efficacy [5]. Several environmental and process factors are known to induce aggregation, such as the low pH employed during the viral inactivation step [4] or the shear stress induced from pumps [5]. Therefore, the formation of high molecular weight (HMW) species is unavoidable and the measurement of this CQA is crucial to elicit a real-time control of the aggregation inducing factors.

Several analytical techniques are available for the study and characterization of protein aggregates such as dynamic light scattering or Raman spectroscopy [6]. However, these techniques are characterized by lengthy analysis times [1, 7]. Fluorescent dyes, such as SYPRO Orange and 4-4-bis-1-phenylamino-8-naphthalene sulfonate (Bis-ANS), are sensitive to the hydrophobicity of the surrounding environment. Since aggregate formation generates hydrophobic unfolded protein structures, these fluorescent tags can be used to rapidly detect this phenomenon [8-10]. The dye's fluorescence intensity significantly intensifies when in the contact to the hydrophobic patches, providing a straightforward and instantaneous measurement [3]. Fluorescent dyes can be used as a stand-alone characterization method [10, 11] or in combination with other analytical techniques [12] for a rapid measurement,

demonstrating the great potential of applying it in a PAT tool. Miniaturized sensors are considered to be a possible solution to speed up the analytical measurements of CQAs due to the inherent short operation time [3]. Additionally, microfluidic chips are characterized by the use of minimal amounts of samples (in the μL or nL-scale) and, depending on the material, being relatively affordable and easily fabricated [13]. Therefore, by combining the advantages of fluorescence-based methods with the miniaturization of analytical technologies, a miniaturized tool for real-time detection of mAb aggregates can be achieved, with the microfluidic device working at-line.

When designing a fluorescent dye-based miniaturized sensor, a major problem arises: the fluorescent dye stream needs to be fast and efficiently mixed with the mAb sample stream. The small characteristic dimensions of such sensors combined with the low fluid velocities typically used leads to low Reynolds numbers (Re) and, consequently, to the presence of a laminar flow regime [14]. In such regimes, fluids flow in parallel layers, with no disruption, and mixing is dominated by molecular diffusion, an inherently slow process. Therefore, to preserve the small dimensions of microfluidic devices and to increase their throughput, it is essential to increase the contact area of the fluidic layers and induce chaotic advection to obtain the necessary fast and efficient mixing [15, 16]. Several strategies have been used to enhance the mixing efficiency in laminar flow regimes, including the passive mixing methods [16, 17]. Passive mixing is accomplished by altering the structure or configuration of microfluidic channels [3], such as using distinct zigzag angles [18], serpentine configurations [14, 19] or the incorporation of obstructions in the middle of the channel [20]. The simple design, fabrication and operation of the microfluidic chips employing passive methods [14] make them the preferred approach. Even though many passive micromixers have been reported in literature, the mixing performance of the devices was determined under dissimilar conditions from those required for a fluorescent dye-based sensor. A screening of possible geometries and, subsequently, its mixing efficiency must then be performed, taking into account the characteristics of the fluorescent dye and the mAb streams.

In the present study, the development of a micromixer channel to mix a fluorescent dye with a mAb stream is demonstrated, to potentially be used as real-time aggregate detection tool. First, the design of a passive mixing channel employing different geometries to induce the mixing of two streams is discussed. To study the mixing efficiency of each proposed design, a computational fluid dynamic (CFD) model was developed. From all the assessed geometric configurations, a zigzag channel with a

45⁰ angle, providing a residence time of 30 seconds, showed the highest mixing efficiency. The proposed zigzag mixing channel is experimentally validated, first, resorting to colour dyes, and then to a fluorescent tagged IgG molecule (FITC-IgG).

4.2. MATERIALS AND METHODS

Poly(dimethylsiloxane) (PDMS) was purchased as a Sylgard 184 elastomer kit (Dow Corning, Midland, MI, USA). Standard food colorant dyes (blue and yellow dyes) were obtained from Jo-La (Bharco Foods B.V., Diemen, The Netherlands). IgG from human serum conjugated with the fluorescent dye FITC was acquired from Sigma-Aldrich (Sigma-Aldrich Chemie BV, Zwijndrecht, The Netherlands). Sodium phosphate monobasic dehydrate, di-sodium hydrogen phosphate and sodium chloride were purchased from Sigma-Aldrich, Merck (Merck KGaA, Darmstadt, Germany) and VWR Chemicals (VWR International, Radnor, PA, United States), respectively.

4.2.1. MICROFLUIDIC STRUCTURE DESIGN

Four micromixers with different geometries were designed in AUTOCAD® (Version 23.0): a zigzag, a curved serpentine, a square serpentine and a straight T-mixer channel (**Figure 4.1**). All designed micromixers display two inlets from which the working fluids are supplied separately. The two inlets are connected by a T-joint that leads the fluids to the mixing channel, which, at the end, is also connected to a straight channel, the outlet channel, through which the mixed fluids exit the device. Additionally, geometric variations of the zigzag micromixer were explored, varying the zigzag angle, ϕ, at 30⁰, 45⁰, 60⁰ and 82⁰.

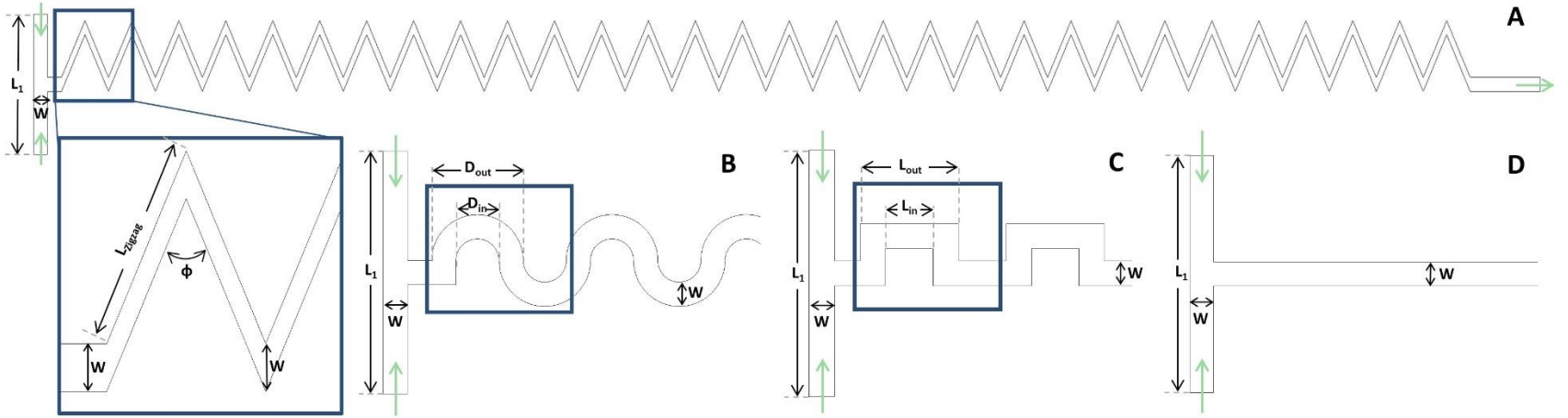

*Figure 4.1 - Schematic representation of the designed passive mixing structures, each with 30 mixing units and a total length of the mixing channel of around 26.25 mm: **A)** Zigzag channel, with φ=45⁰; **B)** Curved serpentine; **C)** Square serpentine and **D)** T-mixer. The description and value of each parameter can be found in Table 1. In blue, the mixing unit from each designed structure is highlighted. The green arrows indicate the flow of both liquids entering in the two inlets and the resulting mixed liquid exiting in the outlet.*

4.2.2. Numerical Simulations

4.2.2.1. Numerical Model

Commercial CFD software COMSOL Multiphysics (Version 5.6) was employed to analyse the flow patterns and mixing behaviour inside the designed micromixers. Two interfaces, *Laminar Flow* and *Transport of Diluted Species*, were utilized, with the multiphysics node *Reacting Flow, Diluted Species* applied to couple the interfaces (**Figure 4.2**). The *Laminar Flow* interface was used to compute the velocity and pressure fields by solving the Navier-Stokes and continuity equations. The fluid was assumed to be Newtonian and the flow incompressible, laminar and at steady-state, and can be expressed as:

$$\rho(v \cdot \nabla)v = \nabla \cdot [-pI + \mu(\nabla v + (\nabla v)^T)] \quad \textbf{(1)}$$

$$\rho\nabla \cdot (v) = 0 \quad \textbf{(2)}$$

where ρ is the density, v is the velocity, p is the pressure, I is the identity matrix and μ is the dynamic viscosity of the fluid. The velocity field obtained was then used to calculate the concentration field using the *Transport of Diluted Species* interface, which solved the convention-diffusion equation:

$$\nabla \cdot (D_c \cdot \nabla c) = v \cdot \nabla c \quad \textbf{(3)}$$

where D_c is the diffusion coefficient and c is the concentration. To solve **Equations (1)**, **(2)** and **(3)**, the following boundary conditions were set: 1) the velocity and mass flux are zero at the walls of the channel; 2) the fluid velocity and concentration at the inlets are defined; and 3) the static pressure at the outlet was set to zero. Since the *Laminar Flow* interface is used to simulate single-phase fluids, a single input of density and of viscosity had to be used. However, both fluids used in the study had dissimilar values of density and viscosity. Thus, density and viscosity of the mixed fluid were defined, at each point of the channel, as a function of the fraction of fluid supplied at inlet 1 present at that point ($f_{inlet1,i}$):

$$\rho_{fluid} = \rho_{inlet1} \cdot f_{inlet1,i} + \rho_{inlet2} \cdot (1 - f_{inlet1,i}) \quad \textbf{(4)}$$

$$\mu_{fluid} = \mu_{inlet1} \cdot f_{inlet1,i} + \mu_{inlet2} \cdot (1 - f_{inlet1,i}) \quad \textbf{(5)}$$

The multiphysics node *Reacting Flow, Diluted Species* was then used to couple the concentration field, obtained from the *Transport of Diluted Species* interface, as an input to the *Laminar Flow* interface, to compute the value of $f_{inlet1,i}$.

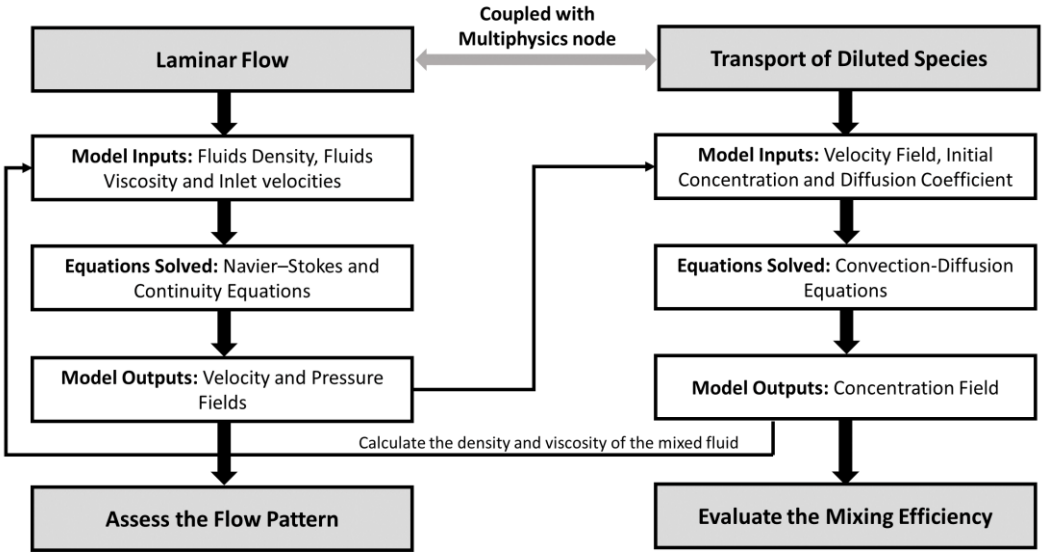

Figure 4.2 - Schematic representation of the numerical model developed to analyze the flow pattern and mixing efficiency of the designed micromixers, with the interfaces adopted and their inputs and outputs.

Since COMSOL Multiphysics is based on the finite element method (FEM), the designed structures needed to be divided into a mesh comprised of a number of small units of simpler shapes. The structures were then discretized using quadrilateral and triangular elements. Grid independence tests were carried out with different numbers of mesh elements. For the initial studies into the different geometries, to save computational time and power, a mesh of 1.22×10^5, 2.73×10^5, 3.31×10^5 and 2.53×10^5 elements were selected for the T-Mixer, Square Serpentine, Curved Serpentine and Zigzag Channel, respectively. For the angle variation studies in the zigzag micromixer, a mesh of 1.68×10^5, 2.50×10^5 and 3.18×10^5 elements for ϕ of 30^0, 45^0 and 60^0, were chosen, respectively.

The mixing index (MI) of each proposed micromixer was evaluated based on the standard deviation of the concentration at a given cross section [21]:

$$MI = 100\% - \frac{\sigma}{\sigma_{max}} = \frac{\sqrt{\sum_{i=1}^{N}(c_i - c_m)^2}}{\sqrt{\sum_{i=1}^{N}(c_0 - c_m)^2}} \quad (6)$$

where σ is the standard deviation of the point concentration to the optimal concentration at a given cross section, σ_{max} is the standard deviation of the concentration at a completely unmixed section, c_i is the concentration at a sample point i, c_m is the optimal concentration ($50\ g\ L^{-1}$), c_0 is the point concentration at a

completely unmixed cross section (0 or 100 $g\ L^{-1}$) and N is the total number of sampling points. MI will thus vary between 0, totally unmixed state, and 100%, completely mixed state.

4.2.2.2. Model Implementation

Firstly, with the proposed numerical model, all the designed micromixers were tested for the mixing efficiency, using two-dimensional (2D) numerical simulations. An aqueous mAb solution and a highly diluted fluorescent dye solution were used as the working fluids for the numerical analysis. A density of 998 $kg\ m^{-3}$ and a viscosity of $1.01 \times 10^{-3}\ Pa \cdot s$ were applied for the fluorescent dye solution [22]. For the mAb solution, a density of 1037 $kg\ m^{-3}$ [23], a viscosity of $6 \times 10^{-3}\ Pa \cdot s$ [24], a diffusion coefficient of $1.5 \times 10^{-11}\ m^2\ s^{-1}$ [24] and a concentration of 100 $g\ L^{-1}$ were assumed. Since no mAb is present in the fluorescent dye stream, its concentration was defined at zero. Different ranges of both inlet velocities were employed, ranging from 1×10^{-5} to $1 \times 10^{-2}\ m\ s^{-1}$.

The numerical model was also used for three-dimensional (3D) numerical simulation for the zigzag structure with $\phi = 45^0$. The height of the microchannel was defined at 100 µm. The previously described proprieties for the mAb and fluorescent dye solutions were used as working fluids. Both inlet velocities were set to $1 \times 10^{-3}\ m\ s^{-1}$ and a mesh with 3.28×10^6 elements was selected to perform this study.

Additionally, a parametric study was performed for the zigzag structure with $\phi = 45^0$, using multiphysics study type *Parametric Sweep* and *All combinations* as the type of sweep. The 3D numerical model was used, with the same defined variables, except for the viscosity and density of the mAb solution. The set of mAb solutions viscosities used were: 2×10^{-3}, 4×10^{-3}, 6×10^{-3} and $8 \times 10^{-3}\ Pa \cdot s$. For the diffusion coefficient, the values studied were: 1×10^{-11}, 5×10^{-11}, 7.5×10^{-11} and $10.5 \times 10^{-11}\ m^2\ s^{-1}$. Since *All combinations* was selected as the type of sweep, the model was solved for all combinations of viscosity and diffusion coefficient values, with a mesh of 8.50×10^5 elements.

4.2.3. Experimental Validation

4.2.3.1. Structure Fabrication

Two microfluidic devices were fabricated: a T-mixer straight microchannel (100 µm high x 100 µm wide x 26.3 mm long) and a zigzag microchannel (100 µm high x 100 µm wide x 17.2 mm long) with two inlets and one outlet (each 100 µm wide). The designed

mold was ordered from INESC Microsystems and Nanotechnologies (Lisbon, Portugal) and the structures were fabricated using a 7:1 mixture of PDMS and curing agent. After being degassed, the mixture is poured onto the mold and baked at 80^{0}C for 45 minutes. After the PDMS is cured, the chip is removed from the mold and the inlets and outlet are punched. Finally, the PDMS chip is bonded to a glass substrate and sealed with a 20:1 mixture of PDMS to curing agent.

4.2.3.2. Color Dyes and FITC-IgG

A syringe pump KD Scientific 200 (KD Scientific Inc, Holliston, MA, United States) was used to pump in two different streams into the microfluidic structure, with a flow rate of 1 µL min^{-1}. Firstly, the micromixer was validated using two color dyes (blue and yellow), and then with a fluorescent tagged IgG molecule (FITC-IgG) and a buffer solution (50 mM sodium phosphate buffer, 150 mM sodium chloride, pH 7.2, prepared in Milli Q water). FITC-IgG was diluted to a concentration of 5 mg mL^{-1} with the same buffer. An inverted fluorescence microscope (Leica DMI 5000 M, 10× objective, Leica Microsystems BV, The Netherlands) and a digital camera (Leica DFC300 FX, Leica Microsystems BV, The Netherlands) were used for the acquisition of bright field and fluorescence images. The fluorescence images of FITC-IgG were obtained by using a Leica L5 filter cube (excitation: BP 460-488 nm; emission: 502-547 LP nm). All the acquired images were processed and analyzed using Image J.

The mixing efficiency was then analyzed based on the color RGB (red, green and blue) components of the images obtained. For the color dye validation, the image was split and each generated image measured according to a grayscale (the value of each pixel is a single sample representing the amount of light, varying from 0, completely black, to 255, completely white). A circular region of interest (ROI), with a radius of 15 µm, was selected after each mixing unit, in the blue stream, and the color intensity measured. To quantify the color yellow, the green and red measurements were added, and the color blue corresponds to the blue measurement. Considering the blue color, the MI can then be calculated:

$$MI = 100\% - (\%B_{left} - D_{mixed}) \quad (7)$$

where $\%B_{left}$ is the amount of blue present in the ROI and D_{mixed} is the difference of blue to yellow in a 1:1 mixture, which was determined to be 0. Therefore, **Equation (7)** can be rewritten:

$$MI = 100\% - \left(\frac{B_{image} - Y_{image}}{B_{unmixed}} \times 100\%\right) \quad (8)$$

where B_{image} is the amount of blue measured in the ROI, Y_{image} is the amount of yellow measured in the ROI and $B_{unmixed}$ is the amount of blue in an unmixed state, measured in the beginning of the channel. For the FITC-IgG validation, a similar approach was followed for the selection of the ROI. However, since only the green color had to be taken into account, the MI was calculated according to:

$$MI = 100\% \times \frac{G_{buffer}}{G_{mixed}} \quad (9)$$

where G_{buffer} is the amount of green in the ROI of the buffer stream and G_{mixed} is the amount of green in the ROI in a 1:1 mixture of fluorescent dye to buffer.

4.3. Results and Discussion

4.3.1. Design of the Microfluidic Channel

When developing a real-time miniaturized PAT tool for aggregate detection, critical criteria should be fulfilled by the designed structure for a straightforward implementation in a continuous process: 1) the micromixer must not alter the amount of aggregates present in the initial sample; 2) the designed structure should provide high mixing efficiency, with a settled minimum efficiency of 90%; 3) to facilitate process control, the microfluidic device has to provide a fast measurement (within a time range of seconds to a few minutes). Additionally, it is also beneficial that the designed micromixer is simple and easily fabricated, as well as presenting reduced footprint, to allow a smoother implementation. Therefore, considering the imposed criteria, four different microchannel geometries were assessed: a straight T-mixer channel, a square serpentine, a curved serpentine and a zigzag channel (**Figure 4.1**). The mixing length of each of the proposed designs was fixed at around 27 mm, with a total of 30 mixing units. The dimensions of each mixing unit were defined in order to meet this total mixing length (**Table 4.1**) to guarantee that the mixing is dependent not only on the length but also on the flow patterns induced by the different geometries. Furthermore, the T-mixer was also designed as a control to determine to what extent mixing was dependent on the mixing length.

Table 4.1 - Description and the value of the several geometric parameters used in the designed structures (identified in Figure 4.1). The value of the parameter was kept constant in all designed structures, except for φ which was also varied at 82⁰, 60⁰ and 30⁰ a).

Parameter	Description	Measure
L_1	Transverse length of the T-junction	1000 μm
W	Width of the main channel	100 μm
L_{Zigzag}	Length of the zigzag channel diagonal	440 μm
$\Phi^{a)}$	Angle of the zigzag channel	45^0
D_{in}	Diameter of the inner walls of the curved serpentine	180 μm
D_{out}	Diameter of the outer walls of the curved serpentine	380 μm
L_{in}	Length of the inner walls of the square serpentine	190 μm
L_{out}	Length of the outer walls of the square serpentine	390 μm

Firstly, to perform a comparative analysis of each microchannel geometry, and subsequently, its mixing efficiency, a CFD model was developed. Resorting to COMSOL Multiphysics, two interfaces, Laminar Flow and Transport of Diluted Species, were employed, with the multiphysics node Reacting Flow, Diluted Species coupling the interfaces (Figure 4.2). These numerical simulations were conducted under conditions that mimic those found in practice for the detection of mAb aggregates. Since the fluorescent dye solutions commonly used to analyse aggregates are highly diluted, the proprieties of water at 20⁰C were used [22]. The mAb solution was considered to have the composition commonly found in the formulation step, high protein and low excipients concentrations, with a mAb concentration of 100 $g\ L^{-1}$ being employed. Then, the properties of the mAb solution (diffusion coefficient, viscosity and density) were based on this concentration [23, 24] chosen to test the designed structures under the most unfavourable conditions.

To compare the mixing performance of the proposed designs, the MI at the end of each mixing channel was calculated (**Equation (6)**) and is shown in Figure 4.3**A**. A wide range of inlet velocities, from 1×10^{-5} to $1 \times 10^{-2}\ m\ s^{-1}$, was used to assess its impact on the mixing efficiency, resulting in a Reynolds number (Re) ranging from 3×10^{-4} to 0.3. At low velocities (and subsequently low Re), viscous forces are dominant. Consequently, the strength of the secondary flows is not sufficient to significantly disturb the parallel fluid layers and mixing is solely dominated by molecular diffusion. Thus, the high MI observed for lower velocities across all structures is due to longer residence times and larger contact areas. As the inlet velocities and Re increases, a decrease in the MI is observed due to shorter retention

times and, thus, less efficient molecular diffusion. These parallel fluid layers are represented in the T-mixer velocity arrow plot obtained from COMSOL (**Figure 4.3B**), where it is possible to observe the fluid flowing in parallel without any path crossing. By analysing the remaining arrow plots (**Figure 4.3C-E**) at the velocity of $1 \times 10^{-3}\ m\ s^{-1}$, the designed structures presented regions where the parallel layers were disturbed and the streams path crossed. For example, the zigzag structure (**Figure 4.3E**) showed a disturbance area next to the corner of the structure. Likewise, the square serpentine structure (**Figure 4.3C**) exhibited several disturbance regions near the turns. These path crossing areas were then responsible for increasing the MI since they increase the contact area between the fluids. Because these areas were more pronounced in the square serpentine, followed by the zigzag and lastly by the curved serpentine (**Figure 4.3D**), it was expected the mixing efficiency would follow the same order. However, the square serpentine showed a lower MI. The presence of more predominant void areas (in blue) is observed, where the fluid is not able to reach. These void areas might counterbalance the path crossing phenomenon, especially at higher velocities. The curved serpentine, where the void areas are almost negligible, presents a higher MI than the square serpentine. Thus, the mixing in the designed structures will depend on the balance of these two phenomena, the presence of path crossing and void areas in the channel. The zigzag structure was more efficient because the presence of void volumes was more favourably counterbalanced by the presence of path crossing regions, having a MI of at least 90% at all tested velocities. Therefore, this zigzag geometry will then be explored to further increase its mixing efficiency.

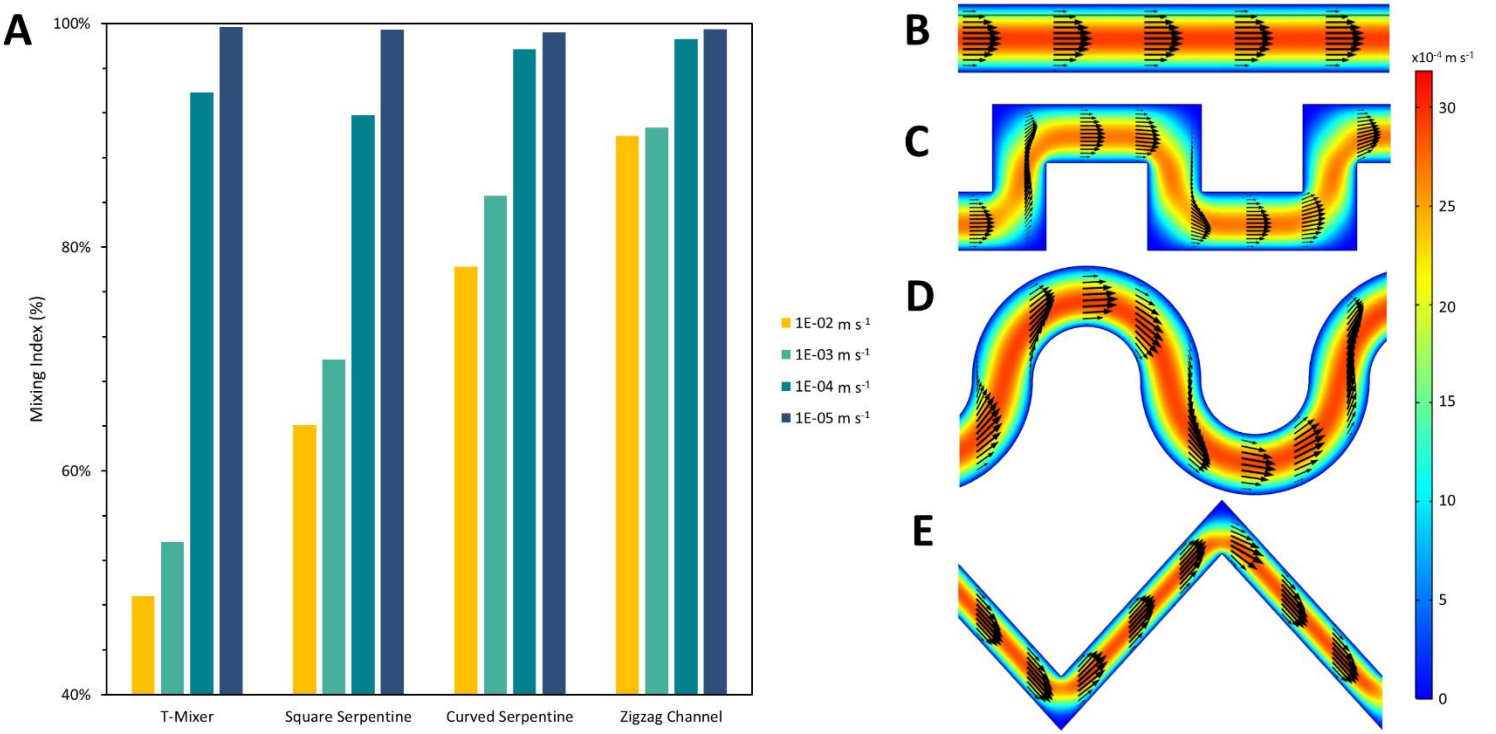

*Figure 4.3 - **A)** Mixing index of each of the passive micromixers, with 30 mixing units, at the exit of the channel, with different velocities defined at both inlets: 1×10^{-2}, 1×10^{-3}, 1×10^{-4} and 1×10^{-5} $m\,s^{-1}$, with a Reynolds number varying from 3×10^{-4} to 0.3. Velocity arrow plots obtained from COMSOL, in the last mixing unit, at $v = 1 \times 10^{-3}$ $m\,s^{-1}$: **B)** T-mixer; **C)** Square Serpentine; **D)** Curved Serpentine; and **E)** Zigzag channel ($\varphi = 82^0$).*

To further manipulate the two aforementioned mixing phenomena and enhance the MI, variations in the zigzag angle were performed, ranging from the initial 82º to 30º. From **Figure 4.4E**, by decreasing the angle to 45º, a higher MI is obtained compared to the initial 82º, especially at higher velocities. The decrease in the path crossing area is then more favourable to induce the mixing, even though the void area of the corner increases (**Figure 4.4A**, **C**-**D**). When decreasing the zigzag angle to 30º angle, the MI slightly drops. The increase on the void area is no longer counterbalanced by the increase in the flow disturbance area (**Figure 4.4B**). When comparing the MI reached with 45º and 60º angles, only a 1% difference is encountered at all velocities tested. Although the 60º angle presents a slightly higher MI, the 45º angle presents a smaller footprint structure, an important imposed design criteria. Hence, the zigzag channel with a 45º angle will be the design selected to create this fluorescent dye-based PAT tool.

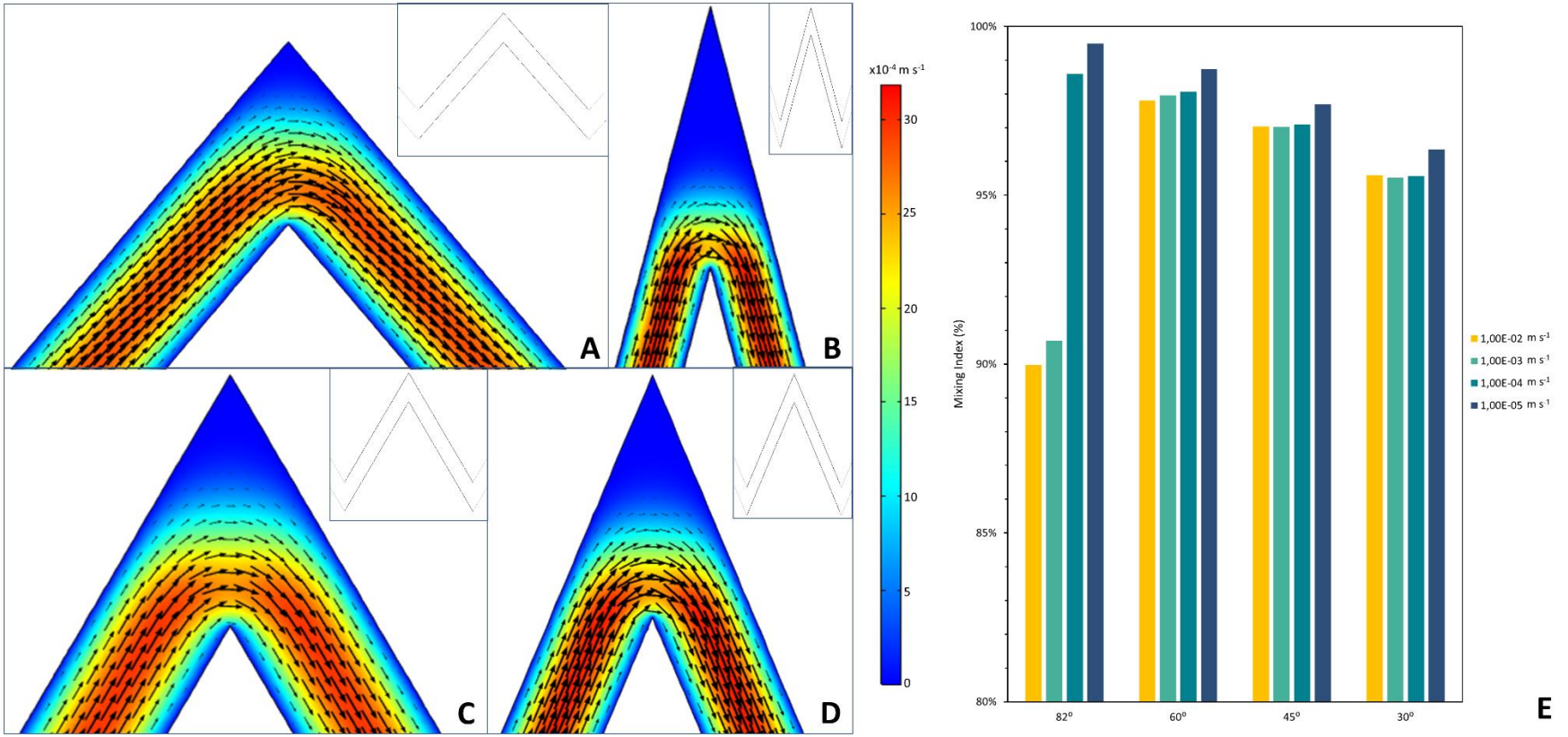

Figure 4.4 - Geometric variation of the angle, φ, and the corresponding velocity arrow plots obtained from COMSOL, in the last mixing unit, at $v = 1 \times 10^{-3}\ m\ s^{-1}$*: **A)** 82°; **B)** 30°; **C)** 60°; and **D)** 45°. **E)** Mixing index of each of the geometric variations, with 30 mixing units, at the exit of the channel, with different velocities defined at both inlets:* 1×10^{-2}, 1×10^{-3}, 1×10^{-4} *and* $1 \times 10^{-5}\ m\ s^{-1}$.

4.3.2. 3D Simulations

The CFD model was firstly developed and implemented in 2D since it demands less computational resources and time than its 3D counterpart. Thus, the 2D simulations were used as a screening tool into mixing efficiency of the different geometries, while the more physically accurate 3D simulations were used to confirm the previously obtained results. A velocity of $1 \times 10^{-3}\ m\ s^{-1}$ was used since fluid velocities of this order of magnitude are commonly used in microfluidic devices [16, 17]. The results obtained for the MI in the 3D simulations are present in **Figure 4.5A** (■). At the exit of the structure, a slightly higher MI of approximately 98% was obtained, when compared to 97% of the 2D simulations. This difference might be due to the extra dimension of the height of the channel taken into account in the 3D simulations. Thus, the path crossing of both fluids also occurs vertically, providing better and faster mixing. Additionally, in the 3D simulations, the MI of 98% is already achieved after the 5th mixing unit. Then, based on the 3D simulations, the final zigzag structure can have less than 30 mixing units. Nevertheless, the MI obtained is solely based on CFD simulations. Thus, these results have to experimentally validated and the selection of the optimal number of mixing units should be based on the latter.

Other design requirements were also evaluated with the 3D model. The shear rate which the mAb molecule would be subjected to in the microchannel was addressed since one of the design requirements is that the structure itself must not affect the amount of aggregates. According to the 3D simulations, the shear rate which the fluid is exposed to was below $1.76 \times 10^{3}\ s^{-1}$. Bee *et al.* [25] exposed highly concentrated mAb solutions to shear rates between 2×10^{4} and $2.5 \times 10^{5}\ s^{-1}$ for 5 minutes. No aggregation in the stressed samples were detected by several analytical techniques (dynamic light scattering, analytical ultracentrifugation, etc.). Hence, the structure, which calculated a lower shear rate, is not expected to change the sample's level of aggregation.

Pressure drop, the difference of pressure in the beginning and in the end of the mixing channel, was also evaluated within the microchannel to assess the integrity of the device. A pressure drop of $4.5 \times 10^{3}\ Pa$ across the structure was calculated. Therefore, the pressure drop was sufficiently small for cheap fabrication materials, like PDMS, to be used without jeopardizing the integrity of the structure during its operation.

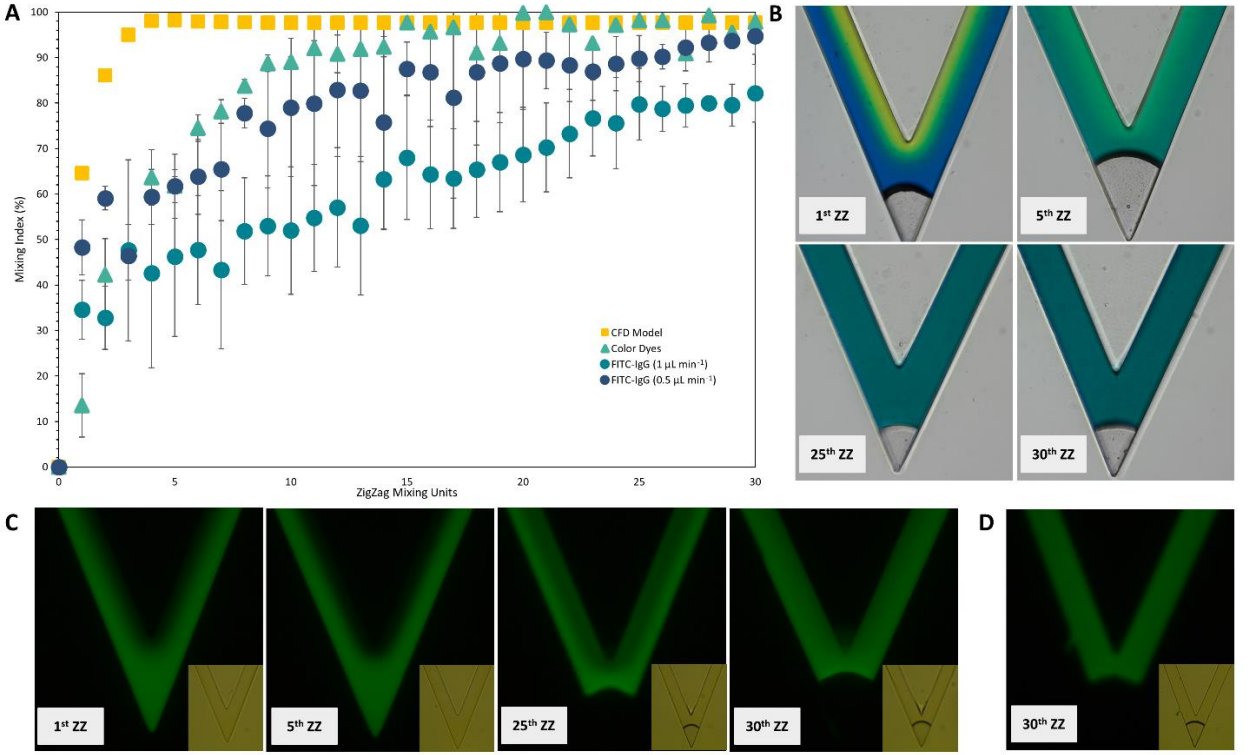

Figure 4.5 - ***A)*** *Comparison of the mixing index obtained from the 3D CFD model ( ), the experimental validation using color dyes ( ), and using the FITC-IgG molecule, at a flow rate of 1 µL min^{-1} and 0.5 µL min^{-1} (and , respectively). All experimentally measured MI values are the average of two experiments and the error bars represent the standard deviation (±SD).* ***B)*** *Bright field microscope images from the experimental validation of the zigzag channel using color dyes, from the 1st, 5th, 25th and 30th zigzag unit, acquired with the objective 10x.* ***C)*** *Fluorescence microscope images from the experimental validation of the zigzag channel using FITC-IgG, at a flow rate of 1 µL min^{-1}, from the 1st, 5th, 25th and 30th zigzag unit, acquired with the objective 10x, exposure time of 50 ms and gain 0.* ***D)*** *Fluorescence microscope images from the experimental validation of the zigzag channel using FITC-IgG, at a flow rate of 0.5 µL min^{-1}, from the 30th zigzag unit, acquired with identical conditions to* ***C)****.*

The mixing length (L_{mix}) of 26.25 mm was also determined based on the following equation:

$$L_{mix} = 2 \times N_{MU} \times L_{zigzag} \quad \textbf{(10)}$$

where N_{MU} is the number of mixing units, 30, and L_{zigzag} is the length of the zigzag channel diagonally (Table 4.1). Knowing the mixing length, the mixing time can be calculated, taking also into account the length of the T-junction and velocity used. A mixing time (t) of 27.5 seconds was achieved for the designed structure, showing that it is not only able to provide a high mixing efficiency, but also a fast measurement in the time range of seconds.

Lastly, one imposed requirement was a reduced footprint of the micromixer, which was determined using the mixing length and amplitude of the zigzag angle. A 10.75 mm^2 footprint was calculated, satisfactory for a passive mixer, which normally ranges from a few mm^2 to cm^2 [26].

4.3.3. Parametric Studies

The excipients typically found in mAb formulations may impact the fluid properties. Additionally, the micromixer can be used in other steps of the mAb manufacturing process, where the mAb solution properties will differ from those previously chosen in the CFD simulations. Plus, different mAbs typically present quite disparate transport properties [24]. A robust structure which can provide rapid and efficient mixing over a broad range of mAb solutions conditions is then crucial. Therefore, to take into consideration the impact of different excipients and solution properties, a parametric study for the MI was performed to cover a wide range of conditions. The viscosity was varied between 2×10^{-3} and 8×10^{-3} $Pa \cdot s$ and the diffusion coefficient between 1×10^{-11} and 10.5×10^{-11} $m^2\ s^{-1}$, values found in literature [24, 27, 28]. The MI obtained for all the assessed values, viscosity and diffusion coefficient, can be found in Table 4.2. The mixing efficiency is mainly dependent on the viscosity: solutions with lower viscosities reached higher MI values. At higher viscosities, some parts of the structure were unavailable and, therefore, mixing was hindered in those regions. Nevertheless, only slight differences in the MI were reached, with values ranging from 97% to almost 100% for all combinations of viscosity and diffusion coefficient tested. The robustness of the mixing efficiency of the proposed structure is then demonstrated. The developed PAT tool is able to be used as an universal method to detect the formation of aggregates through all the various steps in the manufacturing process.

Table 4.2 - Mixing index obtained in the parametric study for the zigzag structure with φ = 45⁰, varying the diffusion coefficient, D_c, between 1×10^{-11} and 10.5×10^{-11} $m^2 s^{-1}$, and the viscosity, μ, between 2×10^3 and 8×10^3 Pa s, of the mAb stream properties in the 3D numerical model.

$\mu(Pa\ s)$	$D_c\ (m^2 s^{-1})$			
	1×10^{-11}	5×10^{-11}	7.5×10^{-11}	10.5×10^{-11}
2×10^3	99.94%	99.89%	99.87%	99.86%
4×10^3	98.57%	98.61%	98.63%	98.65%
6×10^3	97.83%	97.87%	97.89%	97.91%
8×10^3	97.40%	97.40%	97.42%	97.45%

4.3.4. Experimental Validation

With the final design for the micromixer achieved, a zigzag channel with a 45⁰ angle and 98% of mixing efficiency, the next step was to experimentally validate the calculated MI. Firstly, the zigzag and a T-mixer channel (with an identical mixing length) were fabricated and, resorting to standard colour dyes, the MI was experimentally validated. Blue and yellow dyes were used and the formation of green throughout the channel was analysed, with the results obtained present in **Figure 4.5A** (▲). When analysing **Figure 4.5B**, it is possible to observe the formation of the colour green throughout the mixing channel, with a perfect mixing of blue and yellow being achieved by the 25th mixing unit. Even though a MI of 98% is still reached by the end of the channel, the mixing is considerably slower. The high MI is not achieved by the 5th mixing unit (**Figure 4.5B**) as the CFD model predicted, but on the 15th mixing unit. The colour dyes possess different physical proprieties than the highly concentrated mAb solution used in the 3D simulations, explaining the slower mixing. Nevertheless, it still provides satisfying mixing and indicates that the zigzag channel is able to efficiently mix two streams. Furthermore, the T-mixer channel was also validated and was able to reach a mixing of 52%, a similar value to the one obtained in the CFD model, 54%. Mixing is then solely due to molecular diffusion in this structure, reinforcing the ability of zigzag design to enhance the mixing.

Next, the zigzag channel was experimentally validated with a fluorescent tagged IgG molecule, FITC-IgG, mixed with a buffer solution. The MI found for the FITC-IgG is described in **Figure 4.5A** (●). A MI of 86% is achieved, slightly lower than the expected value of 98%. For the FITC-IgG molecule, a degree of labelling (DoL) of 10 was calculated according to The and Feltkamp [29]. Thus, ten molecules of FITC are labelling a single molecule of IgG, which can significantly alter the physical proprieties

of the antibody [30]. This high DoL will thus lead to a different mAb molecule, with a dissimilar diffusion coefficient to the ones assessed during the simulation work, explaining the small difference encountered for the MI. Additionally, the T-mixer was also validated with the FITC-IgG molecule and a MI of 49% was determined. Therefore, even though the proprieties of the molecule can influence the characteristics of the mAb stream to be mixed, a high MI is still reached for the designed channel, proving that in fact the zigzag geometry enhances mixing. Since molecular diffusion, which is dependent on the residence time of the molecule in the channel, plays a crucial role in mixing, by reducing the flow rate, the IgG molecule will then have enough mixing time to achieve proper mixing. For example, by using a flow rate of 0.5 $\mu L\, min^{-1}$, a MI of around 95% (**Figure 4.5A** (●) and **D**) is achieved. Nevertheless, the zigzag geometry allows for the generation of some advection, by folding the laminar flow and allowing the streamlines to cross each other. The different MIs experimentally obtained for the T-mixer and for the zigzag channel clearly demonstrate the mixing efficiency provided by the latter. Therefore, the mass transport of the mAb molecule is not solely due to diffusion but also due to the path disturbance provided by the proposed geometry.

4.4. Concluding Remarks

The design and development of a miniaturized mixer for the creation of a fluorescent dye-based PAT tool for aggregate detection is here described. Resorting to a passive mixing induction, by using different geometries and subsequent variations, the mixing of two streams in the microscale is achieved. A CFD model in COMSOL Multiphysics was developed to assess the mixing efficiency of four proposed designs: a straight, a zigzag, a curved serpentine and a square serpentine channel. From the screening of the various geometries, the zigzag channel presented the highest mixing efficiency. The mixing occurs due to a balance of the presence of path crossing and void areas induced by the zigzag angle. Therefore, the zigzag channel with a 45° angle showed a high MI, of around 98%, in the 3D simulation. The design criteria imposed were all fulfilled: 1) the micromixer is expected not to alter the amount of aggregates due to the low shear rate calculated; 2) a high mixing efficiency of above 90%; is achieved; 3) a real-time measurement is accomplished in under 30 seconds. Furthermore, due to the low pressure drop and reduced footprint, the micromixer is easy to fabricate in PDMS and to operate. A wide range of mAb solutions conditions were also tested in the CFD model by varying the viscosity and diffusion coefficient to assess the robustness of the developed micromixer. A MI of at least 97% was obtained for all

combinations of conditions tested, demonstrating the capability to detect aggregates in a variety of manufacturing processes.

The final designed micromixer was then experimentally validated, first, resorting to colour dyes, and then to a fluorescent tagged IgG molecule (FITC-IgG). A MI of 98% was obtained in the end of the channel with the colour dyes, validating the mixing efficiency proposed by the CFD model. For the FITC-IgG validation, a MI of 86% was reached at the end of the channel. This lower value can be explained by the high DoL of this molecule, which can significantly impact the mAb physical proprieties [30]. Nevertheless, even though small differences are encountered between the CFD model and experimental validation (**Figure 4.5A**), the proposed zigzag channel is still able to induce mixing in a fast and efficiently manner. The next step will be to verify the capability of the proposed structure to actually detect aggregates. Due to the high affinity of the fluorescent dyes to mAb aggregates, it was assumed that if the solutions were in contact, the fluorescent dyes would instantly interact with the aggregates and a fluorescence signal would be emitted. However, this assumption still needs to be experimentally validated. Nevertheless, a simple design for providing efficient mixing of two streams under 30 seconds was hereby demonstrated.

4.5. REFERENCES

[1] São Pedro, M. N., Silva, T. C., Patil, R., Ottens, M., White paper on high-throughput process development for integrated continuous biomanufacturing. Biotechnol Bioeng 2021, 118, 3275-3286.

[2] Grilo, A. L., Mantalaris, A., The Increasingly Human and Profitable Monoclonal Antibody Market. Trends Biotechnol 2019, 37, 9-16.

[3] São Pedro, M. N., Klijn, M. E., Eppink, M. H. M., Ottens, M., Process analytical technique (PAT) miniaturization for monoclonal antibody aggregate detection in continuous downstream processing. J Chem Technol Biotechnol 2021.

[4] Walchli, R., Ressurreicao, M., Vogg, S., Feidl, F., *et al.*, Understanding mAb aggregation during low pH viral inactivation and subsequent neutralization. Biotechnol Bioeng 2020, 117, 687-700.

[5] Thomas, C. R., Geer, D., Effects of shear on proteins in solution. Biotechnol Lett 2011, 33, 443-456.

[6] Mahler, H. C., Friess, W., Grauschopf, U., Kiese, S., Protein aggregation: pathways, induction factors and analysis. J Pharm Sci 2009, 98, 2909-2934.

[7] Somasundaram, B., Pleitt, K., Shave, E., Baker, K., Lua, L. H. L., Progression of continuous downstream processing of monoclonal antibodies: Current trends and challenges. Biotechnol Bioeng 2018, 115, 2893-2907.

[8] Hawe, A., Sutter, M., Jiskoot, W., Extrinsic fluorescent dyes as tools for protein characterization. Pharm Res 2008, 25, 1487-1499.

[9] Paul, A. J., Schwab, K., Prokoph, N., Haas, E., *et al.*, Fluorescence dye-based detection of mAb aggregates in CHO culture supernatants. Anal Bioanal Chem 2015, 407, 4849-4856.

[10] He, F., Phan, D. H., Hogan, S., Bailey, R., *et al.*, Detection of IgG aggregation by a high throughput method based on extrinsic fluorescence. J Pharm Sci 2010, 99, 2598-2608.

[11] Oshinbolu, S., Shah, R., Finka, G., Molloy, M., *et al.*, Evaluation of fluorescent dyes to measure protein aggregation within mammalian cell culture supernatants. J Chem Technol Biotechnol 2018, 93, 909-917.

[12] Hawe, A., Friess, W., Sutter, M., Jiskoot, W., Online fluorescent dye detection method for the characterization of immunoglobulin G aggregation by size exclusion chromatography and asymmetrical flow field flow fractionation. Anal Biochem 2008, 378, 115-122.

[13] Sia, S. K., Whitesides, G. M., Microfluidic devices fabricated in poly(dimethylsiloxane) for biological studies. Electrophoresis 2003, 24, 3563-3576.

[14] Javaid, M. U., Cheema, T. A., Park, C. W., Analysis of Passive Mixing in a Serpentine Microchannel with Sinusoidal Side Walls. Micromachines (Basel) 2017, 9.

[15] Cai, G., Xue, L., Zhang, H., Lin, J., A Review on Micromixers. Micromachines (Basel) 2017, 8.

[16] Lee, C.-Y., Wang, W.-T., Liu, C.-C., Fu, L.-M., Passive mixers in microfluidic systems: A review. Chemical Engineering Journal 2016, 288, 146-160.

[17] Ward, K., Fan, Z. H., Mixing in microfluidic devices and enhancement methods. J Micromech Microeng 2015, 25.

[18] Tsai, C. D., Lin, X. Y., Experimental Study on Microfluidic Mixing with Different Zigzag Angles. Micromachines (Basel) 2019, 10.

[19] Rhoades, T., Kothapalli, C. R., Fodor, P. S., Mixing Optimization in Grooved Serpentine Microchannels. Micromachines (Basel) 2020, 11.

[20] Alam, A., Afzal, A., Kim, K.-Y., Mixing performance of a planar micromixer with circular obstructions in a curved microchannel. Chemical Engineering Research and Design 2014, 92, 423-434.

[21] Hashmi, A., Xu, J., On the quantification of mixing in microfluidics. J Lab Autom 2014, 19, 488-491.

[22] Perry, R. H., Green, D. W., Maloney, J. O., Perry's Chemical Engineers Handbook. McGraw-Hill 1997.

[23] Pathak, J. A., Sologuren, R. R., Narwal, R., Do clustering monoclonal antibody solutions really have a concentration dependence of viscosity? Biophys J 2013, 104, 913-923.

[24] Woldeyes, M. A., Qi, W., Razinkov, V. I., Furst, E. M., Roberts, C. J., How Well Do Low- and High-Concentration Protein Interactions Predict Solution Viscosities of Monoclonal Antibodies? J Pharm Sci 2019, 108, 142-154.

[25] Bee, J. S., Stevenson, J. L., Mehta, B., Svitel, J., *et al.*, Response of a concentrated monoclonal antibody formulation to high shear. Biotechnol Bioeng 2009, 103, 936-943.

[26] Khosravi Parsa, M., Hormozi, F., Jafari, D., Mixing enhancement in a passive micromixer with convergent–divergent sinusoidal microchannels and different ratio of amplitude to wave length. Computers & Fluids 2014, 105, 82-90.

[27] Pindrus, M. A., Shire, S. J., Yadav, S., Kalonia, D. S., The Effect of Low Ionic Strength on Diffusion and Viscosity of Monoclonal Antibodies. Mol Pharm 2018, 15, 3133-3142.

[28] Sudrik, C., Cloutier, T., Pham, P., Samra, H. S., Trout, B. L., Preferential interactions of trehalose, L-arginine.HCl and sodium chloride with therapeutically relevant IgG1 monoclonal antibodies. MAbs 2017, 9, 1155-1168.

[29] The, T. H., Feltkamp, T. E. W., Conjugation of Fluorescein Isothiocyanate to Antibodies. Immunology 1970, 18, 865 - 873.

[30] São Pedro, M. N., Azevedo, A. M., Aires-Barros, M. R., Soares, R. R. G., Minimizing the Influence of Fluorescent Tags on IgG Partition in PEG-Salt Aqueous Two-Phase Systems for Rapid Screening Applications. Biotechnol J 2019, 14, e1800640.

Chapter 5

Application of a Fluorescent Dye-based Microfluidic Sensor for Real-time Detection of mAb Aggregates

The lack of process analytical technologies (PAT) able to provide real-time information and process control over a biopharmaceutical process has long impaired the transition to continuous biomanufacturing. For the monoclonal antibody (mAb) production, aggregate formation is a major critical quality attribute (CQA) with several known process parameters (i.e. protein concentration and agitation) influencing this phenomenon. The development of a real-time tool to monitor aggregate formation is then crucial to gain control and achieve a continuous processing. Due to an inherent short operation time, miniaturized biosensors placed after each step can be a powerful solution. In this work, the development of a fluorescent dye-based microfluidic sensor for fast at-line PAT is described, using fluorescent dyes to examine possible mAb size differences. A zigzag microchannel, which provides 90% of mixing efficiency under 30 seconds, coupled to an UV-Vis detector, and using four FDs, was studied and validated. With different generated mAb aggregation samples, the FDs Bis-ANS and CCVJ were able to robustly detect from, at least, 2.5 to 10% of aggregation. The proposed FD-based micromixer is then ultimately implemented and validated in a lab-scale purification system, demonstrating the potential of a miniaturized biosensor to speed up CQAs measurement in a continuous process.

Published as: São Pedro, M.N., Eppink M.H.M., & Ottens, M. (2023), *Application of a fluorescent dye-based microfluidic sensor for real-time detection of mAb aggregates*, Biotechnology Progress, e3355, (https://doi.org/10.1002/btpr.3355)

5.1. INTRODUCTION

The creation of process analytical technologies (PAT) for fast analytics and control is still one of the major challenges to tackle when implementing continuous bioprocessing into biopharmaceutical processes. To elicit a response for fluctuations in operational conditions, in-line or at-line sensors need to be placed within the manufacturing process to provide a real-time measurement of product critical quality attributes (CQAs) [1]. A common monitored CQA is protein aggregation, especially in the biomanufacturing of monoclonal antibodies (mAbs). Even though the presence of high molecular weight (HMW) species in the final formulation can enhance immune response, their appearance is inevitable [2]. For example, the increasing protein concentration [3] and agitation [4] are known aggregation inducing factors. Hence, a PAT tool for the detection of mAb HMW species is crucial to allow to control their formation.

Fluorescent dyes (FD), such as 4-4-bis-1-phenylamino-8-naphthalene sulfonate (Bis-ANS), SYPRO Orange and Nile Red, are a widely used analytical technique to detect and study aggregation [5, 6]. These dye's fluorescence intensifies (when compared to its intensity in the presence of the monomeric mAb form) in the presence of hydrophobic unfolded protein structures, a common characteristic in aggregate formation [5]. In particular, the FD Bis-ANS binds to these hydrophobic residues through hydrophobic interactions of the aromatic rings, present in its structure [7]. Additionally, a novel class of fluorescent molecular rotors, such as Thioflavin T (ThT), 9-(2-Carboxy-2-cyanovinyl)julolidine (CCVJ) and Proteostat, have recently appeared as possible alternatives to the previously described classic probes. These molecular rotors rotate freely in solution and when their movement is restricted, these FDs emit fluorescence [8, 9]. For example, when ThT binds to amyloid fibrils (insoluble proteinaceous materials formed during protein-misfolding events), through β-sheet-rich deposits, their FD's movement is constrained and it increases dramatically its fluorescence [10]. Since both classes provide a fast, stable and straightforward result [11], these FDs can be taken into consideration when creating a real-time PAT tool to measure aggregation [12]. To further speed up the analytical measurement, miniaturized sensors are considered a promising solution. The inherent short operation time, the minimal amounts of sample (nL or μL) and the easiness of fabrication and affordability are major benefits provided by the implementation of a miniaturized PAT tool [12]. A zigzag microfluidic structure was designed and developed for a FD-based aggregate detection: this micromixer will then allow the

mixing of a mAb sample with a FD [13]. This zigzag microchannel, represented in Figure 5.1 (with its geometric measurements described in Table 5.1) provides a mixing efficiency of around 90% within 30 seconds. In total, this microchannel has 30 mixing zigzag units, adding to 26.25 mm of mixing length. Additionally, due to the low shear forces, this structure is expected not to alter the amount of aggregates during the measurement and, due to the low pressure drop, the micromixer is easy to operate and fabricate. More information on the development of this structure and its characteristics can be found in São Pedro *et al.* [13].

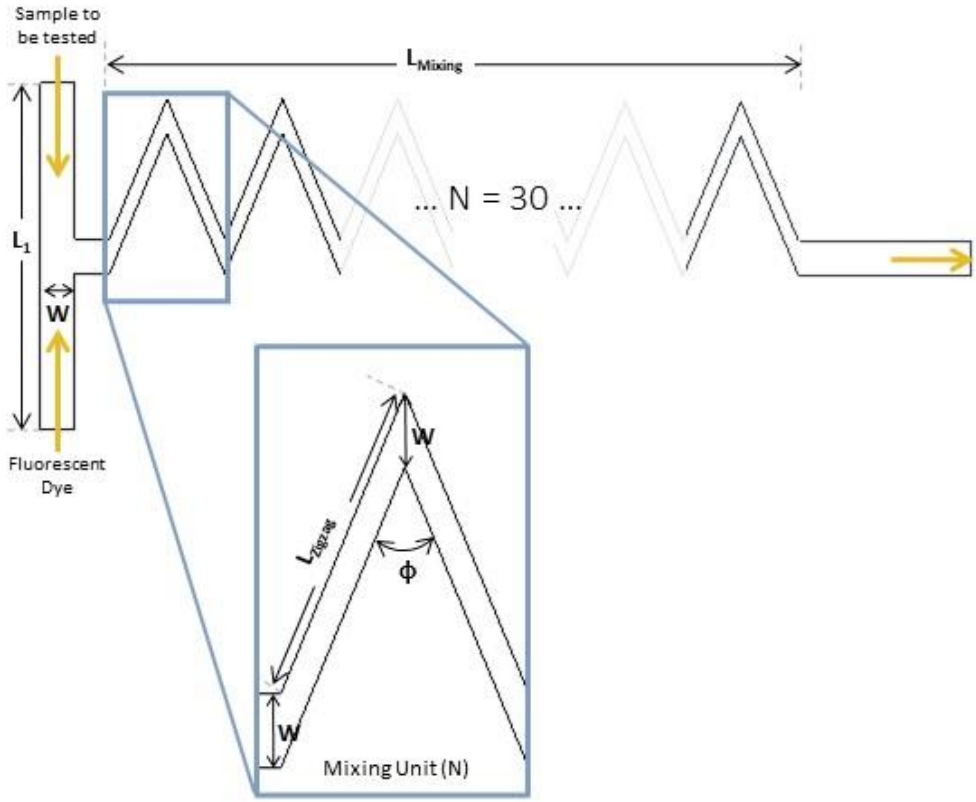

Figure 5.1 - Schematic representation of the micromixer structure, with the measurement of each parameter described in Table 5.1. In blue, the zigzag mixing unit (N) of the micromixer is highlighted, with the structure having a total of 30 N. The orange arrows indicate the flow of both liquids entering in the two inlets and the resulting mixed liquid exiting in the outlet.

Table 5.1 - Measurement of each geometric parameters used in the micromixer (identified in Figure 5.1) [13]. L1 corresponds to the transverse length of the T-junction, W to the width of the main channel, L_{Zigzag} to the length of the zigzag channel diagonal, Φ to the angle of the zigzag channel and L_{Mixing} to the mixing length, calculated based on the number of mixing units, 30, and the length of the zigzag channel diagonally.

Parameter	Measurement
L_1	1000 µm
W	100 µm
L_{Zigzag}	440 µm
Φ	45^0
L_{Mixing}	26.25 mm

Therefore, this microfluidic structure was designed to be able to produce an immediate aggregate detection in a continuous downstream process. However, this micromixer was only experimentally validated for its mixing efficiency. The ability of the proposed structure to actually detect aggregates still needs to be assessed. In this present work, firstly, a high-throughput (HT) screening of four different FDs is performed: the hydrophobic sensitive Bis-ANS and Nile Red and the molecular rotors ThT and CCVJ. The required FD concentration to be later employed in the micromixer is reached, as well as an early assessment into possible limits of detection intrinsic to each FD. After, resorting to different types of aggregates, the micromixer is used to identify aggregation using a UV-Vis detector: an increase in the UV signal is observed when aggregation is detected. Finally, the micromixer is validated in a chromatographic unit operation. Anion exchange (AEX) chromatography in an ÄKTA™ Avant unit was performed in flow-through (FT) mode to remove aggregates, with the micromixer implemented within the system. An increase in the UV signal was observed in the eluate, with the presence of aggregates later confirmed by analytical size exclusion chromatography (SEC-UPLC), while the FT (containing the product) did not produce any signal. A miniaturized FD-based PAT tool is then demonstrated, being able to robustly detect all types of aggregates which can arise in a downstream process.

5.2. Materials and Methods

Poly(dimethylsiloxane) (PDMS) was purchased as a Sylgard 184 elastomer kit (Dow Corning, Midland, MI, USA) and dimethylsiloxane-(60-70% ethylene oxide) block copolymer was acquired from Gelest (Pennsylvania, USA). Sodium phosphate monobasic dehydrate, ammonium sulphate and sodium citrate hydrate were purchased from Sigma-Aldrich (New Jersey, United States). Di-sodium hydrogen

phosphate and sodium chloride (NaCl) were bought from VWR Chemicals (VWR International, Pennsylvania, United States). Acetic acid was obtained from Fluka (Honeywell, North Carolina, United States) and citric acid from J.T. Baker (VWR International, Pennsylvania, United States). The mAb employed in this study was supplied by Byondis B.V. (Nijmegen, The Netherlands), with an isoelectric point of 8.6.

Regarding the FDs used, ThT, CCVJ and Nile Red were purchased from Sigma-Aldrich (New Jersey, United States), whereas Bis-ANS was acquired from Invitrogen (Massachusetts, United States). For the preparation of the stock solutions, the dye ThT was dissolved in MilliQ water and filtered through a 0.2 µm Whatman syringe filter (Merck, New Jersey, United States). The exact concentration was calculated from measuring the UV absorbance at 412 nm, using a molar extinction coefficient of 36 000 M^{-1} cm^{-1} [14]. Bis-ANS was dissolved in methanol (Sigma-Aldrich, New Jersey, United States) and the exact concentration calculated at 385 nm, with a molar extinction of 16 790 M^{-1} cm^{-1} [15]. Finally, CCVJ and Nile Red were dissolved in dimethyl sulfoxide (Fluka, Massachusetts, United States), and the exact concentration calculated at 440 nm and 552 nm, with the molar extinction of 25 404 M^{-1} cm^{-1} and 19 600 M^{-1} cm^{-1}, respectively [8].

5.2.1. Stressing of mAb Formulations

The provided mAb was stored at a concentration of 6 mg mL^{-1} in sodium acetate buffer, pH 4.5, at -80°C. An early characterization of this sample was performed and the presence of 4% of aggregation was detected, being referred from here on as the storage aggregates. To remove these HMW species, size exclusion chromatography (SEC) was performed on an ÄKTA™ Avant system (Cytiva, Massachusetts, United States). An HiPrep™ 16/60 Sephacryl S-300 HR column (Cytiva, United States) was used, with the elution being performed with 50 mM sodium phosphate buffer, 150 mM NaCl, pH 7.2, at a flow rate of 0.5 mL min^{-1}. The collected fraction of the purified monomer was then concentrated to 5 mg mL^{-1}, using the amicon ultra-15 centrifugal filters (Merck, New Jersey, United States).

Protein aggregation was then induced to the purified mAb solution, in 1.5 mL eppendorfs, using different types of aggregation factors such as time, temperature, low pH shift or freeze-thawing (F/T). Time aggregates were generated by storing the mAb purified sample at 4°C for, at least, 4 weeks. Temperature aggregates were induced by incubating the mAb purified sample at 75°C for 10 minutes, using a thermomixer

(Eppendorf, Hamburg, Germany) operated at 600 rpm. Low pH shift aggregates were produced by dialyzing the mAb purified sample with 50 mM sodium citrate buffer, 500 mM NaCl, pH 3, using the amicon ultra-15 centrifugal filters. F/T aggregates were generated by incubating the purified mAb sample at -80°C for one hour followed by thawing at 25°C. The freeze-thaw cycle was repeated five times.

5.2.2. Characterization of the Stressed Formulations

After the different types of aggregates were generated, an initial characterization of each sample was performed using the following analytical techniques:

5.2.2.1. SEC-UPLC

The mAb concentration and the percentage of aggregation of each stressed sample is determined by analytical SEC in an UltiMate 3000 UHPLC System (Thermo Fisher Scientific, Massachusetts, United States). 5 µL of sample was injected in an ACQUITY UPLC Protein BEH SEC 200 Å column (Waters, Massachusetts, United States) and run with the 100 mM sodium phosphate buffer, pH 6.8, for 10 minutes. The flow rate used was 0.3 mL min^{-1} and the protein was detected at 280 nm.

5.2.2.2. Hydrophobic Interaction Chromatography (HIC)

The hydrophobicity of each stressed formulation was assessed by HIC, according to Goyon *et al.* [16]. A HiTrap™ Butyl FF column (CV of 1 mL), purchased from Cytiva (New Jersey, United States), was employed. An adsorption buffer of 3.5 M ammonium sulfate and 0.1 M phosphate buffer, pH 7, and an elution buffer of 0.1 M phosphate buffer, pH 7, were used. A gradient was performed from 25 to 100% of the elution buffer in 20 CV at a flow rate of 1 mL min^{-1}.

5.2.2.3. Dynamic Light Scattering (DLS)

The presence of larger aggregates was determined by DLS, performed in Zetasizer APS with the Protein Size Standard Operating Procedure (SOP) of the Zetasizer Software (Version 8.02, Malvern Panalytical, United Kingdom). 100 µL of each of the stressed formulations were measured in a 96-well plate at the fixed angle of 90°, at a laser wavelength of 830 nm and a temperature of 25°C. The samples were measured in triplicates and each sample was measured three time by the instrument.

5.2.3. HT Screening of FDs

The HT screening of the selected FDs was performed in a Tecan EVO Freedom 200 robotic station (Tecan, Switzerland), equipped with a plate reader (InfiniTe Pro 200),

a robotic manipulator (RoMa) arm (to move microplates to the different positions) and one liquid handing arm (LiHa). Corning 96-well NBS™ microplate (Merck, New Jersey, USA), made of white polystyrene, were used for the measurement of the fluorescence emission spectra. From the FDs stock solutions previously prepared, several diluted FD solutions were prepared with MilliQ water, with the concentration range tested present in Table 5.2. Then, 100 µL of each of the generated aggregates (maintaining the concentration of 5 mg mL^{-1}) were pipetted into a well by the liquid handling robot, followed by the addition of 100 µL of the FD. Hence, a one-to-one ratio of sample to FD was used, which would be later applied in the micromixer measurements. After, the microplate is transported to the plate reader, where it is mixed at 600 rpm for 2 minutes and the fluorescence spectrum of each sample recorded according to the wavelengths described in Table 5.2. Extra blank measurements were performed where the mAb aggregate samples were replaced by buffer only. Then, the fluorescence signal recorded was subtracted from each mAb induced aggregation sample measurement to remove any buffer interference on the fluorescence signal.

Table 5.2 - FDs employed in the HT screening, with the excitation and emission wavelengths used, the concentration range tested and the determined optimal concentration.

Fluorescent Dye	Excitation Wavelength (nm)	Emission Wavelengths (nm)	Concentration Range Tested	Optimal Concentration
ThT	415	465 – 600	1 – 5 mM	1 mM
CCVJ	435	465 – 650	0.5 – 50 µM	1 µM
Bis-ANS	380	450 – 600	0.5 – 5 µM	0.5 µM
Nile Red	550	600 – 750	25 – 100 µM	75 µM

5.2.4. Aggregate Detection with the Micromixer

5.2.4.1. Structure Fabrication

The zigzag microfluidic device (100 µm high x 100 µm wide x 17.2 mm long) presents two inlets and one outlet, each 100 µm wide (Figure 5.1) [13]. The dimensions of this micromixer are also described in Table 5.1. The designed mold was ordered from INESC Microsystems and Nanotechnologies (Lisbon, Portugal) and the structures were fabricated according to Gokaltun *et al.* [17] to reduce the inherent hydrophobicity of PDMS. Dimethylsiloxane-(60-70% ethylene oxide) block copolymer, comprised of poly(ethylene glycol) (PEG) and PDMS segments (PDMS-PEG), were blended with PDMS during device manufacturing, using a 10:1:0.0025 mixture of PDMS, curing

agent and PDMS-PEG. After being degassed, the mixture is poured onto the mold and baked at 70^{0}C overnight. After the PDMS is cured, the chip is removed from the mold and the inlets and outlet are punched. Finally, the PDMS chip is bonded to a glass substrate and sealed with a 20:1 mixture of PDMS to curing agent.

5.2.4.2. UV-Vis Measurement

A syringe pump KD Scientific 200 (KD Scientific Inc, Massachusetts, United States) was used to pump both mAb sample and FD into the micromixer structure, with a flow rate of 1 µL min^{-1}. The FD concentrations used were the optimal concentrations determined in the HT screening, present in **Table 5.2**. Before starting the measurement, the UV signal is first auto-zero resorting to a solution composed of the FD with the sample buffer, with a ratio of one-to-one. The autozero is performed to eliminate any interference from the dye's intrinsic fluorescence. After the two fluids were mixed in the microstructure, the fluid is sent to an inline UV-Vis detector (SPD-20AV, Shimadzu, Kyoto, Japan) which contains a microflow cell (0.2 µL). Two wavelengths were selected to perform the measurement for each FD, taking into consideration the results previously obtain in the HT screening: CCVJ, with excitation wavelength (λ_{exc}) of 435 nm and the emission wavelength (λ_{em}) of 520 nm; ThT, with λ_{exc} of 415 nm and λ_{em} of 520 nm; Bis-ANS, with λ_{exc} of 380 nm and λ_{em} of 520 nm; and Nile Red, with λ_{exc} of 550 nm and λ_{em} of 650 nm. After the connection of the micromixer to the UV-Vis detector, the aggregation measurement starts and the UV signal is recorded until is stable for at least 10 minutes. Then, after the signal stabilization, the micromixer is disconnected from the UV-Vis detector and the UV signal is once more autozero with the FD and sample buffer mixture. This procedure was repeated for all generated aggregate samples with each of the FDs selected in this study.

5.2.4.3. AEX Validation

An ÄKTA™ Avant unit was used to perform an anion exchange chromatography (AEX) for the removal of aggregates, resorting to a 1 mL Capto™ adhere column (Cytiva, Massachusetts, United States). This system was equipped with: three pumps (pumps A, B and sample pump) with inlet valves in each to be able to select different buffers, a column valve, an outlet valve, three versatile valves, two UV monitors and a 10 mL Superloop™ (Cytiva, Massachusetts, United States). The sample pump was employed to inject the FD into the micromixer structure, using a flow rate of 3 µL min^{-1} (0.003 mL min^{-1}). The versatile valves were used to incorporate the superloop and the micromixer in the system. The superloop will collect the FT and eluate from the AEX

column, and then send it to the micromixer channel for aggregate detection. Thus, the reduction of the pump flow rate to 3 µL min^{-1} necessary for aggregate detection in the micromixer can be achieved. Additionally, two UV monitors were employed: UV1, placed after the micromixer, to detect the increase of signal due to the presence of HMW species; and UV2, placed after the column valve, to monitor the chromatographic run. The chromatography system was controlled with the research software Orbit, a control and data acquisition system developed at Lund University (Lund, Sweden). Orbit communicates with UNICORN™ and creates the necessary instructions to run a continuous process, which then sends the information to an ÄKTA™ unit. More information on the software Orbit is described elsewhere [18, 19].

The buffers and flow rates used for the AEX chromatography run were based on GE Healthcare [20], for a sample concentration of 60 mg mL^{-1}. The AEX operation was performed in flow through (FT) mode, with a mAb sample stressed by low pH induction, resulting in 6% aggregation. The selected FD was CCVJ ([CCVJ] = 1 µM, λ_{exc} = 435 nm, λ_{em} = 520 nm). Aggregate detection is performed during 60 minutes, after the collection of the FT and eluate from the AEX column in the superloop. Apart from the autozero of the UV signal, an extra phase was incorporated after aggregate detection where water is injected in the micromixer and in the connection tubes to clean and remove any remaining sample or FD.

5.3. Results and Discussion

5.3.1. Aggregate Induction and Characterization

To create the necessary aggregation PAT tool, the designed micromixer should be able to detect the widest type and size range of aggregates which can arise during a biomanufacturing process. Thus, the first part of this work was to generate a broad sample variety, with aggregates possessing different physical and chemical characteristics, resorting to different induction factors. Using a mixture of mAb aggregate samples, the FDs and the micromixer will be later tested to assess the capability to detect all types of aggregates. The provided mAb already presented 4% of aggregation, becoming the first mAb sample to be tested, the hereby named storage aggregates. Then, to remove any remaining HMW species, SEC was performed and a purified mAb sample obtained, which unsurprisingly presented 0% of aggregation. Since mAb aggregate formation depends on the type of stress used [4], protein aggregation in the purified mAb sample was then induced using a variety of aggregation factors: time, temperature, low pH shift or F/T.

The level of aggregation was determined by SEC-UPLC (Table 5.3), ranging from 2.5% (time aggregates) to 10% aggregation (low pH aggregates). Additionally, SEC allowed to detect oligomers in the size range of 1 nm to 25 nm [2], with the presence of dimers and trimers across all aggregation samples. The presence of larger aggregates was then assessed by DLS, which can detect oligomers in the size range of 10 nm to 5 µm [2]. The results obtained by this analytical technique are described in Table 5.3 and in Figure 5.S1**B**. While the monomer mAb form presents a size of 12.5 nm, all the induced aggregates exhibit HMW species with larger sizes, especially the time and F/T aggregates (up to 1 µm). The storage aggregates similarly display larger dimensions, being mainly composed of trimers and HMW species up to 640 nm, as generally aggregates increase in size (and amount) in a time-dependent manner [2]. Additionally, F/T as an aggregation induction factor, when performed with NaCl, forms larger particles (in the micron range) due to the decrease of colloidal stability [4].

The mAb monomeric form and the resulting induced aggregates were also characterized according to their hydrophobicity by HIC [16]. The results obtained are also presented in Table 5.3, with the corresponding chromatograms obtained in Figure 5.S1**A**. In HIC, the retention of the molecule in the column is solely due to interactions between the surface amino acids and the stationary phase. Hence, different retention times and profiles are due to conformational changes, when compared to the monomer form. Temperature and low pH induced aggregates have a later retention time and profile, with the conformational changes suffered making them more hydrophobic when compared to the remaining samples. This increase in hydrophobicity happens when the antibody is exposed to strong destabilizing conditions, such as low pH (pH 3.0) and high temperatures (75^0C): the level of unfolding exposes a larger number of hydrophobic patches [21]. Nevertheless, a wide variety of different types of aggregates, ranging in terms of the level of aggregation, size and hydrophobicity, were generated. Since the type of stress that the mAb solution suffers greatly influences its physical and chemical properties [4], and in an integrated continuous process a variety of aggregation inducing factors are employed, it was crucial to have an extensive sample set. Since the objective is to create a PAT tool which covers the entire size range or type of aggregates, it is imperative that the micromixer (with the selected FD to be employed) can detect all mAb induced aggregation samples.

Table 5.3 - Aggregation samples generated resorting to different induction factors (purified mAb, time, storage, F/T, temperature and low pH induced aggregates). These samples were used in the HT screening of the FDs and in the UV-Vis detection with the micromixer. The type of aggregate induction, with the corresponding buffer used, the resulting percentage of aggregation (obtained by SEC-UPLC) and the characterization of each sample (achieved by DLS and HIC) is here described. More information on this characterization can be found in Supplementary Material (Figure 5.S1). Na-Pb corresponds to sodium phosphate, NaCl to sodium chloride, NaOAc to sodium acetate and Na-Citrate to sodium citrate.

Aggregation Sample	Buffer	% Aggregation (SEC-UPLC)	Size (SEC-UPLC and DLS)	Hydrophobicity (HIC)
Purified mAb	50 mM Na-PB Buffer, 150 mM NaCl, pH 7.2	0	Monomer 165 kDa / 12.5 nm	-
Time Aggregates	50 mM Na-PB Buffer, 150 mM NaCl, pH 7.2	2.5	Mainly Dimers 375 kDa / 320 – 1000 nm	-
Storage Aggregates	25 mM NaOAc + 5 mM NaCl, pH 4.5	4	Mainly Trimers 500 kDa / 60 – 640 nm	-
F/T Aggregates	50 mM Na-PB Buffer, 150 mM NaCl, pH 7.2	7	Mainly Dimers 375 kDa / 20 – 40 & 640 – 1000 nm	-
Temperature Aggregates	50 mM Na-PB Buffer, 150 mM NaCl, pH 7.2	6	Trimers 500 kDa / 40 - 80 nm	+
Low pH Aggregates	50 mM Na-Citrate + 500 mM NaCl, pH 3	10	Trimers 500 kDa / 40 - 160 nm	++

5.3.2. HT Screening of FDs

Several commercially available FDs have been used to detect mAb aggregation [5, 8, 11]. However, the minimal concentration required to produce a measurable signal for each FD when applied in the micromixer was still unknown. Hence, a HT screening of each FD was performed to determine the FD concentration to be employed in the micromixer. Additionally, possible constrains regarding the limit of detection of each FD can be assessed. A broad literature review on the use of these FDs was already performed in São Pedro *et al.* [22], which includes the concentration and wavelengths used in each reported publication. Based on this information, the concentration range tested is described in Table 2 as well as the excitation and emission wavelengths used.

The optimal concentration for each FD was reached (**Table 5.2**), with the fluorescence spectra recorded for the best condition represented in **Figure 5.2**. As expected, all FDs had strong fluorescence signals for the majority of the mAb induced aggregation samples, with most being able to distinguish as little as 2.5% of aggregation. Moreover, the purified mAb sample displayed almost no fluorescence intensity across all four FDs. Nevertheless, Bis-ANS and Nile Red, both hydrophobic sensitive FDs, do not produce a major increase in fluorescence intensity for the F/T aggregates, when compared to the mAb purified sample. The F/T aggregates do not contain any exposed hydrophobic regions in the unfolded aggregated structure which would produce a fluorescence intensity increase by these two FDs. Previous studies indicate that the mAb native structure is retained to a high degree after F/T, with the sample mainly be composed of native-like IgG molecules [23]. The HIC characterization confirms this hypothesis since the hydrophobicity of the F/T aggregates did not increase compared to the mAb monomer form, showing the same retention time and profile. Additionally, Nile Red also does not produce a fluorescence signal for the time aggregate detection, the sample with the lowest level of aggregation, which indicates the dye's limit of detection. Therefore, Nile Red will only be suitable to be applied in mAb samples which present more than 2.5% of aggregation.

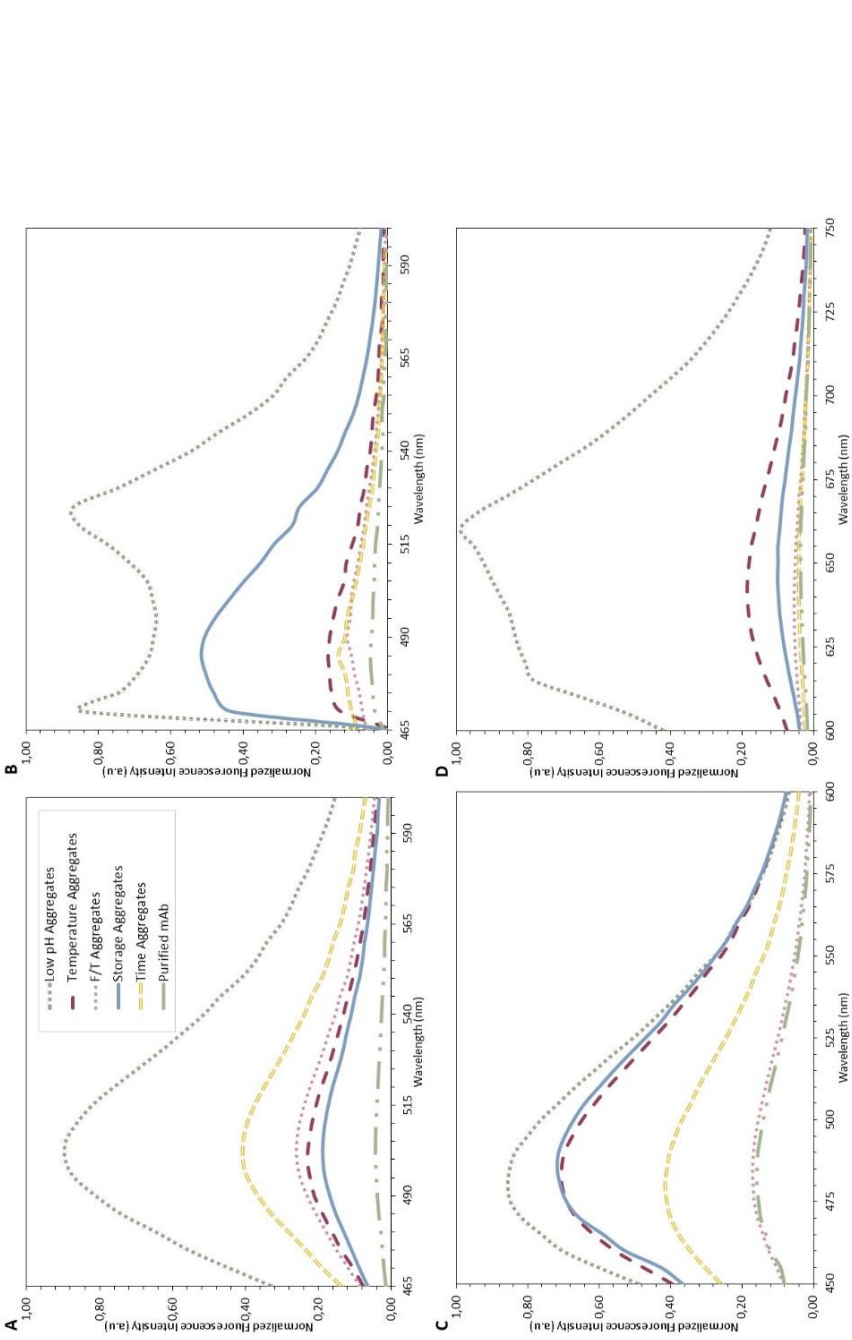

*Figure 5.2 - Optimized fluorescence spectra of the different FDs studied, resorting to the different type of aggregates (purified mAb, time, storage, F/T, temperature and low pH induced aggregates): **A)** ThT, at a concentration of 1 mM; **B)** CCVJ, at a concentration of 1 μM; **C)** Bis-ANS, at a concentration of 0.5 μM; and **D)** Nile Red, at a concentration of 75 μM. The excitation and emission wavelengths, as well as the tested concentrations, can be found in Table 5.2.*

Furthermore, for all FDs employed, it is possible to observe that the fluorescence signal measured does not directly correlate with the quantity of mAb aggregates in the sample. For example, as seen in **Figure 5.2A**, the storage aggregates display a higher fluorescence signal than the remaining mAb samples, except the low pH aggregates. However, the storage aggregates only present 4% of aggregation. The fluorescence intensity not only depends on the amount of aggregates, but also on the properties of such aggregates [15]. Ultimately, a straightforward quantification of aggregation based on the FD signal is, up to the moment, not possible. The aggregate measurement provided by the FDs and, subsequently, the micromixer, will only be qualitative, not quantitative.

5.3.3. Application of Micromixer

5.3.3.1. UV-Vis Sensor

With the FD concentration defined, the next step was to validate the developed micromixer for mAb aggregation detection resorting to a standard UV-Vis detector. Each FD, with the mAb aggregation sample to be tested, were simultaneously pumped in the microfluidic structure where both streams mixed under 30 seconds. A flow rate of 1 µL min^{-1} was employed, which provides a mixing efficiency of around 90% [13]. The resulting fluid is then sent to an inline UV-Vis detector where, if an increase of the signal is observed, aggregation is detected. The emission wavelength of each FD was selected according to the HT screening performed beforehand, choosing a wavelength close to the peak of the fluorescence intensity signal. Before starting the measurement, the UV signal is auto-zero with a solution composed of FD and the sample buffer (ratio one-to-one) to eliminate any possible interference from the FD intrinsic fluorescence. As observed in **Figure 5.3A**, after the micromixer is connected to the UV-Vis detector, the signal is allowed to stabilize for, at least, 10 minutes before finishing the measurement by disconnecting the micromixer and auto-zero again with the same FD and sample buffer solution. Similar procedure was repeated for all four FDs and all mAb aggregate samples, with the results obtained presented in **Figure 5.4**. However, not all FDs were able to be successfully employed in the UV-Vis detector. Nile Red, as observed in **Figure 5.3B** for the detection of storage aggregates, does not produce a stable signal over the imposed 10 minutes time range. The signal decreases during the measurement due to the aggregation of the FD. Nile Red self-associates in dimers in the micromixer and subsequently, in the tubes connecting to the UV-Vis detector, due to the dye's poor solubility in water [24]. These aggregates interfere with the aggregate measurement and, since the majority of the buffers used during the mAb

purification chain are composed by water, Nile Red cannot be applied as a FD to detect aggregation within a continuous integrated process. Therefore, Nile Red was discarded as a FD to be further used in this miniaturized PAT tool.

Nevertheless, all the remaining FDs, ThT, CCVJ and Bis-ANS, were able to successfully provide a stable measurement and detect aggregation (**Figure 5.4**). The purified mAb sample, with 0% aggregation, yields no measurable UV signal across all three FDs. Moreover, all the aggregate samples displayed great increases in the UV signal when the aggregation measurement started. Although ThT could detect all the different mAb induced aggregation samples, the UV signal from the temperature and low pH aggregates is relatively less than the remaining (storage and F/T aggregates). ThT binds to intermolecular β-sheets formed in high-order aggregates, being an indicator of amyloid structure [25, 26]. Hence, the lower ThT signal indicates that the temperature and low pH aggregation mechanism is not accompanied by β-sheet formation, but by the exposure of the hydrophobic patches. The HIC results already showed the increase in the hydrophobicity of these two samples when compared to the mAb monomer form (**Table 5.3**). Therefore, since not all mAb aggregation mechanisms will lead to a β-sheet formation, ThT is no longer considered a suitable FD to be applied and will not be further explored. Nonetheless, Bis-ANS and CCVJ exhibit an ample increase in the UV signal and are suitable to be used in the micromixer. Once again, the UV signal obtained does not directly correlate with the amount of aggregates in each sample: for example, for Bis-ANS, the time aggregates produce a similar UV signal than for the temperature aggregates. Thus, FD detection of aggregation depends more on the proprieties of the aggregates than the amount, providing a merely qualitative measurement. The limit of detection (LoD) of the developed PAT tool is intrinsically connected to the LoD of the FD. Therefore, to properly use the developed PAT tool, further investigation into the LoD of the FD is needed. Additionally, in the past years, there has been the development of novel FDs, like Proteostat, which might be better suitable to detect other types of aggregates [9] and might be an alternative option to be applied in the micromixer. Nevertheless, with CCVJ and Bis-ANS being able to produce measurable UV signals, it was demonstrated the potential of using the two FDs to successfully detect HMW species.

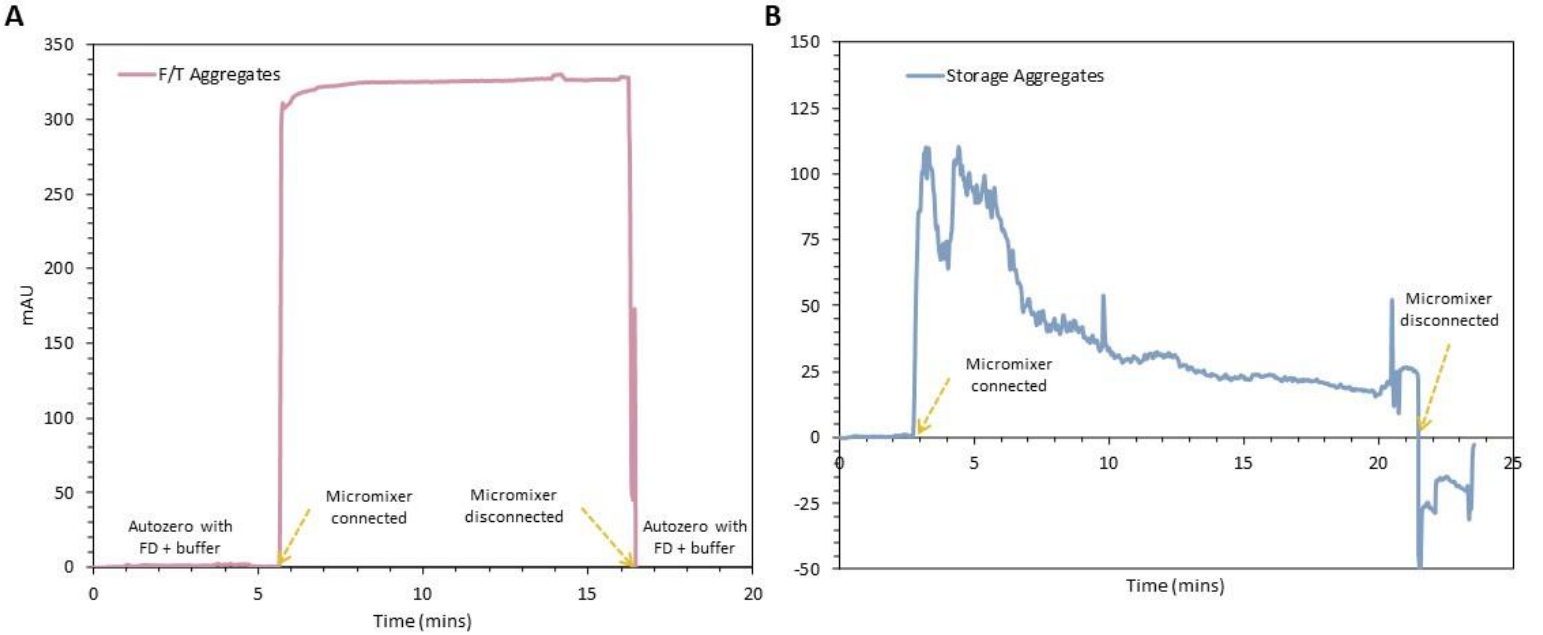

Figure 5.3 - UV signal measured for: ***A)*** *F/T aggregates detected with ThT ([ThT] = 1 mM, λ_{exc} = 415 nm, λ_{em} = 520 nm); and* ***B)*** *Storage aggregates detected with Nile Red ([Nile Red] = 75 µM, λ_{exc} = 550 nm, λem = 650 nm). The measurement starts with the autozero of the UV signal with a solution composed of the FD and the sample buffer, mixed in a ratio of one-to-one. Then, the micromixer is connected to the UV-Vis detector to start the aggregation detection. After the stabilization of the signal for at least 10 minutes, the micromixer is disconnected and the signal once more autozero with the FD and sample buffer mixture.*

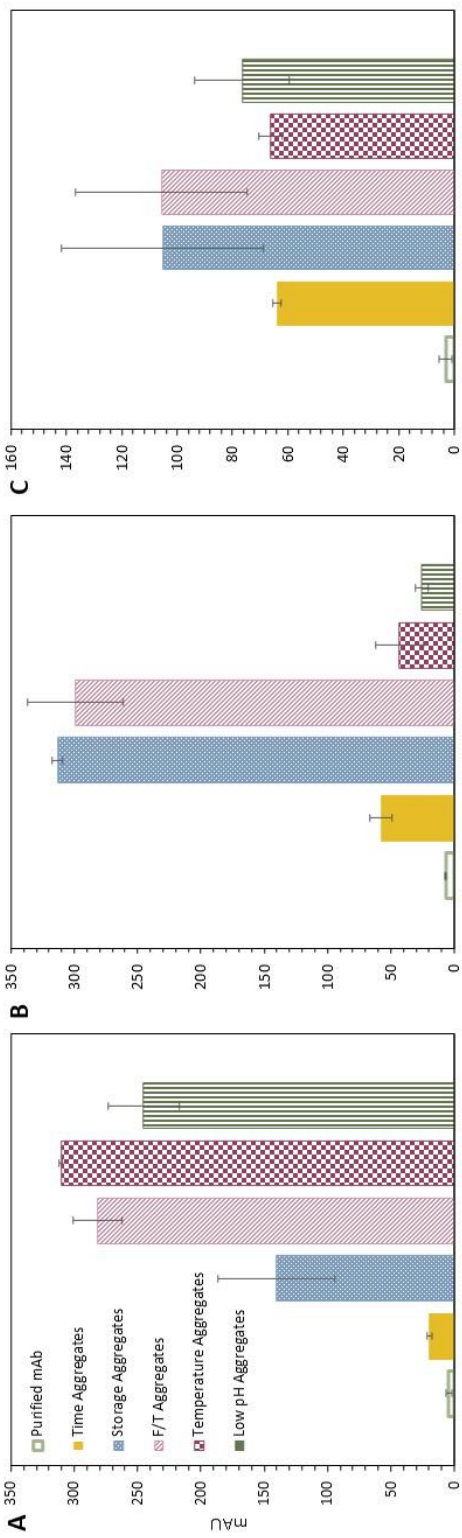

Figure 5.4 - UV signal measured for each induced aggregation sample (purified mAb, time, storage, F/T, temperature and low pH induced aggregates) and the FDs: A) CCVJ ([CCVJ] = 1 μM, λ_{exc} = 435 nm, λ_{em} = 520 nm); B) ThT ([ThT] = 1 mM, λ_{exc} = 415 nm, λ_{em} = 520 nm); and C) Bis-ANS ([Bis-ANS] = 0.5 μM, λ_{exc} = 380 nm, λ_{em} = 520 nm). The UV measured values are the average of two experiments and the error bars represent the standard deviation (±SD).

Finally, one of the design constrains when developing this fluorescent dye-based microfluidic sensor was that the micromixer would not alter the amount of aggregates [13]. To confirm that indeed the micromixer was not affecting the sample's aggregation levels, the mAb aggregate samples were collected after the UV-Vis detection and analysed by SEC-UPLC. No increase in the level of aggregation was observed for any analysed sample (data not shown). Therefore, the developed microfluidic sensor fulfils all the design constrains of a PAT tool: a real-time measurement of mAb aggregation in a continuous process can be achieved, with the micromixer providing 90% of mixing efficiency within 30 seconds [13].

5.3.3.2. AEX Validation

The final evaluation of the fluorescent dye-based micromixer was to employ it in a chromatographic operation for aggregate detection. AEX chromatography was performed in a flow-through (FT) mode for the removal of aggregates, which has been previously optimized [20]. The micromixer was then implemented in a standard ÄKTA™ Avant unit, with the addition of an extra UV sensor, one 10 mL superloop and three versatile valves (**Figure 5.5A** and **B**). The extra UV sensor (UV2) was used to monitor the chromatographic run whereas the UV already present in the ÄKTA™ unit (UV1) was placed after the micromixer to detect the aggregation signal provided by the FD. The superloop was added, after the chromatography column, to collect the FT and the eluate (**Figure 5.5A**). The pumps already existing in the system, pump A and B, were not only used for the chromatographic run but also to pump the FT/eluate collected in the superloop directly to the micromixer (**Figure 5.5B**). Therefore, to allow the reduction of flow rate for aggregate detection in the micromixer, the incorporation of the superloop was crucial. Due to pump limitations for lower flows, a flow rate of 3 µL min^{-1} was applied, which is still able to provide a high mixing efficiency (around 85%). Additionally, the sample pump (SampP) injects the FD directly into the micromixer, with a similar flow rate.

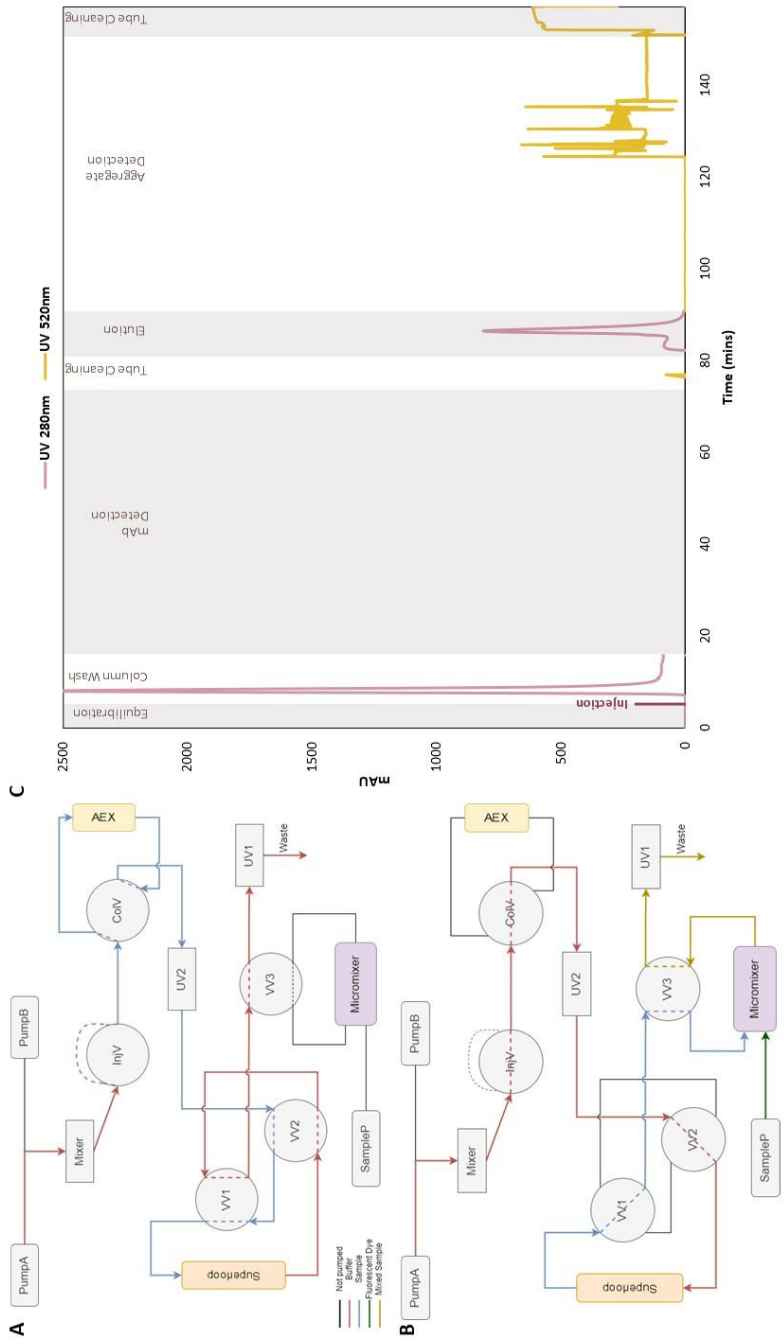

Figure 5.5 - Process diagrams of the integration of the micromixer in an AEX chromatographic run in an ÄKTA™ Avant system, performed for the removal of mAb aggregates: ***A)*** *Sample application in the AEX column, with the subsequent collection of the FT in a superloop; and* ***B)*** *Aggregate detection of the collected sample in the micromixer. The red line represents the pathway of the different buffers pumped in by Pump A and B, whereas the blue line exemplifies the pathway performed by the sample in the system. The sample pump (SampP) is used to inject the fluorescent dye into the micromixer (green line), which, when mixed with the mAb sample (gold yellow line), is then sent to the UV1 detector. Black lines represent inactive flow paths.* ***C)*** *AEX chromatographic run performed in FT mode for aggregate removal, using a low pH induced sample with 6% aggregation (60 mg mL^{-1}) and CCV] ([CCV] = 1 µM, λ_{exc} = 435 nm, λ_{em} = 520 nm) as the FD. Firstly, after the column equilibration, mAb sample is injected in the column and the FT is collected in the superloop. The sample is then directed to the micromixer where is mixed with the FD at a flow rate of 3 µL min^{-1}, with the signal detection being performed during 60 minutes. Then, the tubes and micromixer are cleaned with water and the same procedure is repeated for the elution of the AEX column.*

From the results obtained in the UV-Vis detector, CCVJ, a molecular rotor, showed a more significant UV signal increase, around 300 mAU, being the preferred FD to be used in this validation. A mAb sample, with a concentration of 60 mg mL^{-1}, was stressed by low pH induction, obtaining a 6% level of aggregation (Table 5.4). This aggregation sample was then injected onto an AEX column, with the results obtained found in Figure 5.5**C**. First, after the column equilibration and sample injection, the FT is collected in the superloop. Then, a FT sample is sent to the micromixer, where when mixed with the FD, no UV signal was detected. Hence, the FT sample exhibits no aggregation, with AEX column being able to bind all the aggregates. The level of aggregation was later confirmed by SEC-UPLC (Table 5.4), which merely identified 0.4% of aggregates. Later, after cleaning the micromixer and the attached tubes with water and disposing the remaining sample in the superloop, the AEX elution was performed and collected. The detection procedure is repeated once more, and for the eluate, the UV signal increased. Even though theoretically the pump system can handle flow rates starting at 1 µL min^{-1}, the ÄKTA™ system still has some limitations when using lower flow rate. The presence of air bubbles is visible on the UV signal, especially in the first minutes after the signal increases. Nevertheless, the signal was allowed to stabilize and aggregation was still detected using the micromixer sensor. The detection time was initially defined to be 60 minutes which needs to be considerably reduced to provide a real-time analysis. Since the micromixer can provide an efficient mixing under 30 seconds [13], modifications to the external ÄKTA™ setup have to be perform to decrease of the overall measurement time. For example, by reducing the connection tubes which connect the versatile valve to the micromixer, this decrease of measuring time can be achieved. The aggregate detection was again confirmed by SEC-UPLC, with the eluate collected presenting 5% of aggregation (Table 5.4). Thus, even if a long measuring time was defined, the proposed micromixer was still able to successfully detect aggregation.

Table 5.4 - Aggregation levels and concentration determined by SEC-UPLC for each collected sample from the AEX chromatographic run.

	Aggregation (%)	Concentration (mg mL^{-1})
Initial Sample	6	60.0
FT Sample	0.4	2.0
Eluate Sample	5	0.5

Recently, with the development of the PAT framework, several PAT tools have been successfully implemented to detect aggregation in the required time frame for decision making and control [27, 28]. For example, Patel *et al.* [29] has used a multi-

angle light scattering (MALS) system coupled to ÄKTA™ unit to real-time quantify the formation of aggregates. However, extra equipment such as a MALS system is not as readily available as a standard UV-Vis detector to detect aggregation. If the detection time can be significantly decreased, the increase in the UV signal can be used as a cut-off point to stop collecting the mAb product. When developing this PAT sensor, several design constrain were imposed including: the overall cost of the technique had to be minimal and the microfluidic chip simple to operate [22]. By using a zigzag micromixer and a simple extra UV monitor connected to a ÄKTA™ unit, these design constrains are met since no external equipment and setup is required, which would increase the cost and complexity of the developed PAT tool. Although FDs have inherent limitations regarding the quantification of the HMW species, a simple zigzag micromixer was firstly designed [13] and hereby applied and tested. Thus, this work demonstrates that the miniaturization of the analytical technique discussed by São Pedro *et al.* [22] is a powerful solution to speed up the CQAs measurement in a continuous process.

5.4. Concluding Remarks

A PAT fluorescent dye-based microfluidic sensor was hereby introduced and developed, being able to detect all different types of aggregates tested. From a SEC purified mAb sample, with 0% of aggregation, several induction factors were used to create a large variety of mAb aggregates, which presented different physical and chemical properties. A HT screening was then performed to assess the required concentration, emission wavelength and limit of detection of each FD to later be applied in the micromixer. This microfluidic chip was then connected to an UV-Vis detector and tested to detect mAb aggregation with all the stressed samples. Even though Nile Red and ThT were not suitable to be applied due to intrinsic limitations of the dye, Bis-ANS and CCVJ provide a measurable signal when aggregates were present in the analyzed sample. However, a measurement resorting to FDs will merely be qualitative, not yet being possible to quantify aggregation based on its signal. The FD signal is more dependent on the type of aggregate than its amount, making this developed PAT tool able to solely detect protein aggregation. Ultimately, the micromixer was validated in an AEX chromatographic run for the removal of mAb aggregates. An increase of the UV signal was observed on the eluate sample, which presented 5% of aggregation, whereas the FT sample, with 0.4% of aggregation, was not (**Figure 5.5C** and **Table 5.4**). Even though further investigation into the LoD of each FD should be performed, it was demonstrated that the micromixer can efficiently

and robustly detect several type of aggregates and can be easily incorporated in a downstream unit operation.

Although the micromixer was able to successfully detect aggregation in a chromatography run, the measurement was still performed for 60 minutes. To create a real-time measurement, this detection time ought to be significantly reduced. By decreasing the connection tubes length in the ÄKTA™ system and/or introducing an extra phase in the Orbit software to fill these tubes with sample prior to the measurement, this time reduction should be achieved. Nevertheless, a fluorescent dye-based microfluidic sensor was demonstrated, being able to effectively detect a wide range of mAb aggregates. Furthermore, the micromixer was capable of handling the higher flow rates and pressure inherent to the ÄKTA™ system, demonstrating the potential of miniaturizing the analytical technique to accelerate CQAs measurement to the required time frame for process control.

5.5. REFERENCES

[1] São Pedro, M.N., Silva, T.C., Patil, R. and Ottens, M., White paper on high-throughput process development for integrated continuous biomanufacturing. Biotechnol Bioeng 2021, 118(9), 3275-86.

[2] Bansal, R., Gupta, S. and Rathore, A.S., Analytical Platform for Monitoring Aggregation of Monoclonal Antibody Therapeutics. Pharm Res 2019, 36(11), 152.

[3] Schermeyer, M.-T., Wöll, A.K., Kokke, B., Eppink, M. and Hubbuch, J., Characterization of highly concentrated antibody solution - A toolbox for the description of protein long-term solution stability. mAbs 2017, 9(7), 1169-85.

[4] Telikepalli, S.N., Kumru, O.S., Kalonia, C., Esfandiary, R., *et al.*, Structural characterization of IgG1 mAb aggregates and particles generated under various stress conditions. J Pharm Sci 2014, 103(3), 796-809.

[5] He, F., Phan, D.H., Hogan, S., Bailey, R., *et al.*, Detection of IgG aggregation by a high throughput method based on extrinsic fluorescence. J Pharm Sci 2010, 99(6), 2598-608.

[6] Paul, A.J., Bickel, F., Rohm, M., Hospach, L., *et al.*, High-throughput analysis of sub-visible mAb aggregate particles using automated fluorescence microscopy imaging. Anal Bioanal Chem 2017, 409(17), 4149-56.

[7] Bothra, A., Bhattacharyya, A., Mukhopadhyay, C., Bhattacharyya, K. and Roy, S., A fluorescence spectroscopic and molecular dynamics study of bis-ANS/protein interaction. Journal of Biomolecular Structure and Dynamics 1998, 15(5), 959-66.

[8] Hawe, A., Filipe, V. and Jiskoot, W., Fluorescent molecular rotors as dyes to characterize polysorbate-containing IgG formulations. Pharm Res 2010, 27(2), 314-26.

[9] Oshinbolu, S., Shah, R., Finka, G., Molloy, M., *et al.*, Evaluation of fluorescent dyes to measure protein aggregation within mammalian cell culture supernatants. J Chem Technol Biotechnol 2018, 93(3), 909-17.

[10] Biancalana, M. and Koide, S., Molecular mechanism of Thioflavin-T binding to amyloid fibrils. Biochim Biophys Acta 2010, 1804(7), 1405-12.

[11] Paul, A.J., Schwab, K., Prokoph, N., Haas, E., *et al.*, Fluorescence dye-based detection of mAb aggregates in CHO culture supernatants. Anal Bioanal Chem 2015, 407(16), 4849-56.

[12] São Pedro, M.N., Klijn, M.E., Eppink, M.H.M. and Ottens, M., Process analytical technique (PAT) miniaturization for monoclonal antibody aggregate detection in continuous downstream processing. J Chem Technol Biotechnol 2021.

[13] São Pedro, M.N., Santos, M.S., Eppink, M.H.M. and Ottens, M., Design of a microfluidic mixer channel: First steps into creating a fluorescent dye-based biosensor for mAb aggregate detection. Biotechnology Journal 2022.

[14] Sulatskaya, A.I., Lavysh, A.V., Maskevich, A.A., Kuznetsova, I.M. and Turoverov, K.K., Thioflavin T fluoresces as excimer in highly concentrated aqueous solutions and as monomer being incorporated in amyloid fibrils. Sci Rep 2017, 7(1), 2146.

[15] Hawe, A., Friess, W., Sutter, M. and Jiskoot, W., Online fluorescent dye detection method for the characterization of immunoglobulin G aggregation by size exclusion chromatography and asymmetrical flow field flow fractionation. Anal Biochem 2008, 378(2), 115-22.

[16] Goyon, A., D'Atri, V., Bobaly, B., Wagner-Rousset, E., *et al.*, Protocols for the analytical characterization of therapeutic monoclonal antibodies. I - Non-denaturing chromatographic techniques. J Chromatogr B Analyt Technol Biomed Life Sci 2017, 1058, 73-84.

[17] Gokaltun, A., Kang, Y.B.A., Yarmush, M.L., Usta, O.B. and Asatekin, A., Simple Surface Modification of Poly(dimethylsiloxane) via Surface Segregating Smart Polymers for Biomicrofluidics. Sci Rep 2019, 9(1), 7377.

[18] Gomis-Fons, J., Andersson, N. and Nilsson, B., Optimization study on periodic counter-current chromatography integrated in a monoclonal antibody downstream process. J Chromatogr A 2020, 1621, 461055.

[19] Gomis-Fons, J., Schwarz, H., Zhang, L., Andersson, N., *et al.*, Model-based design and control of a small-scale integrated continuous end-to-end mAb platform. Biotechnol Prog 2020, 36(4), e2995.

[20] GE Healthcare, Selective removal of aggregates with Capto adhere. Application note 28-9078-93 AB 2012.

[21] Arosio, P., Rima, S. and Morbidelli, M., Aggregation mechanism of an IgG2 and two IgG1 monoclonal antibodies at low pH: from oligomers to larger aggregates. Pharm Res 2013, 30(3), 641-54.

[22] São Pedro, M.N., Klijn, M.E., Eppink, M.H.M. and Ottens, M., Process analytical technique (PAT) miniaturization for monoclonal antibody aggregate detection in continuous downstream processing. Journal of Chemical Technology & Biotechnology 2021, 97(9), 2347-64.

[23] Hawe, A., Kasper, J.C., Friess, W. and Jiskoot, W., Structural properties of monoclonal antibody aggregates induced by freeze-thawing and thermal stress. Eur J Pharm Sci 2009, 38(2), 79-87.

[24] Ray, A., Das, S. and Chattopadhyay, N., Aggregation of Nile Red in Water: Prevention through Encapsulation in beta-Cyclodextrin. ACS Omega 2019, 4(1), 15-24.

[25] Li, Y., Mach, H. and Blue, J.T., High throughput formulation screening for global aggregation behaviors of three monoclonal antibodies. J Pharm Sci 2011, 100(6), 2120-35.

[26] Sahin, E., Grillo, A.O., Perkins, M.D. and Roberts, C.J., Comparative effects of pH and ionic strength on protein-protein interactions, unfolding, and aggregation for IgG1 antibodies. J Pharm Sci 2010, 99(12), 4830-48.

[27] Rathore, A.S., Yu, M., Yeboah, S. and Sharma, A., Case study and application of process analytical technology (PAT) towards bioprocessing: use of on-line high-performance liquid chromatography (HPLC) for making real-time pooling decisions for process chromatography. Biotechnol Bioeng 2008, 100(2), 306-16.

[28] Rolinger, L., Rudt, M., Diehm, J., Chow-Hubbertz, J., *et al.*, Multi-attribute PAT for UF/DF of Proteins-Monitoring Concentration, particle sizes, and Buffer Exchange. Anal Bioanal Chem 2020, 412(9), 2123-36.

[29] Patel, B.A., Gospodarek, A., Larkin, M., Kenrick, S.A., *et al.*, Multi-angle light scattering as a process analytical technology measuring real-time molecular weight for downstream process control. MAbs 2018, 10(7), 945-50.

Chapter 5

Application of a Fluorescent Dye-based Microfluidic Sensor for Real-time Detection of mAb Aggregates

Supplementary Material

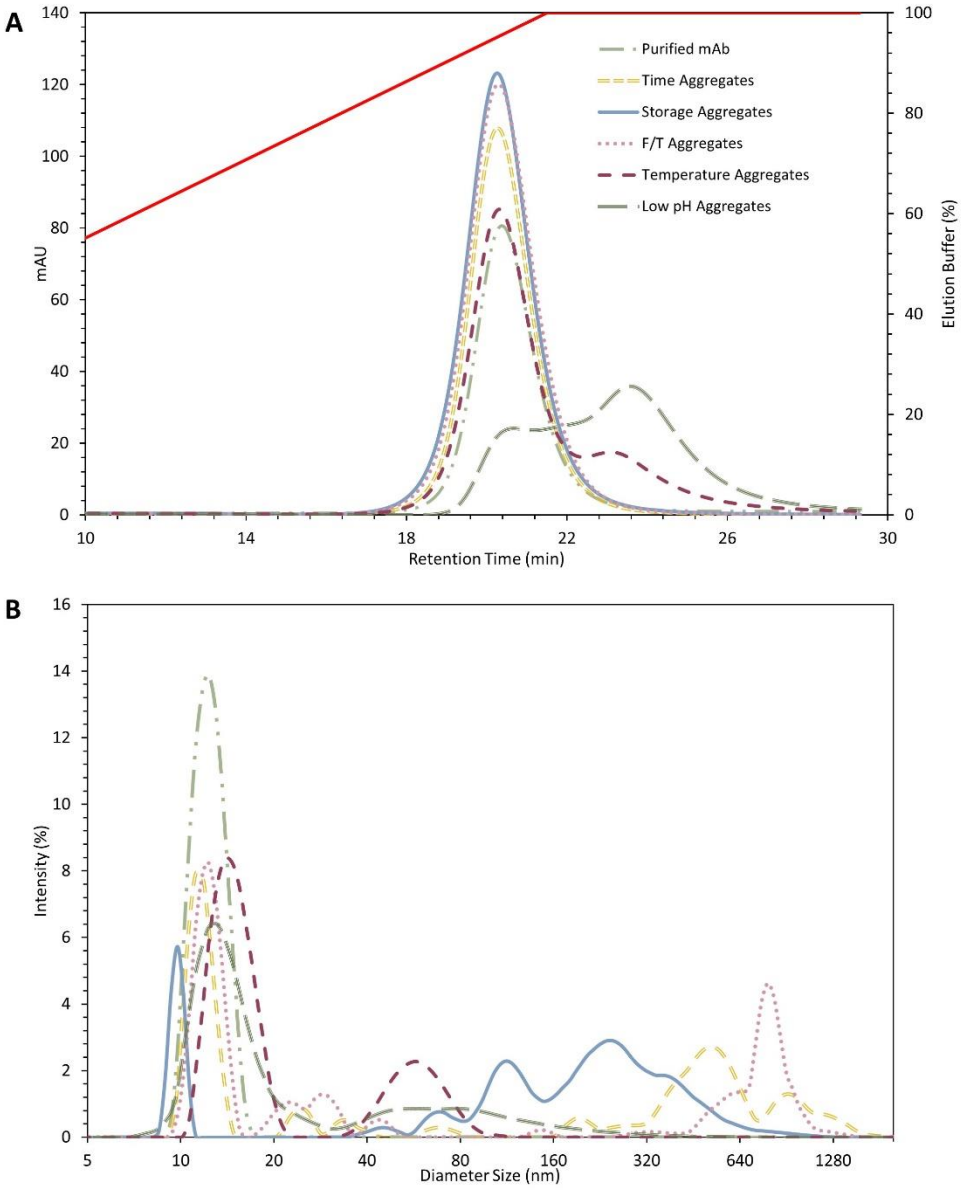

*Figure 5.S1 - Characterization of the different aggregation samples (purified mAb, time, storage, F/T, temperature and low pH induced aggregates) by: **A)** HIC, according to Goyon et al. [16], to assess any possible changes in hydrophobicity of the generated aggregates when compared with the purified sample; **B)** DLS, to determine the presence of larger aggregates in the generated samples.*

Chapter 6

Real-time Detection of mAb Aggregates in an Integrated Downstream Process

The implementation of continuous processing in the biopharmaceutical industry is hindered by the scarcity of process analytical technologies (PAT). To monitor and control a continuous process, PAT tools will be crucial to measure real-time product quality attributes such as protein aggregation. Miniaturizing these analytical techniques can increase measurement speed and enable faster decision-making. A fluorescent dye (FD)-based miniaturized sensor has previously been developed: a zigzag microchannel which mixes two streams under 30 seconds. Bis-ANS and CCVJ, two established FDs, were employed in this micromixer to detect aggregation of the biopharmaceutical monoclonal antibody (mAb). Both FDs were able to robustly detect aggregation levels starting at 2.5%. However, the real-time measurement provided by the microfluidic sensor still needs to be implemented and assessed in an integrated continuous downstream process. In this work, the micromixer is implemented in a lab-scale integrated system for the purification of mAbs, established in an ÄKTA™ unit. A viral inactivation and two polishing steps were reproduced, sending a sample of the product pool after each phase directly to the microfluidic sensor for aggregate detection. An additional UV sensor was connected after the micromixer and an increase in its signal would indicate that aggregates were present in the sample. The at-line miniaturized PAT tool provides a fast aggregation measurement, under 10 minutes, enabling better process understanding and control.

Published as: São Pedro, M.N., Isaksson, M., Gomis-Fons, J., Eppink M.H.M., Nilsson, B. & Ottens, M. (2023), *Real-time detection of mAb aggregates in an integrated downstream process*, Biotechnology & Bioengineering, 1–12 (https://doi.org/10.1002/bit.28466);

6.1. INTRODUCTION

A challenge in the implementation of continuous biomanufacturing by the biopharmaceutical industry is the shortage of process analytical technologies (PAT) [1, 2]. A real-time measurement of certain critical quality attributes (CQAs), such as protein aggregation, is imperative to provide decisive information for subsequent steps and to facilitate process control [3]. For the biomanufacturing of monoclonal antibodies (mAbs), the presence of high molecular weight (HMW) species is undesirable [4]. With several known aggregation inducing factors being present in the downstream process [5, 6], a PAT tool capable to detect the formation of these HMW species is essential. Miniaturized biosensors as in-line or on-line PAT tool could speed up the analytical measurement to the required time frame for decision-making. The inherent short operation time, the small sample volume required (in the scale of nL or µL) and the easiness of fabrication are just a few advantages provided by the miniaturization of the analytical technique [7].

Fluorescent dyes (FD), such as 4-4-bis-1-phenylamino-8-naphthalene sulfonate (Bis-ANS) and 9-(2-Carboxy-2-cyanovinyl)julolidine (CCVJ), have been employed to detect and study protein aggregation [8]. The fluorescence of these molecules is intensified due to changes in the hydrophobicity, Bis-ANS [9], or the viscosity of the surrounding environment, CCVJ [10]. Since these dyes provide an immediate and straightforward measurement of aggregation, a FD-based microfluidic biosensor for aggregate detection was designed and developed. A zigzag micromixer, represented in **Figure 6.1**, is capable of effectively mixing two different streams within 30 seconds [11]. The micromixer is comprised of two inlets and one outlet, where the mixing occurs due to the 45^0 zigzag design, with a total of 30 mixing units. This zigzag structure was applied to detect the presence of HMW species in a variety of mAb aggregation samples, induced by different induction factors (like temperature, freeze-thawing or low pH incubation). Depending on the FD employed, the developed micromixer was able to robustly detect, at least, 2.5% of aggregation [12].

Although the micromixer was able to successfully detect aggregation in a single unit operation, an anion exchange (AEX) chromatography [12], further validation in an integrated downstream process is still required. Therefore, in this work, the developed PAT tool will be assessed for aggregate detection in a lab-scale integrated system, established in an ÄKTA™ Avant unit. The final steps of a mAb purification scheme were carried out: a low-pH viral inactivation (VI) step followed by two polishing steps, a bind-and-elute cation exchange (CEX) and a flow-through (FT) AEX

chromatography step. The presence of aggregates in the final purification steps is critical, especially after the polishing steps, since these steps were designed and developed to remove any product related impurities. After each unit operation, a sample of either the FT pool or the eluate was directly sent to the micromixer for aggregate detection. An increase in the UV absorbance would mean that aggregates were present in the sample, which would subsequently be confirmed by off-line analytical size exclusion chromatography (SEC-UPLC). The micromixer was able to effectively detect aggregation in the samples validated with an offline measurement, demonstrating the potential of creating a real-time measurement by the miniaturization of the analytical technique.

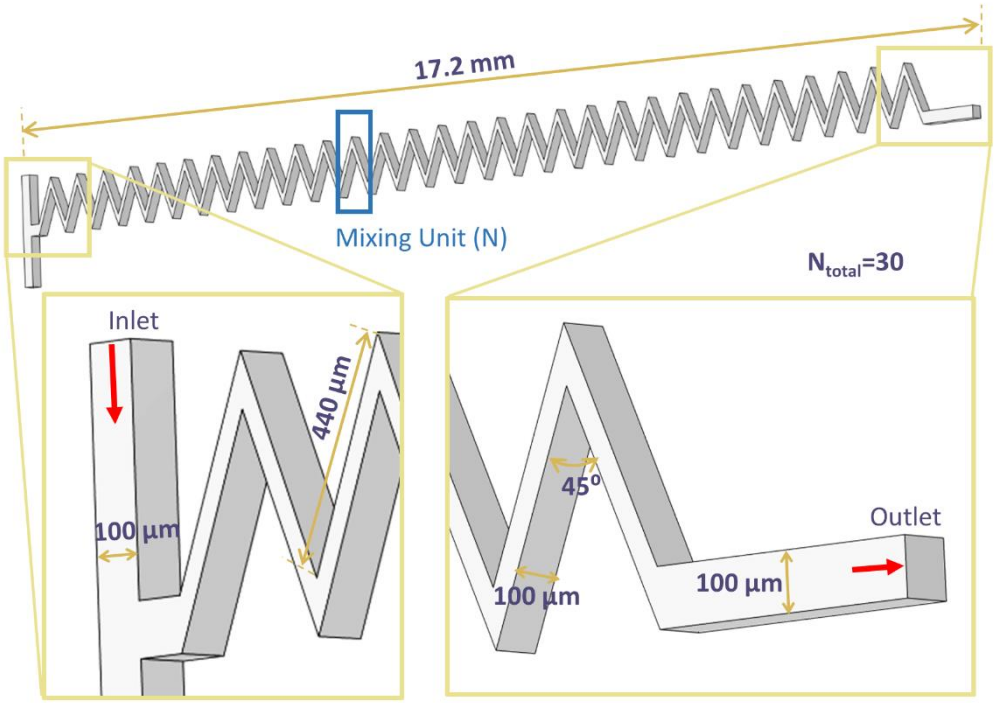

Figure 6.1 - 3D schematic representation of the micromixer structure, with the relevant measurements described. The zigzag mixing unit (N) of the micromixer is highlighted in blue, with the structure being a consecutive repetition of 30 N and having a total mixing length of around 27 mm (calculated based on the 30 N and the length of the zigzag channel diagonally, 440 µm). The red arrows indicate the flow of both liquids entering in one of the inlets and the resulting mixed liquid exiting at the outlet.

6.2. Materials and Methods

Poly(dimethylsiloxane) (PDMS) was purchased as a Sylgard 184 elastomer kit (Dow Corning, Midland, MI, USA). Dimethylsiloxane-(60-70% ethylene oxide) block copolymer was acquired from Gelest (Pennsylvania, USA). Sodium phosphate monobasic dehydrate was purchased from Sigma-Aldrich (New Jersey, United States). Di-sodium hydrogen phosphate and sodium chloride were bought from VWR Chemicals (VWR International, Pennsylvania, United States), whereas sodium acetate was purchased from Merck Aldrich (New Jersey, United States). Acetic acid was obtained from Fluka (North Carolina, United States) and sodium hydroxide from J.T. Baker (VWR International, Pennsylvania, United States). Regarding the FDs, CCVJ and Bis-ANS were purchased from Sigma-Aldrich (New Jersey, United States) and Invitrogen (Massachusetts, United States), respectively. The mAb used was supplied by Byondis B.V. (Nijmegen, The Netherlands), with an isoelectric point of 8.6.

The integrated downstream process was implemented in an ÄKTA Avant system (**Figure 6.2**), controlled by the software UNICORN™ 7.5 (Cytiva, Uppsala, Sweden). This ÄKTA unit was equipped with: three pumps (pumps A, B and sample pump) with inlet valves in each to be able to select different buffers; a column valve (ColV); a loop valve (LoopV); an inlet (InlS) and an outlet (OutV) valve; four versatile valves (VV); an injection valve (InjV); two UV monitors; conductivity and pH sensors; and a 10 mL and two 50 mL superloops™ (all from Cytiva, Massachusetts, United States).

6.2.1. Sample Preparation

The mAb sample was stored in sodium acetate buffer, pH 4.5, at -80°C, in a concentration of 6 mg mL^{-1}. This sample was dialyzed with 50 mM sodium acetate buffer, 100 mM NaCl, pH 5, using amicon ultra-15 centrifugal filters, and concentrated to 40 mg mL^{-1}.

To prepare the stock solutions of the FD dyes, CCVJ was dissolved in dimethyl sulfoxide (Fluka, Massachusetts, United States) and Bis-ANS in methanol (Sigma-Aldrich, New Jersey, United States). The exact concentration of each FD stock solution was calculated from the UV absorbance: for CCVJ at 440 nm, with the molar extinction of 25 404 M^{-1} cm^{-1}; and for Bis-ANS at 385 nm, with a molar extinction of 16 790 M^{-1} cm^{-1}. From the stock solutions, the FD solution was diluted with MilliQ water to a concentration of 1 µM for CCVJ and to 0.5 µM for Bis-ANS [12].

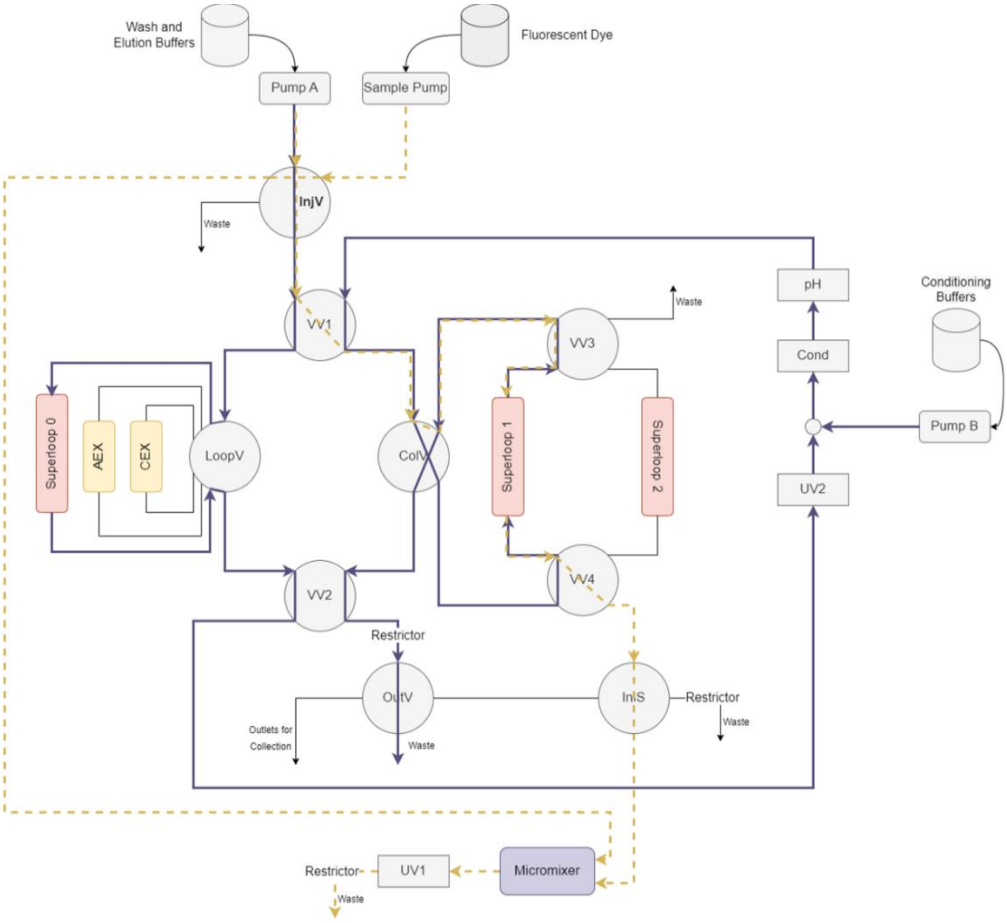

Figure 6.2 - Process diagram of the integrated downstream setup with the implementation of the real-time PAT micromixer. The dark blue line represents the flow path for the sample injection in the VI step: Pump A is used to transfer the mAb sample stored in superloop 0, connected to the loop valve (LoopV), to superloop 1, where the VI step occurs, passing through UV2, conductivity (Cond) and pH meter. Since the mAb sample is stored at pH 5, Pump B is used for the in-line sample conditioning to decrease the sample's pH to 3. Similar flow paths are used for the wash and elution of the CEX and AEX chromatography steps, also connected to the loop valve, where the FT or the eluate pools are stored in superloop 1/2. The dashed gold line indicates the flow path used for aggregate detection with the micromixer: the sample pump is used to inject the fluorescent dye into the micromixer through the injection valve (InjV); while, simultaneously, the stored sample in superloop 1 is injected in the micromixer by Pump A. Both streams are mixed in the micromixer structure and the resulting mixed fluid is sent to the UV1 sensor, where, if there is aggregation, an increase in the signal is observed. Black lines represent inactive flow paths.

6.2.2. Aggregate Detection

6.2.2.1. Microstructure Fabrication

The zigzag micromixer (100 µm high x 100 µm wide x 17.2 mm long) presents two inlets and one outlet (Figure 6.1). More information on the dimensions and characteristics of the micromixer channel are found in São Pedro *et al.* [11]. In terms of the structure fabrication, the designed mold was ordered from INESC Microsystems and Nanotechnologies (Lisbon, Portugal). To reduce the inherent hydrophobicity of PDMS and protein adsorption to the micromixer walls, the structures were fabricated according to Gokaltun *et al.* [13]. Dimethylsiloxane-(60-70% ethylene oxide) block copolymer, comprised of poly(ethylene glycol) (PEG) and PDMS segments (PDMS-PEG), were blended with PDMS during device manufacturing, using a 10:1:0.0025 ratio of PDMS, curing agent and PDMS-PEG. After being degassed, the mixture was poured onto the mold and baked at 70ºC overnight. After the PDMS was cured, the chip was removed from the mold and the inlets and outlet were punched in the microstructure. Finally, the PDMS chip was bonded to a glass substrate and sealed with a 20:1 mixture of PDMS to curing agent.

6.2.2.2. Off-line Analytics

The mAb concentration and level of aggregation was determined off-line by analytical size exclusion chromatography (SEC) in an UltiMate 3000 UHPLC System (Thermo Fisher Scientific, Massachusetts, United States). 5 µL of each sample was injected in an ACQUITY UPLC Protein BEH SEC 200 Å column (Waters, Massachusetts, United States), using the running buffer 100 mM sodium phosphate buffer, pH 6.8. After the sample injection, the flowrate was set to 0.3 mL min^{-1} for 10 minutes and the protein detection was performed at 280 nm.

6.2.3. Integrated Downstream Process

6.2.3.1. Process Conditions and Buffers

The integrated downstream process included three steps: a low-pH VI; followed by a CEX step in bind/elute mode; and finally an AEX step in FT mode, starting with the injection of 1 mL of mAb sample (concentration of 40 mg mL^{-1}). The VI step was performed at a pH of 3.0 for 60 minutes, in one of the 50 mL superloop. The CEX column used was a 1 mL HiTrap® Capto™ S ImpAct and the AEX resin was a 1 mL HiTrap® Capto™ Adhere (both obtained from Cytiva, Uppsala, Sweden). In total, seven different buffers were used for the loading, elution and stripping of the columns,

described in Table 6.1. The choice of these buffers, as well as the column volumes and flow rates employed, were based on GE Healthcare [14]. Each step was optimized separately and in batch mode beforehand to assess the formation and removal of mAb aggregates. Between several unit operations/steps, the sample buffer conditions had to be adjusted. This was performed through in-line conditioning by dilution. For the VI, the pH of the initial sample had to be lowered from 5.0 to 3.0. A solution of 0.2 M of hydrochloric acid was used, with a dilution ratio of 4:1. To increase the pH after the VI, a 100 mM sodium acetate, 150 mM sodium hydroxide solution was employed, with a dilution ratio of 4:1. Before the AEX column, the CEX eluate was diluted in-line with a ratio of 1:1, with 50 mM sodium phosphate solution, pH 6.8. A cleaning-in-place of each column was performed with 1M NaOH.

Table 6.1 - Buffers used in the integrated downstream set-up experiments. NaOAc corresponds to sodium acetate, Na-Pb to sodium phosphate and NaCl to sodium chloride.

		Buffer
	Initial Sample	50 mM NaOAc + 100 mM NaCl, pH 5.0
VI	**Incubation**	37.5 mM NaOAc + 75 mM NaCl, pH 3.0
CEX	**Equilibration**	50 mM NaOAc + 60 mM NaCl, pH 5.0
	Elution	50 mM NaOAc + 240 mM NaCl, pH 5.0
	Stripping	50 mM NaOAc + 500 mM NaCl, pH 5.0
AEX	**Equilibration**	25 mM NaOAc + 25 mM Na-Pb + 120 mM NaCl, pH 6.2
	Stripping	37.5 mM NaOAc + 75 mM NaCl, pH 3.0

6.2.3.2. Process Setup

The developed system configuration for the implementation of the microfluidic chip in an ÄKTA Avant unit is shown in Figure 6.2. Pump A was used for the equilibration, elution and stripping buffers and Pump B was mainly employed for the in-line conditioning buffers. The sample pump was applied to inject the FD into the micromixer structure, passing through the InjV (Figure 6.2, dashed gold line). The four VVs were used to guide the flow path and to incorporate the two 50 mL superloops in the system. The VI step was performed in superloop 1 (Figure 2, dark blue line). For the remaining process steps, the two superloops independently collected the eluate from the CEX column, and the FT and the eluate of the AEX column. These samples were shortly stored in superloops 1 or 2 to be later sent to the micromixer channel for aggregate detection. Another particularity of the developed setup was the addition of three different restrictors. By adding these restrictors, the overall process pressure was maintained which was crucial to preserve the integrity of

the microfluidic mixer. The LoopV contained the two chromatographic columns and the 10 mL superloop, from where the mAb sample was injected to start the process (superloop 0). The ColV was used as a versatile valve, guiding the flow path and allowing the connection to the two 50 mL superloops. By switching the ColV position, the superloops could either be filled (**Figure 6.2**, dark blue line) or emptied (**Figure 6.2**, dashed gold line). The OutV was utilized in the sampling of what was collected in the superloop and not further injected in the next step. For example, the FT of the AEX column, i.e. the mAb purified product, the stripping of the CEX column and the elution of the AEX column were collected and later analyzed off-line to determine the level of aggregation. The flow paths for remaining phases, such as the CEX column equilibration and elution, are represented in **Figure 6.S1** for a better understanding of the process set-up.

Additionally, two separate UV monitors were employed in this system: UV1, a U9-M monitor able to measure up to three wavelengths; and UV2, a U9-L detector, able to measure only one wavelength. UV1 was placed after the micromixer, to be able to detect aggregation due to the increase in UV absorbance; and UV2, at 280 nm, monitored the chromatographic run, placed after the VV2. The pH and conductivity sensor were also placed after UV2 to monitor the chromatography process.

6.2.3.3. Micromixer Implementation

The micromixer provides around 90% of mixing efficiency when both streams are simultaneously pumped into the structure at 1 µL min^{-1} [11]. Due to the ÄKTA's inherent pump limitations for lower flows, a flow rate of 3 µL min^{-1} (0.003 mL min^{-1}) was used, which still provided a high mixing efficiency, of around 85%, determined according to São Pedro *et al.* [12]. With the incorporation of the two 50 mL superloops, this reduction of pump A's flow rate to 3 µL min^{-1} for aggregate detection in the micromixer could be achieved.

To implement the FD-based PAT tool in an ÄKTA unit, several challenges had to be tackled to enable a fast analytical measurement, under 10 minutes: (1) by placing the micromixer close to the InlS valve (**Figure 6.S2**), the volume of the connection tubes, was reduced as much as possible; (2) before the analytical measurement was started, the connection tubes were filled with sample; (3) to clean and remove any remaining sample or FD, the connection tubes and micromixer were flushed with water at a flow rate of 5 µL min^{-1} after each aggregate detection (**Figure 6.S3**); and, finally, (4) to eliminate any interference from the FD's intrinsic fluorescence, before the measurement, the UV signal was auto-zeroed with FD and sample buffer in the

micromixer. Regarding the wavelengths used in UV1 for aggregate detection, for the FD CCVJ, the selected excitation wavelength (λexc) was of 435 nm and the emission wavelength (λem) of 520 nm. For the FD Bis-ANS, the selected λexc was of 385 nm and the λem of 520 nm [12].

6.2.3.4. Process Control

The ÄKTA systems are normally controlled by the Unicorn software. However, the Unicorn software has several limitations as, for example, operating an ÄKTA system with customized flow paths or introducing process control features. The Orbit software, written in Python, was developed at the department of Chemical Engineering, Lund University (Lund, Sweden). With Orbit, direct communication and control of ÄKTA equipment is enabled via two different protocols (OPC and REST API), and customized control strategies can be implemented, thus overcoming these limitations. In this work, the ÄKTA Avant was controlled via Orbit and a pooling control strategy was implemented: the pooling cut-off times of the collection of the FT and eluate pools of the polishing steps in both 50 ml superloops were based on the UV absorbance at a wavelength of 280 nm, measured on-line by the UV2 monitor [15]. More information on Orbit and how the controller functions can be found in Gomis-Fons *et al.* [16] and Lofgren *et al.* [17], with several examples on its use described elsewhere [18-20].

6.3. Results and Discussion

6.3.1. Design of the Downstream Process

To assess the micromixer ability to detect the presence of HMW species in a biomanufacturing process, the final steps of the purification process of mAbs were implemented and integrated in an ÄKTA system. The main goal was to directly send a sample to the micromixer for aggregate detection (**Figure 6.3A**). However, the purification steps were firstly optimized separately and an early assessment of the level of aggregation was performed. Basing the experimental buffers (**Table 6.1**) and process conditions on the mAb downstream processes implemented elsewhere (GE Healthcare [14] and Gomis-Fons *et al.* [21]), the three unit operations were reproduced, and the volumes necessary for in-line conditioning were determined. The resulting chromatograms of the bind-and-elute CEX and FT AEX are presented in **Figure 6.3B** and **C**, respectively. The level of aggregation after each unit operation was determined by SEC-UPLC, and is described in **Table 6.2**. With the optimization of each step, the elimination of HMW species was accomplished, with the final mAb product

containing merely 0.1% of aggregation. Therefore, the designed integrated process is expected to efficiently remove the aggregates, and the developed PAT tool should only detect aggregation in the VI and the CEX steps, but not in the AEX FT, the final purified product.

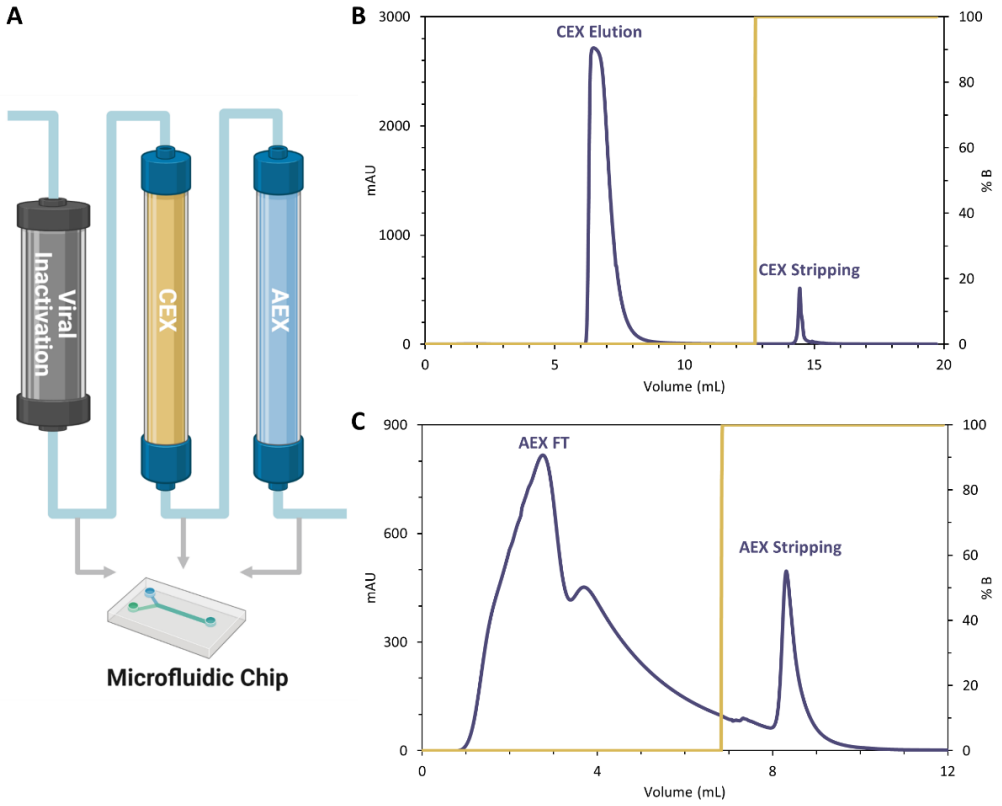

*Figure 6.3 - **A)** Schematic representation of the unit operations implemented in the integrated downstream setup: VI, a CEX and a AEX chromatography step. A sample of each collected phase is sent directly to the micromixer structure, where mAb aggregation is detected within 10 minutes. Each unit operation was optimized separately beforehand: first, the mAb sample was incubated at pH 3 for 60 minutes, and the resulting sample was injected in a **B)** CEX column, in a bind-and-elute mode; followed by a **C)** AEX step, in a FT mode. The buffers employed can be found in Table 6.1, the same buffers used in the integrated system. Each sample was also analyzed by SEC-UPLC to determine the aggregation level (Table 6.2) to confirm aggregate removal within the downstream process.*

Table 6.2 - Aggregation levels and concentration determined by SEC-UPLC for each collected sample from the batch optimization experiments.

	Aggregation (%)	Concentration (mg mL^{-1})
Initial Sample	2.7	36.5
VI Incubation	2.8	28.7
CEX Stripping	3.2	11.6
AEX FT	0.1	2.0
AEX Stripping	13.8	0.4

6.3.2. Implementation of the Micromixer in a Downstream Process

The next step was to incorporate and integrate all the steps in an ÄKTA Avant unit, with the implementation of the PAT microfluidic chip (Figure 6.2, Figure 6.S1 and 6.S3). Several extra modules were added to a standard ÄKTA unit: a LoopV, four VVs, one extra UV monitor, and three superloops, one of 10 mL and two 50 mL. The function of each additional module is extensively described in Section 2.3.2. The microfluidic chip was operated at a flow rate of 3 µL min^{-1} (0.003 mL min^{-1}), which provided a mixing efficiency of around 85% [12]. Pump A and sample pump inject the sample and the FD into the micromixer, respectively. The incorporation of two superloops in the system was crucial since it allowed to perform not only the VI step, but also to collect the eluate from the CEX column, as well as the FT and the eluate of the AEX column. Thus, the mAb samples could be stored and later directly sent to the micromixer to detect the presence of HMW species (Figure 6.2, dashed gold line), using a reduced pump A's flow rate. Additionally, with the addition of three restrictors, the system's pressure could be maintained, without the presence of any pressure spikes which could damage the integrity of micromixer or cause the disconnection of the tubes to the micromixer. Thus, a single microfluidic chip could be constantly reused for every measurement performed.

The micromixer was previously validated to successfully detect aggregation in an FT AEX unit operation [12]. However, the detection time, starting with the pumping of the sample to be mixed with the FD and finishing with forwarding the mixed fluid to the UV sensor, took a total of 60 minutes. Hence, since the micromixer was not able to provide a real-time measurement, a major challenge when integrating this microfluidic sensor was to significantly reduce this detection time. Several design measures and procedures were implemented to decrease this measuring time to merely 10 minutes, explained in detail in Section 6.2.3.3. Rathore *et al.* [22] used an online-HPLC system to perform pooling of a chromatography column based on

product CQAs, like aggregation. The time of analysis in the HPLC was reduced to 11 minutes, allowing for a real-time decision making for the chromatographic pooling. Therefore, the measuring time of the PAT micromixer was aimed to be reduced to the 10-minutes mark. Furthermore, to eliminate any interference from the FD's intrinsic fluorescence, the UV signal was auto-zeroed with the injection of FD and the sample buffer in the micromixer before the measurement.

6.3.3. Aggregate Detection

With the process set up in the ÄKTA system, the final mAb purification steps were reproduced and, after each phase, a sample was directly sent to the developed PAT tool for aggregate detection. Firstly, resorting to the viscosity-sensitive FD CCVJ, a run was performed in the integrated downstream process and the results can be found in Figure 6.4. The UV signal at 280 nm (dark blue line) was recorded by UV2, controlling the process, whereas the UV signal at 520 nm (dashed gold line) was recorded by UV1. The UV signal at 520 nm was defined to monitor the λem of the FD CCVJ, meaning that when there was an increase in absorbance, aggregation was present in the analyzed sample. Once more, off-line SEC-UPLC was performed to confirm and determine the level of aggregation of the collected samples which were not loaded into the next purification step (Table 6.3).

Table 6.3 - Aggregation levels and concentration determined by SEC-UPLC for each collected sample from the integrated downstream runs, for the fluorescent dyes CCVJ ([CCVJ] = 1 μM, λexc = 435 nm, λem = 520 nm) and Bis-ANS ([Bis-ANS] = 0.5 μM, λexc = 380 nm, λem = 520 nm). The AEX stripped sample collected was not enough to be analyzed by SEC-UPLC in the CCVJ run. The CEX FT and the AEX Stripping sample for the Bis-ANS run did not contain mAb sample, therefore aggregation was not detected (ND).

	CCVJ		**Bis-ANS**	
	Aggregation (%)	Concentration (mg mL^{-1})	Aggregation (%)	Concentration (mg mL^{-1})
Initial Sample	4.8	39.3	5.2	40.6
CEX FT	ND	0	ND	0
CEX Stripping	32.9	2.4	31.1	3.3
AEX FT	0.9	0.6	0.6	0.6
AEX Stripping		-	ND	0

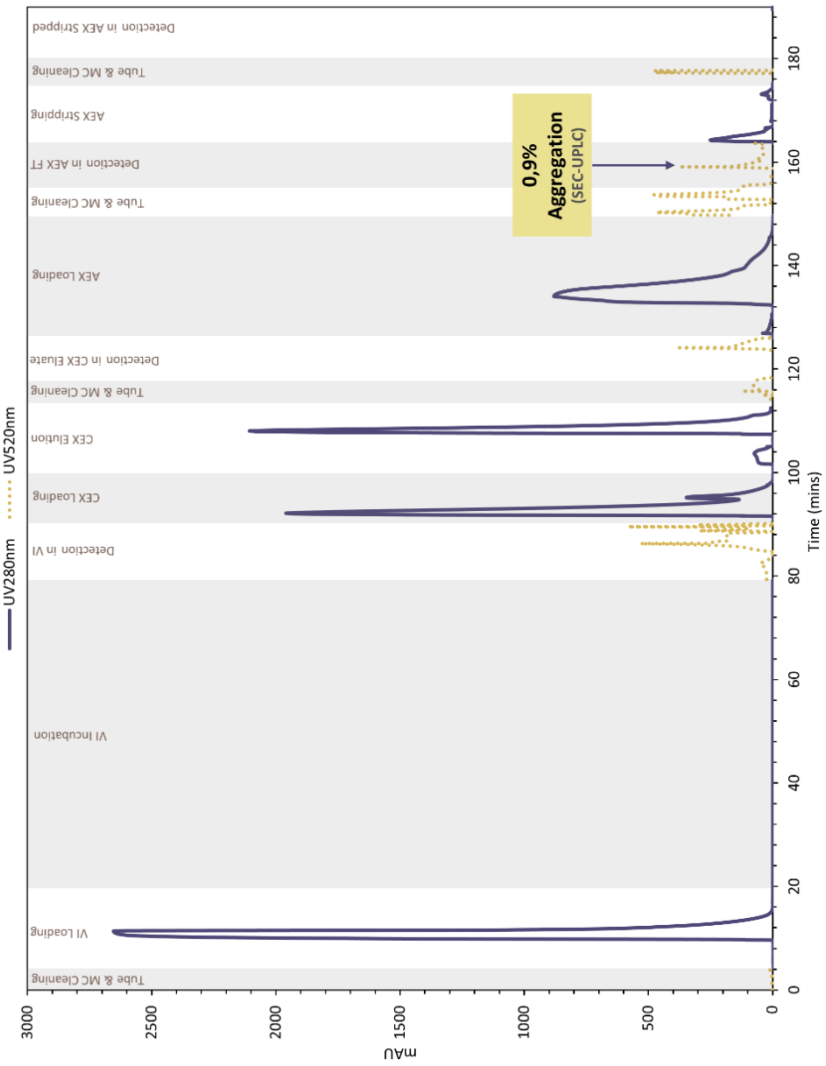

Figure 6.4 - Chromatographic profile for a single run in the integrated downstream set-up: VI, CEX and AEX, with CCVJ ([CCVJ] = 1 μM, λexc = 435 nm, λem = 520 nm) as the fluorescent dye used for detection. The mAb sample ([mAb] = 40 mg mL⁻¹) first undergoes the viral inactivation step, where it is incubated at pH 3 for 60 minutes, followed by CEX in bind-and-elute mode and a FT AEX step. Before each measurement, the micromixer structure is cleaned with water. The UV signal at 280 nm (UV2) is used to monitor the chromatography run whereas the UV signal at 520 nm (UV1) is employed for aggregate detection. The UV1 signal was autozeroed with buffer and fluorescent dye in the micromixer before each analysis. The examined samples in the microfluidic structure were also analyzed by SEC-UPLC to determine the aggregation level (Table 6.3).

The integrated run started with the cleaning of the micromixer and connection tubes. Afterwards, the mAb sample was injected from the 10 mL superloop 0 to the 50 mL superloop 1, loading the VI step (Figure 6.2, dark blue line). Since the injection of the mAb sample required the passage through the UV2 detector, the first peak observed at 280 nm in Figure 6.4 corresponds to this VI loading. During the VI loading, pump B performed sample conditioning by in-line dilution, lowering the mAb pH solution from 5.0 to 3.0. The sample was incubated for 60 minutes, while the equilibration of the CEX and AEX columns were taking place. After the VI step, a mAb sample was directly sent to the microfluidic sensor for aggregate detection (**Figure 6.2**, dashed gold line). A significant increase in the UV absorbance at 520 nm can be observed (Figure 6.4), which means HMW species are present in the mAb sample. Then, a bind-and-elute CEX was performed, with the eluate also being analyzed in the micromixer. Once again, an increase in the UV signal at 520 nm can be detected, which means that the first polishing step does not completely remove all HMW species present. Subsequently, the CEX eluate was loaded onto the AEX column and the FT was collected for aggregate analysis. Surprisingly, the microfluidic sensor detected HMW species in the AEX FT, i.e., the final purified product, which was not expected since the process was optimized for aggregate removal. The off-line analysis by SEC-UPLC revealed that the mAb final product still contained 0.9% of aggregation (Table 6.3). Hence, the FD CCVJ can detect aggregation in samples containing as low as 1% of HMW species. Nevertheless, aggregate detection using FDs is more related to the properties of the aggregates than actually their amount [23]. Therefore, FDs will only provide a qualitative measurement, not quantitative, and an absolute value for its limit of detection (LOD) should not be defined. Later, the AEX column was stripped and the sample pool was sent for aggregate detection and posterior off-line analysis. The micromixer was not able to detect aggregation, which could not be confirmed by the SEC-UPLC analysis since not enough volume was collected. A possible explanation is, since a larger percentage of aggregation was encountered in the mAb product, the absence of a signal in UV1 from the AEX strip sample is due to a poor separation of the HMW species in the final polishing step. Additionally, the AEX strip sample might be too diluted for the FD CCVJ being able to detect aggregation. Since sample collection in each of the superloops is controlled by the UV signal at 280 nm provided by the UV2 monitor, the shortage of volume collected from the stripping of the AEX column already indicated a very diluted sample (Table 6.3). Nonetheless, the micromixer was successfully implemented and applied, detecting aggregation where HMW species were indeed present during the mAb purification process.

Furthermore, the micromixer sensor was also tested with the hydrophobicity sensitive FD Bis-ANS. The results are described in **Figure 6.5**, with the off-line analysis by SEC-UPLC being found in **Table 6.3**. An identical process was performed, starting with the VI step and followed by the two polishing steps. Similarly to CCVJ, an increase in the UV signal at 520 nm is observed in the VI and CEX eluate samples. Hence, aggregation was effectively detected by the micromixer once more. However, for the AEX FT, the UV absorbance never increased during the 10 minutes measuring time. Consequently, aggregation was not detected in the mAb final product, which was later analyzed off-line. The mAb final product contained merely 0.5% of aggregates, which was not detected by the FD Bis-ANS. The regulatory guidelines provided by the United States and the European Pharmacopeia recommend that the mAb final formulation has to be 'practically/essentially free' of insoluble aggregates (100 nm to 100 µm), which have been reported to cause immunogenicity [24, 25]. Even though the size of these aggregates would still need to be assessed, 0.5% of aggregation on the final mAb formulation can be considerable acceptable (if the HMW species present are mainly reversible soluble aggregates). Therefore, Bis-ANS can be an ideal choice to be employed in the mAb purification process since it only provides an increase of the UV signal at 520 nm for samples with around 2% of aggregation [12]. Additionally, for the stripping of the AEX column, the micromixer was able to effectively detect aggregation, which was expected (**Table 6.2**). Once more, the developed miniaturized PAT tool, using Bis-ANS, successfully detected aggregation in an integrated downstream process. Thus, the FD can be chosen with respect to the maximum recommended concentration of aggregates in the final mAb formulation: the UV signal would only increase if the aggregate level is above the recommended limit.

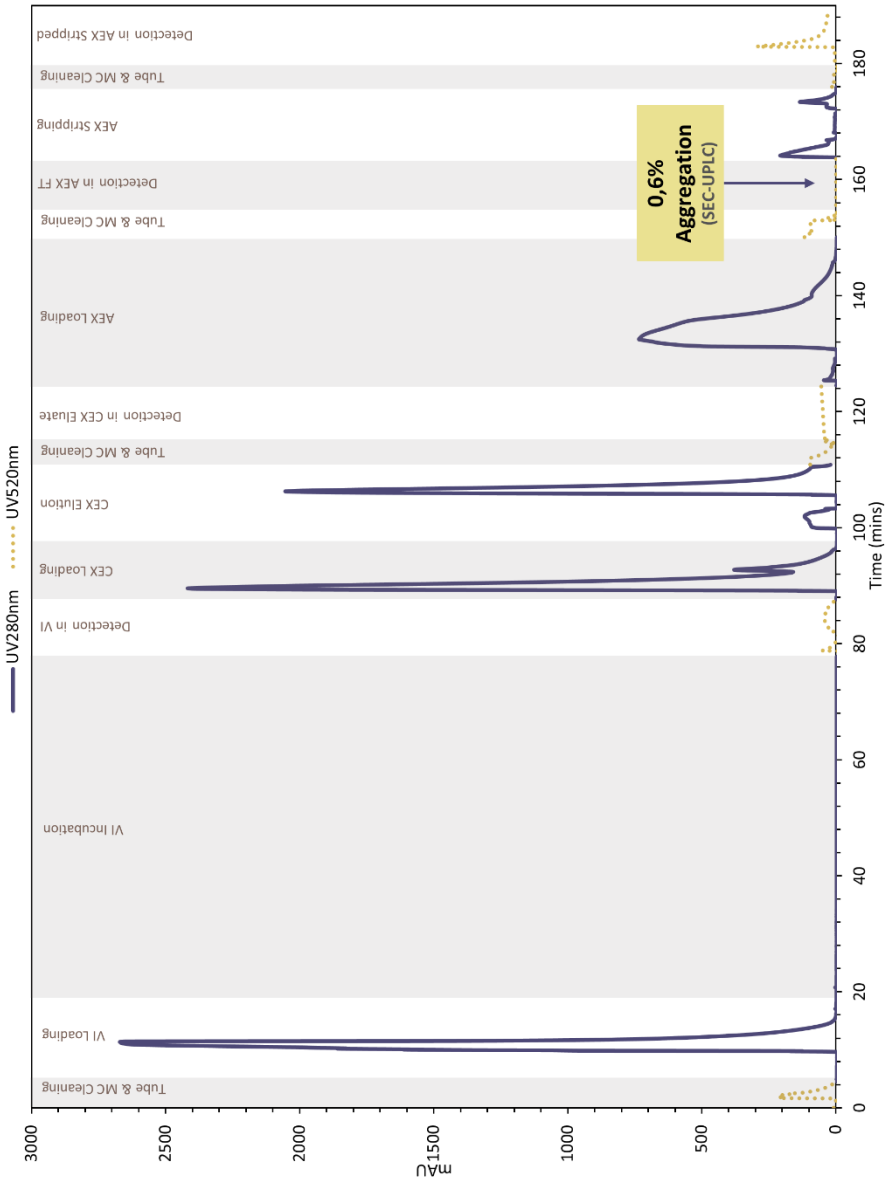

Figure 6.5 - Chromatographic profile for a single run in the integrated downstream set-up: VI, CEX and AEX, with Bis-ANS ([Bis-ANS] = 0.5 µM, λexc = 380 nm, λem = 520 nm) as the fluorescent dye used for detection. The same chromatography run was performed as in Figure 6.4, with the examined samples in the microfluidic structure analyzed by SEC-UPLC to determine the aggregation level (Table 6.3).

6.3.4. Potential and Limitations of the Micromixer

The main goal was to develop a PAT tool capable of real-time detection of aggregation in an integrated continuous downstream process. Although the miniaturized PAT tool fulfilled the requirement of detecting the presence of HMW species, this microfluidic sensor cannot be implemented in a truly continuous process. However, the majority of the implemented continuous downstream operations are actually merely semi-continuous, such as the periodic counter current (PCC) chromatography. The loading of the harvest feed is performed continuously but the washing and elution of the chromatography columns is not, with a discontinuous output of material. Therefore, the developed PAT micromixer could still be easily implemented.

Due to the inherent low flow rates employed in the micromixer, the addition of two superloops was essential to store the product pools. A reduction to lower flow rates, while using the ÄKTA system pumps, could be achieved without jeopardizing the entire purification process. Although the ÄKTA's pumps can technically employ these low flow rates, the entrance of air bubbles could be observed as not enough back pressure was generated. In **Figure 6.4**, a sudden increase in the UV signal at 520 nm can be seen at the start of every measurement. The presence of air bubbles result in these oscillations in the UV signal, which might affect the stability of the aggregation measurement. These air bubbles are primarily caused by switching of valve positions and thus flow paths, and the pump´s limitation for lower flow rates, making their appearance unavoidable. For example, the sudden peak observed in the tube cleaning before the AEX stripped pool (**Figure 6.4**) detection can be attributed to an air bubble. Nevertheless, if the UV signal ends up stabilizing, as seen for the AEX FT pool, the aggregate detection provided by the micromixer is reliable, which was later confirmed by an off-line analysis.

The LOD for this miniaturized PAT tool is directly correlated with the LOD of the FD employed. Depending on the level of aggregation allowed in the final biopharmaceutical formulation, CCVJ and Bis-ANS may be great options to be applied. Recently, several novel FDs have emerged, such as Proteostat, which seems to be better suited to detect small soluble aggregates [10]. Hence, the choice of the ideal FD will be critical to produce a reliable aggregate detection and it should be selected according to the needs of removing aggregates in a specific process. Furthermore, even though this work focused on the purification of a biopharmaceutical mAb, these FDs can detect aggregation across a variety of different proteins [26-28]. Hence, the

developed micromixer can be employed in several purification processes where protein aggregation is a CQA.

Unfortunately, a quantification of the degree of aggregation is not yet possible. Since the signal provided by the FD is directly related to the type of aggregate rather than actually its amount, a quantification cannot be achieved [23]. For example, in **Figure 6.5**, similar UV signals at 520 nm can be observed throughout the process (VI, CEX eluate and AEX stripped sample), even though the amount of aggregates in each sample differs (**Table 6.2** and **6.3**). Therefore, this microfluidic sensor is limited to offering a qualitative measurement. For aggregate quantification, the possibility of miniaturizing other analytical techniques should be examined since the developed micromixer demonstrated that its miniaturization produces a real-time measurement. Hydrodynamic chromatography and asymmetrical flow field-flow fractionation (AF_4) could be powerful alternatives to be miniaturized and implemented in the developed integrated system [7].

Nevertheless, the developed PAT tool presents two major advantages when compared to other already reported analytical approaches for a real-time measure of aggregation: the sample volume collected for analysis (30 µL) is negligible, being easily implemented in several biomanufacturing steps; and, since only an extra UV monitor is necessary to perform the analytical measurement, a fluorescent dye-based microfluidic sensor is a relatively affordable alternative. For example, Patel *et al.* [29] created a real-time aggregation measurement by coupling a Multi-angle Light Scattering (MALS) detector to a purification unit. Even though an immediate and in-line measurement is achieved, the cost associated to a MALS detector make this technique not readily available in a biomanufacturing site. Other analytical techniques pose a similar challenge, with an extra and complicated external set-up required to perform the measurement which increases production costs: Raman spectrometry [30], near-infrared spectroscopy [31] and light scattering [32].

6.4. Concluding Remarks

A PAT fluorescent dye-based microfluidic sensor was successfully implemented in an integrated downstream process, and it was capable of detecting aggregation after each unit operation. Firstly, the final steps in the integrated downstream process for the purification of mAbs, composed of the VI and two polishing steps, were optimized separately for aggregate removal. Then, to implement the previously developed micromixer, an integrated downstream system was developed in an ÄKTA system. A

sample was directly sent for aggregate analysis after each step in the purification chain. By adding two superloops and one extra UV sensor, the implementation of the microfluidic sensor was achieved: the two superloops allowed the collection of the mAb samples to be sent for analysis, reducing the flow rate; while the extra UV sensor permitted the monitoring of the chromatographic run while the already existing UV was used for the aggregation measurement. Additionally, several strategies were employed to reduce the measuring time of the microsensor from 60 to 10 minutes, such as reducing the connection tubes length or filling them with sample/FD beforehand. The microfluidic sensor effectively and robustly detected aggregation when using two distinct FDs, CCVJ and Bis-ANS, which was later confirmed off-line. Depending on the regulatory guidelines for the presence of aggregate in the final formulation of the mAb, a more (CCVJ) or less (Bis-ANS) sensitive FD can be selected to detect aggregation in the micromixer.

Although the developed PAT tool cannot produce a quantifiably measurement of the level of aggregation, the microfluidic chip does allow a rapid detection of HMW species. With the implementation in the integrated system, a real-time measurement was achieved, even under the desired 10 minutes. Therefore, the miniaturization of the analytical technique effectively speeds up the measurement. With the ability to measure real-time CQAs, immediate feedback and control of the process parameters can be achieved. For example, while performing the measurement, a control strategy can be implemented if an increase in the UV signal at 520 nm occurs.

6.5. REFERENCES

[1] São Pedro, M.N., Silva, T.C., Patil, R. and Ottens, M., White paper on high-throughput process development for integrated continuous biomanufacturing. Biotechnol Bioeng 2021, 118(9), 3275-86.

[2] Chopda, V., Gyorgypal, A., Yang, O., Singh, R., *et al.*, Recent advances in integrated process analytical techniques, modeling, and control strategies to enable continuous biomanufacturing of monoclonal antibodies. Journal of Chemical Technology & Biotechnology 2021, 97(9), 2317-35.

[3] Mandenius, C.-F. and Gustavsson, R., Mini-review: soft sensors as means for PAT in the manufacture of bio-therapeutics. Journal of Chemical Technology & Biotechnology 2015, 90(2), 215-27.

[4] Bansal, R., Gupta, S. and Rathore, A.S., Analytical Platform for Monitoring Aggregation of Monoclonal Antibody Therapeutics. Pharm Res 2019, 36(11), 152.

[5] Walchli, R., Ressurreicao, M., Vogg, S., Feidl, F., *et al.*, Understanding mAb aggregation during low pH viral inactivation and subsequent neutralization. Biotechnol Bioeng 2020, 117(3), 687-700.

[6] Telikepalli, S.N., Kumru, O.S., Kalonia, C., Esfandiary, R., *et al.*, Structural characterization of IgG1 mAb aggregates and particles generated under various stress conditions. J Pharm Sci 2014, 103(3), 796-809.

[7] São Pedro, M.N., Klijn, M.E., Eppink, M.H.M. and Ottens, M., Process analytical technique (PAT) miniaturization for monoclonal antibody aggregate detection in continuous downstream processing. Journal of Chemical Technology & Biotechnology 2021, 97(9), 2347-64.

[8] Paul, A.J., Bickel, F., Rohm, M., Hospach, L., *et al.*, High-throughput analysis of sub-visible mAb aggregate particles using automated fluorescence microscopy imaging. Anal Bioanal Chem 2017, 409(17), 4149-56.

[9] He, F., Phan, D.H., Hogan, S., Bailey, R., *et al.*, Detection of IgG aggregation by a high throughput method based on extrinsic fluorescence. J Pharm Sci 2010, 99(6), 2598-608.

[10] Oshinbolu, S., Shah, R., Finka, G., Molloy, M., *et al.*, Evaluation of fluorescent dyes to measure protein aggregation within mammalian cell culture supernatants. J Chem Technol Biotechnol 2018, 93(3), 909-17.

[11] São Pedro, M.N., Santos, M.S., Eppink, M.H.M. and Ottens, M., Design of a microfluidic mixer channel: First steps into creating a fluorescent dye-based biosensor for mAb aggregate detection. Biotechnology Journal 2022.

[12] São Pedro, M.N., Eppink, M.H.M. and Ottens, M., Application of a fluorescent dye-based microfluidic sensor forreal-time detection of mAb aggregates. Biotechnology Progress 2023.

[13] Gokaltun, A., Kang, Y.B.A., Yarmush, M.L., Usta, O.B. and Asatekin, A., Simple Surface Modification of Poly(dimethylsiloxane) via Surface Segregating Smart Polymers for Biomicrofluidics. Sci Rep 2019, 9(1), 7377.

[14] Healthcare, G., Continuous chromatography, Downstream Processing of a Monoclonal Antibody. 2015 Report 29170800 AA 2015.

[15] Lofgren, A., Andersson, N., Sellberg, A., Nilsson, B., *et al.*, Designing an Autonomous Integrated Downstream Sequence From a Batch Separation Process - An Industrial Case Study. Biotechnol J 2018, 13(4), e1700691.

[16] Gomis-Fons, J., Lofgren, A., Andersson, N., Nilsson, B., *et al.*, Integration of a complete downstream process for the automated lab-scale production of a recombinant protein. J Biotechnol 2019, 301, 45-51.

[17] Lofgren, A., Gomis-Fons, J., Andersson, N., Nilsson, B., *et al.*, An integrated continuous downstream process with real-time control: A case study with periodic countercurrent chromatography and continuous virus inactivation. Biotechnol Bioeng 2021, 118(4), 1664-76.

[18] Schwarz, H., Gomis-Fons, J., Isaksson, M., Scheffel, J., *et al.*, Integrated continuous biomanufacturing on pilot scale for acid-sensitive monoclonal antibodies. Biotechnol Bioeng 2022, 119(8), 2152-66.

[19] Gomis-Fons, J., Schwarz, H., Zhang, L., Andersson, N., *et al.*, Model-based design and control of a small-scale integrated continuous end-to-end mAb platform. Biotechnol Prog 2020, 36(4), e2995.

[20] Moreno-González, M., Keulen, D., Gomis-Fons, J., Gomez, G.L., *et al.*, Continuous adsorption in food industry: The recovery of sinapic acid from rapeseed meal extract. Separation and Purification Technology 2021, 254.

[21] Gomis-Fons, J., Andersson, N. and Nilsson, B., Optimization study on periodic counter-current chromatography integrated in a monoclonal antibody downstream process. J Chromatogr A 2020, 1621, 461055.

[22] Rathore, A.S., Yu, M., Yeboah, S. and Sharma, A., Case study and application of process analytical technology (PAT) towards bioprocessing: use of on-line high-performance liquid chromatography (HPLC) for making real-time pooling decisions for process chromatography. Biotechnol Bioeng 2008, 100(2), 306-16.

[23] Hawe, A., Friess, W., Sutter, M. and Jiskoot, W., Online fluorescent dye detection method for the characterization of immunoglobulin G aggregation by size exclusion chromatography and asymmetrical flow field flow fractionation. Anal Biochem 2008, 378(2), 115-22.

[24] den Engelsman, J., Garidel, P., Smulders, R., Koll, H., *et al.*, Strategies for the assessment of protein aggregates in pharmaceutical biotech product development. Pharm Res 2011, 28(4), 920-33.

[25] van Beers, M.M. and Bardor, M., Minimizing immunogenicity of biopharmaceuticals by controlling critical quality attributes of proteins. Biotechnol J 2012, 7(12), 1473-84.

[26] Lindgren, M., Sörgjerd, K. and Hammarström, P., Detection and Characterization of Aggregates, Prefibrillar Amyloidogenic Oligomers, and Protofibrils Using Fluorescence Spectroscopy. Biophysical Journal 2005, 88(6), 4200-12.

[27] Bai, Y., Wan, W., Huang, Y., Jin, W., *et al.*, Quantitative interrogation of protein co-aggregation using multi-color fluorogenic protein aggregation sensors. Chemical Science 2021, 12(24), 8468-76.

[28] Maarschalkerweerd, A.v., Wolbink, G.-J., Stapel, S.O., Jiskoot, W. and Hawe, A., Comparison of analytical methods to detect instability of etanercept during thermal stress testing. European Journal of Pharmaceutics and Biopharmaceutics 2011, 78(2), 213-21.

[29] Patel, B.A., Gospodarek, A., Larkin, M., Kenrick, S.A., *et al.*, Multi-angle light scattering as a process analytical technology measuring real-time molecular weight for downstream process control. MAbs 2018, 10(7), 945-50.

[30] Yilmaz, D., Mehdizadeh, H., Navarro, D., Shehzad, A., *et al.*, Application of Raman spectroscopy in monoclonal antibody producing continuous systems for downstream process intensification. Biotechnol Prog 2020, 36(3), e2947.

[31] Thakur, G., Hebbi, V. and Rathore, A.S., An NIR-based PAT approach for real-time control of loading in Protein A chromatography in continuous manufacturing of monoclonal antibodies. Biotechnol Bioeng 2020, 117(3), 673-86.

[32] Rolinger, L., Rudt, M., Diehm, J., Chow-Hubbertz, J., *et al.*, Multi-attribute PAT for UF/DF of Proteins-Monitoring Concentration, particle sizes, and Buffer Exchange. Anal Bioanal Chem 2020, 412(9), 2123-36.

Chapter 6

Real-time Detection of mAb Aggregates in an Integrated Downstream Process

Supplementary Material

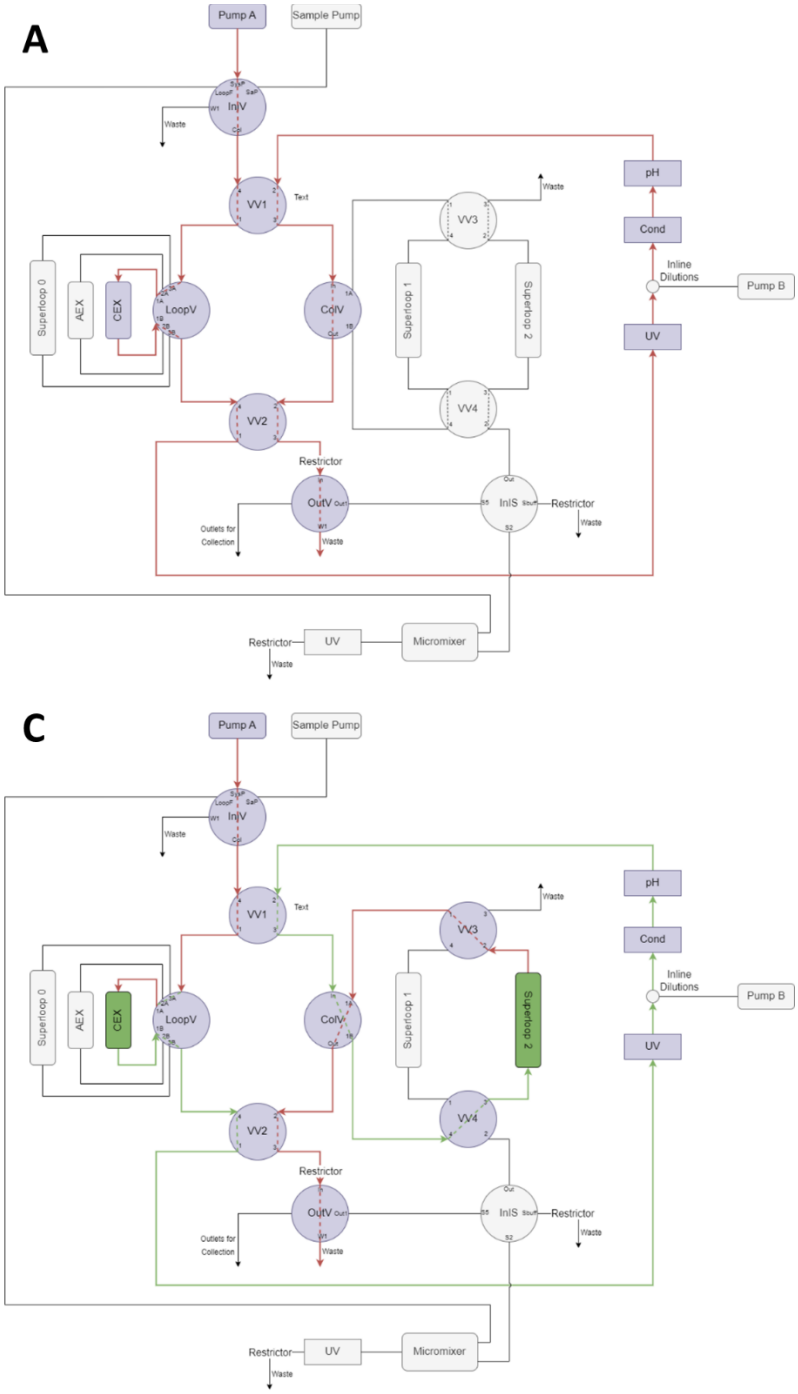

*Figure 6.S1 - Process diagram of the integrated downstream setup for the remaining phases of the CEX and AEX chromatography: **A** – equilibration of the CEX column; **B** – loading of the CEX column from the VI step; **C** – elution of the CEX column; and **D** – loading of the AEX column. For the stripping of the AEX column, the flow path of C is repeated, just changing the position of the*

(continues next page)

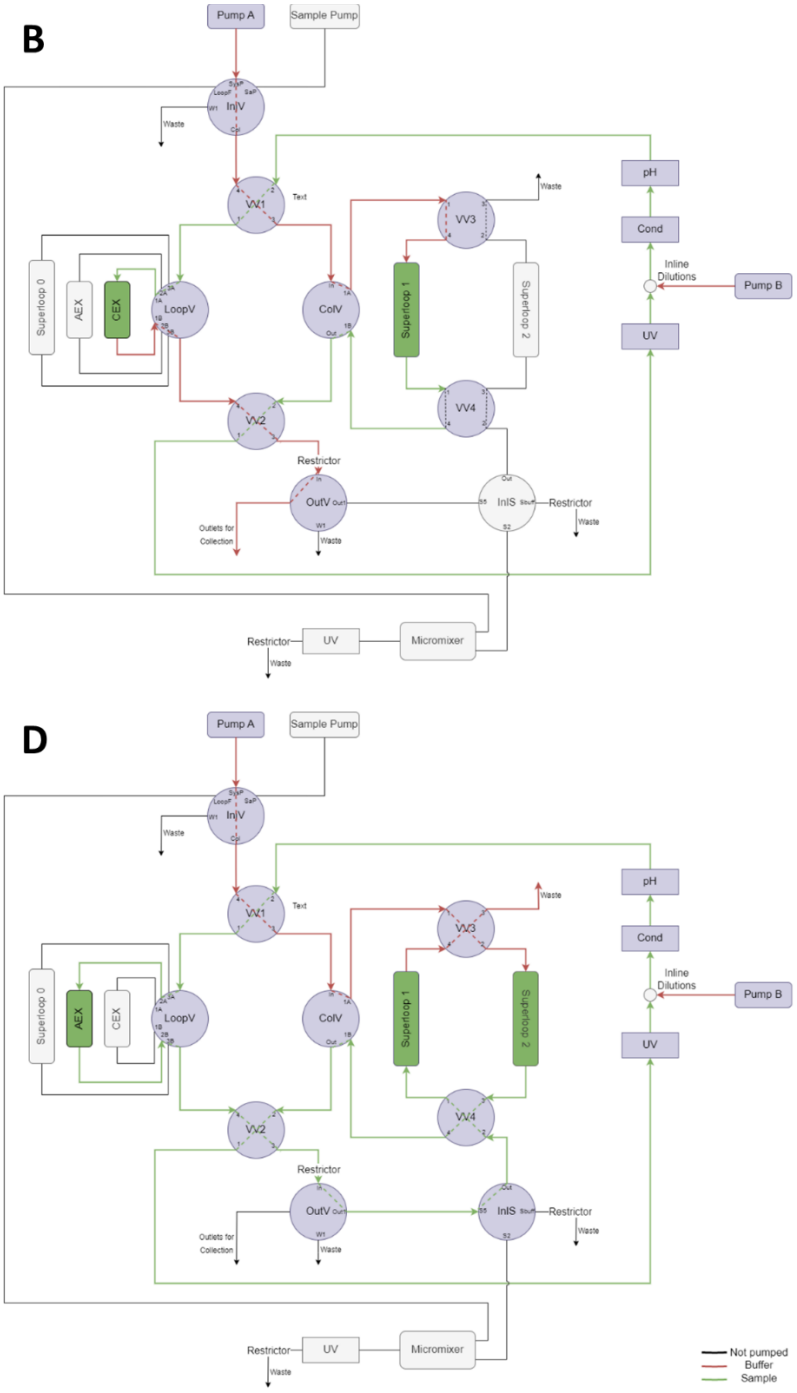

Figure 6.S1 ***(continuation)*** *- Loop valve. For the aggregate detection of each sample collected, the flow path represented in Figure 6.2, the dashed gold line, is reproduced every time. The red line represents the flow path performed by the several buffers used, pumped in from Pump A (process buffers) or Pump B (in-line conditioning buffers), the green line indicates the flow path which the mAb sample performs, whereas the black line represents inactive flow paths.*

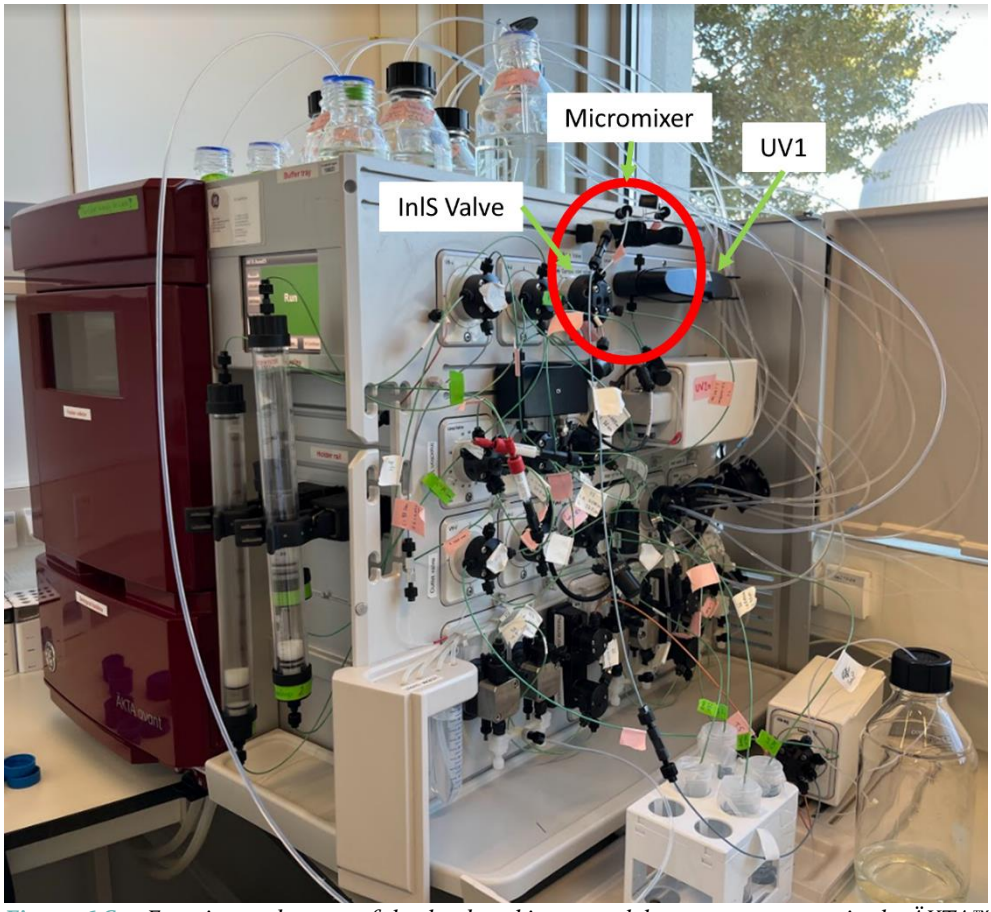

Figure 6.S2 - Experimental set-up of the developed integrated downstream system in the ÄKTA™ Avant unit. In red, the implemented microfluidic chip is highlighted: the connection tubes length between the micromixer and the inlet valve (InlS) or the UV1 were reduced to decrease the measuring time.

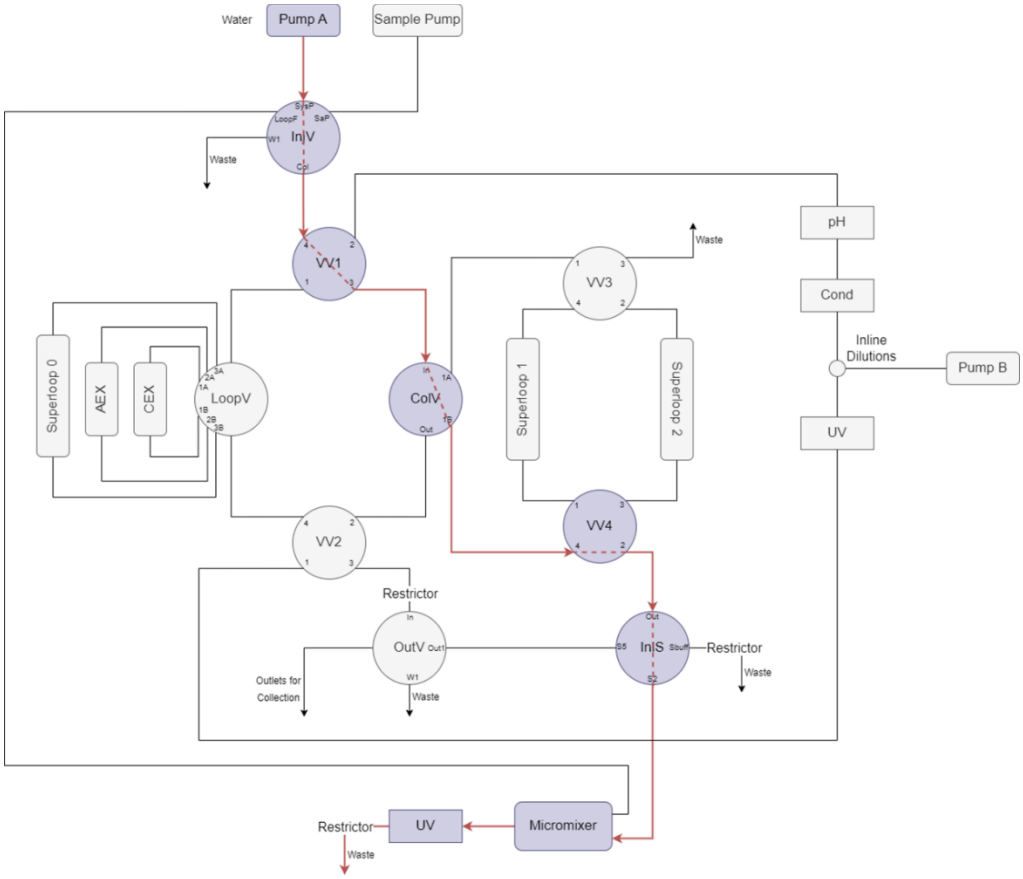

Figure 6.s3 - Process diagram of the integrated downstream setup for the cleaning of the micromixer with water. Pump A, through the injection valve (InjV), the column valve (ColV), the versatile valve 4 (VV4) and the inlet valve (InlS), injects water in the micromixer to clean it and the connection tubes at 5 µL min^{-1}.

Chapter 7

Conclusions and Outlook

7.1. General Conclusions

This PhD thesis describes the development of a microfluidic chip which provides a real-time detection of high molecular weight (HMW) species in an integrated downstream process. A zigzag micromixer was designed, applied and ultimately validated in a lab-scale mAb purification process. Using FDs and an UV detector, when an increase in the UV signal was observed, aggregates were detected by the micromixer. The work developed hereby demonstrated that the miniaturization of the analytical technique is a potential solution to create a real-time measurement. In particular:

- To implement an end-to-end continuous process in the biopharmaceutical industry, further development of process analytical technology (PAT) tools is crucial to gather critical quality attributes (CQAs) information in the process and elicit a timely response to facilitate control (Chapter 2);
- The miniaturization of an analytical technique is a powerful solution to create a real-time measurement due to its short reaction times (Chapter 3);

- mAb aggregation is inevitable in a continuous downstream process, with several well-established analytical techniques available to be miniaturized, such as Dynamic Light Scattering (DLS), Raman Spectroscopy (RS) and Circular Dichroism. FDs were considered a viable option for miniaturization since the measurement takes place within seconds, providing an immediate result (**Chapter 3**);
- Resorting to a computational fluid dynamics (CFD) model to determine the mixing efficiency, a zigzag mixing microchannel was designed and developed for the detection of aggregates labelled with a fluorescent dye (FD). This micromixer provides a mixing efficiency of circa 90% under 30 seconds, determined with a fluorescent tagged IgG molecule (**Chapter 4**);
- Two FDs, Bis-ANS and CCVJ, were applied successfully in the micromixer and detect a wide range of aggregate types, generated by a variety of induction factors: low pH, temperature, time and freeze-thawing (**Chapter 5**);
- A lab-scale purification process was set-up in an ÄKTA™ unit, reproducing the last downstream steps of the mAb production: VI step followed by two chromatographic polishing steps, cation (CEX) and anion exchange (AEX) chromatography, responsible for aggregate removal. The developed micromixer was incorporated in the system and able to effectively detect aggregation, with a sample of each unit operation being directly sent for analysis (**Chapter 6**);

7.2. Comparison of the Developed Micromixer with Available PAT Tools

Although the implementation of PAT tools in a continuous downstream processing remains fairly unexplored in the biopharmaceutical industry, numerous examples have already been reported for real-time aggregate detection and quantification. **Table 7.1** describes some of the latest publications regarding PAT tools for an aggregation measurement employed in a downstream unit operation.

Table 7.1 - Several examples of published PAT tools for the detection of mAb aggregation in a downstream process: the analytical technique chosen, the PAT application and the measuring time is described.

Analytical Technique	PAT application	Measuring Time	Reference
HPLC	On-line	11 minutes	Rathore *et al.* [1]
Raman Spectroscopy (RS)	In-line	15 minutes	Yilmaz *et al.* [2]
Light Scattering (DLS)	On-line	2 minutes	Rolinger *et al.* [3]
Light Scattering (MALS)	In-line	1 second	Patel *et al.* [4]
Near Infrared Spectroscopy (NIR)	On-line	3 seconds	Thakur *et al.* [5]
FD-based Micromixer	At-line	< 10 minutes	This thesis

A variety of analytical techniques have been explored and applied for aggregate detection and quantification. Ideally, the analysis should be performed in situ in the stream, i.e., an in-line measurement, such as RS and multi angle light scattering (MALS). However, an on-line measurement (where a sample is removed from the process stream for analysis and later returned) are also applied as long as the information collected is available within the required time frame for decision-making. Although the developed PAT tool only allows for an at-line measurement (where the sample is removed and analysed), the sample volume collected for analysis (30 µL) is negligible, even if the micromixer is implemented in several purification steps. The measuring time is rather longer, especially when compared to the NIR and the light scattering techniques, but still within the required time for pooling decisions in a chromatography step [1]. Hence, with the process information collected within the required time range, a control strategy can be implemented if an increase in the UV signal is observed.

When comparing with the remaining PAT tools, the micromixer's main advantage is that no additional large equipment is required to perform the measurement, only a simple UV monitor. All mentioned examples in the literature have an external experimental setup: a high performance liquid chromatography (HPLC) system [1], a Raman analyser [2], a Zetasizer [3], a MALS detector [4] and a NIR system [5]. As demonstrated in **Chapter 6**, the micromixer can be easily incorporated in a chromatographic system, decreasing the complexity of the experimental setup. With a simple UV monitor, readily available in a regular laboratory or in a biomanufacturing site, the FD-based PAT tool can robustly detect HMW species. Since no extra

equipment is necessary to perform the measurement, the costs of the developed analytical technique are minor. Thus, a cost-effective PAT tool has been developed for the detection of aggregates, still able to provide information in a time frame that enables process control.

7.3. Other Analytical Alternatives for Miniaturization

The findings described in this PhD thesis showed that the miniaturization of the analytical technique to produce a real-time measurement is not only a viable option, it is the perfect solution. To control a continuous process, the analytical measurement of CQAs has to be produced in a few seconds to minutes. When working with miniaturized biosensors, due to its inherent small operation time, a fast measurement can be achieved. For example, the Archimedes system, developed by Malvern Instruments and described in detail in **Chapter 3**, already employs a microchannel to perform the analytical measurement [6]. Furthermore, the miniaturization of the analytical technique leads to: (1) minor sample volumes used for the analysis, in a µL or nL-scale; (2) portability; (3) lower costs, especially if fabricated in a relative inexpensive material (such as the polymer PDMS); (4) design versatility; and (5) potential for parallel operation [7, 8]. Even though the use of FDs only provided a qualitative measurement of aggregation, **Chapter 3** presents a variety of other possibilities of miniaturization of analytical techniques for aggregate detection.

Hydrodynamic Chromatography (HDC) separates the molecules according to their size. Large particles will only access the central region of the microchannel with the highest flow velocity due to the parabolic shape of the flow profile [9]. Therefore, larger molecules will be transported faster, arriving first to the end of the microchannel. With a simple detection method placed at the end of the microchannel, like a standard UV detector, HMW species can be detected if the retention time of the analyte is lesser than of a monomer molecule. This HDC-based microfluidic chip would then be easily implemented into the developed integrated system (**Chapter 6**), using the extra UV detector to monitor the early appearance of the aggregates. Thus, future efforts should be employed in designing and developing a HDC-based microfluidic chip: a long and flat separation channel, with a large aspect ratio. Due to the planar chip configuration, numerical simulations using a CFD software (similar approach to **Chapter 4**) should be the first step to assess if the microfluidic chip can be fabricated in relative cheap polymer materials, like PDMS. PDMS has propensity to collapse, so a possible incorporation of columns within the separation channel or a

change in the fabrication material needs to be first investigated. Additionally, HDC has not been employed to separate mAb aggregates from its monomer form. Resorting to CFD simulations once again, an early assessment into the separation efficiency can also be achieved.

RS is another solid alternative for the miniaturization of the analytical technique for aggregate detection. RS has been heavily used in real-time measurement of several CQAs and in process control, especially in the upstream production of mAbs [10-12]. However, in the downstream process, RS has been quite unexplored, especially for aggregate detection. Although this analytical technique provides quantitative information, the intrinsically weak Raman signal and the interference of fluorescence are drawbacks for RS implementation. The miniaturization of RS would not only expedite the measurement (from 15 minutes [2] to a few seconds), but also increase the sensitivity and accuracy of the analytical technique. Waveguide-confined and surface-enhanced RS (**Chapter 3**) are strong examples of employed design and fabrication techniques which improved the weak RS signal. Regarding aggregate detection, several studies have been reported where RS is used to discriminate between different HMW species. For example, Zhang *et al.* [13] developed a model, combining RS and a multivariate analysis, which differentiates aggregation levels in different mAb product samples. Therefore, with the enhancement of sensitivity provided by the miniaturization combined with the novel models, RS can be considered a serious contender for the detection and quantification of aggregates. Although extra equipment would be required to perform the analytical measurement, the gain of analytical information will overcome the complexity of the experimental set-up. RS has the advantage of being robust and non-destructive, while providing information about secondary structure, tertiary structure, and aggregation mechanisms [14].

Other possibilities for miniaturization are the analytical techniques which provide information on the conformational stability, i.e., the methods which assess 3D-structural changes in the mAb monomer structure. RS, circular dichroism and mass spectrometry are examples of analytical techniques which allow to study protein aggregation due to changes in the conformational stability. The complexity of the microfluidic chip and the required external equipment set-up are major downsides when miniaturizing these techniques. However, conformational stability methods can be considered a better option for process control since it allows for an in-line measurement with minimal sample preparation. Hence, it is recommended that the

conformational stability techniques are further explored concerning its miniaturization and developed further for aggregate quantification. Nevertheless, the associated costs of developing a conformational stability microfluidic chip (the fabrication material and the extra equipment necessary for the analysis) might need to be taken into consideration.

7.4. Further Research in PAT Development for Aggregate Detection

Miniaturization of the analytical technique was demonstrated to bring a novel and powerful opportunity to create a real-time measurement. Additionally, difficulties regarding instrumentation and limit of detection of each analytical technique can also be addressed and solved by miniaturizing the measurement (Chapter 3). However, more challenges have risen with the development of such PAT tools, such as data handling. A major challenge is to extract relevant information from the large quantities of raw data and measurements. RS, previously discussed, and the remaining conformational stability techniques produce a large amount of spectral data. Multivariate data analysis (MVDA), such as partial least squares (PLS) and principal component analysis (PCA), can then be applied to extract useful information and create soft sensors [2, 10, 11]. Therefore, efforts should be made in instrumentation improvement in parallel with developing new multivariate mathematical approaches to withdraw valuable process data.

To establish a continuous biomanufacturing, all unit operations within the production process need to be linked to create a single flow. Thus, when two unit operations are integrated, the yield and performance of a unit operation is severely depending on the yield and performance of the previous unit operation. Output monitoring on each unit operation is then of the utmost importance to ensure a robust process and maintain product quality [15]. Therefore, one of the main challenges to have all process unit operations fully integrated is to have real-time information on product attributes, provided by the PAT sensors, to be able to control the process via feedback and/or feed-forward control strategies [16]. In feedback control systems, corrective measures are taken automatically after disturbances affect product quality whereas, in a feed-forward control strategy, proactive actions are taken before process disturbances impact product quality, with a control algorithm required to generate the necessary control actions. A proportional integral derivative (PID) controller or model predictive controller are used for feedback control. PID is easier and relatively straightforward

to implement, being the preferred and most reported advanced control strategy, considering purity and yield as the control output [17, 18]. Process efficiency in the mAb production is mainly evaluated by the purity of the final product, which reflects in the total elimination of product related impurities (i.e. aggregates). Therefore, the development of PAT tools which evaluate real-time the presence of such impurities will aid the implementation of a robust process control strategy. Nevertheless, the delay in implementing PAT and control strategies for protein aggregation is not only due to the absence of robust and inexpensive sensors, but mostly on the lack of complete understanding on how the process parameters influence product CQAs [16]. Protein aggregation still remains a poorly understood phenomenon, with several known environmental factors and process parameters known to induce it (**Table 1.2**). A better understanding on the mechanisms behind protein aggregation would improve process control and performance. Until now, PAT tools to detect aggregation have been employed mainly for pooling decisions [1, 4]. With a greater knowledge on aggregation mechanisms, a PID feedback control strategy on the process parameters influencing this occurrence can be developed and later implemented. Additionally, feed-forward control should not be overlooked, being already applied for a chromatographic separation [19]. Furthermore, with the development of PAT sensors able to collect on-line data, the implementation of Digital Twins in biomanufacturing can be achieved. A Digital Twin is a digital representation of a physical process, with mathematical models being used to design and optimize the different unit operations. Thus, the retrieved data by the sensor can be used in the model to estimate otherwise unmeasured parameters, which, in turn, can then be used for monitoring or in feedback control [20].

7.5. REFERENCES

[1] Rathore, A.S., Yu, M., Yeboah, S. and Sharma, A., Case study and application of process analytical technology (PAT) towards bioprocessing: use of on-line high-performance liquid chromatography (HPLC) for making real-time pooling decisions for process chromatography. Biotechnol Bioeng 2008, 100(2), 306-16.

[2] Yilmaz, D., Mehdizadeh, H., Navarro, D., Shehzad, A., *et al.*, Application of Raman spectroscopy in monoclonal antibody producing continuous systems for downstream process intensification. Biotechnol Prog 2020, 36(3), e2947.

[3] Rolinger, L., Rudt, M., Diehm, J., Chow-Hubbertz, J., *et al.*, Multi-attribute PAT for UF/DF of Proteins-Monitoring Concentration, particle sizes, and Buffer Exchange. Anal Bioanal Chem 2020, 412(9), 2123-36.

[4] Patel, B.A., Gospodarek, A., Larkin, M., Kenrick, S.A., *et al.*, Multi-angle light scattering as a process analytical technology measuring real-time molecular weight for downstream process control. MAbs 2018, 10(7), 945-50.

[5] Thakur, G., Hebbi, V. and Rathore, A.S., An NIR-based PAT approach for real-time control of loading in Protein A chromatography in continuous manufacturing of monoclonal antibodies. Biotechnol Bioeng 2020, 117(3), 673-86.

[6] Hawe, A., Weinbuch, D., Zölls, S., Reichel, A. and Carpenter, J.F. Submicrometer, micrometer and visible particle analysis in biopharmaceutical research and development. Biophysical Characterization of Proteins in Developing Biopharmaceuticals2020. p. 285-310.

[7] Sia, S.K. and Whitesides, G.M., Microfluidic devices fabricated in poly(dimethylsiloxane) for biological studies. Electrophoresis 2003, 24(21), 3563-76.

[8] Kricka, L.J., Miniaturization of analytical systems. Clinical Chemistry 1998, 44, 2008–14.

[9] Striegel, A.M. and Brewer, A.K., Hydrodynamic chromatography. Annu Rev Anal Chem (Palo Alto Calif) 2012, 5, 15-34.

[10] Santos, R.M., Kaiser, P., Menezes, J.C. and Peinado, A., Improving reliability of Raman spectroscopy for mAb production by upstream processes during bioprocess development stages. Talanta 2019, 199, 396-406.

[11] McAvan, B.S., Bowsher, L.A., Powell, T., O'Hara, J.F., *et al.*, Raman Spectroscopy to Monitor Post-Translational Modifications and Degradation in Monoclonal Antibody Therapeutics. Anal Chem 2020, 92(15), 10381-9.

[12] Schwarz, H., Mäkinen, M.E., Castan, A. and Chotteau, V., Monitoring of amino acids and antibody N-glycosylation in high cell density perfusion culture based on Raman spectroscopy. Biochemical Engineering Journal 2022, 182.

[13] Zhang, C., Springall, J.S., Wang, X. and Barman, I., Rapid, quantitative determination of aggregation and particle formation for antibody drug conjugate therapeutics with label-free Raman spectroscopy. Anal Chim Acta 2019, 1081, 138-45.

[14] Ettah, I. and Ashton, L., Engaging with Raman Spectroscopy to Investigate Antibody Aggregation. Antibodies (Basel) 2018, 7(3).

[15] Rathore, A.S., Kateja, N. and Kumar, D., Process integration and control in continuous bioprocessing. Current Opinion in Chemical Engineering 2018, 22, 18-25.

[16] Chopda, V., Gyorgypal, A., Yang, O., Singh, R., *et al.*, Recent advances in integrated process analytical techniques, modeling, and control strategies to enable continuous biomanufacturing of monoclonal antibodies. Journal of Chemical Technology & Biotechnology 2021, 97(9), 2317-35.

[17] Krattli, M., Muller-Spath, T. and Morbidelli, M., Multifraction separation in countercurrent chromatography (MCSGP). Biotechnol Bioeng 2013, 110(9), 2436-44.

[18] Papathanasiou, M.M., Burnak, B., Katz, J., Shah, N. and Pistikopoulos, E.N., Assisting continuous biomanufacturing through advanced control in downstream purification. Computers & Chemical Engineering 2019, 125, 232-48.

[19] Mendhe, R., Thukkaram, M., Patil, N. and Rathore, A.S., Comparison of PAT based approaches for making real-time pooling decisions for process chromatography - use of feed forward control. Journal of Chemical Technology & Biotechnology 2015, 90(2), 341-8.

[20] Udugama1, I., Lopez, P., Gargalo, C., Li, X., Bayer, C., Gernaey, K., Digital Twin in biomanufacturing: challenges and opportunities towards its implementation. Systems Microbiology and Biomanufacturing 2021, 1, 257–27.

Curriculum vitae

Mariana Neves São Pedro was born in Lisbon, Portugal on 26th October 1993. In 2011, she started her BSc. in Biochemistry at Faculdade de Ciências da Faculdade de Lisboa. An early passion for protein purification started to develop, leading her to pursue a more applied MSc. in Biotechnology at the Instituto Superior Técnico, in Lisbon. During her master thesis, she studied the influence of fluorescent tags on monoclonal antibodies partition in miniaturized PEG-salt aqueous two-phase extraction.

After finishing his MSc., Mariana decided to continue exploring her love for downstream processing and challenge herself by pursuing a higher education on the topic. While looking for future opportunities, she worked as a research fellowship in the Institute for Bioengineering and Biosciences, where she assisted in a high-throughput screening of different chromatographic conditions and resins for the purification of antibody fragments.

In 2019, Mariana started a PhD position at Technische Universiteit Delft, part of on the CODOBIO – Continuous Downstream Processing of Biologics research project, an international training programme (ITN) funded in the frame of Marie Skłodowska-Curie Actions. Mariana's project was focused on the design and development of a real-time PAT microfluidic biosensor for the detection of monoclonal antibody aggregation in a continuous downstream process. The results of her research during these past four years are presented here in this thesis.

Acknowledgements

Citing proposition number 6 accompanying this PhD thesis, the work presented in these last 175 pages was not done solely by one person. Fortunately, in this journey, I have met amazing people which have aided this project, either with their technical knowledge or by just being a friendly face I can vent out to. Thus, I will spend the next few pages praising and gushing over them! Warning alert, if you are not confortable with feelings and extra cheesy displays of emotions, I advise you to skip the next section…

First of all, I would like to thank my promotors for, first, giving me the opportunity to perform this PhD, and their supervision over these last four years. **Marcel**, thank you for giving me space to explore my creativity and time to grow as a researcher. Even when you knew something might not work, you always allowed me to try, (fail) and learn from it. **Michel**, thank you for your precious feedback in our meetings and for letting me use Byondis resources and labs to conduct this project.

Também quero agradecer às minhas duas estudantes de mestrado: **Mafalda** e **Maria**. Obrigada por terem escolhido este projecto! Sem o vosso esforço e dedicação, este trabalho seria muito diferente. Mesmo quando tudo parecia correr mal, desde enfrentar uma pandemia até a um Äkta mal-comportado, nunca desistiram e ajudaram-me imenso a construir este biosensor.

I would also like to thank everyone in the CODOBIO consortium, for all input and ideas to this project during our monthly meetings. Special thanks to the visiting PhDs we welcomed in Delft: **Madèlene**, for helping design and develop the integrated system, and **Nacho**, for all the conversations.

In this past four years I have joined a new found family, the **BPE** section**,** which I hereby thank:

Aos meus dois fantásticos paranymphs: **Marina** e **Tiago**. **Marina,** a minha réplica em miniatura, como poderia ter passado estes últimos quatro anos sem ser constantemente confundida contigo? De certeza que a minha experiência teria sido muito diferente (e muito mais aborrecida)… Foste sempre o meu apoio emocional, a minha *cheerleader* pessoal, ouvindo-me e animando-me quando era preciso. Nem te digo o quanto vou sentir falta de ir à janela entre os nossos escritórios para ver se estás

lá ou das tuas visitas à minha secretária só para fazer uma pergunta "rápida". Tu brilhas por dentro e por fora e nunca deixes que ninguém te faça duvidar disto. E agora chegou a tua vez de acabares isto, já não falta muito. Vamo lá Raúl, vamo lá!

Tiago, tens sido o meu *partner in crime* desde o primeiro dia desta aventura (até ao ultimo!) e não teria escolhido melhor. Vou ter imensas saudades de partilhar um escritório contigo todos os dias: desde ouvir-te a martelar frustado no teclado às nossas "pequenas" pausas para gossip. Sempre que saia frustada do laboratório ou de uma reunião, encontrava-te sempre pronto para ouvir os meus desabafos e preocupações. Foste o CT para o meu Wes. Ah, claro, e o menos importante, também te agradeço pelo todo o trabalho que fizemos juntos, foi bastante mais divertido escrever um artigo ou ensinar o advanced course contigo. Espero que tenhas aprendido tanto comigo como eu aprendi contigo (não precisas de agradecer pelas minhas horas passadas a explicar-te a Eurovisão ou HSM).

Song, I can truly say thay this PhD project would not have happened and materialized without you and your knowledge. Not only you have taught me everything that I needed to know in the lab and spent countless hours troubleshooting with me all the problems I encountered, you have help me maintain my mental sanity. Always ready with words of encouragement and the ability to make me laugh, you calmed me down when I was ready to give up. Wherever the future takes me in terms of my career, I already know I will miss you and our life conversations next to the Äkta. But (hopefully) we will have your delicious hotpots to catch up!

Joan, thank you for being unapologetically you! You never judge and you have the ability to make me feel normal in this crazy world. You are my real-life example of hard-work and dedication. With **Daniela**, you make the most fashionable couple that I know!

Oriol and **Marijn**, my favourite MESs two, I know that these past four years have not been easy for you and I only hope I was able to be there for you as you were there for me. You guys are true warriors and I am very happy to slowly have you back! **Marijn**, you are a personified antithesis: you have the purest soul I have ever met while still capable of having an evil sense of humor. You can make me truly laugh. Do not ever change, no matter what happens! **Oriol**, I only wished that you saw yourself the way we all see you: funny, charming and strong. You always make time to listen to me and my problems and some of my favourite memories are the endless conversations we had. When the time comes to have fun and get our hands "dirty", I know I can always count on you.

Daphne, **Roxana** and **Tim**, we have shared so much during this journey, from the normal PhD struggles to amazing trips to conferences (special shoutout to the Otters, 3rd place doesn't seem so bad with you). **Daphne**, I admire your passion and resilience, you were always able to work around and make things happen. And thanks to **Tim** for joining me in the non-engineer team.

To everyone that I had the pleasure to share the office with: **Bianca** and **Mónica**, for the initial guidance and advices, and to **Zulhaj** and **Robin**, for the patience of putting up with me. **Marteen**, your heart and your smile are as big as you and I will miss them when walking everyday into the office. Let's keep singing Bohemian Rhapsody together!

To all the amazing BPE staff: **Adrie**, **Ludo**, **Christiaan**, **Stef**, **Max**, and especially **Kawieta**, this group would not function without you. **Marieke**, thank you for your early guidance into being a researcher and how to properly write a publication. To the old BPE generation, for introducing me to the PhD and to the Netherlands: **Debby**, **Joana**, **Rita**, **Clara** and **Chema**. To **Lars**, my successor in the PhD committee, you have made me proud! To **Mona**, for all your words of guidance and advice. And to the new generation of BPE, hope you have as much fun as I had during your PhD: **Rik**, **Brenda**, **Tamara**, **Hector**, **Ramon**, **Miki**, **Mariana**, **Marika** and **Eduardo**.

E a **Raquel**, tendo sido apenas parte desta família por pouco tempo, és a minha *partner in crime* para a leitura e para ir a concertos. Tu e o Tiago podem sempre contar connosco para jantaradas ou para fazer dogsitting da **Caya** e do **Gu**.

Apart from BPE, I also had the priviledge of being adopted into the EBT family. I always have a blast when we all hang out, always laughing my ass off. To all the friday drinks or crazy activities we shared together (and that we still are going to share): **Samuel**, **Timothy**, **Maxim**, **Lemin**, **Nina**, **Stefan**, **Ali**, you guys are definitely too hot to handle… To **Kiko**, who always has the ability to stay positive and strong, even when life (or a knee) tries to bring you down.

To **Rodoula** and **Angelos**, going to your house is like going to a grandma's house, you will come out nurtured and with 5 quilos more. I will always treasure the wonderful time and trips, all the amazing meals and afternoons spent laying in your sofa. *I'll be there for you, cause you're there for me too.* **Rodoula**, I will miss our hour long coffee breaks and sport sessions (which were basically just another hour long coffee breaks).

To the best PhD committee: **Céline**, **Susan**, **Timmy** and **Sam**. Organizing all the social activities and the symposium was a lot of fun with you!

In the last four years, I was lucky enough to also have gained a third family. Thank you for opening your arms and accepting me in our crazy dysfunctional family: to the annoying little brother (that I never asked for) **Sergio**, the calming and serene **Flo**, the explosion **Marta** and the positive and funny **Ingrid**. To the best neighbours **Ale** and **Georg** for all the movie marathons, game night, lazy Sunday afternoons and all the amazing food/sandwiches we shared together. I will miss it!

Ao pessoal que deixei em Portugal mas que sempre que volto, nada parece ter mudado: **Rosado**, **Lola**, **João**, **Rita**, **Monteiro**, **Susie**, **Cris** e **Raquel**. Ouviram sempre os meus desabafos e preocupações, mesmo com quilómetros de distância. E quando chega a altura de fazer a festa, posso sempre contar com vocês!

Aos meus **pais**, que literalmente sem eles eu não estaria aqui. Obrigada pela noite de paixão que me trouxe a este mundo, por me terem aturado todos estes anos (ufff já vão 30) e por acreditarem sempre em mim. Ao meu irmão **Tomás**, a melhor crise de vesícula, sem ti não me teria tornado a melhor irmã e role model do mundo. Tenho bastante orgulho da pessoa que te tornaste. Vocês apoiaram-me nos meus piores momentos e são os primeiros a celebrar as minhas vitórias, por isto esta vitória é nossa!

Y por último (pero ciertamente no menos importante), tengo que agradecer a **David**. *Yo era ateo, pero ahora creo, porque un milagro como tú ha tenido que bajar del cielo.* Hago mías las palabras de C. Tangana. Durante estos últimos cuatro años, si alguien ha aguantado mis peores momentos y ha estado a mi lado para celebrar los buenos, has sido tú. En cierto modo, esta victoria mía tiene que ser un POCO (no abuses) compartida contigo. Tienes la capacidad de hacerme reír siempre, incluso cuando no quiero. Consigues derretir mi corazón helado. No hay nadie más en este mundo que pueda llevarme a una montaña rusa. Solo tú. Te quiero.

List of Publications

São Pedro, M.N., Isaksson, M., Gomis-Fons, J., Eppink M.H.M., Nilsson, B. & Ottens, M., *Real-time detection of mAb aggregates in an integrated downstream process,* Biotechnology & Bioengineering, 2023, 1–12 (https://doi.org/10.1002/bit.28466);

São Pedro, M.N., Eppink M.H.M., & Ottens, M., *Application of a fluorescent dye-based microfluidic sensor for real-time detection of mAb aggregates*, Biotechnology Progress, 2023, e3355, (https://doi.org/10.1002/btpr.3355);

São Pedro, M. N., Santos, M.S., Eppink M.H.M., & Ottens, M., *Design of a microfluidic mixer channel: First steps into creating a fluorescent dye-based biosensor for mAb aggregate detection*, Biotechnology Journal, 2022, 18, e2200332 (https://doi.org/10.1002/biot.202200332);

São Pedro, M.N., Klijn, M.E., Eppink, M.H. and Ottens, M., *Process analytical technique (PAT) miniaturization for monoclonal antibody aggregate detection in continuous downstream processing*, Journal of Chemical Technology and Biotechnology, 2022, 97, 2347-2364 (https://doi.org/10.1002/jctb.6920);

São Pedro, M. N., Silva, T. C., Patil, R., & Ottens, M.,*White paper on high-throughput process development for integrated continuous biomanufacturing*, Biotechnology and Bioengineering, 2021, 118, 3275– 3286 (https://doi.org/10.1002/bit.27757);

Nascimento, A., **São Pedro, M.N.,** Pinto, I.F., Aires-Barros, M. R., Azevedo, A. M., *Microfluidics as a high-throughput solution for chromatographic process development - The complexity of multimodal chromatography used as a proof of concept*, Journal of chromatography, 2021, 1658, 462618 (https://doi.org/10.1016/j.chroma.2021.462618);

São Pedro, M.N., Azevedo, A. M., Aires-Barros, M. R., Soares R.R.G., *Minimizing the Influence of Fluorescent Tags on IgG Partition in PEG–Salt Aqueous Two-Phase Systems for Rapid Screening Applications*, Biotechnology Journal, 2019, 14, 1800640 (https://doi.org/10.1002/biot.201800640).

Conference Contributions

São Pedro, M.N., Eppink, M.H. and Ottens, M., *Real-time process analytical technology: Fluorescent dye-based miniaturized sensor for aggregate detection,* **Integrated Continuous Biomanufacturing V**, Barcelona, October 2022, Oral Presentation.

São Pedro, M.N., Santos, M.S., Eppink, M.H. and Ottens, M., *Development of a Fluorescent Dye-Based Miniaturized Sensor for Aggregate Detection in Integrated Continuous Processing,* **International Symposium and Exhibition on the Purification of Proteins, Peptides and Polynucleotides (ISPPP) 2021**, Porto, November 2021, Oral Presentation.

São Pedro, M.N., Santos, M.S., Eppink, M.H. and Ottens, M., *Development of a Fluorescent Dye-Based Miniaturized Sensor for Aggregate Detection in Integrated Continuous Processing,* **American Chemical Society Fall 2020**, Online, August 2020, Oral Presentation.

São Pedro, M.N., Eppink, M.H. and Ottens, M., *Miniaturized Sensors for Integrated Continuous Biomanufacturing - Development of a fluorescent dye-based microfluidic chip for the detection of mAb aggregates*, **ESBES 2020 — 13th European Symposium on Biochemical Engineering Sciences**, Online, May 2020, Oral Presentation.

São Pedro, M.N., Eppink, M.H. and Ottens, M., *Miniaturization of Analytics – the case of Continuous Bioprocess*, **High-Throughput Process Development**, Porto, November 2019, Poster.